NATIONAL ADVISORY COMMITTEE FOR AERONAUTICS

TECHNICAL NOTE

No. 1245

Property Fairchild
Engineering Library

SUMMARY OF LATERAL-CONTROL RESEARCH

By Langley Research Department

Compiled by Thomas A. Toll

Langley Memorial Aeronautical Laboratory
Langley Field, Va.

PROPERTY FAIRCHILD
ENGINEERING LIBRARY

Property Fairchild
Engineering Library



Washington

March 1947

CASE FILE
COPY

TABLE OF CONTENTS

	Page
Summary	1
Introduction	1
I - Criterions Used in Lateral-Control Specifications	3
Rolling Performance	3
Control Forces	4
Stick or Wheel Travel	5
Adverse Yaw	5
Lag in Response	5
Control-Free Stability	6
II - Factors Involved in the Lateral-Control Problem	6
Lateral Maneuverability	6
Concept of Lateral Maneuverability	6
Helix Angle	7
Control Force	9
Effects of Wing Twist	11
Effects of Control-System Stretch	14
Effects of Adverse Yaw	14
Weathercock Stability	15
Dihedral	16
Effects of Aspect Ratio	16
Effects of Altitude	16
Effects of Radii of Gyration and Wing Loading	17
Control-Free Stability	18
Flutter	18
III - Testing Procedures and Application of Experimental Results	20
Flight Investigations	20
Procedure for Determining Rolling Performance	20
Description of Maneuver	20
Variables Measured	21
Presentation of Data	22
Procedure for Determining Adverse Yaw	22
Description of Maneuver	22
Variables Measured	23
Presentation of Data	23
Procedure for Determining Aileron Trim Changes with Speed	23
Wind-Tunnel Investigations	23
Two-Dimensional Models	24
Finite-Span Models	28

TABLE OF CONTENTS

	Page
IV - Characteristics of Lateral-Control Devices	30
Conventional Flap-Type Ailerons	30
Plain Ailerons	33
Hinge-Moment Characteristics	33
Lift Characteristics	37
Pitching-Moment Characteristics	38
Flight Tests	39
Ailerons Having Exposed-Overhang Balances	40
Hinge-Moment Characteristics	40
Critical Deflection	43
Effectiveness	44
Design Considerations	45
Flight Tests of Frise Ailerons	46
Ailerons Having Sealed Internal Balances	48
Ailerons Having Linked Tabs	53
Comparisons of Various Balancing Devices	57
Hinge-Moment Characteristics	57
Effect of Angle of Rig	58
Rolling Performance	58
Application to Arrangements Involving Full-Span Flaps	59
Flap-Trailing-Edge Ailerons	59
Drooped Ailerons	60
Ailerons with Retractable Flaps	60
Effects of Air-Flow and Wing-Surface Conditions	61
Boundary-Layer Effects	62
Mach Number Effects	64
Surface-Covering Distortion	67
Spoiler Devices	69
Hinged-Flap Spoilers	71
Retractable-Arc Spoilers	71
Slot-Lip Ailerons	73
Plug-Type Spoiler Ailerons	74
Effects of Mach Number	75

TABLE OF CONTENTS

	Page
V - Booster Mechanisms	75
Aerodynamic Boosters	76
Equations for Control Force	77
Characteristics of Spring-Tab Ailerons	79
Special Spring-Tab Designs	81
Use of Preload	81
Geared Spring Tab	81
Detached Tab	82
Other Aerodynamic Boosters	82
Mechanical Boosters	83
VI - Structural Aspects	84
Integrity of Airplane	84
Rolling Performance	86
Control Forces	86
VII - Application of Equations and Design Charts	86
Illustrative Example	86
Discussion	100
VIII - Status of Lateral-Control Research	101
Conventional Flap-Type Ailerons	102
Rolling Performance	102
Hinge Moments	103
Spoiler Devices	105
Lateral Control with Swept Wings	105
Appendix - Definitions of Symbols	108
References	117

NATIONAL ADVISORY COMMITTEE FOR AERONAUTICS

TECHNICAL NOTE NO. 1245

SUMMARY OF LATERAL-CONTROL RESEARCH

By Langley Research Department

Compiled by Thomas A. Toll

SUMMARY

A summary has been made of the available information on lateral control. A discussion is given of the criterions used in lateral-control specifications, of the factors involved in obtaining satisfactory lateral control, and of the methods employed in making lateral-control investigations in flight and in wind tunnels. The available data on conventional flap-type ailerons having various types of aerodynamic balance are presented in a form convenient for use in design. The characteristics of spoiler devices and booster mechanisms are discussed. The effects of Mach number, boundary layer, and distortion of the wing or of the lateral-control system are considered insofar as the available information permits. An example is included to illustrate the use of the design data. The limitations of the available information and some of the lateral-control problems that remain to be solved are indicated.

INTRODUCTION

The lateral-control research that had been conducted by the NACA prior to 1937, and that was summarized in reference 1, was concerned primarily with the design of lateral-control devices having sufficient effectiveness to enable the pilot of an airplane to keep the wings level at all normal flight speeds. In order to meet that condition large rolling-moment coefficients are required only at speeds approaching the stall; consequently, the provision of adequate rolling performance is principally a problem of the size of the device, the aerodynamic balance being of only secondary importance even for moderately large airplanes.

Between 1937 and 1941 a study was made of the lateral-control characteristics of a large number of combat and noncombat airplanes. The results of that study, reported in reference 2, indicated that the provision of lateral control that is sufficient only to keep the wings level is inadequate, and that a certain minimum standard of rolling performance is desirable for any type of airplane, even at high speeds. Subsequent experience has indicated that combat airplanes may be required to perform rapid rolling maneuvers near maximum speed. The problem of providing aerodynamic balance for light control forces at high speeds therefore has become at least as important as the problem of providing adequate effectiveness of the lateral-control device.

In order to meet the requirements for light control forces the designer has the choice of relying entirely either on aerodynamic balance or on some form of booster mechanism, or of combining a booster mechanism of low capacity with a small amount of aerodynamic balance. In any case, the control forces of fighter airplanes of average size may have to be reduced by amounts corresponding to as much as 95 percent of the unbalanced aileron hinge moments (reference 3). Some of the considerations relating to the provision of light control forces, as well as to other lateral-control problems, are discussed in reference 4.

The purpose of the present paper is to summarize rather completely the available information on lateral control, to point out the limitations of the available information and to indicate some of the problems that remain to be solved. No new investigations were attempted in preparing the present paper, although some of the data and analyses have not previously been published.

The symbols used in presenting the results are defined in the appendix. Figures that give data for use in design are listed in table I.

I - CRITERIONS USED IN LATERAL-CONTROL SPECIFICATIONS

In order to apply the results of theoretical and experimental studies to the design of satisfactory lateral-control devices, the requirements for satisfactory lateral control must be specified exactly. Lateral-control specifications have been limited to the unstalled flight range because the characteristics at and above the stall usually are very erratic. The lateral behavior in stalled flight usually is included in considerations of stalling characteristics.

The first comprehensive set of lateral-control specifications, which represent the present NACA recommendations, was published in reference 5. The present lateral-control specifications of the Air Technical Service Command, Army Air Forces, (reference 6) and of the Bureau of Aeronautics, Navy Department, (reference 7) are identical with each other. In the following paragraphs the significance of the various criterions used in specifying lateral-control characteristics is discussed.

ROLLING PERFORMANCE

Criterions that have been proposed for specifying the rolling performance of an airplane have been based on the time required to attain a given angle of bank, the maximum rolling velocity, the lateral movement of the center of pressure C_l/C_L, and the wing-tip helix angle $pb/2V$. Each of these criterions is subject to certain limitations. The results of the investigation described in reference 2 and some analytical studies have indicated, however, that the criterion based on $pb/2V$ is the most convenient and can be used to specify satisfactorily the rolling performance. The value of this criterion is independent of altitude for given aileron deflections and is independent of airplane size for geometrically similar airplanes.

Because the maneuvering qualities of fighter airplanes are determined by the maximum rate of roll or by the time required to reach a given angle of bank, the values of $pb/2V$ required of such airplanes may be

considerably higher than the values of $pb/2V$ considered sufficient for transport or trainer airplanes. The maneuverability of a fighter airplane near maximum speed is of course very important, but because of considerations of the airplane structure and of the control forces the values of $pb/2V$ required at high speeds cannot be as large as the values of $pb/2V$ required at moderate speeds.

For a given value of $pb/2V$, the rolling velocity p approaches zero as the airspeed approaches zero and may become very large at very high airspeeds. For autogiros or for other low-speed aircraft an additional requirement may specify that a minimum value of the product pb be obtained. For airplanes capable of very high speeds, the maximum required rolling performance may be determined by the maximum value of the rolling velocity p that is desired by the pilot.

A specification of the aileron effectiveness required for maintaining lateral trim in all flight conditions may be desirable for airplanes that might be subjected to extreme asymmetrical power conditions or for airplanes having high positive effective dihedral, which may exist at high lift coefficients when a large amount of sweepback is employed.

CONTROL FORCES

Tests of numerous airplanes have indicated that for all flight conditions the aerodynamic forces should be large enough, compared with the static friction force, to return the control stick or the control wheel approximately to neutral when it is freed and that the forces at high speeds should not be so large that the pilot is unable to attain the specified value of $pb/2V$. The type of force variation within these limits is relatively unimportant, but the force should never decrease to the value of the static friction except near the neutral control setting. It is desirable, however, that the force should continue to increase smoothly with increasing deflection. From considerations of the structural integrity of the airplane it is desirable that the control deflection at high speed be limited by control forces to values within the structural design limitations.

STICK OR WHEEL TRAVEL

In order to provide small control forces, the stick or wheel travel should be as large as possible so that a high mechanical advantage is obtained. The stick or wheel travel usually is restricted however for ease of operation or because of space limitations; that is, the lateral displacement of a control stick is limited by interference with the pilot's leg freedom or by the cockpit width, and the motion of a wheel-type control is limited to the arc through which the wheel can be turned comfortably with one hand. Large increases made in the angular travel of a control wheel to provide light control forces have been found very undesirable.

ADVERSE YAW

Adverse yaw should be considered in the requirements for lateral control because the changes in heading that accompany the use of ailerons may be annoying to the pilot, because the directional stability during steady yawed flight may be reduced when the adverse yaw is excessive, because yaw reduces the rolling velocities unless the rudder is skillfully coordinated with aileron movements, and because the rudder forces required to counteract adverse yaw may be excessive. Some flight investigations and the analysis of reference 8 have indicated that, for highly maneuverable airplanes, critical vertical-tail loads may result from rolls out of accelerated turns or pull-outs unless high sideslip angles are prevented.

As indicated by the analysis presented in reference 9 the induced adverse aileron yawing-moment coefficient is directly proportional to the lift coefficient. The critical condition for investigating aileron yaw, therefore, is near the stalling speed. Requirements for lateral control usually specify the maximum angle of sideslip resulting from the use of the lateral-control device that may be tolerated.

LAG IN RESPONSE

Any lag in time between the deflection of a control and the resulting airplane motion is objectionable to

the pilot. Lag may be dangerous, because it may cause the pilot to overcontrol the airplane. Specifications designed to eliminate lateral-control devices with objectionable lag characteristics limit the interval between the time when the lateral-control device reaches full deflection and the time when maximum rolling acceleration is attained. The permissible lag sometimes is given as a function of the speed and the size of the airplane.

CONTROL-FREE STABILITY

Although the problem of control-free stability has presented little difficulty in the design of ailerons in the past, some tendency toward instability has been exhibited by a few recent aileron designs. The problem is of greatest significance for large airplanes or for high-speed airplanes for which the ailerons may be essentially free even though the pilot has not released the control. Requirements for control-free stability specify that when the control is released after a sudden deflection, the ailerons must return to their trim positions and any oscillations must be heavily damped.

II - FACTORS INVOLVED IN THE LATERAL-CONTROL PROBLEM

LATERAL MANEUVERABILITY

Concept of Lateral Maneuverability

In the present paper the term "lateral maneuverability" is considered to involve those characteristics of an airplane in flight that affect the pilot's ability to produce a rolling velocity. This concept of lateral maneuverability therefore includes the rolling moment as affected by the rigidity of the wing-aileron structure and by adverse yaw, the damping and inertia effects of the wing and of other parts of the airplane, and the control forces that must be exerted by a pilot in order to produce a rolling maneuver.

Helix angle.- For the condition of a pure steady roll about the longitudinal wind axis, the wing-tip helix angle is given satisfactorily for conventional airplanes by the equation

$$\frac{pb}{2V} = \frac{C_l}{C_{l_p}} \tag{1}$$

in which C_l is the total rolling-moment coefficient and C_{l_p} is the damping coefficient of the airplane wing. Equation (1) neglects the damping of other parts of the airplane. Values of C_{l_p}, as determined by lifting-line theory for wings having round tips, are given in reference 9. Values of C_{l_p} with the Jones edge-velocity correction applied are presented in reference 10. A lifting-surface-theory correction to C_{l_p} was obtained in the investigation reported in reference 11. Values of C_{l_p} from reference 11 are presented in figure 1. These values are lower than the original values given in reference 9 by amounts ranging from 13 percent for wings of aspect ratio 6 to 2 percent for wings of aspect ratio 16. Values of C_{l_p} for square-tipped wings of aspect ratio 6 are about 6 percent higher than the values for round-tipped wings given in figure 1. Figure 1 has been prepared in such a manner that values of C_{l_p} can be obtained directly as functions of taper ratio and of geometric aspect ratio provided c_{l_α} is equal to 0.1. Variations in c_{l_α}, whether they are caused by changes in airfoil shape or by changes in Mach number in the subcritical speed range, influence the effective aspect ratio (see reference 12) as well as the value of C_{l_p} for a given effective aspect ratio, and these variations can be accounted for by applying the appropriate value of c_{l_α} to the abscissa and the ordinate of figure 1.

If values of C_l required for estimating $pb/2V$ are not available from test data, values of C_l as

derived from lifting-line theory may be obtained from references 1 and 9. A convenient method for estimating $pb/2V$ that avoids the separate determination of C_l and C_{l_p} is presented in reference 13. In reference 13 a helix-angle parameter γ $\left(\text{equal to } 114.6 \frac{C_{l_\delta}/\frac{\Delta\alpha}{\Delta\delta}}{C_{l_p}}\right)$ is given as a function of the spanwise location of the inboard and outboard aileron tips. For constant-percentage-chord ailerons, the parameter γ is essentially independent of the aspect ratio and the taper ratio of the airplane wing. For convenient application of the units used in the present paper, a chart of the parameter γ' $\left(\text{equal to } \frac{\gamma}{114.6}\right)$ is presented as figure 2. The values of C_{l_p} involved in both γ and γ' are the values given in reference 9. For a rigid unyawed wing not equipped with a linked tab or a spring tab

$$\frac{pb}{2V} = \gamma' \frac{\Delta\alpha}{\Delta\delta} \Delta\delta_a \qquad (2)$$

where $\Delta\delta_a$ is the total deflection (in degrees) of the right and left ailerons.

The helix angle $pb/2V$ is, of course, affected by a number of factors, the most important of which usually are wing flexibility, adverse yaw, and deflection of linked tabs or spring tabs. In preliminary design, these effects sometimes may be estimated and expressed as simple reduction factors to be applied to the value of $pb/2V$ given by equation (2). An empirical equation for use in preliminary design therefore may be written as

$$\frac{pb}{2V} = \gamma' \frac{\Delta\alpha}{\Delta\delta} \Delta\delta_a \left(1 - k_T - k_\beta - k_r - k_t\right) \qquad (3)$$

where the factors k_T, k_β, k_r, and k_t are the reductions in $pb/2V$ (expressed as fractions of the value of $pb/2V$ given by equation (2)) resulting from wing twist, sideslip, yawing velocity, and tab deflection, respectively. The factors k_T, k_β, and k_r are discussed subsequently in this section of the present

paper and the factor k_t is discussed in the section "Ailerons Having Linked Tabs, Part IV." Rough preliminary estimations of airplane rolling performance sometimes are made by assuming that

$$1 - k_T - k_\beta - k_r = 0.8$$

The substitution of this value in equation (3) has given satisfactory results near the stalling speed and at about 0.8 of the maximum level-flight speed for many airplanes. At intermediate speeds values of $pb/2V$ obtained in this manner usually are conservative.

Control force.- The control force during a steady rolling maneuver is related to the aileron hinge-moment coefficients and to the geometry of the aileron system by the equation

$$F = \frac{1}{r} q b_a \bar{c}_a^2 \left[C_{h_{a_{up}}} \left(\frac{\partial \delta_a}{\partial \theta} \right)_{up} - C_{h_{a_{down}}} \left(\frac{\partial \delta_a}{\partial \theta} \right)_{down} \right] \qquad (4)$$

where $C_{h_{a_{up}}}$ and $C_{h_{a_{down}}}$ are the hinge-moment coefficients of the aileron that is deflected upward and of the aileron that is deflected downward, respectively; and $\left(\frac{\partial \delta_a}{\partial \theta} \right)_{up}$ and $\left(\frac{\partial \delta_a}{\partial \theta} \right)_{down}$ are the mechanical advantages of the upgoing and of the downgoing aileron, respectively. In terms of slopes, for ailerons deflected equally up and down

$$F = -\frac{1}{r} q b_a \bar{c}_a^2 \frac{\partial \delta_a}{\partial \theta} \Delta \delta_a C_{h_\delta} \left(1 + \frac{2(\Delta\alpha)_p}{\Delta \delta_a} \frac{C_{h_\alpha}}{C_{h_\delta}} \right) \qquad (5)$$

where $(\Delta\alpha)_p$ accounts for the effect of the rolling velocity on the hinge-moment coefficients and $\frac{\partial \delta_a}{\partial \theta}$ is the rate of change in deflection of a single aileron with change in deflection of the control (stick or wheel). Methods for estimating $(\Delta\alpha)_p$ are given in references 10 and 11. The method of reference 11 permits

the effects of aspect ratio to be accounted for more accurately. A chart for estimating $(\Delta\alpha)_p$, based on the method of reference 11, is presented in figure 3. The factor B_1 of figure 3 is equal to the factor $\frac{A_c E_c + 2}{A_c E_c + 4}$ given in reference 11.

The quantity $\left(1 + \frac{2(\Delta\alpha)_p}{\Delta\delta_a} \frac{C_{h_\alpha}}{C_{h_\delta}}\right)$ of equation (5) frequently is referred to, particularly in British papers, as the response factor K in which the quotient $\frac{2(\Delta\alpha)_p}{\Delta\delta_a}$ usually is assumed in analytical work to be equal to -0.2 for ailerons of average size. The rolling velocity tends to reduce the aileron hinge moments when the response factor is less than 1.0 (positive value of $C_{h_\alpha}/C_{h_\delta}$) and the rolling velocity tends to increase the aileron hinge moments when the response factor is greater than 1.0 (negative value of $C_{h_\alpha}/C_{h_\delta}$). Ailerons frequently have been designed in such a manner that the rolling velocity decreases the aileron hinge moments in order to minimize the amount of aerodynamic balance required for given control forces. This advantage cannot be realized in many designs, however, because considerations associated with the aileron floating tendency in pull-outs and at high angles of sideslip may require that the values of C_{h_α} be maintained as near zero as possible.

A relation between the hinge-moment parameters for constant values of F/q can be obtained if the value of $(\Delta\alpha)_p$ for a given aileron deflection is assumed to be independent of Mach number. From equation (5) the relation is

$$C_{h_\alpha} = \frac{-r}{2b_a\bar{c}_a^2 \frac{\partial\delta_a}{\partial\theta} (\Delta\alpha)_p} \frac{F}{q} - \frac{\Delta\delta_a}{2(\Delta\alpha)_p} C_{h_\delta} \qquad (6)$$

For a given wing-aileron arrangement, therefore, lines representing constant values of F/q may be drawn on a chart in which C_{h_α} is plotted against C_{h_δ}. The

line representing the condition of zero stick force is given by the simple relation

$$C_{h_\alpha} = -\frac{\Delta\delta_a}{2(\Delta\alpha)_p} C_{h_\delta} \qquad (7)$$

Equations (4) to (7) are strictly applicable only to the steady-roll condition. An analysis of aileron control-force characteristics during initiation and reversal of an aileron roll, made by Morgan and Bethwaite in Great Britain, shows that for ailerons having positive values of the ratio $C_{h_\alpha}/C_{h_\delta}$ exceeding 2.0, objectionably high stick forces may be required for a rapid control movement even though the control forces are satisfactory during a steady roll. For most ailerons, however, the ratio $C_{h_\alpha}/C_{h_\delta}$ is considerably lower than 2.0, and the forces required for rapid control movements are not likely to present a serious problem.

Effects of Wing Twist

During a rolling maneuver, the forces resulting from aileron deflection and from wing damping may twist a wing and therefore reduce the aileron effectiveness in proportion to the torque produced. Because the aerodynamic forces increase with the dynamic pressure, the loss in aileron effectiveness also increases with the dynamic pressure. The aileron effectiveness becomes zero, therefore, at some airspeed - called the reversal speed. At speeds in excess of the reversal speed, the airplane rolls in a direction opposite to that which would be obtained for the same aileron deflections at low speeds.

The effects of wing twist on lateral maneuverability may be of considerable importance even at speeds far below the reversal speed. In an analysis presented in reference 14 the rolling performance of a P-47C-1-RE airplane was corrected for the effects of adverse yaw, as measured in flight, and for the effects of Mach number on $\Delta\alpha/\Delta\delta$, as determined from high-speed wind-tunnel tests, in order to isolate the effects of wing twist. The results of this analysis are summarized in figure 4.

At an indicated airspeed of 400 miles per hour wing flexibility is responsible for a 31-percent loss in the aileron effectiveness of the P-47C-1-RE airplane. The reversal speed is at an indicated airspeed of about 545 miles per hour. A somewhat similar analysis made by Morris and Morgan of Great Britain shows that at an indicated airspeed of 400 miles per hour the aileron effectiveness of the British Spitfire airplane is reduced by about 65 percent, principally because of wing twist.

A number of methods have been proposed for calculating the reversal speed or the effect of wing twist on the rolling performance at any speed (see references 13 to 21). These methods differ principally in the degree of accuracy with which the spanwise twist is obtained and in the extent to which the induction effects are accounted for. In addition, these methods differ in their adaptability to the inclusion of the effects of compressibility on the various aerodynamic parameters. Some of the methods (references 14, 17, 19, and 21) require that the actual wing-torsional-stiffness distribution be known, whereas in other methods the torsional stiffness is assumed to follow some simple mathematical law.

Reference 13 points out that significant differences in the torsional stiffness and in the aerodynamic parameters of wings for the same production airplane may be expected to result from differences in fabrication. Because of these uncertainties, the large amount of time required to obtain a solution by one of the most exact methods probably is not justified in the usual case.

In a method proposed in reference 13, the induced-lift effects are taken into account and the wing torsional stiffness is assumed to vary inversely as the cube of the distance from the wing center line. Charts giving values of a rolling-moment-loss parameter τ are presented in reference 13 and equations are given from which the wing torsional stiffness required to meet a given standard of rolling performance may be quickly estimated.

The values of τ given in reference 13 are dependent on the wing taper ratio and on the spanwise locations of the inboard and the outboard aileron tips. A rolling-moment-loss parameter τ' (equal to $\left(\frac{y_r}{b/2}\right)^3 \tau$, where y_r

is the distance from the wing center line to the midspan of the aileron) is roughly independent of the location of the outboard aileron tip. Values of τ' are given in figure 5.

The wing torsional stiffness required for a specified value of the helix-angle reduction factor k_τ may be computed by means of the following general equation:

$$m_{\theta_y} = \frac{1}{\left(\frac{y}{b/2}\right)^3} \frac{b^3}{2A^2 k_\tau} \left\{ \left[\tau' \left(\frac{\partial c_m}{\partial \alpha} \right)_{c_l} \right]_{\text{aileron}} - k_t \left[\tau' \left(\frac{\partial c_m}{\partial \alpha} \right)_{c_l} \right]_{\text{tab}} \right\} \frac{q}{\sqrt{1 - M^2}} \qquad (8)$$

where m_{θ_y} is the wing torsional stiffness at any spanwise station y. Values of $q/\sqrt{1 - M^2}$ for various values of $V\sigma^{1/2}$ and for various altitudes are given in figure 6. The values of $\left(\frac{\partial c_m}{\partial \alpha}\right)_{c_l}$ in equation (8) are for low Mach numbers. If experimental values of $\left(\frac{\partial c_m}{\partial \alpha}\right)_{c_l}$ have been obtained at the Mach numbers for which values of m_{θ_y} are to be computed, these values of $\left(\frac{\partial c_m}{\partial \alpha}\right)_{c_l}$ may be used in equation (8) provided the theoretical factor $\sqrt{1 - M^2}$ is deleted from equation (8). At the reversal speed, the term $(1 - k_\tau - k_\beta - k_r - k_t)$ in equation (3) is zero, and the factors k_β and k_r usually may be assumed to be zero. For a known value of m_{θ_y}, therefore, the reversal speed may be estimated by solving equation (8) for $q/\sqrt{1 - M^2}$ when $k_\tau = 1 - k_t$. If at a given speed V_1 the corresponding helix-angle reduction factor k_{τ_1} is known, the value of k_{τ_2}

corresponding to any other speed V_2 may be calculated as follows:

$$k_{T_2} = k_{T_1} \frac{\left(q/\sqrt{1 - M^2}\right)_2}{\left(q/\sqrt{1 - M^2}\right)_1} \qquad (9)$$

Effects of Control-System Stretch

For ailerons having approximately linear effectiveness and hinge-moment characteristics, the principal effect of any stretch in the control system is simply a reduction in the aileron movement, and consequently in the rate of roll, for a given control deflection. In most instances stretch results in little or no change in the mechanical advantage of the system; therefore, the control force for a given total aileron deflection remains almost unchanged. Control-system stretch may cause large changes in the control forces of ailerons having very nonlinear hinge-moment characteristics.

Effects of Adverse Yaw

Adverse yaw in a rolling maneuver results from the combined effects of an inherent yawing moment of a rolling wing and a yawing moment caused by operation of the lateral-control device. Both these yawing moments normally are adverse over the usual range of flight lift coefficients, when conventional flap-type ailerons are used. The yawing moments of spoiler-type lateral-control devices, however, may be favorable over at least a part of the flight lift-coefficient range. The yawing moment of a rolling wing is caused by an asymmetrical distribution of the drag and by inclination of the lift vectors. The drag effect usually is favorable, but the effect of inclination of the lift vectors invariably is adverse at positive lift coefficients and usually is of considerably greater magnitude than the effect of the drag.

Adverse yaw tends to retard the forward movement of the upgoing wing. When the rudder is not used to counteract the yawing moment, loss in $pb/2V$ results from the sideslip angle - for wings with positive effective dihedral - and from the yawing velocity - for wings at

positive lift coefficients. The corresponding helix-angle reduction factors k_β and k_r usually cannot be estimated accurately - particularly at low speeds - in a preliminary design. Flight tests of present-day airplanes indicate, however, that when conventional flap-type ailerons are used, the value of the sum $k_\beta + k_r$ usually is between 0.2 and 0.3 at landing speeds. If at a lift coefficient C_{L_1}, the corresponding value $\left(k_\beta + k_r\right)_1$ is known, the value $\left(k_\beta + k_r\right)_2$ at any other lift coefficient C_{L_2} may be roughly estimated from the relation

$$\left(k_\beta + k_r\right)_2 = \left(k_\beta + k_r\right)_1 \frac{C_{L_2}}{C_{L_1}} \qquad (10)$$

The effects on rolling velocity of adverse yawing moment may be decreased by increasing the weathercock stability or by decreasing the dihedral.

Weathercock stability.- Modifications that increase the weathercock stability, such as increasing the vertical-tail area, not only permit greater rates of roll to be obtained but also cause the angle of bank for constant aileron deflection to be more nearly a linear function of time (reference 22). Because an increase in vertical-tail area makes possible the performance of a given banking maneuver with decreased aileron deflection, the control forces required for the maneuver are decreased when the vertical-tail area is increased.

The advantages of increasing the vertical-tail area diminish as the vertical-tail area is increased. In conventional airplane designs, however, the vertical tail is seldom of such size that a further increase in vertical-tail area would not give beneficial results. Tests made in the Langley free-flight tunnel indicate that a value of C_{n_β} at least as high as 0.0015 usually is necessary for satisfactory flying qualities.

The effect on lateral maneuverability of changing the tail length while maintaining the same weathercock

stability, thereby increasing the damping in yaw, is shown in reference 23 to be negligible.

Dihedral.- The reduction in lateral maneuverability because of adverse yaw varies almost linearly with the effective dihedral. Poor weathercock stability, when combined with high positive effective dihedral, results in a large opposing action to any rolling motion. This combination may also cause predominance of the lateral oscillation, which is undesirable because of the resultant erratic response to the application of control and the possible discomfort to occupants of the airplane.

Because the banking motion is opposed by the effect of dihedral, increases in dihedral cause increases in the control forces necessary to perform a given maneuver. In general, the effective dihedral should be no larger than is necessary for meeting other criterions.

Effects of Aspect Ratio

Although increases in aspect ratio, while maintaining the same aileron-chord ratio c_a/c and the same aileron-span ratio $\frac{b_a}{b/2}$, may result in slight increases in $pb/2V$ the rolling velocity p will probably decrease with increases in aspect ratio because of the increased wing span required for an airplane of a given weight.

Effects of Altitude

Some of the effects of altitude on lateral maneuverability, as indicated by the analysis reported in reference 24, are summarized in figure 7 for the condition of constant true airspeed. If a lateral-control device that is capable of producing the same maximum rolling-moment coefficient throughout the altitude range is used, the time required to obtain a given angle of bank is greater at the higher altitudes. In order to obtain a given angle of bank in a given time at any altitude, larger rolling-moment coefficients must be applied at the higher altitudes. These results follow from the fact that the value of $pb/2V$ and hence the final steady value of rolling velocity is independent

of altitude, but the initial angular acceleration is reduced at high altitude because of the lower indicated airspeed. If, on the other hand, the aileron deflection is limited to that corresponding to a constant hinge moment, a given angle of bank is obtained in shorter periods of time at the higher altitudes, because greater aileron deflections can be obtained at the reduced indicated airspeed and hence the final value of rolling velocity is higher.

For airplanes having positive values of $C_{h_\alpha}/C_{h_\delta}$, the ratio of the control force required to start a rolling maneuver to the control force required to maintain the maneuver has been shown by Morgan and Bethwaite to be higher at the higher altitudes.

Effects of Radii of Gyration and Wing Loading

An analysis of the effects on lateral maneuverability of variations in the radius of gyration in roll is reported in reference 24. The analysis presented in reference 24 was made for constant wing loading; increases in radii of gyration therefore correspond to increases in moments of inertia. For a given rolling-moment coefficient, the time required to obtain a given angle of bank is increased considerably when the radius of gyration in roll is increased from 0.08b to 0.16b (see fig. 8). The percent increase in the time required to obtain a given angle of bank is greater for short banking maneuvers than for long banking maneuvers because the radius of gyration in roll affects only the acceleration period at the start of a maneuver. Additional analysis presented in reference 24 shows that, in order to obtain a 45° bank in 1/2 second with a typical fighter airplane, the rolling-moment coefficient must be increased by approximately 20 percent when the radius of gyration in roll is increased from 0.08b to 0.16b.

Increases in the radius of gyration in roll have been shown by Morgan and Bethwaite to cause small increases in the control forces required for rapid movements of ailerons having positive values of $C_{h_\alpha}/C_{h_\delta}$.

The influence on any banking maneuver of changes in the radius of gyration in yaw is negligible.

When the radius of gyration in roll is held constant, increases in the moment of inertia in roll caused by increases in wing loading result in effects similar to those obtained by increasing the radius of gyration while maintaining the same wing loading.

CONTROL-FREE STABILITY

A theoretical analysis of the stability of an airplane with ailerons free is reported in reference 25. The stability boundaries were found to be primarily a function of the hinge-moment parameters C_{h_α} and C_{h_δ}. The results of the analysis indicated that, in general, aileron-free stability is not a serious problem for a mass-balanced aileron system, which usually is provided in order to prevent flutter. For ailerons that tend to float with the relative wind (negative C_{h_α}) the only possible type of instability is a divergence or an unstable variation of control force with deflection. The divergence (or zero control force) boundary is defined by equation (7). For ailerons that tend to float against the relative wind (positive C_{h_α}), any possible aileron-free oscillations are heavily damped in a mass-balanced system and are of no practical concern unless the value of C_{h_δ} also is positive. Aileron oscillations have been observed in flight when mass-balanced systems employing ailerons that are overbalanced for small deflections and that have high positive values of C_{h_α} are used. Unbalanced mass behind the hinge line has an unfavorable effect on the damping and tends to shift the boundary for oscillatory instability into the negative range of C_{h_δ}. Ailerons requiring close aerodynamic balance therefore should be mass balanced. The presence of friction in no case causes undamped oscillations if the ailerons are otherwise stable.

FLUTTER

The flutter theory, for two-dimensional air-flow conditions, of wings equipped with conventional unbalanced

flap-type ailerons is presented in reference 26. In reference 27 the effects of the various parameters involved in the flutter problem are investigated systematically and comparisons between the theory and experimental results are made. Reference 27 also shows that three-dimensional effects usually are small. Equations for a three-dimensional solution of the flutter problem are presented in reference 28.

The air-load parameters in the flutter equations are different for balanced ailerons than for unbalanced ailerons. Solutions for the air-load parameters are obtained in references 29 and 30 for ailerons having exposed-overhang balances and in references 29 to 31 for ailerons having tabs. Rigorous solutions for the air-load parameters of ailerons having sealed internal balances have not been obtained, but a method of estimating these parameters is suggested in reference 21.

The influence of the properties of various structural materials and of the plan form and the thickness of wings on flutter characteristics is investigated in reference 32.

Theoretical flutter analyses of wing-aileron systems have been concerned primarily with types of flutter that involve the coupling of either two or three of the following motions: wing flexure, wing torsion, and aileron deflection. The wind-tunnel tests reported in reference 33 show that freedom of a wing to oscillate in a chordwise plane may permit an additional type of flutter. Another possible degree of freedom is introduced when a spring tab is used in conjunction with an aileron.

Any specific type of flutter can be eliminated for a given speed range (with the possible exception of the transonic range) by several different combinations of the various wing and aileron parameters involved in the flutter equations. Elimination of all the basic types of aileron flutter usually can be accomplished by the use of suitable mass balance. The most favorable conditions are obtained when the center of gravity of the aileron is slightly forward of the aileron hinge axis and is at the same elevation - in a direction normal to the chord - as the hinge axis. For ailerons with

spring tabs, both the aileron and the tab should be mass balanced, but as shown by Collar of Great Britain mass balance of a spring tab is favorable only when the distance between the tab hinge axis and the balancing weight is less than $\frac{c_a - c_{st}}{1 - \frac{k_1}{k_2}}$, where k_1/k_2 normally is a negative quantity and is equal to the ratio of tab deflection to aileron deflection with the control (stick of wheel) fixed. Any friction in the aileron system is favorable with regard to flutter, and sufficient friction, which makes the system essentially irreversible, may prevent the basic types of aileron flutter. The intentional use of friction to prevent flutter is not considered desirable, however, because of its adverse effects on control feel. Any slack in the aileron or tab linkage is unfavorable.

III - TESTING PROCEDURES AND APPLICATION OF EXPERIMENTAL RESULTS

In this section of the present paper, a description is given of the methods being used by the Langley Laboratory of the NACA for making flight investigations of lateral-control characteristics. A discussion also is given of some of the most common wind-tunnel test setups, of the limitations of these setups, and of the methods that are being used for applying wind-tunnel data.

FLIGHT INVESTIGATIONS

Procedure for Determining Rolling Performance

Description of maneuver.- The rolling performance of an airplane usually is determined during abrupt aileron rolls made from laterally level, trimmed, straight flight at different indicated airspeeds. Power for level flight ordinarily is used at speeds below the level-flight speed obtainable with maximum continuous

power; above this speed rolls are made during steady diving flight with maximum continuous power. The test altitude is not particularly important unless compressibility effects are involved. In a given series of tests, however, the altitude should be maintained approximately constant.

At each selected speed five rolls in each direction, with a different control deflection for each roll, usually are sufficient. A greater number of control deflections may be necessary for airplanes having very nonlinear lateral-control characteristics. At high speeds the maximum control deflection may have to be restricted in order to ensure that the aerodynamic forces on the ailerons and on other parts of the airplane do not exceed the structural design limits.

Each test roll is made by moving the control (stick or wheel) abruptly to some predetermined deflection and by holding the control at that deflection until the maximum rolling velocity occurs. Until maximum rolling velocity occurs, the rudder is held in its original trim position. Recovery from the maneuver is made by any method the pilot desires. The control should be deflected as rapidly as possible. When control forces permit, full deflection can be reached in about 0.1 to 0.2 second. The desired control deflection usually can be obtained by means of a variable-stop device attached to the stick or control wheel; however, with such an arrangement care must be exercised to ensure that the proper control forces are measured.

Variables measured.- The following variables are measured during the most general investigations for determining the rolling performance of an airplane:

Rolling velocity

Free-stream impact pressure or indicated airspeed

Rudder position

Aileron position

Stick or control-wheel deflection

Stick or control-wheel force

Aileron hinge moments

Pressure altitude

Free-air temperature

Aileron distortion

Presentation of data.- The test results may be plotted in the form of a time history, as illustrated in figure 9, for a roll with ailerons partly deflected. The maximum helix angle $pb/2V$ is computed from the maximum rolling velocity, the wing span, and the true airspeed. The values of aileron force and deflection which occur at the time of maximum rolling velocity should be used, since the steady force that the pilot will be able to hold is of primary interest. When there is a large negative value of C_{h_α} or when there is a spring-tab system with a weak spring, the maximum force and deflection as well as the force and deflection at maximum rolling velocity may have to be considered. Plots usually are made to show the variation of control force and $pb/2V$ with total aileron deflection for each of the test indicated airspeeds. Another very useful plot is one in which the total aileron deflection, the rolling velocity at some standard altitude, and $pb/2V$ are plotted against indicated airspeed for a fixed value of the control force.

When aileron hinge-moment coefficients are to be plotted, the tests should be made with the trim tab locked in one position (preferably neutral), because the variation of hinge-moment coefficient with speed may be somewhat obscured if the control force is trimmed to zero at each speed tested.

Procedure for Determining Adverse Yaw

Description of maneuver.- Tests for determining adverse yaw are made by performing abrupt rudder-fixed rolls at low speeds. The maneuver is similar to that described for determining rolling performance, except that the rolls must be continued beyond the time at which maximum rolling velocity occurs in order to reach the maximum sideslip angle before recovery is started. Because some modern airplanes with powerful ailerons may require a large change in angle of bank (90° or more) in order to reach the maximum sideslip angle for

full aileron deflection, the maneuver may be modified to allow rolls to be made out of an initially banked attitude (not exceeding 45°) in low-acceleration turns. In this maneuver the maximum sideslip angle occurs at a smaller absolute angle of bank. Rolls should be made in both directions with partly deflected ailerons as well as with fully deflected ailerons.

Variables measured.- The variables measured during a maneuver for determining adverse yaw include the sideslip angle, the normal acceleration, and the first six of the items listed in the previous section on the determination of rolling performance. The sideslip angle usually is measured by means of a freely swiveling vane mounted on its vertical axis at the end of a boom extending ahead of the airplane wing.

Presentation of data.- A time history of the important variables obtained during a maneuver for determining aileron yaw may be plotted as illustrated in figure 10. Another useful plot is one in which the maximum change in sideslip angle is given as a function of the total aileron deflection.

Procedure for Determining Aileron Trim

Changes with Speed

A complete flight investigation of lateral-control characteristics should include measurements of aileron trim changes with speed for straight, laterally level flight. These measurements are made by trimming the aileron control force to zero at level-flight speed with normal rated power and with the airplane in the clean condition, and then by measuring the aileron control forces and the aileron deflections required to trim in laterally level straight flight at various other speeds with rated power and with power off. Because the lateral position of the airplane center of gravity may have a large effect on aileron trim variations, the lateral center-of-gravity position should be determined and specified, especially if large unsymmetrical weight distributions are possible with the airplane being tested.

WIND-TUNNEL INVESTIGATIONS

Close approximations to the maneuvers that are performed during flight investigations of lateral-control

characteristics can be obtained in wind tunnels only when dynamic models are used and are permitted to fly freely. The Reynolds numbers and the model scales for such tests are necessarily very low and consequently the air-flow conditions and the structural details of the ailerons may be very different for the model than for the airplane. In the usual case, accurate simulation of the air-flow conditions and the structural details has seemed more important than accurate simulation of the flight maneuver. Wind-tunnel aileron-development programs therefore are conducted almost invariably on large static models for which high Reynolds numbers may be obtained.

Two-Dimensional Models

Ailerons frequently are investigated in two-dimensional flow because such an arrangement permits the use of the largest possible model scale for a given wind tunnel, because variables associated with wing plan form are eliminated, and because two-dimensional models are simpler and less costly than finite-span models. In spite of the fact that large Reynolds numbers can be obtained with two-dimensional models, the results of tests of such models are extremely limited in their application to specific designs. Limitations result from the inadequacy of the available methods for computing finite-span characteristics from two-dimensional data. For the most part, these methods are based on lifting-line theory, in which the following two assumptions are made:

(1) The induced downwash angle may be considered to be constant along the chord of a finite-span wing.

(2) The wing wake leaves the lifting line in a planar sheet.

Although these assumptions result in small errors in the helix angles computed from the results of tests of two-dimensional models, they result in much larger errors in the aileron hinge-moment characteristics. Computations based on lifting-surface theory (reference 34) show that the induced downwash angle may vary considerably along the chord of a finite-span wing, especially at sections near the wing tip. This variation in downwash angle results in a chordwise load in addition to the load considered by lifting-line theory. The nonlinearity of finite-span hinge-moment curves, as compared with two-dimensional hinge-moment curves, probably is a result of the rolling up of the wing-wake sheet, especially at high angles of attack and at large aileron deflections.

Equations based on lifting-line theory are given in reference 35 for computing finite-span hinge-moment parameters of full-span control surfaces from two-dimensional data. These equations may be expressed as follows:

$$\left(c_{h_\alpha}\right)_{LL} = \frac{c_{L_\alpha}}{c_{l_\alpha}} c_{h_\alpha} \tag{11}$$

$$\left(c_{h_\delta}\right)_{LL} = c_{h_\delta} - \frac{\Delta\alpha}{\Delta\delta} c_{h_\alpha}\left(1 - \frac{c_{L_\alpha}}{c_{l_\alpha}}\right) \tag{12}$$

For the evaluation of equations (11) and (12) the value of the ratio $c_{L_\alpha}/c_{l_\alpha}$ can be assumed to equal $\frac{A}{A + 2.5}$ (see reference 36). The effects of the actual span-load distributions of a wing and of a partial-span aileron are accounted for more accurately in the following equations, which were first presented in reference 37:

$$\left(c_{h_\alpha}\right)_{LL} = \frac{1}{\frac{b_a}{b/2}\bar{c}_a^2} c_{L_\alpha} \int \frac{c_{h_\alpha}}{c_{l_\alpha}} \frac{c_l}{c_L} c_a^2 d\frac{y}{b/2} \tag{13}$$

$$\left(c_{h_\delta}\right)_{LL} = \frac{1}{\frac{b_a}{b/2}\bar{c}_a^2}\left[\int c_{h_\delta} c_a^2 d\frac{y}{b/2} + \int c_{h_\alpha} \frac{\Delta\alpha}{\Delta\delta}\left(\frac{1}{c_{l_\alpha}} \frac{c_s}{c} \frac{cc_l}{c_s a} - 1\right) c_a^2 d\frac{y}{b/2}\right] \tag{14}$$

where the integrations are carried over the span of the aileron. The span-load parameters $\frac{c_l}{c_L}$ and $\frac{cc_l}{c_s a}$

(α in radians) may be obtained from references 38 and 9, respectively. Equations (13) and (14) probably give the most accurate values for the finite-span hinge-moment parameters that may be obtained by methods based on lifting-line theory; however, because of the basic limitations of the theory, the refinements of these equations do not, at the present time, seem to be worth while for preliminary design work. For most wing-aileron arrangements, values obtained from equations (13) and (14) are very close to values obtained from the simplified relations expressed by equations (11) and (12).

The effects of the chordwise variation in the downwash angle on the hinge-moment parameter C_{h_α} are evaluated for a few specific cases in reference 37. A lifting-surface-theory correction for thin airfoils is obtained in the form of an increment $\left(\Delta C_{h_\alpha}\right)_{LS}$, which can be added to the value of C_{h_α} obtained from lifting-line theory. The use of the lifting-surface-theory correction is shown in reference 37 to give values of C_{h_α} that are in good agreement with the experimental slopes - for three models - measured over small ranges of angle of attack. Since the publication of reference 37 similar satisfactory checks have been obtained for several other models. Charts from which approximate values of $\left(\Delta C_{h_\alpha}\right)_{LS}$ may be obtained for almost any finite-span control surface were prepared from data given in reference 11 and are presented in figure 11. The factor B_2 $\left(\text{given as } F/\left(c_f/c\right)^2 \text{ in reference 11}\right)$ in figure 11 depends for its value on the moment about the hinge axis of the load caused by the chordwise variation of the downwash angle and for exposed-overhang balances is a function of the chord of the control surface and of the chord of the balance. The factor B_2 for sealed internal balances depends on the completeness of the seal as well as on the chords of the control surface and of the balance. The value of B_2 for internally balanced control surfaces having chords up to 40 percent of the wing chord can be approximated from figure 11 by assuming the internal-balance chord to be equivalent to about eight-tenths of the same exposed-overhang-balance chord. The value of C_{h_α} for a

finite-span model therefore may be expressed as

$$C_{h_\alpha} = \left(C_{h_\alpha}\right)_{LL} + \left(\Delta C_{h_\alpha}\right)_{LS} \tag{15}$$

where $\left(C_{h_\alpha}\right)_{LL}$ is obtained from equation (11) or equation (13) and $\left(\Delta C_{h_\alpha}\right)_{LS}$ is obtained from figure 11.

No systematic corrections to $\left(C_{h_\delta}\right)_{LL}$ have yet been obtained for ailerons, but the available data indicate that such corrections may be as large as the corrections to $\left(C_{h_\alpha}\right)_{LL}$. No simple solution has yet been found for the problem of the nonlinearity of the hinge-moment curves of finite-span models.

Because of the inadequacy of the present theory for application to the computation of finite-span hinge-moment coefficients, corrections for the effects of finite span usually are not applied when stick forces are estimated from two-dimensional data; consequently such computations generally are considered to be of value only for comparing the effects of modifications to a given aileron.

In the estimation of stick forces and rates of roll the two-dimensional lift and hinge-moment data may be plotted either against aileron deflection or against angle of attack. The wing lift coefficient of the airplane must be computed for the flight speed for which stick-force computations are to be made. From this value of wing lift coefficient the section lift coefficient and the corresponding section angle of attack, at the midspan of the aileron, can be estimated from the theoretical span-load distribution for the condition of zero rolling velocity.

The airplane control force is computed from the section hinge-moment coefficients at specified deflections of the upgoing and downgoing ailerons. The values of the hinge-moment coefficients should be taken at the angle of attack for zero rolling velocity corrected by

an increment $(\Delta\alpha)_p$ (from fig. 3) to account for the effect of the rolling velocity. The control force is computed from the equation

$$F = \frac{1}{r} q b_a \bar{c}_a^2 \left[(c_{h_a})_{up} \left(\frac{\partial \delta_a}{\partial \theta} \right)_{up} - (c_{h_a})_{down} \left(\frac{\partial \delta_a}{\partial \theta} \right)_{down} \right]$$

The helix angle pb/2V may be estimated for the rigid unyawed wing from the equation

$$\frac{pb}{2V} = \gamma' \Delta\alpha$$

where the value of γ' for the particular wing-aileron arrangement is obtained from figure 2. The value of $\Delta\alpha$ is obtained from the two-dimensional lift data and is the change in angle of attack that results in a change in section lift coefficient equal to the change caused by the total aileron deflection for which the stick force is estimated.

Finite-Span Models

For equal test Reynolds numbers, results obtained from tests of finite-span models are considered to be much more reliable than results obtained from tests of two-dimensional models. In order to obtain high Reynolds numbers in tests of finite-span models, aileron investigations frequently are made on models that represent only the outer panels of airplane wings. A model of this type usually is mounted in such a manner that one wall of the wind tunnel may serve as a reflection plane at the root section of the model. The model scale for a given wind tunnel, therefore, may be more than twice as large as the scale for a complete model. The large model scale available allows accurate simulation of most of the structural details of the airplane wing panel. A disadvantage of tests of partial-span models results from the fact that large corrections (especially to the rolling-moment coefficients) must be applied in order to make the wind-tunnel data applicable to free-air conditions.

Wind-tunnel tests have been made of full-scale outer wing panels of actual airplane construction. For wind tunnels that are not large enough to accommodate complete full-scale airplanes, tests of this type present the only possibility for a wind-tunnel model to simulate accurately an airplane wing panel while under aerodynamic load. The results of such tests are very useful.

Data obtained from aileron investigations on partial-span wing models usually are analyzed by estimating the airplane stick forces and helix angles in steady rolls. When aileron investigations are conducted on complete airplane models, the static lateral-stability parameters as well as the aileron characteristics may be determined. Such data sometimes are analyzed by estimating the airplane rolling and yawing velocities as functions of time after the ailerons have been deflected. Good agreement with the actual rolling and yawing velocities, as measured in flight, have been obtained when the computation methods of reference 39 have been used.

A method for estimating airplane helix angles and stick forces from wind-tunnel data on tests of static models is given in reference 11. This method may be applied most conveniently when the increments of rolling-moment coefficients caused by aileron deflection and the aileron hinge-moment coefficients are plotted against angle of attack. Equations (1) and (4) are used in the computations. For a given indicated airspeed, values of C_l and C_{h_a} for the upgoing and the downgoing ailerons are taken at angles of attack corresponding to the indicated airspeeds but corrected by an amount $(\Delta\alpha)_p$ (from fig. 3) to account for the rolling velocity. Because the value of $(\Delta\alpha)_p$ depends on the total rolling-moment coefficient, which, in turn, depends to some extent on the angle of attack of the parts of the wing over which the ailerons extend, values of $(\Delta\alpha)_p$ are determined most accurately as a result of a series of successive approximations. In the usual case two approximations are sufficient.

IV - CHARACTERISTICS OF LATERAL-CONTROL DEVICES

CONVENTIONAL FLAP-TYPE AILERONS

The most common lateral-control device of present-day airplanes is the conventional flap-type aileron. The popularity of this device results principally from its simplicity, from the fact that the response to aileron deflection is almost instantaneous, and because the rolling moments and the hinge moments usually are approximately linear functions of the aileron deflection. Disadvantages result from the unfavorable yawing moments, from the pitching moments that tend to twist the wing in a manner that reduces the rate of roll, from the difficulties involved in providing the proper amount of aerodynamic balance, and from the necessity for limiting the spans of conventional high-lift flaps.

The characteristics of flap-type ailerons have been studied extensively with the object of obtaining designs that require minimum amounts of aerodynamic balance in order to obtain given rates of roll with given control forces. Analysis presented in reference 1 indicates that, in this respect, ailerons having long spans and narrow chords have an advantage over ailerons having short spans and wide chords. An additional advantage is obtained if the ailerons are designed in such a manner that the aileron chords increase, rather than decrease, as the outboard tip is approached (see reference 40).

In order to allow the greatest possible span of the high-lift device, short wide-chord ailerons are desirable. Flight tests (reference 41) of ailerons having chords equal to 40 percent of the wing chord indicated that these ailerons were unsatisfactory because, during sideslip, large control forces had to be applied in order to prevent the forward wing from "digging in" and thus overcoming the dihedral effect. This characteristic is associated with a tendency for the ailerons to float with the wind and therefore is alleviated by the use of a balancing device that reduces this floating tendency.

A common arrangement for reducing aileron control force has involved the combination of a strong upfloating tendency with a differential aileron linkage that permits greater up-aileron deflections than down-aileron deflections. Fixed tabs, deflected downward, sometimes are used in order to increase the upfloating tendency. Arrangements of this kind are discussed in detail in reference 1. A disadvantage of such arrangements results from the fact that the upfloating tendency usually is greatest at the lowest speeds and, consequently, the greatest effect on the control forces occurs at the lowest speeds. A design that gives acceptable control forces at high speeds therefore may give overbalance at low speeds.

A means for decreasing the variation of control force with speed is indicated by an arrangement involving the combination of a downfloating tendency with a differential linkage that permits greater down-aileron deflections than up-aileron deflections. The practicability of this arrangement has not yet been established, however, by flight tests.

The pertinent results of a number of wind-tunnel investigations of balanced ailerons were collected and are published as reference 42. A second collection (reference 43) was made of wind-tunnel data that are more nearly applicable to airplane-tail control surfaces. Because the balances used on tail control surfaces are essentially the same as the balances used on ailerons, the data from both collections, as well as some data on ailerons and tail control surfaces obtained since the publication of these collections, have been used in most of the present analysis. More accurate evaluation of the effects of such parameters as aspect ratio and aileron chord is believed to have been obtained from the use of the two sets of data than would have been obtained from the use of aileron data alone. The correlations presented in this section of the present paper therefore should be applicable to tail control surfaces as well as to ailerons, except when an indication is given that only aileron data have been used.

Data on control surfaces with beveled-trailing-edge balances, sealed internal balances, exposed-overhang balances, and tabs had been correlated previously, and the results are published as references 44, 45, 46, and 47, respectively. The published correlations have been modified for presentation in the present paper when simplifications could be made or when additional data

permitted more accurate evaluations of some of the geometric parameters. For the most part, the correlations apply only to the small ranges of angle of attack and of aileron deflection over which the characteristics are linear. Estimates of characteristics at large angles of attack and at large aileron deflections can be made by means of the test data of reference 42.

Because the characteristics of some ailerons are extremely sensitive to Mach number or to any condition that affects the boundary layer, the correlations have been derived from data that were obtained under approximately the same test conditions. The data that have been correlated were obtained at low Mach numbers and under conditions for which transition from laminar to turbulent flow could be expected to occur quite far forward on the airfoils. The effects of Mach number, Reynolds number, surface roughness, and air-stream turbulence are discussed under the heading "Effects of Air-Flow and Wing-Surface Conditions, Part IV." Because of a scarcity of test data only qualitative or rough quantitative evaluations of these effects may be made. The methods presented herein therefore are not considered to be sufficiently reliable to enable a designer to arrive at a satisfactory final aileron configuration without some development work in flight or on a large-scale wind-tunnel model. The methods are useful, however, for making preliminary designs or for deciding the manner in which existing ailerons should be modified in order to obtain desired changes in characteristics.

In most cases the hinge-moment parameters of balanced ailerons may be estimated most conveniently by considering the plain aileron and the effect of the balance, separately, as follows:

$$\left(c_{h_\alpha}\right)_{\substack{\text{balanced}\\\text{aileron}}} = \left(c_{h_\alpha}\right)_{\substack{\text{plain}\\\text{aileron}}} + \left(\Delta c_{h_\alpha}\right)_{\text{balance}} \tag{16}$$

$$\left(c_{h_\delta}\right)_{\substack{\text{balanced}\\\text{aileron}}} = \left(c_{h_\delta}\right)_{\substack{\text{plain}\\\text{aileron}}} + \left(\Delta c_{h_\delta}\right)_{\text{balance}} \tag{17}$$

The value of C_{h_α} for the plain aileron may be calculated from equation (15) when the two-dimensional parameter c_{h_α} for the plain aileron is known. The value of C_{h_δ} for the plain aileron should be estimated from available data (such as that of reference 42) on a finite-span model having approximately the same wing plan form, relative aileron span, aileron chord, and trailing-edge angle as the proposed arrangement. Variations in trailing-edge angle seem most important, but these may be accounted for with fair accuracy by means of a correlation of the effects of trailing-edge angle on C_{h_δ}.

Equations (16) and (17) are well adapted for application of the available correlations of the effects of aerodynamic balances on aileron hinge-moment parameters. The greater part of the data used in deriving the correlations was obtained from tests of finite-span models. Variations in aspect ratio are accounted for by empirical aspect-ratio correction factors. The correlations therefore are considered to be more reliable when applied to finite-span models than when applied to two-dimensional models.

Plain Ailerons

The term "plain aileron" as used herein includes any conventional flap-type aileron, regardless of contour, that is not equipped with any form of overhang balance, tab balance, or external balance.

Hinge-moment characteristics.- The hinge-moment characteristics of ailerons have been found to be critically dependent on the aileron contour near the trailing edge. Ailerons on airfoils without cusped trailing edges, such as those having the thickness distribution defined in reference 48, usually require considerably less overhang or tab balance than ailerons on airfoils having cusped trailing edges. In general, any increase in trailing-edge angle, whether obtained by changing the basic airfoil section or by modifying the contour of a given airfoil section, may be expected to reduce the degree of unbalance of the plain aileron. The greatest balancing effect of a large trailing-edge angle occurs at small angles of attack and at small

aileron deflections; therefore, the hinge-moment curves of ailerons having large trailing-edge angles usually are characterized by a high degree of nonlinearity.

An explanation of the balancing effect resulting from the use of a large trailing-edge angle can be made on the basis of an effective change in airfoil camber. As an approximation, the effective contour of an airfoil in a viscous fluid is the contour obtained by adding the boundary-layer-displacement thickness at each airfoil surface to the geometric ordinates of that surface. Changes in angle of attack or in aileron deflection cause increases in the boundary-layer-displacement thickness on the surface of the airfoil where the pressure gradient becomes more adverse and cause decreases in the boundary-layer-displacement thickness on the surface of the airfoil where the pressure gradient becomes less adverse. These changes in boundary-layer-displacement thickness cause changes in the effective camber of the airfoil which, in turn, cause reductions in the incremental aileron lift and hinge moment for given changes in angle of attack and in aileron deflection. Changes in camber near the trailing edge are much more important with regard to hinge moments than with regard to lift, and the magnitudes of such camber changes seem to depend to a large extent on the trailing-edge angle, the greater changes occurring for the larger trailing-edge angles. An open gap at the nose of an aileron allows the boundary-layer air to flow from the high-pressure airfoil surface to the low-pressure airfoil surface. The effective change in camber and consequently the effect of the boundary layer on the hinge moments, particularly for ailerons having large trailing-edge angles, therefore are greater when the gap is open than when the gap is sealed.

When an aileron is beveled, dimensions other than the trailing-edge angle affect the hinge-moment characteristics, but the principal effects of such dimensions seem to be on the ranges of angle of attack and of aileron deflection over which the increased trailing-edge angle is most effective in changing the hinge-moment slopes. Ailerons having bevels of large chords (25 to 40 percent of the aileron chord) and large radii of curvature between the bevels and the parts of the ailerons forward of the bevels usually are more satisfactory than ailerons having bevels of small chords and small radii of curvature.

The trailing-edge angles of various true-contour and straight-sided airfoils have been plotted against the airfoil thickness in figure 12. The straight-sided airfoils considered are those having the rear parts of their contours formed by straight lines drawn from the trailing edge tangent to the true airfoil contour. For all airfoils the trailing-edge angle is defined arbitrarily as the angle between lines drawn from the airfoil surfaces at the trailing edge to the airfoil surfaces at about 0.98c.

For most finite-span ailerons, the trailing-edge angle varies along the aileron span. An effective trailing-edge angle for such an aileron can be considered to be the constant trailing-edge angle for which the parameters c_{h_α} and c_{h_δ} would be the same as for the variable trailing-edge angle. Such an effective trailing-edge angle $\bar{\phi}$ can be determined approximately by the following expression

$$\bar{\phi} = \frac{1}{b_a \bar{c}_a^{\,2}} \int_{y_i}^{y_o} \phi c_a^{\,2} \, dy \qquad (18)$$

The hinge-moment parameters c_{h_α} and c_{h_δ} for true-contour, bulged, beveled, and straight-sided sealed ailerons on various two-dimensional models are plotted against the trailing-edge angle in figure 13. Some additional information on the models from which these data were obtained is given in table II. Aileron chords of 0.15c, 0.20c, 0.30c, and 0.40c are considered. This correlation is useful for obtaining rough estimates of the values of the two-dimensional hinge-moment parameters of plain ailerons provided the aileron chord and the trailing-edge angle are known. The hinge-moment parameters seem to increase almost linearly as the trailing-edge angle is increased from 6° to about 30°. A further increase in trailing-edge angle is not likely to produce much additional balance. Within the linear range, the incremental changes in section hinge-moment parameters appear to vary with the incremental change

in trailing-edge angle approximately in accordance with the following relations:

$$\Delta c_{h_\alpha} = 0.0005\ \Delta\phi \qquad (19)$$

$$\Delta c_{h_\delta} = 0.0004\ \Delta\phi \qquad (20)$$

The effect of a gap on the hinge-moment parameters is shown in figure 14 for a 0.30c plain aileron with various trailing-edge angles. For the airfoil considered (NACA 0009) the hinge-moment characteristics are almost unchanged by a gap at the nose of a true-contour aileron. For a trailing-edge angle larger than that of the true-contour aileron, the gap causes both c_{h_α} and c_{h_δ} to become less negative. The variation with trailing-edge angle of c_{h_α} is about 20 percent greater and the variation with trailing-edge angle of c_{h_δ} is about 50 percent greater when the gap is 0.005c than when the gap is sealed. The magnitude of the effect of gap may vary considerably on different airfoils, but the trends indicated in figure 14 are typical of most of the airfoils that have been investigated. The greatest effect of the gap usually is at small angles of attack and at small aileron deflections. The hinge-moment curves therefore may be expected to be more nonlinear with the gap open than with the gap sealed.

Extrapolation of the curves of figure 14 through small trailing-edge angles indicates that opening the gap may make c_{h_α} and c_{h_δ} more negative. This effect has been observed on airfoils with cusps, but the effect may be considerably greater than that indicated by figure 14, especially for thick airfoils if the maximum thickness is relatively far back.

The effects of changing the trailing-edge angles of five finite-span models (see table II) are given in figure 15. The incremental changes in c_{h_α} and c_{h_δ} are plotted against the product of an aspect-ratio correction factor and the incremental change in trailing-edge angle $\frac{A}{A+2}\Delta\phi$. The finite-span data are in fair

agreement with curves having the slopes obtained in the correlation of two-dimensional data (equations (19) and (20)). The equations of the correlation curves for finite-span models are as follows:

$$\Delta C_{h_\alpha} = 0.0005 \frac{A}{A + 2} \Delta\emptyset \qquad (21)$$

$$\Delta C_{h_\delta} = 0.0004 \frac{A}{A + 2} \Delta\emptyset \qquad (22)$$

The aspect-ratio correction factor $\frac{A}{A + 2}$ as used herein is strictly an empirical factor and was chosen simply for convenience and because its use brings the available data on the incremental hinge-moment slopes into fair agreement, regardless of the aspect ratio of the model. This factor also has been found applicable to the effects of plain-overhang and internal balances on both C_{h_α} and C_{h_δ}.

Lift characteristics.- Modifications that affect the hinge-moment parameters of plain ailerons generally have some influence on the lift parameters. The effect of the trailing-edge angle on the lift-curve slope, relative to the lift-curve slope obtained by extrapolating to zero trailing-edge angle, is given in figure 16. The effect of a gap also is expressed in a ratio form in figure 17. Although the effect of the gap was expected to be greatest for the most forward positions of the gap, no systematic variation could be detected within the range of aileron chords investigated.

A correlation of the available data on aileron effectiveness is published as reference 54, which shows that, by the use of the section aileron effectiveness factor, the aileron rolling-moment coefficients may be computed with sufficient accuracy by the methods of lifting-line theory. An analysis of the effects of aileron modifications on the rolling-moment coefficients therefore reduces to an analysis of the effects of these modifications on the section aileron effectiveness factor.

Some of the faired correlation curves of reference 54 are reproduced in figure 18. Curves are given

for large and small aileron deflections and for sealed and open gaps. The data used in obtaining these curves are for low Mach numbers and for a small range of trailing-edge angle, the average trailing-edge angle being about 10°. Data also are given in reference 54 on the variation of the effectiveness factors with trailing-edge angle as determined from tests of several airfoils. These data are replotted in figure 19 as ratios of the effectiveness factor at the various trailing-edge angles to the effectiveness factor at a trailing-edge angle of 10°. The effectiveness factor of an aileron with a given chord and trailing-edge angle may be estimated by multiplying the value obtained from figure 18 by the appropriate ratio obtained from figure 19.

Pitching-moment characteristics.- An analysis of the pitching-moment characteristics - in terms of the the parameter $\left(\partial c_m/\partial \alpha\right)_{c_l}$ - of plain ailerons having various chords is presented in reference 55. A correlation of the effects of trailing-edge modifications on the pitching-moment parameter $\left(\partial c_m/\partial \delta_a\right)_{c_l}$ is given in reference 56. The parameters $\left(\partial c_m/\partial \alpha\right)_{c_l}$ and $\left(\partial c_m/\partial \delta_a\right)_{c_l}$ are related to each other by the expression

$$\left(\frac{\partial c_m}{\partial \alpha}\right)_{c_l} = -\frac{\left(\frac{\partial c_m}{\partial \delta_a}\right)_{c_l}}{\left(\frac{\Delta \alpha}{\Delta \delta}\right)}$$

This relationship, the pitching-moment data of references 55 and 56, and values of the parameter $\Delta\alpha/\Delta\delta$ obtained from figures 18 and 19 have been used to construct curves giving values of the parameter $\left(\partial c_m/\partial \alpha\right)_{c_l}$ for various aileron-chord ratios and for various trailing-edge angles (fig. 20). Values of the parameter $\left(\partial c_m/\partial \alpha\right)_{c_l}$ are directly proportional to values of the wing torsional stiffness required for a given reduction in $pb/2V$ resulting from wing twist. (See equation (8).) Figure 20 indicates that reductions in the required wing

torsional stiffness may be obtained by increasing the aileron-chord ratio c_a/c or by increasing the trailing-edge angle ϕ.

A correlation of the effects of trailing-edge modifications on the airfoil aerodynamic-center location, indicated by the parameter $\left(\partial c_m/\partial c_l\right)_{\delta_a}$, is given in reference 56. The trailing-edge angle and the airfoil thickness at 0.9c were used as parameters in obtaining that correlation, the results of which are summarized in figure 21. In general, when the trailing-edge angle is increased, the airfoil aerodynamic center moves forward.

Flight tests.- The effects of aileron contour modifications were investigated in flight during an aileron development program for the XP-51 airplane. The original ailerons for this airplane were sufficiently effective per unit deflection, but because of small aileron travel $\left(\delta_{a_{max}} = \pm 10^\circ\right)$ the maximum effectiveness at level-flight speeds was fairly low. The ailerons were very satisfactory, however, at diving speeds because with the high mechanical advantage of this airplane almost full aileron deflection was possible without excessive stick forces.

The purpose of the development program was to obtain an aileron design that would permit the use of an increased deflection range, particularly at the level-flight speeds, without increasing the stick forces. In order to reduce the aileron hinge moments at the higher deflections, the aileron profile was thickened and beveled at the trailing edge to give an average trailing-edge angle of 25°. (See fig. 22.) Flight tests of this aileron were made with the aileron linkage altered to give maximum aileron deflections of ±20° with the original maximum stick travel. The aileron nose gap was unsealed for these tests.

A comparison of the results of flight tests of the original and the modified ailerons is shown in figure 22. Both sets of ailerons were equipped with balancing tabs. At indicated airspeeds less than 300 miles per hour the helix angle $pb/2V$ obtainable with a 50-pound stick force was approximately doubled by changing from the original to the modified ailerons. For a 50-pound stick

force the deflections of the modified ailerons that were obtainable were considerably reduced at diving speeds, but because the deflections still were greater than ±10°, the helix angle was always higher than the helix angle obtainable with the original ailerons.

During the course of the investigation, ailerons having trailing-edge angles of 32° also were investigated. These ailerons were overbalanced for small deflections, but for large deflections, the stick forces were about the same as the stick forces for the ailerons with trailing-edge angles of 25°. Sealing the nose gap reduced but did not entirely eliminate the overbalance for small deflections. At an indicated airspeed of 320 miles per hour, a condition for which the ailerons were overbalanced, a free-control oscillation of the sealed ailerons was recorded when the control stick was deflected and then released. A time history, shown in figure 23, indicates that the aileron oscillated steadily between 7° and -10° with a period of about 0.5 second. Similar oscillations could not be induced at lower speeds. No oscillations were experienced under any conditions with the ailerons that had trailing-edge angles of 25°.

Ailerons Having Exposed-Overhang Balances

Hinge-moment characteristics.- The addition of an exposed-overhang balance (either plain or Frise) to the nose of a plain aileron results in a balancing effect, because changes in pressure caused by changes in angle of attack or aileron deflection are permitted to act on a part of the movable surface that is ahead of the hinge line and because additional balancing pressures are produced over the overhang as it protrudes into the air stream.

Correlations of the effects of plain-overhang and Frise balances on the hinge-moment parameters C_{h_α} and C_{h_δ} have been made on the basis of three empirical factors, each of which is related to some physical property of the wing-aileron arrangement. An aspect-ratio correction factor $\frac{A}{A+2}$ performs the same function

as the lift-curve-slope factor used in reference 46. A factor F_1, which is related to the overhang length, is defined as follows:

$$F_1 = \left[\left(\frac{\bar{c}_b}{\bar{c}_a}\right)^2 - \left(\frac{t/2}{\bar{c}_a}\right)^2\right]\frac{b_b}{b_a}$$

A factor F_2', which is related to the nose shape of the balance, is in general the product of an area-moment ratio and a basic nose-shape factor F_2, where F_2 is defined by the expression

$$F_2 = 1 - \sqrt{1 - \left(\frac{1 + \bar{c}_{b_1}/\bar{c}_a}{1 + \bar{c}_b/\bar{c}_a}\right)^2}$$

The general expression for the nose-shape factor F_2' for each of the various nose types considered is given in figure 24. The symbols M_O, M_B, M_C, and so forth that appear in the area-moment ratios (fig. 24) refer to moments about the aileron hinge axis of the profile areas of exposed-overhang balances of types corresponding to the subscripts O, B, C, and so forth. The balance profile area is defined as the total profile area of the aileron ahead of the hinge axis. For any balance having a nose shape formed by circular arcs (nose types O, A, B, D, and G of fig. 24)

$$F_2' = F_2$$

Charts for determining F_1 and F_2 are given in figure 25.

Correlations of the incremental effects of plain-overhang and Frise balances on the hinge-moment parameters C_{h_α} and C_{h_δ} are presented in figure 26. Some additional information regarding the models considered is given in table III. The increment ΔC_{h_δ} is expressed

as a function of the three factors $\frac{A}{A+2}$, F_1, and F_2', but the increment ΔC_{h_α}, being relatively independent of the nose shape, is expressed as a function of only $\frac{A}{A+2}$ and F_1. The equations of the correlation curves are as follows:

$$\Delta C_{h_\alpha} = 0.017 \frac{A}{A+2} F_1 \qquad (23)$$

$$\Delta C_{h_\delta} = 0.10 \frac{A}{A+2} F_1 F_2' \qquad (24)$$

The correlation of ΔC_{h_δ} for Frise balances does not necessarily apply at zero aileron deflection but does apply to the negative range of aileron deflection where the effect of the balance is greatest. In the positive range of aileron deflection, Frise balances have almost no effect on aileron hinge moments.

The data used in the correlation of ΔC_{h_δ} of figure 26 were obtained from finite-span aileron models and from two-dimensional models, but the data used in the correlation of ΔC_{h_α} were obtained only from tests of finite-span aileron models. When compared on the basis of the same correlation factors, the available two-dimensional data on ΔC_{h_α} were in poor agreement with the finite-span data. The available data on finite-span tail control surfaces indicate that for such surfaces the incremental slopes ΔC_{h_α} and ΔC_{h_δ} that are attributable to a given overhang balance are about 30 percent greater than the incremental slopes indicated by figure 26.

Charts for estimating the required length of overhang for balances having several representative nose shapes are presented in figure 27. For a given design problem, the value of the product F_1F_2' corresponding to the required value of ΔC_{h_δ} must first be obtained from the correlation presented in figure 26. The value of $\bar{c}_b/\bar{c}_a$ required for this value of F_1F_2' may then be estimated from figure 27 for any of the nose shapes considered. The charts given in figure 27 were derived

for ailerons on airfoils having the thickness distribution defined in reference 46. These charts may be used, however, to obtain first approximations to the required overhangs for ailerons on airfoils having other thickness distributions. For such airfoils, more reliable values for the required overhangs can be obtained by calculating the value of the product F_1F_2' corresponding to the first-approximation value of $\bar{c}_b/\bar{c}_a$ from the expressions given in figure 24 for F_2' and the charts of figure 25 for F_1 and F_2. If the calculated value of F_1F_2' does not agree with the required value obtained from figure 26, a new value of $\bar{c}_b/\bar{c}_a$ must be assumed and the process repeated until satisfactory agreement is obtained between the required and the calculated values of F_1F_2'.

Critical deflection.- The deflection range of ailerons having exposed-overhang or Frise balances usually must be restricted within limits defined by some critical deflection $\delta_{a_{cr}}$, beyond which the overhang ceases to have a favorable effect on C_{h_δ} and the lift ceases to increase linearly with deflection. In an analysis reported in reference 46, an attempt was made to correlate $\delta_{a_{cr}}$ with the product F_1F_2', which was used in the correlation of ΔC_{h_δ}. The correlation was not satisfactory, however, because $\delta_{a_{cr}}$ seemed to be influenced much more strongly by the nose shape than by the overhang length, and smaller values of $\delta_{a_{cr}}$ usually were obtained for rearward locations of the maximum airfoil thickness than for forward locations of the maximum airfoil thickness. A somewhat better correlation of $\delta_{a_{cr}}$ (see fig. 28) was obtained in reference 46 in terms of the factor $\frac{F_2'\sqrt{F_1}}{1 - l^2}$, where l is the distance (as a fraction of the wing chord) from the minimum pressure point for the basic airfoil pressure distribution to the airfoil leading edge. For the plain overhangs of figure 28, the values of $\delta_{a_{cr}}$ were somewhat larger numerically for negative deflections

than for positive deflections because most of the airfoils considered were cambered. Although the test values are somewhat scattered from the faired curves, the given relation should be sufficiently reliable to serve as a rough guide in preliminary design work or to make estimates of the change in $\delta_{a_{cr}}$ that might be expected to result from minor modifications to the overhangs or most shapes of balances already in use.

Increases in the critical deflection $\delta_{a_{cr}}$ may be expected to result from increases in the aileron-balance nose radii, from decreases in the balance chord, and from forward movements of the airfoil minimum pressure point. Other means for changing the critical deflection are available, however. Appreciable increases in $\delta_{a_{cr}}$ of exposed-overhang balances have been obtained by equipping the balance nose with a slat or a slot or by bulging the surfaces of the control near the hinge line. With the possible exception of the addition of the slot or the slat, however, any known modification that results in an increased value of $\delta_{a_{cr}}$ reduces the aerodynamic balance for small deflections.

Effectiveness.- The lift-effectiveness parameter $\Delta\alpha/\Delta\delta$ is changed somewhat by an overhang balance and the magnitude of the change is dependent on the gap at the balance nose. A correlation of these effects is given in reference 46 and the faired curves of that correlation are reproduced in figure 29. The value of $\Delta\alpha/\Delta\delta$ increases as the balance (defined by the product F_1F_2') is increased and the rate of increase is greater for the larger gaps. For the sealed-gap condition the increase in $\Delta\alpha/\Delta\delta$ with increased aileron balance results from an increase in c_{l_δ}, whereas, for highly balanced ailerons, the increase in $\Delta\alpha/\Delta\delta$ with increased gap size is caused primarily by a decrease in c_{l_α}. The values given in figure 29 are applicable only to small deflections, and because of the reduction with increased balance of the critical deflection $\delta_{a_{cr}}$, the maximum lift increment of a highly balanced aileron usually is considerably less than the maximum lift increment of the corresponding plain aileron.

Design considerations.- A given value of ΔC_{h_δ} usually can be obtained by many variations of balance length and nose shape, ranging from rather short and blunt balances to longer balances with sharp or medium noses. The increment ΔC_{h_α} is relatively independent of nose shape, particularly for sealed balances. By careful selection of the overhang and the nose shape, therefore, many combinations of values of C_{h_α} and C_{h_δ} can be obtained.

The fact that $\delta_{a_{cr}}$ varies approximately as $F_2' \sqrt{F_1}$, whereas ΔC_{h_δ} varies as $F_1 F_2'$, indicates that for the same degree of balance a larger increment of lift probably can be obtained from an aileron having a long overhang and a moderate nose shape (type B, C, or D of fig. 24) than from an aileron having a short overhang and a blunt nose shape (similar to type A).

Other considerations impose limitations on the most desirable length of overhang. A long overhang requires that a large part of the fixed structure of the wing be cut away to allow free movement of the balance. The large breaks in the airfoil surface that result from the use of medium or sharp nose shapes have been found to increase the drag.

A nose shape of type C if designed for slight underbalance at low deflections may give overbalance at moderately large deflections, because the peak negative pressure over the protruding balance moves forward and increases in magnitude as the aileron deflection approaches the critical value. All the pointed nose shapes (types D, E, or F) show a greatly increased balancing effect when the nose protrudes above or below the airfoil contour, unless the air flow already has separated from the aileron at that deflection. This condition normally should be avoided by restricting the available aileron deflection.

The Frise type of aileron balance was developed as a possible means for increasing the profile drag of the upgoing aileron, and therefore, for reducing the adverse yawing moment. This property cannot be

realized with most airplanes, however, because almost no increase in profile drag is obtained until the air flow separates from the protruding nose. A small amount of flexibility in the control system may cause severe aileron shake when the aileron is near the deflection at which separation begins. At higher deflections the aileron may be stable, but the hinge moments usually are excessive and the lift effectiveness is reduced.

A disadvantage of the Frise balance results from its ineffectiveness for reducing hinge moments at positive aileron deflections. Frise ailerons may have to be overbalanced for negative deflections, therefore, in order to reduce the net hinge moments of the two ailerons to values that can be handled by the pilot. This condition causes the stresses in the aileron linkage system to be much higher than they would be for a balance that is equally effective for positive and negative deflections. High stresses in a flexible control system not only aggravate the tendency to shake, but may allow an aileron to be "snatched" to a large negative deflection during certain critical airplane maneuvers, as, for example, a roll while pulling out of a high-speed dive.

Flight tests of Frise ailerons.- An investigation was conducted on the XP-40-1 airplane to determine means of alleviating the aileron shake that occurred at moderate negative deflections. The original ailerons and a number of modified ailerons were tested. The various aileron profiles are shown in figure 30, together with a tabulation of some of the important aileron characteristics. The modifications consisted principally of bulging the lower surface or of adding a slat at the lower surface of the balance nose. Either of these modifications was found to reduce the shake, but the bulged ailerons, when used with the original differential linkage, were unsatisfactory because they required excessive control forces. The aileron with a nose slat at an angle of 32° seemed most satisfactory, because the shake was almost entirely eliminated, the stick forces at high deflections were reduced, and the maximum value of $pb/2V$ was increased.

An aileron development program for the P-47C-1-RE airplane was undertaken not only to reduce the aileron shake, but also to reduce the aileron stick forces at large aileron deflections. The original ailerons (fig. 31)

for this airplane had very small radii of curvature at the balance noses, and although the stick forces were very light for small aileron deflections, flow separation from the balance nose caused very high stick forces at large aileron deflections. Modified ailerons (fig. 31) having increased nose radii and increased balance chords were designed and were tested in flight. Preliminary tests showed that these ailerons tended to overbalance when used with the original linkage (maximum deflections of -16° and 12°). Tests made with the linkage arrangement changed to give maximum deflections of ±15° indicated that, although the available $pb/2V$ was increased, the stick forces were heavier than with the original ailerons. A Republic differential unit, which gives a higher mechanical advantage for small deflections than for large deflections, was then installed. Comparisons of the characteristics of this aileron arrangement with the characteristics of the original ailerons are given in figure 31. Because of the greater available deflection range, the modified ailerons were more effective at low speeds than the original ailerons, but at an indicated airspeed of 400 miles per hour, the value of $pb/2V$ obtainable with 50 pounds stick force was greater for the original ailerons. Decreasing the maximum deflections of the modified ailerons to ±13.4° caused these ailerons to be more effective than the original ailerons throughout the speed range. No aileron shake was reported during tests of the modified ailerons.

The fact that control-system stretch may have a large effect on stick-force characteristics was shown during tests of a P-40F airplane equipped with highly balanced Frise ailerons linked for maximum deflections of ±24°. The aileron profile and a comparison between forces measured for the actual elastic control system and forces computed for an assumed rigid system are presented in figure 32. As in many Frise aileron systems, the ailerons tested were overbalanced for negative deflections and were underbalanced for positive deflections. Because of control-system stretch, therefore, the positive deflections generally were smaller and, before flow separation had occurred, the negative deflections generally were greater than the deflections that would be obtained for the same stick position with a rigid control system. The air flow separates from the nose of the upgoing aileron at a given deflection regardless of stick position, and a large increase in aileron hinge moment results. The total available deflection of the

two ailerons therefore was less for the flexible system than for the rigid system, and the reduction was greater at high speeds than at low speeds. Computed stick forces presented in figure 33 show that the variation of stick force with stick position becomes more nonlinear as the flexibility of the system is increased and that a given amount of flexibility is more unfavorable at the higher speeds. Stretch has been known to cause violent overbalance of some aileron systems that incorporated differential aileron motions.

Ailerons Having Sealed Internal Balances

The internal type of aerodynamic balance has certain advantages over other balance types, particularly in application to high-speed airplanes. These advantages result from the fact that the lift, drag, and pitching-moment characteristics and the chordwise pressure distributions of a wing with a plain sealed aileron are unaffected by the addition of a sealed internal balance.

Sealed internal balances for use with ailerons usually consist of a plate (attached rigidly to the aileron nose) in a chamber that is vented to the air stream in such a manner that a pressure difference across the plate is created principally by aileron deflection and to a lesser degree by changes in the angle of attack. A flexible seal connects the nose of the balance plate to the forward wall of the balance chamber.

Sealed internal balances are considered to be more suitable to analytical treatment than other types of aerodynamic balance because the balancing force is obtained from the pressure difference between two chambers in which the air is essentially static. The balancing moment, therefore, can be derived from the geometry of the system provided the pressure difference is known. The characteristics of an aileron having almost any arrangement of the balance plate and of the flexible seal can be calculated, therefore, from the characteristics measured for one particular balance configuration. If the resultant pressure coefficient is constant along the aileron span, the increment of hinge-moment coefficient caused by the balance is related to

the resultant-pressure coefficient and to the geometry of the system by the following equation:

$$\Delta C_{h_a} = \frac{1}{2} P_R \left[\left(\frac{\bar{c}_{bp}}{\bar{c}_a} \right)^2 (1 + m_s) - \left(\frac{\bar{t}/2}{\bar{c}_a} \right)^2 \right] \frac{b_b}{b_a} \qquad (25)$$

where $\bar{c}_{bp}$ is the root-mean-square chord of the balance plate and m_s is the ratio of the moment contributed by the flexible seal to the moment contributed by the balance plate.

Values of m_s have been determined analytically (reference 58) and checked experimentally (reference 59). The experimental investigation included a number of arrangements for which the deflection of the balance plate is restricted and the shape of the flexible seal is constrained by balance-chamber cover plates. Some of the experimentally determined values of m_s for several typical balance arrangements are presented in figure 34. For all arrangements represented by figure 34, the seal was attached to the forward wall of the balance chamber at the vertical location corresponding to the intersection of an extension of the balance plate (at zero deflection) with the forward wall of the balance chamber. When the resultant pressure coefficient P_R and the balance plate deflection δ_{bp} are of the same algebraic sign, values of m_s always should be taken from figure 34 at positive values of δ_{bp}, regardless of the actual sign of δ_{bp}. If, on the other hand, P_R and δ_{bp} are of opposite sign, values of m_s should be taken at negative values of δ_{bp}.

The effect of a sealed internal balance frequently is calculated approximately from the following equation:

$$\Delta C_{h_a} = \frac{1}{2} P_R \left[\left(\frac{\bar{c}_b}{\bar{c}_a} \right)^2 - \left(\frac{\bar{t}/2}{\bar{c}_a} \right)^2 \right] \frac{b_b}{b_a}$$

$$= \frac{1}{2} P_R F_1 \qquad (26)$$

where $\bar{c}_b$ is the root-mean-square of the overhang, the nose of which is assumed to be located midway between the two points of attachment of the flexible seal, and F_1 is the overhang factor used in the correlation of data on plain-overhang and Frise balances. (See fig. 25.)

Computations based on the seal arrangements considered in figure 34 indicate that for some arrangements values of ΔC_{h_α} computed from equation (26) may be considerably in error. The error is small, however, for the arrangements that appear to give the most desirable aileron hinge-moment characteristics. Such arrangements involve small gaps ($0.1c_{b_p}$ or less) and seals that are just wide enough to be tangent to the cover plate of the balance chamber when the aileron is at maximum deflection. Equation (25) is always recommended for use, however, when the exact seal configuration is known and when the resultant pressures across the balance plate have been accurately determined for the particular wing-aileron arrangement that is being considered.

In many instances the exact seal configuration is not well defined or the resultant pressure coefficients are unknown. Approximate correlations of the effect of sealed internal balances on the hinge-moment parameters, C_{h_α} and C_{h_δ}, therefore, are convenient. Such correlations (fig. 35) have been obtained from the available experimental data (see table IV) without taking into consideration the effect of airfoil profile on the resultant pressures and with the assumption that the geometrical relations expressed by equation (26) are sufficiently reliable. These correlations are intended to supersede those given in reference 45. The equations of the faired correlation curves are as follows:

$$\Delta C_{h_\alpha} = 0.14 \frac{A}{A + 2\left(\frac{\bar{c}_a}{\bar{c}}\right)^2} F_1 \qquad (27)$$

$$\Delta C_{h_\delta} = 0.09 \frac{A}{A + 2\sqrt{\frac{\bar{c}_a}{\bar{c}}}} F_1 \qquad (28)$$

These correlations are believed to be most reliable when the following conditions apply:

(1) The balance plates are attached rigidly to noses of the ailerons and the vents are as close to the hinge line as practicable

(2) There is no leakage across the seal

(3) The cover plates are of airfoil contour

Small variations in any of these conditions may cause large changes in the effect of an internal balance.

An indication of the probable effects of changes in the chordwise location of the balance-chamber vents (determined from data of references 43 and 45) is given in figure 36 for an aileron of 18-percent chord. Moving the vents forward of the hinge line causes P_{R_α} to increase and P_{R_δ} to decrease. For internal balances of the type considered in the correlations, the variation of the resultant pressure across the balance plate with deflection usually is about two-thirds the variation of the peak resultant pressure at the hinge with deflection.

The characteristics of internally balanced ailerons have been found to be very sensitive to the alinement of the cover plates just forward of the vents. The effects of misalinement as determined in a few tests, are shown in figure 37 (data from reference 45). When small aileron deflections and small changes in angle of attack are considered, bending the cover plates slightly out normally decreases the effect of the balance on C_{h_α} and increases the effect of the balance on C_{h_δ}. Bending the cover plates out usually decreases the deflection range for which the balance has an effect on the hinge-moment slopes, probably because of the earlier separation of the flow. For large aileron deflections the control forces may be larger when the cover plates are bent out than when the cover plates are of true contour.

The loss in balancing effect caused by leakage across the balance plate is significant because of the difficulties involved in installing completely sealed internal balances, because some means usually must be

provided for draining water from the upper balance chamber, and because of the convenience of making small adjustments to the amount of aerodynamic balance by varying the amount of leakage.

Leakage across the balance plate of an internally balanced aileron affects the aileron hinge moments by reducing the pressure difference across the balance plate and by altering the flow conditions behind the balance-chamber vents. In an analysis presented in reference 45, a correlation of wind-tunnel data on the effects of leakage was obtained by expressing the incremental effect of the internal balance on C_{h_δ} as a function of the ratio of leak area to vent area (see fig. 38). For this correlation the vent area is defined as the minimum area between one balance-chamber cover plate and the nose of the aileron. This correlation neglects any effect of leakage on the flow conditions behind the vents. For most true-contour ailerons this effect is small and the correlation that was obtained by neglecting this effect has been found to apply satisfactorily in most instances.

The effect of leakage on the flow conditions behind the balance-chamber vents may be important for thick cusped airfoils having their maximum thickness located far back. Data obtained from tests of such an airfoil in two-dimensional flow (reference 52) are compared in figure 38 with the data used to obtain the original correlation. For the model of reference 52 leakage causes the flow to separate at the aileron hinge and thereby causes a large change in the external pressure distribution. (See fig. 39.) The change in pressure distribution not only causes an increase in the aerodynamic moment over the part of the aileron behind the hinge but, because of the reduction in the external pressures in the vicinity of the balance-chamber vents, also causes a large reduction in the pressure difference across the balance plate. For the model of reference 52, the value of C_{h_δ} for the aileron with $0.75c_a$ overhang and with a ratio of leak area to vent area of 1.0 is more negative than the value of C_{h_δ} for the plain sealed aileron.

Flow through the balance-chamber vents, which results from leakage across the balance plate, may be expected to alter the boundary-layer conditions in such a

manner that the balancing effect of a large trailing-edge angle is increased (see fig. 14). The effect of leakage on the hinge moments of an internally balanced aileron therefore can be expected to be smaller when the trailing-edge angle is large than when the trailing-edge angle is small. When the leakage does not cause the flow to separate at the aileron hinge, the effect of leakage on the hinge moments of an internally balanced aileron having a large trailing-edge angle may be less than the effect indicated by the correlation curve (fig. 38).

The available data have indicated that the percent reduction in ΔC_{h_α} resulting from leakage is about the same as the percent reduction in ΔC_{h_δ}.

Ailerons Having Linked Tabs

A tab that is linked in such a manner that the tab deflection depends only on the aileron deflection is commonly called a linked tab. Such a tab is a very convenient device in that it can be combined with any of the aileron balances that already have been discussed and because the balancing or unbalancing effect can be altered readily by changing the ratio of tab deflection to aileron deflection.

A unique characteristic of a linked tab is that a large change in C_{h_δ} can be produced without causing any appreciable change in C_{h_α}; a small effect on C_{h_α} introduced by the tab linkage usually may be neglected. Almost any desired values of C_{h_α} and C_{h_δ} can therefore be obtained by combining the linked tab with one of the other balancing devices.

Because a balancing linked tab deflects in a direction opposite to that of the aileron to which it is attached, a reduction occurs in the net lift resulting from aileron deflection. An analysis of a large amount of pressure-distribution data on an NACA 0009 airfoil (reference 43) indicates that the most efficient trailing-edge balancing tab is one having a chord between 20 percent and 25 percent of the aileron chord, because such a tab produces the least change in lift for a given

change in aileron hinge moment. On the other hand, a linked tab used to augment the lift of an aileron (leading or unbalancing tab) should produce the greatest change in lift for a given change in aileron hinge moment. A tab of this type is most efficient when the tab chord is equal to about 50 percent of the aileron chord.

The influence of a linked tab on aileron effectiveness can be calculated by considering the tab to be a small aileron and by using the methods for calculating aileron effectiveness that already have been explained. The change in aileron effectiveness can be expressed in a form convenient for some analyses by means of the helix-angle reduction factor k_t, which can be given with sufficient accuracy for preliminary design by the equation

$$k_t = -\frac{b_t}{b_a}\frac{\left(\frac{\Delta\alpha}{\Delta\delta}\right)_{tab}}{\left(\frac{\Delta\alpha}{\Delta\delta}\right)_{aileron}}\frac{\partial\delta_t}{\partial\delta_a} \tag{29}$$

In the usual case, a tab linked for balancing should be placed at the spanwise location corresponding to the maximum aileron chord in order to produce the most balance for a given change in aileron effectiveness.

The effect of linked tabs on the hinge moments of ailerons is expressed in the present analysis as a function of the deflection ratio $\partial\delta_t/\partial\delta_a$ and of four factors that are defined as follows:

$$F_3 = \frac{b_t}{b_a}\left(\frac{\bar{c}_a'}{\bar{c}_a}\right)^2 \tag{30}$$

$$F_4 = \left(\frac{\bar{c}_t}{\bar{c}_a'}\right)^{0.7} + 0.51\,\frac{\bar{c}_a'}{\bar{c}'} \tag{31}$$

$$F_5 = 1.3 - 0.026\phi \tag{32}$$

$$F_6 = 1 - 0.85\left[\left(\frac{\bar{c}_b'}{\bar{c}_a'}\right)^2 - \left(\frac{\bar{t}'/2}{\bar{c}_a'}\right)^2\right] \tag{33}$$

The factor F_3 accounts for the effects of the span and the spanwise location of the tab. The factor F_4 accounts for the effects of the tab chord and the aileron chord. The factor F_5 accounts for the effect of the trailing-edge angle, and the factor F_6 accounts for the effect of the tab on the pressure difference across an aileron overhang balance (either exposed or internal). The inclusion of the factor F_6 in the tab correlation makes unnecessary an adjustment in the increment ΔC_{h_δ} resulting from an aileron overhang balance for the effect of the tab on the pressures across the overhang balance.

For wings having linear taper, constant-percentage-chord ailerons and tabs, and tabs beginning at the inboard ends of the ailerons, the ratio $\bar{c}_a'/\bar{c}_a$ involved in the factor F_3 can be evaluated with sufficient accuracy for most design work by means of the relation

$$\frac{\bar{c}_a'}{\bar{c}_a} = 1.0 + 0.4\left(1 - \frac{b_t}{b_a}\right)(1 - \lambda) \tag{34}$$

where λ is the wing taper ratio. The factors F_3, F_4, and F_5 can be evaluated conveniently from the charts given in figure 40. An inspection of the factor F_6 reveals that the term

$$\left[\left(\frac{\bar{c}_b'}{\bar{c}_a'}\right)^2 - \left(\frac{\bar{t}'/2}{\bar{c}_a'}\right)^2\right]$$

is similar to the expression for the overhang factor F_1 used in the correlations of exposed-overhang and sealed internal balances, with the exceptions that the various chord and thickness elements are the root-mean-squares of values measured over the tab span rather than over the aileron span, and the overhang-span ratio b_b/b_a is omitted. This term in the factor F_6 can be evaluated, therefore, from the chart given for F_1 in figure 25.

The correlation of the effect of linked tabs on the aileron hinge-moment parameter C_{h_δ} is given in figure 41 (data from reference 47). Some information regarding the models considered in the correlation is given in table V. The equation of the correlation curve is

$$\Delta C_{h_\delta} = 0.022 F_3 F_4 F_5 F_6 \left(-\frac{\partial \delta_t}{\partial \delta_a}\right) \qquad (35)$$

This equation may be used to estimate the incremental change in C_{h_δ} of an aileron resulting from a given linked tab or to estimate the configurations of tabs that are capable of producing a given change in C_{h_δ} of an aileron.

The effect of a tab on aileron hinge moments usually decreases slightly when a gap is opened at the nose of the aileron. This effect is illustrated in figure 42 for a model in two-dimensional flow.

The effect of a gap at the nose of a tab may be very large, although the available data on this effect are too inconsistent to permit any reliable correlation. For some ailerons, such a gap has resulted in a reduction of the tab balancing effect by as much as 50 percent. In any design the tab gap should be sealed or at least made as small as possible.

Comparisons of Various Balancing Devices

Hinge-moment characteristics.- The correlations that have been presented may be used to illustrate the relative effects of the various balancing devices on the hinge-moment parameters C_{h_α} and C_{h_δ}. The variations in these parameters that might be expected to accompany the addition of each of the balances to a 0.25c plain aileron on an assumed fighter-airplane wing (fig. 43) are shown in figure 44. By means of methods, which already have been described, the values of C_{h_α} and C_{h_δ} of the true-contour plain aileron are estimated to be -0.0012 and -0.0065, respectively.

A line of zero stick force (see equation (7)) is indicated in figure 44 for an aileron extending from $0.55\frac{b}{2}$ to $0.97\frac{b}{2}$. Constant values of F_s/q over the ranges of angles of attack and of aileron deflections for which the parameters C_{h_α} and C_{h_δ} are applicable may be represented by lines drawn parallel to the line of zero stick force. Because of the positive slope of the line of zero stick force, the increment ΔC_{h_δ} required for a given reduction in stick force is largest for balances that produce the greatest change in C_{h_α} for a given change in C_{h_δ}. In the order of increasing effects on C_{h_α} for a given effect on C_{h_δ}, the various balances may in general be listed as follows: balancing tab, sealed internal balance, plain-overhang balance, and balance obtained by increasing the trailing-edge angle.

The comparisons given in figure 44 were obtained from the correlations that were derived from low Mach number data. The results given are not necessarily applicable, therefore, at high Mach numbers.

The combinations of two or possibly three types of balance may be desirable in order to obtain specified values of the aileron hinge-moment parameters or in order to avoid the difficulties that are encountered almost invariably when a large amount of one type of balance is used. The effects of such combinations on

the aileron hinge-moment parameters may be illustrated by means of figure 44. Because moderate changes in trailing-edge angle have only a small influence on the incremental effects of exposed-overhang or sealed internal balances, the curves representing these balances may originate from any point on the curve representing various trailing-edge angles. The curve representing the balancing tab may originate from any point on the curve representing various trailing-edge angles, or on the curves representing various overhang balances (exposed or internal), but the increment ΔC_{h_δ} attributable to a given linked tab is altered by variations in the trailing-edge angle or in the aileron overhang.

Because of the desirability of obtaining increased rolling moments for given aileron deflections, consideration frequently has been given to a combination involving a very wide-chord sealed internal balance and an unbalancing (leading) tab. Such an arrangement, although probably satisfactory for commercial airplanes, has been considered undesirable for military airplanes because of the possibility of the tab being shot away, thus leaving the ailerons overbalanced.

Effect of angle of rig.- An analysis reported in reference 64 was made to determine the effects on the stick-force characteristics of changes in the angle of rig of beveled ailerons, of ailerons having Frise balances, and of ailerons having sealed internal balances. The results of the analysis are summarized in figure 45. The stick-force characteristics of the ailerons having Frise balances were found to be very sensitive to the angle of rig, whereas the stick-force characteristics of ailerons having beveled trailing edges or sealed internal balances seemed to be relatively insensitive to the angle of rig. In general, when there is no differential in the linkage system, only ailerons having decidedly nonlinear hinge-moment curves, particularly at aileron deflections near 0°, may be expected to be sensitive to changes in rigging.

Rolling performance.- Data have been collected on the rolling-performance characteristics of a number of fighter airplanes of American and foreign manufacture. Pertinent details of the wing-aileron arrangements of these airplanes are given in table VI. All the balancing devices that have been discussed are represented.

Comparisons are made on the basis of the helix angle $pb/2V$ and the rolling velocities obtainable at 10,000 feet altitude with a 50-pound stick force (figs. 46 and 47). An accurate rating of the balanced ailerons is not possible from the data presented. The only conclusion to be drawn perhaps is that good performance can be obtained from ailerons having any of the various balances, provided sufficient care is exercised in the design and development. The wide variations in the performance of airplanes having Frise ailerons may be an indication of the well-known fact that Frise ailerons are extremely sensitive to each of a large number of design parameters.

Application to Arrangements Involving Full-Span Flaps

Several methods for incorporating conventional flap-type ailerons in arrangements that involve full-span lift flaps have been proposed. In some of the more promising arrangements, the lateral-control system is made up of a combination of conventional ailerons with a spoiler-type lateral-control device. Only the characteristics of the conventional ailerons are considered at this time. The characteristics of spoiler-type devices are discussed in the section of the present paper entitled "Spoiler Devices, Part IV."

Flap-trailing-edge ailerons.- In some full-span-flap arrangements, conventional ailerons are installed in the rear parts of the lift flaps (references 65 to 69). For such arrangements, conventional aileron balancing devices can be used, although the aileron chord may have to be limited to about 10 percent of the wing chord. In order to obtain a reasonable amount of lateral control, the aileron span must be long, although only a small increase in lateral control is obtained by extending the ailerons inboard of stations $0.2\frac{b}{2}$ from the plane of symmetry.

The rolling-, yawing-, and hinge-moment characteristics of a plain aileron at the trailing edge of a slotted flap (reference 67) are presented in figure 48. When the flap is retracted the aileron characteristics present no unusual problems. When the flap is deflected, the aileron maintains most of its effectiveness for negative deflections but is relatively ineffective for positive deflections. These characteristics are such

that in order to obtain the best rolling performance a differential aileron motion should be used when the flap is deflected but not necessarily when the flap is retracted. The use of the differential with flaps deflected may cause some ailerons to be overbalanced, however, if the ailerons are designed for close aerodynamic balance when the flaps are retracted.

The yawing characteristics of an airplane having a lateral-control device consisting only of flap-trailing-edge ailerons may be expected to be very unfavorable when the lift flaps are deflected, because the adverse induced aileron yawing-moment coefficient varies directly with the lift coefficient, and because the variations in profile drag caused by aileron deflection also contribute an adverse yawing moment.

Considerations of over-all characteristics indicate that when full-span flaps are fully deflected, lateral control should be obtained from some device other than conventional ailerons at the trailing edges of the flaps.

Drooped ailerons.- Ailerons outboard of partial-span flaps sometimes are drooped and operated differentially when the flaps are deflected. In other arrangements a single flap or the rear flap of a double-slotted-flap combination is used to provide lateral control as well as lift. The lateral-control characteristics for all of these arrangements are very similar to the lateral-control characteristics for flap trailing-edge ailerons; that is, when the ailerons are drooped the aileron effectiveness for positive deflections is low and the adverse yawing moments for either positive or negative deflections are high. The problem of providing aerodynamic balance for lateral control while maintaining an efficient high-lift device, may be more difficult for drooped ailerons than for flap-trailing-edge ailerons.

Ailerons with retractable flaps.- A number of investigations have been made of conventional flap-type ailerons in combination with lift flaps that may be retracted ahead of the ailerons. In an early adaptation of this arrangement the flap moved rearward as it was deflected, but no gap was left between the flap nose and the lower surface of the wing. The lower surface

of the aileron, therefore, was completely shielded by the deflected flap. In spite of this shielding effect, flight tests (reference 70) indicated that the ailerons were nearly as effective with flaps deflected as with flaps retracted, and the yawing characteristics at a given lift coefficient were less unfavorable with the flaps deflected than with the flaps retracted.

Wind-tunnel tests indicate that some improvement in the characteristics of ailerons with retractable flaps can be obtained if a gap is left between the nose of the deflected flap and the lower surface of the wing. An arrangement of this kind may consist either of an approximately full-span, narrow-chord aileron in combination with a single full-span flap (reference 71) or of a partial-span aileron in combination with full-span duplex flaps (references 72 and 73). Although the aileron effectiveness may be somewhat less when the flap is at some intermediate position than when the flap is retracted, the aileron effectiveness can be even higher when the flap is fully deflected than when the flap is retracted. This fact is demonstrated by the data (fig. 49) obtained from the tests reported in reference 71. The indicated flap positions correspond approximately to positions on the flap path selected in reference 71. When the flap is fully deflected, only small positive aileron deflections are effective in increasing the rolling moment, but negative deflections as large as -30° are effective. A differential aileron motion should be used, therefore, to obtain maximum rolling moment. A tendency toward overbalance of the differentially operated aileron is indicated by the large negative floating angle when the flap is fully deflected. Data given in reference 71 indicate, however, that this tendency is reduced by increasing the chord of the sealed internal balance.

Although the yawing-moment characteristics of flap-type ailerons used with retractable flaps generally are not favorable, at a given wing lift coefficient the yawing moments usually are less unfavorable with flaps deflected than with flaps retracted.

Effects of Air-Flow and Wing-Surface Conditions

The preceding discussion has been concerned primarily with the characteristics of ailerons under

certain very restricted conditions; that is, the Mach number was low, transition was assumed to occur far forward on the airfoil, and the ailerons were of sufficiently rigid construction to prevent any appreciable distortion by the aerodynamic forces. In the present section the effects of deviations from the previously assumed conditions are discussed and some information is provided from which rough quantitative estimates of these effects may be made. The applicability of the information is limited by the fact that the available data are not sufficient to permit an accurate determination of the relative importance of the various factors concerned.

Boundary-layer effects.- Large variations in aileron characteristics may result from changes in the thicknesses of the boundary layers at the surfaces of an aileron. At low Mach numbers the thickness of a boundary layer depends largely on the chordwise location of the region of transition from laminar to turbulent flow. For a given airfoil the most important factors that govern the transition location are the airfoil surface condition, the Reynolds number, and the air-stream turbulence. The relative importance of each of these factors is not easily established, but experience indicates that for almost any airfoil, transition near the leading edge may be brought about by the wing roughness that may result from conventional airplane fabrication methods or by a Reynolds number within the flight range of some airplanes. The turbulence that exists in some wind tunnels is sufficient to induce transition near the leading edge for most airfoils.

In a recent unpublished theoretical study, values of the section hinge-moment parameters c_{h_α} and c_{h_δ} in viscous flow were computed for ailerons having small trailing-edge angles. The method used was based on the concept that differences in the thicknesses of boundary layers at the upper and lower airfoil surfaces effectively alter the camber of the airfoil. Computations of the parameter c_{h_δ} were made for the conditions of fixed transition at the leading edge and at 0.5c, and computations of the parameter c_{h_α} were made for the condition of fixed transition at the leading edge. (See fig. 50.) Conditions of fixed transition location may not represent accurately the boundary-layer conditions

that are most likely to be encountered in flight, because for most airplane wings changes in the transition locations on the upper and lower wing surfaces can be expected to result from changes in angle of attack or in aileron deflection. The results presented in figure 50 therefore are considered to be of use principally for illustrating the possible magnitude of the effects of the boundary layer rather than for providing numerical values of the hinge-moment parameters for use in design.

Wind-tunnel investigations of aileron characteristics frequently include tests of a model with smooth airfoil surfaces and with roughness strips or wires near the airfoil leading edge. The fact that the effects of roughness strips at the airfoil leading edge may be expected to be greater when the trailing-edge angle is large than when the trailing-edge angle is small is illustrated in figure 51. In these tests the addition of roughness strips at the leading edge resulted in positive increments of c_{h_δ} of 0.0005 and 0.0025 for trailing-edge angles of 6° and 33°, respectively. The roughness strip also caused a somewhat greater reduction in c_{l_δ} when the trailing-edge angle was large than when the trailing-edge angle was small. The available data are insufficient to show the effects of trailing-edge angle on the changes in c_{h_α} and c_{l_α} caused by the addition of the transition strip, but these effects are expected to be somewhat similar to the effects on c_{h_δ} and c_{l_δ}.

The transition location on the upper surface of a smooth low-drag airfoil usually moves forward very rapidly as the angle of attack, corresponding to the upper limit of the low-drag range, is exceeded. A similar effect usually occurs on the lower surface as the angle of attack is decreased below the lower limit of the low-drag range. Curves of C_{h_a} plotted against α may be characterized by an irregular shape, therefore, as indicated in figure 52. The shapes of these curves are such that a large sudden change in the floating tendency of an aileron may be expected at the limits of the low-drag range. This effect is most noticeable for low-drag airfoils having large trailing-edge angles. The irregularities in the curves of C_{h_a} plotted against α do not occur when conditions are such that extensive laminar flow is prevented (fig. 52).

At a given angle of attack extensive laminar flow may occur over a wide range of control-surface deflections. Curves of C_{h_a} plotted against δ_a, therefore, are not characterized by the irregularities noted in the curves of C_{h_a} plotted against α. Roughening the airfoil surface may cause the slope C_{h_δ} to be less negative through the greater part of the normal deflection range.

The variation of transition location with angle of attack usually is less for smooth conventional airfoils (those having the thickness distribution defined in reference 48) than for smooth low-drag airfoils. Test results indicate, as expected, that for approximately equal trailing-edge angles, the effect of adding roughness strips near the leading edge generally is smaller for the conventional airfoils than for the low-drag airfoils.

Geometric parameters associated with overhang balances do not seem to be of much significance with regard to boundary-layer effects. In the usual case, the resultant-pressure parameters P_{R_α} and P_{R_δ} are more positive over the entire airfoil chord when the transition location is far back than when the transition location is far forward. The increased balancing effect caused by the more positive values of these parameters forward of the hinge line usually is small, however, when compared with the unbalancing effect of the increased positive values of these parameters near the aileron trailing edge.

The effectiveness of a linked tab in changing aileron hinge moments usually is diminished by conditions that tend to increase the boundary-layer thickness. The addition of roughness strips at 0.25c of one model having a 0.09c tab resulted in a 25-percent reduction in the rate of change of control-surface hinge-moment coefficient with tab deflection.

Mach number effects.- The following discussion concerns Mach number effects only in the range of subsonic speed.

In most wind-tunnel tests variations in Mach number are obtained simply by varying the tunnel speed. The indicated Mach number effects therefore include changes

in boundary-layer conditions caused by simultaneous changes in Reynolds number and, for some wind tunnels, by changes in the turbulence of the air stream. Because variations in either Reynolds number or in Mach number within the subcritical speed range may result in forward movements in the transition location, the true effect of Mach number is difficult to isolate from most wind-tunnel data. When the transition location is fixed and when the Reynolds number is held constant, variations in Mach number within the subcritical speed range seem to have small effects on the boundary-layer thickness.

The profiles of 3 two-dimensional models that were tested in the Langley 8-foot high-speed tunnel over a wide range of Mach numbers are shown in figure 53. The variations with Mach number of the normal-force parameters c_{n_α} and c_{n_δ} are shown in figure 54 and the variations of the effectiveness factor $\Delta\alpha/\Delta\delta$, relative to the values of this factor obtained by extrapolating to $M = 0$, are shown in figure 55. Increasing the Mach number from 0 to 0.7 decreases the value of $\Delta\alpha/\Delta\delta$ by 12 percent for the Frise aileron, by 35 percent for the true-contour plain aileron, and by 50 percent for the beveled aileron. These reductions in $\Delta\alpha/\Delta\delta$, particularly for the true-contour plain aileron and for the beveled aileron, probably are greater than the reductions that would have been obtained if the aileron nose gap had been sealed. Several unpublished investigations have shown that an open nose gap may cause large losses in control-surface effectiveness with increased Mach number. In the usual case, for ailerons having either open gaps or sealed gaps, the reduction in $\Delta\alpha/\Delta\delta$ is quite gradual until shock occurs on the airfoil. At speeds in excess of the speed at which shock occurs, the reduction in $\Delta\alpha/\Delta\delta$ is more rapid, probably because a trailing-edge flap cannot induce pressure changes forward of a shock wave.

The variations with Mach number of the hinge-moment parameters (fig. 56) of the three ailerons considered agree qualitatively with results obtained from other investigations of smooth airfoils. The test data available indicate that when the trailing-edge angle is small, the parameters c_{h_α} and c_{h_δ} usually increase in absolute magnitude as the Mach number is increased. When the trailing-edge angle is large, the hinge-moment parameters of smooth low-drag airfoils almost invariably

become more positive when the Mach number is increased by increasing the tunnel speed, and the hinge-moment parameters sometimes change from negative to positive at some speed within the test range of Mach number. The large variations in the hinge-moment parameters noted between Mach numbers of 0.15 and 0.40 (fig. 56(c)) probably do not result simply from compressibility effects, which would be expected to be small over this Mach number range. A large part of the indicated effects may be caused by variations in transition location resulting from increased Reynolds number as the airspeed is increased. The fact that a given change in the trailing-edge angle of a smooth low-drag airfoil may produce much greater effects on the hinge-moment parameters at high Mach numbers than at low Mach numbers is indicated in figure 57.

When an exposed-overhang balance (either Frise or plain) is used, the center of pressure of the aileron load resulting from aileron deflection usually moves forward as the critical Mach number is approached. The parameter C_{h_δ} therefore tends to become less negative. This effect may cause the aileron to become overbalanced near the critical Mach number, even though the trailing-edge angle is small. Adverse compressibility effects probably will be encountered at a lower Mach number with ailerons having small nose radii than with ailerons having large nose radii.

Some unpublished data on an internally balanced aileron with a small trailing-edge angle have indicated that the effect of Mach number on aileron hinge moments is small until shock occurs in the vicinity of the balance-chamber vents. When shock on either the upper or the lower surface is in the vicinity of the vent, the variation of aileron hinge moments with either deflection or angle of attack may become very nonlinear. Internally balanced ailerons may become very heavy when shock moves to the rear of the vents because deflection of the aileron then can produce little, if any, pressure difference across the balance plate.

Only a small amount of data is available on the variation with Mach number of the balancing effect of a tab. The results of two unpublished investigations indicate, however, that for ailerons having small trailing-edge angles, the balancing effect of a tab is

essentially unchanged until shock is sufficiently developed to cause flow separation from the airfoil surface.

The aileron hinge-moment parameters of an assumed fighter airplane (fig. 43) equipped with each of the three ailerons shown in figure 53 were estimated from the section data by methods described previously in the present paper. The results of the computations are presented in figure 58, on which lines of constant F_s/q for aileron deflections of $\pm 5^\circ$ have been drawn (see equation (6)). The computations indicate that the stick force for the true-contour plain aileron would increase with Mach number at a rate considerably in excess of the rate of increase of the dynamic pressure, whereas at Mach numbers greater than about 0.2 the beveled aileron would be overbalanced. For the deflection range considered in figure 58, the Frise aileron was less sensitive to Mach number effects than either the true-contour aileron or the beveled aileron. Additional data given in reference 74 indicate, however, that at large negative deflections, the Frise aileron may be very sensitive to Mach number effects because of the critical nature of the flow over the protruding nose of the balance.

Surface-covering distortion.- Contour changes caused by aerodynamic forces may be of sufficient magnitude to produce objectionable stick-force characteristics for ailerons that otherwise would be satisfactory. The type and extent of covering distortion depends on the external pressure distribution over the surfaces of the aileron, on the pressure inside the aileron, on the initial tension of the covering material, on the modulus of elasticity of the covering material, and on the method of attachment of the covering material. Different vent locations may cause positive, negative, or static internal pressures.

An analysis of the effects of surface-covering distortion on aileron characteristics has been made by Bryant and Holoubok in Great Britain. A somewhat similar analysis is applied to elevators in reference 75. Typical distorted aileron contours for extreme internal-pressure conditions are illustrated in figure 59. For either large positive or large negative internal pressures the changes in stick force caused by distortion result chiefly from changes in the trailing-edge angle

as the airspeed is increased. Because such pressures stress the covering material and thus increase the rigidity of the covering material, the change in camber caused by the external-pressure differential between the upper and the lower surfaces of the aileron is reduced.

Positive internal pressures cause both surfaces of the aileron to bulge. Bulging of the forward part of the aileron seems to have little effect on the hinge-moment parameters, but the increase in trailing-edge angle causes these parameters to become less negative. The stick forces, therefore, are decreased and may become overbalanced if the undistorted aileron is designed to give stick forces within the required limits. In the case of one airplane equipped with fabric-covered ailerons, the internal pressure became so great during a high-speed dive that fabric failure resulted.

Negative internal pressures cause both aileron surfaces to be drawn in with the result that the trailing-edge angle is decreased. The parameters C_{h_α} and C_{h_δ} therefore become more negative and the stick forces may increase to such an extent that the pilot's ability to roll the airplane may be seriously restricted at high speeds.

The data presented in figures 54 to 56 for the true-contour plain aileron and for the beveled aileron may be used to illustrate the effect of trailing-edge angle on the stick forces of a fighter airplane (fig. 43). The change in stick force per degree change in trailing-edge angle for aileron deflections of $\pm 5^\circ$ is given as a function of Mach number in figure 60. The results indicate that the incremental stick force caused by a 1° change in trailing-edge angle may be of the order of magnitude of the maximum allowable stick force for the assumed airplane.

For internal pressures near static pressure, changes in stick force caused by distortion may result chiefly from changes in aileron camber. Under this condition the covering material is not highly stressed by the internal pressure; therefore, the external-pressure differential can cause both surfaces to bow in the same direction. The aileron surface-covering distortion that occurred for such a pressure condition during

flight tests of a P-40F airplane at an indicated airspeed of 350 miles per hour is shown in the photographs of figure 61.

The effect of a change in camber on the variation of hinge-moment coefficient with aileron deflection is very similar to the effect produced by an unbalancing tab with a linkage ratio that increases progressively with increasing speed. Increased stick forces again result and the increases for this condition may be of greater magnitude than for the condition of negative internal pressure; furthermore, the changes in the hinge-moment parameters are greatest for small aileron deflections because for small aileron deflections the surface covering is stressed the least and can deflect most rapidly. This condition results in a nonlinear variation of stick force with aileron deflection.

In the foregoing discussion careful consideration of distortion effects is shown to be necessary in the design of ailerons for high-speed airplanes. As suggested by Bryant and Holoubok, the problem may be attacked in two ways. The distortion may be allowed but controlled by proper venting in order to obtain desirable stick forces throughout the speed range, or the greater part of the distortion may be prevented by using very close rib spacing or a stiff covering material. The second solution is far more satisfactory from aerodynamic considerations, but it has the disadvantage of increasing the aileron weight. Distortion that occurs near the trailing edge, however, seems to have much greater effects on aileron characteristics than distortion that occurs near the hinge line; thus, the greater part of the distortion effects probably can be eliminated by stiffening only the rear 25 percent of the aileron.

SPOILER DEVICES

Some success has been obtained with lateral-control devices that project from the wing surfaces into the air stream. When located near the wing leading edge and when projected above the upper surface of the wing, these devices reduce the lift of the wing by spoiling the flow and thereby produce a rolling moment that is roughly

proportional to the lift coefficient. The name spoiler has been applied to these devices. The effectiveness of similar devices placed near the wing trailing edge is more nearly independent of the lift coefficient. The name spoiler also is used commonly in referring to devices located near the trailing edge, even though the action of such devices is more like the action of split flaps than like that of the devices to which the name spoiler originally was applied.

The spoiler-type lateral-control devices illustrated in figure 62 are representative of most of the arrangements of these devices for which experimental results are available. Although certain aerodynamic characteristics are critically dependent on specific details of the spoiler arrangement, some statements may be made with regard to the characteristics of spoiler devices in general.

Flight tests as well as wind-tunnel tests have indicated that when a spoiler is located far forward on a wing, an appreciable time lag may occur between a movement of the spoiler and the aerodynamic response resulting from that movement, and that small spoiler projections may produce very little rolling moment or even a rolling moment in a direction opposite to that desired. As spoilers are moved rearward, the time lag is reduced, and in general the effectiveness for small spoiler projections is improved. In these respects spoilers located at about 0.7c have proved satisfactory in flight, although the final rolling moments at high positive lift coefficients are somewhat less for such spoilers than for spoilers located far forward.

The fact that spoiler control is obtained simply through a decrease in lift of one wing has resulted in the criticism that difficulty may be experienced in raising a wing that had dropped. Such a difficulty can hardly be of a serious nature, however, because the decrease in lift caused by spoiler control usually results in a movement of the axis of rotation of no more than 20 percent of the wing semispan away from the plane of symmetry.

The greatest advantage of spoiler devices perhaps results from their adaptability to arrangements that involve full-span lift flaps. An important advantage, especially for tailless airplanes, results from the fact

that the yawing moments caused by spoiler control may be favorable over a large part of the angle-of-attack range. The pitching-moment characteristics of spoilers (fig. 63) are less adverse from considerations of wing twist than the pitching-moment characteristics of conventional flap-type ailerons; the rolling effectiveness usually increases with lift coefficient; and some lateral control may be retained beyond the stall.

Hinged-Flap Spoilers

An investigation of a number of configurations of spoilers of the hinged-flap type (fig. 62(a)) on plain wings and on wings with split flaps and slotted flaps is reported in reference 79. Though the effectiveness of such spoilers is about the same as the effectiveness of some other spoiler devices, the hinge-moment characteristics generally are unsatisfactory unless a balancing device is provided. Some degree of balance may be obtained with a small plate that projects into the air stream below the wing as the spoiler is deflected (reference 80).

Retractable-Arc Spoilers

Investigations of retractable-arc spoilers (fig. 62(b)) are reported in references 65, 70, 77, and 81. When such spoilers are located sufficiently far rearward, the lag characteristics and the effectiveness for small spoiler projections generally are satisfactory with flaps retracted. With split flaps or slotted flaps deflected, spoiler projections as large as 0.02c may be ineffective, however, in producing rolling moment. Experience with the P-61 airplane has indicated that with slotted flaps deflected, the rolling effectiveness resulting from small spoiler projections may be improved either by opening a slot just behind the spoiler or by sealing the slot of the lift flap. Elimination of the flap slot, however, has detrimental effects on the lift and drag of the wing with flaps deflected.

The hinge-moment characteristics of retractable-arc spoilers can be varied considerably by changing the width of the spoiler plate, the angle of the upper surface of the spoiler, or the distance between the spoiler pivot

axis and the center of curvature of the spoiler plate. In most cases, however, the type of variation of hinge moment with spoiler projection that results in the most desirable stick feel can be obtained only through the use of some auxiliary device. A solution of this problem was obtained on the P-61 airplane by combining small conventional ailerons ("guide ailerons"), located near the wing tips, with retractable-arc spoilers (fig. 64).

The wheel-force and rolling-performance characteristics of the P-61 airplane have been measured in flight with both spoilers and ailerons in operation and with only spoilers in operation. The results are shown in figure 65. The characteristics were considered satisfactory when both spoilers and ailerons were used. For the spoilers alone the wheel forces were very small, but the force variation with wheel deflection did not seem unsatisfactory for this airplane. Wind-tunnel tests indicate, however, that for spoilers that are thicker than those used on the P-61 airplane, undesirable control-force characteristics may result from a tendency for the spoilers to be pulled small distances out of the wing and from large forces required to hold large spoiler projections. The minimum thickness of a spoiler may be limited by the rigidity required to prevent flexural vibrations.

The rolling velocities obtainable with spoilers alone on the P-61 airplane generally were only about one-third less than the rolling velocities obtainable with spoilers and guide ailerons. At small wheel deflections, however, the use of the guide ailerons resulted in greater improvements in the lateral-control characteristics, particularly at low speeds.

The yawing characteristics of the P-61 airplane with spoilers and guide ailerons are favorable at high speeds and at moderate speeds and are only slightly unfavorable at landing speeds. (See section entitled "Effects of Adverse Yaw, Part II.")

The maximum speeds of airplanes may be reduced somewhat by the increased profile drag associated with the small spoiler projections required to maintain the wings level in flight. The use of a guide aileron appears to offer an advantage in this respect, especially when the movement of the guide aileron leads that of the spoiler at small control deflections.

The simultaneous operation of spoilers and conventional ailerons (located just behind the spoilers) has been considered as a possible means of decreasing the aileron hinge moments and of providing large rolling moments. Investigations have been made of several such arrangements, one of which is reported in reference 77. Although the yawing- and the rolling-moment characteristics seem promising, difficulties probably would be encountered in selecting a linkage that would provide desirable stick-force characteristics throughout the speed range. The relative aileron and spoiler motions required for desirable stick-force characteristics depend to a large extent on the spoiler hinge moments and on the variation of rolling moment with spoiler projection. Both the hinge- and rolling-moment characteristics of spoilers may be very nonlinear for some flight speeds. Wind-tunnel tests show that the hinge moments of ailerons located immediately behind spoilers may be strongly influenced by the variations in flow conditions that result from nonlinear spoiler effectiveness.

Slot-Lip Ailerons

A slot-lip aileron consists essentially of a small flap hinged near the front of a slot through a wing. In some arrangements (fig. 62(c) and references 79 and 82) the slot is fixed in the wing structure some distance forward of the high-lift device. Experience has indicated, however, that from considerations of time lag, profile drag, and wing structure, certain advantages are provided by an aileron formed from the lip just forward of a slotted flap (fig. 62(d) and references 65 to 67 and 69). The discussion in the following paragraph concerns this type of slot-lip aileron.

A slot-lip aileron in the neutral position lies close to the lift flap when retracted. Only small positive aileron deflections therefore may be used, and the operation of the aileron for this flap condition necessitates the use of a complicated linkage arrangement or of a cam. Because of this difficulty and because slot-lip ailerons are less effective with flaps retracted than with flaps deflected, a lateral-control system including a conventional flap-trailing-edge aileron for use with flaps retracted and a slot-lip aileron for use with flaps deflected is considered superior to a system

that consists only of a slot-lip aileron. Flight tests (reference 69) indicate that with the combined system good lateral control can be obtained with an airplane having full-span lift flaps.

Plug-Type Spoiler Ailerons

Some of the disadvantages of the retractable-arc spoiler are overcome with the plug-type spoiler aileron (fig. 62(e) and references 79 and 83 to 85). This device is designed in such a manner that a slot through the wing is opened as the plug is projected into the air stream. Data from wind-tunnel tests (fig. 66) have indicated that plug-type spoiler ailerons when used with slotted flaps are very promising, but these ailerons when used with split flaps may be unsatisfactory because of low effectiveness for small projections.

The tests reported in references 79 and 83 indicate that hinge-moment characteristics of the type that result in satisfactory stick feel can be obtained. For some airplanes, however, the plug may have to be quite narrow or some alternative means may have to be provided in order to avoid excessive stick forces.

In order to simplify the linkage arrangement the plug-type spoiler aileron is designed to allow projections either above or below the neutral position. Projections below the neutral position can be expected to contribute little or no effectiveness.

The spoiler and lift-flap arrangement of the P-61 airplane (fig. 64), when tested with spoiler slot and flap slot open, included the essential features intended for the plug-type spoiler aileron with slotted flap. Flight tests indicated that the effectiveness characteristics of this arrangement are very good, but during the tests a severe chordwise vibration of the spoiler plate occurred. Sealing the spoiler slot eliminated the vibration but reduced the effectiveness of the spoiler, particularly for small spoiler projections when the lift flap was deflected. Satisfactory effectiveness characteristics for small spoiler projections were obtained by sealing the flap slot. The performance of the P-61 airplane is considered satisfactory with this configuration, even though the efficiencies of both the spoiler and the flap were reduced by sealing the slots.

Effects of Mach Number

Results of wind-tunnel tests (references 77 and 86) indicate that the rolling-moment coefficient, resulting from a given projection of a spoiler located at 0.75c, increases rapidly as the Mach number is increased to about 0.72, which is approximately the Mach number at which shock would be expected to occur on the wing. An abrupt reduction in rolling-moment coefficient is indicated as the Mach number is increased from 0.72 to 0.75 - the maximum test Mach number. The effectiveness of a conventional flap-type aileron on the same model also decreased, though less abruptly, over the same Mach number range. From considerations of effectiveness, therefore, when shock occurs on a wing, a spoiler located near the wing trailing edge does not seem to offer an advantage over a conventional flap-type aileron.

Unpublished high-speed wind-tunnel tests indicate that spoiler effectiveness at supercritical Mach numbers probably can be improved by locating the spoiler forward of the 0.75c location. The forward location may also be advantageous from considerations of wing twist as is indicated in figure 63. As discussed previously, the lateral control obtainable from a spoiler located far forward may be unsatisfactory at low speeds because of lag in response and ineffectiveness for small spoiler projections. Spoiler control at high Mach numbers may be satisfactory in these respects, although a forward spoiler may possibly cause buffeting.

V - B O O S T E R M E C H A N I S M S

The control-force reduction provided by any of the conventional aerodynamic balances that already have been described depends on the aileron deflection and on the dynamic pressure of the air stream but not on the force supplied by the pilot. A device that supplies a control-force reduction that is proportional to the force supplied by the pilot, regardless of the aileron deflection or of the dynamic pressure, commonly is referred to as a "booster mechanism."

The use of conventional aerodynamic balances on large or high-speed airplanes is limited by the sensitivity of the control forces to small changes in the

hinge-moment parameters. Experience has indicated that changes in the values of C_{h_α} and C_{h_δ} of approximately ± 0.0010 may occur because of slight variations in the construction of different ailerons for the same airplane. Changes caused by Mach number effects and by surface-covering distortion may be considerably greater. Such changes cause large variations in the control-force characteristics of some present-day airplanes. For future high-speed airplanes the problem of providing close aerodynamic balance will be more difficult. In many cases, therefore, the use of a booster mechanism in conjunction with ailerons that are not closely balanced probably will be desirable. The optimum degree of aerodynamic balance has not been definitely established, but the condition expressed by the relation

$$C_{h_\delta}\left[1 + \frac{2(\Delta\alpha)_p}{\Delta\delta_a}\frac{C_{h_\alpha}}{C_{h_\delta}}\right] = -0.0020 \qquad (36)$$

probably is satisfactory for ailerons on most combat airplanes. The use of a booster mechanism on some low-speed airplanes may be desirable because the control forces then can be predicted quite accurately and therefore the required development work is reduced.

Booster mechanisms may be classified as aerodynamic or mechanical. Aerodynamic boosters utilize power from the air stream to deflect the aileron, whereas mechanical boosters utilize a hydraulic or an electric power supply contained within the airplane.

AERODYNAMIC BOOSTERS

In the most common type of aerodynamic booster, a tab is used to deflect the aileron. Such devices have been called servotabs, Flettner tabs, flying tabs, booster tabs, or spring tabs in previous papers. In the present paper a servotab is defined as the arrangement shown in figure 67(a) and an ordinary spring tab is defined as the arrangement shown in figure 67(b). A servotab is equivalent to a spring tab with the spring omitted. A modified arrangement that is herein called a geared spring tab is shown in figure 67(c). This

device differs from an ordinary spring tab in that when the aileron is moved with the stick free at zero airspeed, the tab deflects with respect to the aileron in the same manner as a conventional balancing (or unbalancing) tab.

Equations for Control Force

Equations for calculating the control-force characteristics of control surfaces with spring tabs have been derived by Gates of Great Britain. The characteristics of the ordinary spring tab (fig. 67(b)) are completely defined when the constants k_1, k_2, and k_3 are specified. These constants are defined by the following formulas in which δ_a and F are the deflection and the control force of an aileron, respectively, and δ_{st} is the spring-tab deflection:

$$\theta = k_1\delta_a + k_2\delta_{st} \tag{37}$$

$$F = k_3\delta_{st} \tag{38}$$

For the ordinary spring tab (fig. 67(b)) the relation between the control force, the aileron hinge moment, and tab hinge moment when the system is in equilibrium is given by the formula

$$-F = \frac{H_a}{rk_1}$$

$$= \frac{H_{st} + \delta_{st}rk_2k_3}{rk_2} \tag{39}$$

Within the range of linear hinge-moment characteristics, H_a and H_t can be expressed in terms of the aileron and tab hinge-moment parameters, and by means of equations (37) to (39) the following general equation can be derived for the stick force resulting from the deflection of one aileron:

$$F = -\frac{\delta_a}{rk_1}\left\{\frac{2\dfrac{(\Delta\alpha)_p}{\frac{pb}{2V}}\gamma'\dfrac{\Delta\alpha}{\Delta\delta}\left[\left(\dfrac{\partial C_{h_a}}{\partial\alpha}\right)_{tf}+\dfrac{rk_2k_3\left(\dfrac{\partial C_{h_a}}{\partial\alpha}\right)_{\delta_a,\delta_{st}}}{\left(\dfrac{\partial C_{h_{st}}}{\partial\delta_{st}}\right)_{\alpha,\delta_a}qb_{st}\bar{c}_{st}^{\,2}}\right]+\left[\left(\dfrac{\partial C_{h_a}}{\partial\delta_a}\right)_{tf}+\dfrac{rk_2k_3\left(\dfrac{\partial C_{h_a}}{\partial\delta_a}\right)_{\alpha,\delta_{st}}}{\left(\dfrac{\partial C_{h_{st}}}{\partial\delta_{st}}\right)_{\alpha,\delta_a}qb_{st}\bar{c}_{st}^{\,2}}\right]}{1-\dfrac{k_2\left(\dfrac{\partial C_{h_a}}{\partial\delta_{st}}\right)_{\alpha,\delta_a}b_a\bar{c}_a^{\,2}}{k_1\left(\dfrac{\partial C_{h_{st}}}{\partial\delta_{st}}\right)_{\alpha,\delta_a}b_{st}\bar{c}_{st}^{\,2}}+\dfrac{rk_2k_3}{\left(\dfrac{\partial C_{h_{st}}}{\partial\delta_{st}}\right)_{\alpha,\delta_a}qb_{st}\bar{c}_{st}^{\,2}}}\right\}qb_a\bar{c}_a^{\,2} \qquad (40)$$

In equation (40) values of $(\Delta\alpha)_p \Big/ \frac{pb}{2V}$ for any specific wing-aileron arrangement can be obtained from figure 3, and the tab-floating parameters $\left(\frac{\partial C_{h_a}}{\partial \alpha}\right)_{tf}$ and $\left(\frac{\partial C_{h_a}}{\partial \delta_a}\right)_{tf}$, which represent the variations of aileron hinge-moment coefficient against angle of attack and against aileron deflection with tab free, are defined by the expressions

$$\left(\frac{\partial C_{h_a}}{\partial \alpha}\right)_{tf} = \left(\frac{\partial C_{h_a}}{\partial \alpha}\right)_{\delta_a, \delta_{st}} - \frac{\left(\frac{\partial C_{h_{st}}}{\partial \alpha}\right)_{\delta_a, \delta_{st}} \left(\frac{\partial C_{h_a}}{\partial \delta_{st}}\right)_{\alpha, \delta_a}}{\left(\frac{\partial C_{h_{st}}}{\partial \delta_{st}}\right)_{\alpha, \delta_a}}$$

$$\left(\frac{\partial C_{h_a}}{\partial \delta_a}\right)_{tf} = \left(\frac{\partial C_{h_a}}{\partial \delta_a}\right)_{\alpha, \delta_{st}} - \frac{\left(\frac{\partial C_{h_{st}}}{\partial \delta_a}\right)_{\alpha, \delta_{st}} \left(\frac{\partial C_{h_a}}{\partial \delta_{st}}\right)_{\alpha, \delta_a}}{\left(\frac{\partial C_{h_{st}}}{\partial \delta_{st}}\right)_{\alpha, \delta_a}}$$

Equation (40) is directly applicable to an aileron with a spring tab. For an aileron with a servotab the constant k_3 is zero. Both the constants k_2 and k_3 are zero for an aileron without a tab.

Characteristics of Spring-Tab Ailerons

When applied to aileron control the spring tab provides the advantage of reducing the control force at high speeds to low values without making the control force unduly light at low speeds. The characteristic

variation of control force with indicated airspeed for spring-tab ailerons is shown in figure 68. The control-force variation with indicated airspeed is much less than that given by the "speed-squared" law. Various other types of control-force variation with indicated airspeed for a given aileron deflection may be obtained by aerodynamically balancing or overbalancing the tab. Some of these possibilities are illustrated in figure 69.

As a result of the smaller increase in control force with airspeed, the rolling velocity obtainable with a given control force may continue to increase with increasing airspeed for spring-tab ailerons, whereas for conventional aerodynamically balanced ailerons, the rolling velocity varies approximately inversely as the airspeed within the range for which the aileron deflection is limited by the control force.

The measured rolling-performance characteristics of an F6F-3 airplane equipped with the original production ailerons and with spring-tab ailerons are compared in figure 70. At an indicated airspeed of 400 miles per hour the value of $pb/2V$ obtainable with a stick force of 30 pounds was about 70 percent higher with the spring-tab ailerons than with the original production ailerons. At indicated airspeeds less than about 200 miles per hour, the spring-tab ailerons were less effective than the original ailerons because the amount of stick travel that was effective in deflecting the ailerons was reduced by the amount of stick travel required to deflect the spring tabs. A large part of the loss in aileron effectiveness that was encountered at low speeds with these ailerons probably could have been avoided by changing the gearing of the ailerons to increase the value of $\partial\delta_a/\partial\theta$ with tab locked.

The principal design difficulties introduced by the spring tab involve the provision of adequate structural strength to withstand the increased rolling velocities obtainable at high speeds and the problem of avoiding flutter. Although the use of spring tabs may allow large aileron deflections at high speeds, any danger of aileron overbalance because of compressibility effects or surface-covering distortion can be reduced because the ailerons do not have to be closely balanced.

Theoretical calculations of spring-tab flutter have shown that the aileron and the tab should be mass balanced about their hinge lines and that the tab balance weight should be close to the tab hinge line. The required mass-balance weight therefore may be rather large. Experimental evidence relating to the mass-balance weight required to prevent flutter is lacking; however, several production airplanes successfully use spring-tab ailerons with no mass balance on the tab. Any tendency toward flutter may be aggravated by slack in the linkage system of either the aileron or the tab.

Some spring-tab ailerons may have a tendency to float up symmetrically, especially in accelerated maneuvers at high speeds. This tendency is discussed in reference 87 and, as shown by Morgan, Bethwaite, and Nivison of Great Britain, it can be reduced by increasing the negative value of k_1/k_2. This upfloating tendency generally is not serious when the value of k_1/k_2 is more negative than -3.0.

Special Spring-Tab Designs

Use of preload.- If the spring in a spring tab is preloaded and any tab movement is thus prevented until a certain control force is exceeded, the control-force characteristics for forces below the preload are the same as those for an aileron without a tab; also, at forces above the preload the variation of force with deflection is the same as that for a spring-tab aileron without preload. At those speeds for which the tab may become operative, the variation of control force with aileron deflection therefore is nonlinear. The use of preload may be desirable in order to obtain increased effectiveness from the ailerons in low-speed flight. If a small amount of friction is present in the tab system, an amount of preload equal to the friction may be desirable to center the tab and therefore to avoid erratic changes in the lateral trim.

Geared spring tab.- By means of the geared spring-tab arrangement (fig. 67(c)), the control force required to deflect an aileron at low speeds may be reduced if the tab deflection has a balancing action or increased if the tab deflection has an unbalancing action. At

very high speeds the control-force characteristics are approximately the same for a geared spring tab and for an ordinary spring tab. An advantage of a spring tab geared to lead, or unbalance, the aileron is that at low airspeeds this arrangement may give greater aileron effectiveness per degree aileron deflection than an aileron without a tab. A discussion of the use of geared spring tabs for elevator control is given in reference 88, and with slight modifications the theoretical results derived in that report may be applied to aileron control.

Detached tab.- A detached tab, consisting of a tab mounted on booms that extend back from the trailing edge of the aileron, may have certain advantages over the more common inset tab. Because of the greater moment arm of the detached tab, a smaller tab area may be used. The adverse effect of the tab on the aileron effectiveness therefore is reduced. Preliminary calculations indicate that the detached tab may not have to be mass balanced in order to prevent tab-aileron flutter, although the aileron may require additional balancing weights in order to provide mass balance about the aileron hinge line. Detached tabs in the wing wake may, however, have a greater tendency to buffet than inset tabs. Wind-tunnel tests of a detached tab, as well as of conventional spring tabs, are reported in reference 89.

Other Aerodynamic Boosters

Very little work has been done on aerodynamic boosters that do not use tabs to deflect the ailerons. Some experimental work, however, has been done on a variable-pitch windmill that is used to drive the ailerons. This device was first tried on a British bomber in 1919. Wind-tunnel tests of a similar device, called the whirleron, were made recently in the Langley Laboratory of the NACA. The operation of this device is similar to the operation of a servotab except that the pilot's effort is used to change the pitch of the blades of a small windmill rather than to deflect a tab. A whirleron has an advantage over a tab in that the operation of a whirleron does not cause a decrease in aileron effectiveness. A very small windmill is required; for example, a windmill that is 9 inches in diameter should be adequate to deflect an aileron on an airplane of the medium-bomber class. Unpublished

results of wind-tunnel tests show that the whirleron is a promising means of control, but care is required in design to avoid undesirable control forces resulting from friction and from inertia effects on the windmill blades.

Another type of aerodynamic booster that has been proposed consists of a piston linked to the aileron and operated by the dynamic pressure of the air stream. Disadvantages of this device result from the difficulty of providing space for the piston size required and from the difficulty of avoiding high frictional forces.

MECHANICAL BOOSTERS

Several hydraulic and electrical booster systems have been tested, but only a few hydraulic boosters have proved at all successful for use on the primary flight controls. No attempt is made to describe herein the many hydraulic and electrical mechanisms that have been tried, but some general considerations as to the requirements of such systems are discussed. In order for the aileron-control characteristics obtained with a booster to be similar to those with the conventional control, the aileron position should be proportional to the stick position and the force exerted by the pilot should be multiplied by a constant. The maximum rate of movement of the aileron should equal or exceed the rate that can be applied by the pilot when conventional aerodynamically balanced ailerons are used. This requirement implies that a large amount of instantaneous power should be available to move the aileron for a short period of time. This requirement has in the past restricted the use of electrical boosters because of the heavy weight of the electrical equipment required to provide sufficient power. With a hydraulic mechanism energy may be stored in an accumulator to supply large amounts of power for rapid aileron movements, and the hydraulic pump need be only sufficiently large to supply the average power required by the booster over a long period of time.

The desired control feel has been supplied in some hydraulic booster mechanisms by a small piston connected to the control stick, which transmits a part of the force applied to the aileron back to the pilot. In

another system a direct mechanical linkage is used between the control stick and the control surface. The main disadvantages of hydraulic systems that have been used in the past are complication, vulnerability, and lack of reliability.

In spite of the generally poor results that have been obtained in the past with mechanical boosters, these devices probably will continue to be of interest, especially for airplanes intended to fly at high Mach numbers. For these cases, aerodynamic boosters may be unsatisfactory and some more positive means of operating the controls may be desirable. The use of a mechanical booster mechanism in connection with an irreversible aileron linkage seems to be a logical method for eliminating the possibility of aileron shake when shock occurs on a wing. Aileron mass balance probably is not necessary in an irreversible system.

VI - STRUCTURAL ASPECTS

A brief summary of the structural considerations related to lateral control seems desirable, even though some of these considerations already have been pointed out in various sections of the present paper.

INTEGRITY OF AIRPLANE

The problem of providing the strength necessary to prevent structural failure of any of the airplane components that are subjected to increased stress during a rolling maneuver becomes increasingly difficult as airplanes are designed for higher speeds. Variations in Mach number may cause large changes in the magnitude and in the distribution of the aerodynamic load on wings and on ailerons. The investigation reported in reference 74 shows that the aerodynamic load on a Frise aileron increases more rapidly with Mach number when the aileron is deflected negatively than when the aileron is deflected positively. The large sudden changes in the aileron load that usually take place when shock occurs on the wing may result in severe aileron shake, which imposes high dynamic loads on the wing, the aileron, the support

fittings, and the control linkage. The provision of a rigid control linkage is an aid to the pilot's ability to control any tendency toward shake.

A recent unpublished analysis indicates that the loads on the primary wing structure are likely to be higher during a rolling pull-out than during a simple pull-out and that the critical loading condition probably occurs in a maneuver that combines high rolling velocity and high rolling acceleration with the maximum normal acceleration.

Large positive internal aileron pressures have resulted in complete failure of fabric-covered ailerons and in failure of the rivets used to attach metal skin to aileron ribs. Loads of this type can be controlled to some extent by careful selection of the vent locations, but the possibility of high skin stresses resulting from inadvertent variations in the vent locations should not be overlooked.

The aileron hinge-moment characteristics must be considered in the structural design of the various components of the aileron linkage system. Ailerons having hinge-moment characteristics that are unsymmetrical with respect to zero aileron deflection may impose large loads in the linkage system even though the complete aileron system is closely balanced. For the same control forces, therefore, the loads in the linkage system may be much greater for Frise ailerons than for conventional arrangements of beveled ailerons or of ailerons having plain-overhang balances, internal balances, or tab balances.

A tendency toward severe chordwise flexural vibration of retractable-arc spoilers has occurred in some installations. Retractable-arc spoilers must be made sufficiently rigid to prevent vibration.

Vertical-tail failures have occurred as a result of sideslip caused by adverse aileron yawing moments in rolling pull-outs. Increased size of the vertical tail reduces the sideslip angle which, in turn, reduces the vertical-tail load. (See reference 8.)

ROLLING PERFORMANCE

For most conventional airplane designs, any flexibility of the wing or of the lateral-control system results in a loss in rolling performance, and the loss increases almost linearly with the dynamic pressure. Loss in rolling performance for given aileron deflections results from structural deformation of the wing and aileron. Loss in rolling performance because of decreased aileron deflections results from cable stretch or deformation of push-pull rods, bell cranks, pulleys, and pulley brackets.

Most present-day airplanes are required to meet a given standard of rolling performance. The required rigidity of the various structural components involved should therefore be specified from considerations of the required performance. The required torsional rigidity of the wing can be estimated conveniently by the use of methods discussed previously in the present paper.

CONTROL FORCES

In the process of estimating airplane control forces, a definite aileron contour and definite aileron deflections must be assumed. Contour deformations may cause large variations in control forces and, consequently, such deformations should be maintained at a minimum even though little possibility for structural failure exists. Variations in the relative deflections of the right and left ailerons, because of stretch in the control system, may result in undesirable control-force characteristics, particularly when a differential linkage system is used.

VII - APPLICATION OF EQUATIONS AND DESIGN CHARTS

ILLUSTRATIVE EXAMPLE

The procedure to be followed in the preliminary design of ailerons for specific airplanes depends to a

large extent on other aspects of the airplane design. In the present example an investigation is made of the various spanwise and chordwise parts of the wing that must be allocated to the aileron plus balance in order that specified rates of roll with specified stick forces may be obtained. The aileron configuration chosen in this design consists of a sealed internally balanced aileron with a combination of a spring tab and a linked tab. Equations and charts, which already have been presented in the present paper, are used in arriving at the various combinations of aileron and tab dimensions that would be expected to meet certain required conditions. The method used may be applied to ailerons having either exposed-overhang balances or beveled trailing-edge balances rather than the sealed internal balances that are considered herein.

The assumed airplane has the geometric constants and the wing plan form indicated in figure 43. The assumed performance requirements are that a value of $pb/2V$ of 0.09 be obtained with a stick force of 30 pounds for an airspeed of 320 miles per hour at sea level, and that the wing torsional stiffness should be such that the loss in $pb/2V$ resulting from wing twist does not exceed 20 percent at an airspeed of 400 miles per hour at sea level. Although these requirements concern only the high-speed flight condition, aileron characteristics at low airspeeds as well as at high airspeeds should be investigated in practice.

The chord ratios selected for the linked tab and the spring tab of each of the possible ailerons are

$$\frac{\bar{c}_{lt}}{\bar{c}_{a'}} = 0.25$$

$$\frac{\bar{c}_{st}}{\bar{c}_{a'}} = 0.25$$

These chord ratios were selected because they may be expected to produce approximately the maximum changes in aileron hinge moment for given changes in aileron effectiveness.

For an aileron with a spring tab, an aileron deflection exists above which the loss in aileron effectiveness resulting from increased spring-tab deflection is greater than the gain in aileron effectiveness resulting from increased aileron deflection. No advantage is obtained, therefore, in exceeding this deflection. For large airplanes or high-speed airplanes the value of this deflection corresponds approximately to the limits of the range of linear hinge-moment characteristics; for internally balanced ailerons the limits of this range are usually about $\pm 12^\circ$ or $\pm 15^\circ$. The maximum tab deflections should not greatly exceed the limits of the range of linear tab effectiveness. For the present example the following maximum deflections of the aileron and of the tabs, as used for each of the ailerons investigated, are assumed:

$$\delta_{a_{max}} = \pm 12^\circ$$

$$\delta_{lt_{max}} = \pm 15^\circ$$

$$\delta_{st_{max}} = \pm 15^\circ$$

Computations have been made of the geometric constants required for each of a number of ailerons when various values of $\frac{\bar{c}_b + \bar{c}_a}{\bar{c}}$ and of $\frac{\bar{c}_a}{\bar{c}}$ are assumed. The procedure is illustrated in detail only for the case of

$$\frac{\bar{c}_b + \bar{c}_a}{c} = 0.40$$

and

$$\frac{\bar{c}_a}{\bar{c}} = 0.25$$

The balance chord ratio therefore is

$$\frac{\bar{c}_b}{\bar{c}_a} = 0.60$$

The procedure used is as follows:

Step (1):

Compute the aileron effectiveness parameter $\frac{\Delta\alpha}{\Delta\delta}$. Values of $\left(\frac{\Delta\alpha}{\Delta\delta}\right)_o$ - the effectiveness parameter at low Mach numbers and at trailing-edge angles of about 10° - are given in figure 18. The effect of variations in trailing-edge angle is given in figure 19. A rough estimate of the effect of Mach number can be made by means of the data of figure 55. From this data a value of the factor $\left(\frac{\Delta\alpha}{\Delta\delta}\right)_M \Big/ \left(\frac{\Delta\alpha}{\Delta\delta}\right)_{M=0}$ corresponding to the trailing-edge angle of the proposed aileron is obtained by interpolating between the curves for the true-contour plain aileron and the beveled aileron at the Mach number of the design condition. A conservative value of the parameter $\frac{\Delta\alpha}{\Delta\delta}$ probably is yielded by this procedure because the data of figure 55 are given for small open nose gaps. The reduction in $\frac{\Delta\alpha}{\Delta\delta}$ with increased Mach number usually is greater when the nose gap is open than when the nose gap is sealed. For the present design condition, $\bar{\phi}$ = 15° (from fig. 12 and equation (18)), M = 0.42, and therefore

$$\frac{\Delta\alpha}{\Delta\delta} = 0.53 \times 0.98 \times 0.90$$

$$= 0.47$$

Step (2):

Estimate the aileron hinge-moment parameters. The hinge-moment parameters of a balanced aileron may be expressed by equations (16) and (17), in which the incremental parameters attributable to the balance are given by equations (21) and (22) for a trailing-edge modification, by equations (23) and (24) for an exposed overhang balance, by equations (27) and (28) for a sealed

internal balance, and by equation (35) for a linked tab. The value of C_{h_α} for the plain aileron is given by equation (15) in which $\left(C_{h_\alpha}\right)_{LL}$ may be obtained from equation (11). Equations for the hinge-moment parameters of an aileron with a completely sealed internal balance and with a linked tab therefore may be written as follows:

$$C_{h_\alpha} = \frac{C_{L_\alpha}}{c_{l_\alpha}} \left(c_{h_\alpha}\right)_{\substack{\text{plain}\\\text{aileron}}} + \left(\Delta C_{h_\alpha}\right)_{LS} + 0.14 \frac{A}{A + 2}\left(\frac{\bar{c}_a}{\bar{c}}\right)^2 F_1 \quad (41)$$

$$C_{h_\delta} = \left(C_{h_\delta}\right)_{\substack{\text{plain}\\\text{aileron}}} + 0.09 \frac{A}{A + 2}\sqrt{\frac{\bar{c}_a}{\bar{c}}}\, F_1 + \left(\Delta C_{h_\delta}\right)_{lt} \quad (42)$$

where the increment $\left(\Delta C_{h_\delta}\right)_{lt}$ is the increment of C_{h_δ} attributable to the linked tab and $\left(C_{h_\delta}\right)_{\substack{\text{plain}\\\text{aileron}}}$ must be estimated from test data. The ratio $C_{L_\alpha}/c_{l_\alpha}$ can be assumed to equal $\frac{A}{A + 2.5}$.

For the assumed airplane

$$\frac{C_{L_\alpha}}{c_{l_\alpha}} = \frac{6}{6 + 2.5}$$

$$= 0.706$$

$$c_{h_\alpha} = -0.0037 \qquad \text{(from fig. 13)}$$

$$\left(\Delta C_{h_\alpha}\right)_{LS} = 0.0014 \times 1.01$$

$$= 0.0014$$ (from fig. 11; the inboard aileron tip assumed to be located at $\frac{y_i}{b/2} = 0.55$. Relatively large variations in $\frac{y_i}{b/2}$ have only small effects on $\left(\Delta C_{h_\alpha}\right)_{LS}$.)

$$\frac{A}{A + 2} = \frac{6}{6 + 2}$$

$$= 0.75$$

$$\left(\frac{\bar{c}_a}{\bar{c}}\right)^2 = (0.25)^2$$

$$= 0.0625$$

$$\sqrt{\frac{\bar{c}_a}{\bar{c}}} = \sqrt{0.25}$$

$$= 0.5$$

$$F_1 = 0.338 \qquad \left(\text{from fig. 25 at } \frac{\bar{t}/2}{\bar{c}_a} = 0.15\right)$$

The value of C_{h_δ} for the plain aileron must be estimated from test data for a finite-span wing model having approximately the same geometric characteristics as the wing of the proposed airplane. A suitable model is that having the flat-sided aileron for which data are presented in figure D 35 of reference 42. The value of C_{h_δ} for that model is about -0.0044, the trailing-edge angle is 17.5°, and the seal and hinge line are located in such a manner that the aileron has a small effective overhang ($F_1 = 0.045$). The value of C_{h_δ} should be corrected to a trailing-edge angle of 15° and to $F_1 = 0$ by means of equations (22) and (28). For the proposed airplane, therefore

$$\left(C_{h_\delta}\right)_{\substack{\text{plain}\\ \text{aileron}}} = -0.0044 - 0.0007 - 0.0014$$

$$= -0.0065$$

Equations (41) and (42) now may be written as

$$C_{h_\alpha} = 0.706(-0.0037) + 0.0014 + (0.14 \times 0.75 \times 0.0625 \times 0.338)$$

$$= 0.0010$$

$$C_{h_\delta} = -0.0065 + (0.09 \times 0.75 \times 0.5 \times 0.338) + \left(\Delta C_{h_\delta}\right)_{lt}$$

$$= 0.0049 + \left(\Delta C_{h_\delta}\right)_{lt}$$

Step (3):

Estimate the balance requirements of the linked tab and of the spring tab. The value of $2(\Delta\alpha)_p/\Delta\delta_a$ in equation (36) may be assumed to equal -0.2; therefore

$$C_{h_\delta}\left(1 - 0.2\,\frac{C_{h_\alpha}}{C_{h_\delta}}\right) = -0.0020 \qquad (43)$$

The expressions obtained in step (2) for C_{h_α} and for C_{h_δ} now may be substituted in equation (43) as follows:

$$\left(\Delta C_{h_\delta}\right)_{lt} = -0.0020 + (0.2 \times 0.0010) - 0.0049$$

$$= -0.0067$$

The linked tab therefore is unbalancing. The linkage ratio, as determined from the maximum deflections of the aileron and of the linked tab, is

$$\frac{\partial\delta_{lt}}{\partial\delta_a} = \frac{15}{12}$$

$$= 1.25$$

For the purpose of estimating the required span ratio of the spring tab, the assumption is made in this example that the spring tab must be capable of providing aileron hinge moments that are approximately equal in magnitude to the hinge moments of the internally balanced aileron with linked tab; that is,

$$\left(\Delta C_{h_\delta}\right)_{st} = 0.0020$$

The choice of this increment should cause the size of the spring tab to be somewhat conservative.

Step (4):

Estimate the required span ratios of the spring tab and of the linked tab. For either tab, values of the factors F_4, F_5, and F_6 - obtained from equations (31), (32), and (33), respectively - are

$$F_4 = 0.50$$

$$F_5 = 0.90$$

$$F_6 = 0.71$$

Values of the ratio $\bar{c}_a'/\bar{c}_a$ in the expression for the factor F_3 (equation (30)) can be estimated by means of equation (34) provided the inboard ends of the tabs are at the inboard end of the aileron. For the present example the assumption is made that the inboard end of the spring tab is at the inboard end of the aileron and the linked tab is just outboard of the spring tab. In

order to determine the required span of the linked tab the combined span of the spring tab and the linked tab must first be determined. The required values of F_3 are, from equation (35), 0.23 for the spring tab and 0.99 for a fictitious tab having the combined span of the spring tab and the linked tab. From equation (34) and the expression for F_3 the required span ratios are

$$\frac{b_{st}}{b_a} = 0.17$$

$$\frac{b_{st} + b_{lt}}{b_a} = 0.95$$

and therefore

$$\frac{b_{lt}}{b_a} = 0.78$$

Step (5):

Compute the helix-angle reduction factors resulting from tab deflection. For either the linked tab or the spring tab

$$\frac{\left(\frac{\Delta\alpha}{\Delta\delta}\right)_{tab}}{\left(\frac{\Delta\alpha}{\Delta\delta}\right)_{aileron}} = \frac{0.21}{0.53}$$

$$= 0.395 \quad \text{(from fig. 18)}$$

Therefore, from equation (29),

$$k_{lt} = -0.78 \times 0.395 \times 1.25$$

$$= -0.384$$

$$k_{st} = -0.17 \times 0.395 \left(-\frac{15}{12}\right)$$

$$= 0.084$$

and the total reduction factor is

$$k_t = -0.384 + 0.084$$

$$= -0.300$$

Step (6):

Compute the helix-angle reduction factor resulting from wing twist. According to the assumed requirements, the torsional stiffness of the wing should be such that the loss in $pb/2V$ caused by wing twist should not exceed 20 percent for an airspeed of 400 miles per hour at sea level. For the design condition of an airspeed of 320 miles per hour at sea level, substitution in equation (9) of values of $q/\sqrt{1 - M^2}$ from figure 6 gives

$$k_T = 0.2 \times \frac{290}{480}$$

$$= 0.12$$

Step (7):

Estimate the helix-angle reduction factors resulting from adverse yaw. At an airspeed of 100 miles per hour at sea level, the value of the sum $k_r + k_\beta$ is estimated to be approximately 0.2. For level flight, the lift coefficient varies inversely as the square of the speed, and therefore, for an airspeed of 320 miles per hour at sea level, equation (10) gives

$$k_r + k_\beta = 0.2 \frac{100^2}{320^2}$$

$$= 0.02$$

Step (8):

Compute the required aileron span ratio. The various helix-angle reduction factors that have been evaluated in the preceding steps now may be substituted in equation (3). For a value of $pb/2V$ of 0.09

$$\tau' = \frac{0.09}{0.47 \times 24 \times (1 - 0.12 - 0.02 + 0.30)}$$

$$= 0.0068$$

For an outboard aileron tip location of $0.97\frac{b}{2}$, the inboard aileron tip location, as determined from figure 2, is $0.62\frac{b}{2}$. The aileron span ratio therefore is

$$\frac{b_a}{b/2} = 0.97 - 0.62$$

$$= 0.35$$

Step (9):

Compute the required wing torsional stiffness. For the present case, the quantity $\tau'\left(\frac{\partial c_m}{\partial \alpha}\right)_{c_l}$ in equation (8) must be evaluated for the aileron, the linked tab, and the spring tab. Values of τ' and $\left(\frac{\partial c_m}{\partial \alpha}\right)_{c_l}$ may be obtained from figures 5 and 20, respectively. Therefore

$$\left[\tau'\left(\frac{\partial c_m}{\partial \alpha}\right)_{c_l}\right]_{\text{aileron}} = 0.114 \times 0.018$$

$$= 0.00206$$

$$\left[\tau'\left(\frac{\partial c_m}{\partial \alpha}\right)_{c_l}\right]_{\substack{\text{linked} \\ \text{tab}}} = 0.118 \times 0.026$$

$$= 0.00307$$

$$\left[\tau'\left(\frac{\partial c_m}{\partial \alpha}\right)_{c_l}\right]_{\substack{\text{spring}\\ \text{tab}}} = 0.114 \times 0.026$$

$$= 0.00297$$

and the required wing torsional stiffness at station y is, from equation (8)

$$m_{\theta_y} = \frac{1}{\left(\frac{y}{b/2}\right)^3} \frac{43^3}{2 \times 6^2 \times 0.12} \cdot (0.00206 + 0.00118 - 0.00025)\ 290$$

$$= \frac{7900}{\left(\frac{y}{b/2}\right)^3} \quad \text{foot-pounds per degree}$$

The torsional stiffness frequently is specified at the aileron midspan. For the present example the aileron midspan is at $\frac{y}{b/2} = 0.79$, and the required torsional stiffness at that location is

$$m_{\theta_y} = \frac{7900}{0.79^3}$$

$$= 16{,}000 \text{ foot-pounds per degree}$$

Step (10):

Calculate the spring stiffness and the mechanical linkage of the aileron-spring-tab system by means of equations (37) and (39). In this process a value for the ratio k_1/k_2 must be selected. Expressions for the aileron hinge moment H_a and for the tab hinge moment

H_{st} must be obtained in terms of the spring-tab deflection δ_{st}. For the present example

$$\theta_{s_{max}} = 14.8^\circ$$

$$\delta_{a_{max}} = 12^\circ$$

$$r = 2.33 \text{ feet}$$

$$F_s = -\frac{30}{2}$$

$$= -15 \text{ pounds}$$

$$\bar{c}_a = 1.44 \text{ feet}$$

$$b_a = 7.5 \text{ feet}$$

$$\bar{c}_{st} = 0.36 \text{ feet}$$

$$b_{st} = 1.3 \text{ feet}$$

$$q = 262 \text{ pounds per square foot}$$

and it is assumed that

$$\frac{k_1}{k_2} = -3.0 \tag{44}$$

The aileron hinge moment is given by

$$H_a = qb_a\bar{c}_a^2\left[\delta_a c_{h_\delta}\left(1 - 0.2\,\frac{c_{h_\alpha}}{c_{h_\delta}}\right) + \delta_{st}\,\frac{\partial c_{h_a}}{\partial \delta_{st}}\right]$$

in which

$$\frac{\partial C_{h_a}}{\partial \delta_{st}} = \frac{\delta_{a_{max}}}{\delta_{st_{max}}} \left(\Delta C_{h_\delta}\right)_{st}$$

or

$$\frac{\partial C_{h_a}}{\partial \delta_{st}} = -\frac{12}{15} \times 0.0020$$

$$= -0.0016$$

Therefore

$$H_a = 262 \times 7.50 \times 1.44^2 \left[12(-0.0020) + \delta_{st}(-0.0016)\right]$$

$$= -97.6 - 6.5\delta_{st}$$

The spring-tab hinge moment is approximately

$$H_{st} = qb_{st}\bar{c}_{st}^2\delta_{st} \frac{\partial C_{h_{st}}}{\partial \delta_{st}}$$

where the value of $\frac{\partial C_{h_{st}}}{\partial \delta_{st}}$ is estimated by extrapolating the data of figure 13 to be approximately -0.0060. Therefore

$$H_{st} = 262 \times 1.30 \times 0.362 \times \delta_{st} \times (-0.0060)$$

$$= -0.265\delta_{st}$$

The expressions thus obtained for H_a and H_{st}, when substituted in equation (39), give

$$-15 = \frac{-41.9 - 2.79\delta_{st}}{k_1} \tag{45}$$

and

$$-15 = -\frac{0.114\delta_{st}}{k_2} + \delta_{st}k_3 \tag{46}$$

Equation (37) may be written as

$$14.8 = 12k_1 + k_2\delta_{st} \tag{47}$$

A simultaneous solution of equations (44), (45), (46), and (47) yields

$$\delta_{st} = -9.8^\circ$$

$$k_1 = 0.97$$

$$k_2 = -0.323$$

$$k_3 = 1.18 \text{ pounds per degree}$$

The required value of δ_{st} is smaller than the value ($\delta_{st} = -15^\circ$) that was assumed originally. Some margin in spring-tab deflection should be provided, however, to allow for deviations from the conditions assumed in the preliminary design.

DISCUSSION

Computations similar to those made in the section entitled "Illustrative Example, Part VII," have been made for many assumed values of $\frac{\bar{c}_a + \bar{c}_b}{\bar{c}}$ and $\frac{\bar{c}_a}{\bar{c}}$ of internally balanced ailerons. The results are presented

in figure 71. The computations were made for the general case in which consideration is given to ailerons having spring tabs as well as either balancing or unbalancing linked tabs. For specific preliminary-design problems, the investigation may be limited to ailerons having spring tabs and balancing tabs, or to ailerons having only a spring tab, only a linked tab, or no tabs. Considerations regarding the wing structure and the required span of the lift flap usually impose limitations on the chordwise and the spanwise parts of the wing that can be allocated to the ailerons. For the usual case, therefore, the number of aileron configurations that needs be investigated is much less than the number that was considered in order to obtain the data of figure 71.

The results presented in figure 71 indicate that for a given value of $\frac{\bar{c}_a + \bar{c}_b}{\bar{c}}$, the required aileron span is reduced when the hinge axis is moved toward the rear, that is, when the aileron chord c_a is decreased and the balance chord c_b is increased. The decrease in the required aileron span results from the fact that the favorable effect of the variation in the configuration of the linked tab more than compensates for the unfavorable effect of the decrease in aileron chord. For a given percentage loss in $pb/2V$ resulting from wing twist, however, the required wing stiffness increases rapidly as the hinge axis is moved toward the rear. For an aileron not equipped with a linked tab, both the required aileron span and the required wing stiffness are reduced as the aileron chord c_a is increased.

VIII - STATUS OF LATERAL-CONTROL RESEARCH

In the preparation of the present paper, an attempt has been made to discuss rather completely the problems associated with lateral control and to present the available information that is believed to be most useful in the aerodynamic design of lateral-control devices. The inadequacy of the available information for application to some of the airplanes now contemplated is fully

appreciated. This section is therefore included in the present paper in order to establish the present status of some of the most important phases of lateral-control research and to indicate some of the lateral-control problems that remain to be investigated.

Rapid advances in airplane design have increased the importance of certain variables that previously have been largely neglected. These variables are associated primarily with high-speed effects and with the effects of the large changes in boundary-layer conditions that may possibly occur on wings designed for favorable pressure gradients over a large part of the chord.

CONVENTIONAL FLAP-TYPE AILERONS

Rolling Performance

In general, the rolling performance of an airplane at low Mach numbers and at given aileron deflections can be predicted with sufficient accuracy from the available analytical methods provided that a reasonably accurate estimate can be made of the wing torsional rigidity. Reliable estimates of the rolling performance at high Mach numbers can be made only when experimental data on the aileron effectiveness parameter $\Delta\alpha/\Delta\delta$ at the appropriate Mach numbers are available. Reductions in $\Delta\alpha/\Delta\delta$ that usually result from increased Mach number cannot be predicted from the present theory, and the available experimental data are insufficient for accurate quantitative estimates of the variation of $\Delta\alpha/\Delta\delta$ with Mach number for arbitrary wing-aileron arrangements. The available data indicate, however, that as the Mach number is increased to that at which shock occurs on the wing, the smallest reduction in aileron effectiveness is obtained when the aileron nose gap is sealed and when the trailing-edge angle is small. Large losses in aileron effectiveness may occur for any aileron when the Mach number at which shock occurs on the wing is exceeded. The addition of a protruding nose balance usually causes the Mach number at which shock occurs to be decreased.

Hinge Moments

For airplanes not equipped with booster devices the aileron hinge moments usually are of no less importance than the aileron effectiveness. Even though booster devices are used, a reasonably accurate knowledge of the aileron hinge-moment characteristics is necessary for the design of an efficient lateral-control system. The available methods for predicting hinge-moment characteristics are not considered to be sufficiently reliable for direct application to the design of ailerons of a full-scale airplane.

Analytical methods of predicting hinge moments involve the following two fundamental steps:

(1) Determination of the section aileron hinge-moment characteristics

(2) Application of corrections to account for the effects of finite aspect ratio

Section hinge-moment characteristics calculated by methods based on potential-flow theory are very different from the measured characteristics for most airfoil sections, even when laminar flow can be maintained over as much as 60 percent of the airfoil chord. Methods based on viscous-flow theory appear to give results that at low Mach numbers are close to the experimental results for ailerons having small trailing-edge angles. The viscous-flow theory takes into account the transition location and gives a reasonably accurate indication of the effects of changes in the transition location for airfoils having small trailing-edge angles. At the present time, however, the influence of the airfoil shape - particularly the trailing-edge angle - on the aileron hinge-moment characteristics is not adequately accounted for by the viscous-flow theory. The necessity for deriving aspect-ratio corrections to the hinge-moment parameters by methods based on lifting-surface theory, rather than on lifting-line theory, is pointed out in reference 37. At the present time, lifting-surface-theory aspect-ratio corrections have been obtained for the parameter C_{h_α} but not for the parameter C_{h_δ}.

Reasonably accurate estimates of the hinge-moment characteristics of balanced ailerons, at low Mach numbers and under conditions for which transition can be

expected to occur near the airfoil leading edge, can be made by means of the test data of reference 42 and the correlations presented herein.

The available experimental data are insufficient to permit any reliable estimates to be made of the hinge-moment characteristics that may occur at high Mach numbers. Because the effects of Mach number appear to be critically dependent on certain geometric properties of wings and ailerons, a systematic investigation is needed to establish the relative effects of the various geometric parameters on the hinge-moment characteristics and to determine any configurations for which the Mach number effects are a minimum.

Some knowledge of the boundary-layer conditions on the wing of an airplane in flight is necessary in order that any reliable prediction of aileron hinge-moment characteristics may be made either by means of viscous-flow theory or by means of wind-tunnel data. For present-day production airplanes, the assumption usually can be made that the existing boundary-layer conditions correspond to a transition location near the wing leading edge, whether or not the wing is designed for favorable pressure gradients over a large part of the chord. Information is needed, however, on the variations in the boundary-layer conditions that may possibly result from improvements in manufacturing methods and in airfoil design.

In view of the large variations in hinge-moment characteristics that may result from manufacturing irregularities, surface-covering distortion, Mach number effects, or possible boundary-layer effects, the use of nonadjustable aerodynamic balances to provide acceptable control forces on large airplanes or on high-speed airplanes is not considered practical. Satisfactory characteristics sometimes can be obtained by adjusting the amount of leakage in an internal balance or by changing the linkage of a balancing tab. The use of some type of booster mechanism probably will be necessary, however, for most future high-performance airplanes. Some aerodynamic balance is desirable, nevertheless, in order to minimize the required capacity of the booster mechanism and in order that some lateral control can be obtained in case of failure of the booster mechanism. The spring tab has proved to be a satisfactory booster mechanism for many present-day airplanes. When a spring

tab is applied to very large airplanes, however, some aerodynamic balance on the tab may be necessary. Information is needed on the most efficient methods of providing aerodynamic balance on tabs. A mechanical booster mechanism, used in conjunction with irreversible aileron motion, seems most desirable for airplanes designed to fly at speeds at which shock occurs on the wing.

SPOILER DEVICES

A large amount of work has been done on the development of spoiler-type lateral-control devices for small low-speed airplanes. Very little information is available, however, on the characteristics of spoilers at high speeds. The high-speed data that are available indicate that the effectiveness of a spoiler located near the wing trailing edge, like the effectiveness of a conventional flap-type aileron, may be reduced considerably when shock occurs on the wing. Investigations should be made to determine whether improved spoiler effectiveness and satisfactory lag characteristics can be obtained at high speeds by locating the spoiler at some chordwise location other than that established on the basis of low-speed data. Information also is needed on spoiler hinge moments at high speeds, on means of preventing vibration or buffeting, and on the effects of variations in airfoil contour on spoiler characteristics.

LATERAL CONTROL WITH SWEPT WINGS

The possibility of raising the critical speeds of wings by using large amounts of sweep is indicated by the results of a theoretical analysis presented in reference 90. The theory indicates that at lift coefficients near zero the critical Mach number of a wing with sweep is approximately equal to the critical Mach number of the same wing without sweep divided by the cosine of the angle of sweep. A few unpublished experiments have provided at least a qualitative verification of the theory. High angles of sweep are required if the value of the critical flight Mach number is to be raised appreciably above 1.0.

Although the use of large angles of sweep may provide definite advantages at high speeds, certain important problems associated with low-speed lateral-control characteristics are indicated by the results of tests reported in reference 91. Figure 72 shows that for a given deflection in a plane perpendicular to the aileron hinge line, the rolling-moment coefficient caused by a flap-type aileron decreases rapidly with increased angle of sweepback. The rolling-moment coefficient caused by a spoiler located at 0.7c and projected a given distance above a wing surface is affected by angle of sweepback even more than the rolling-moment coefficient caused by a flap-type aileron (fig. 72).

The indicated effect of sweepback on the rolling-moment coefficients (fig. 72) is not a direct indication of the effect of sweepback on the helix angle $pb/2V$ because the value of $pb/2V$ depends on the value of the damping coefficient C_{l_p} as well as on the value of the rolling-moment coefficient. Results obtained from tests in the Langley free-flight tunnel and in the Langley stability tunnel show that the value of the damping coefficient C_{l_p} is reduced as the angle of sweepback is increased.

A fundamental characteristic of swept-back wings is that for a given angle of sweepback the effective dihedral, indicated by the value of the parameter C_{l_ψ}, increases rapidly as the lift coefficient is increased. The test data of figure 73 indicate that for a wing having an angle of sweepback of 45° a rolling-moment coefficient of approximately 0.04 must be provided by a lateral-control device in order to maintain lateral trim at an angle of sideslip of 10° when the wing lift coefficient is 0.6. For the flap-type ailerons considered in figure 72 a total aileron deflection of about 40° must be used in order to supply the required value of the rolling-moment coefficient. The design of a device capable of providing lateral trim and some lateral maneuverability at high angles of sideslip therefore may be very difficult.

The tests that have been made of wings having large amounts of sweep have been conducted primarily for the purpose of exploring the nature of the problems involved. Few, if any, attempts have been made to develop lateral-control devices specifically for swept wings. Because

the problems associated with lateral control, particularly at high lift coefficients, seem to be of a rather serious nature, a large amount of development work is required. Satisfactory solutions of these problems may require that lateral control with swept wings be obtained by devices that are considerably different in principal from either the conventional flap-type ailerons or the spoiler devices that are being used on present-day airplanes.

Langley Memorial Aeronautical Laboratory
National Advisory Committee for Aeronautics
Langley Field, Va., February 14, 1946

APPENDIX

DEFINITIONS OF SYMBOLS

Definitions are given herein of most of the symbols used in the present paper. Symbols having a very restricted usage in the present paper are defined as they are introduced. Although some experimental data on control surfaces other than ailerons are used for illustrative purposes and for the development of correlations, aileron symbols are employed in referring to experimental data regardless of the type of control surface involved. The various spans and the various chords that are referred to in the following list of symbols are measured perpendicular and parallel, respectively, to the plane of symmetry of the airplane. The various deflections are measured in planes perpendicular to the hinge lines.

c_l airfoil section lift coefficient

c_{l_1} additional lift coefficient at a section caused by an angle-of-attack change over wing

c_n airfoil section normal-force coefficient

c_m airfoil section pitching-moment coefficient

c_{h_a} aileron section hinge-moment coefficient

C_L wing lift coefficient

C_l rolling-moment coefficient

C_n yawing-moment coefficient

C_{h_a} hinge-moment coefficient of aileron $\left(\frac{H_a}{qb_a\bar{c}_a^2}\right)$

C_{h_s} spoiler hinge-moment coefficient $\left(\frac{H_s}{qb_s\bar{c}_s\bar{d}}\right)$

C_{h_t} tab hinge-moment coefficient $\left(\frac{H_t}{qb_t\bar{c}_t^2}\right)$

C_{l_p}	damping coefficient, that is, rate of change of rolling-moment coefficient C_l with wing-tip helix angle $pb/2V$
P	pressure coefficient
P_R	resultant pressure coefficient ($P_{Lower} - P_{Upper}$)
m_s	seal moment ratio for internally balanced aileron; ratio of balancing moment of flexible seal to balancing moment of thin-plate overhang
$pb/2V$	helix angle of roll, radians
p	angular velocity in roll, radians/sec
b	span of wing, ft
V	true airspeed, ft/sec unless otherwise noted
V_i	indicated airspeed, mph
F	control force (stick force with subscript s, wheel force with subscript w), lb
H_a	aileron hinge moment, ft-lb
H_t	tab hinge moment, ft-lb
H_s	spoiler hinge moment, ft-lb
q	dynamic pressure, lb/sq ft ($\rho V^2/2$)
ρ	mass density of air, slugs/cu ft
σ	ratio of mass density of air at altitude to mass density of air at standard sea-level conditions
b_a	span of aileron, ft
b_b	span of balance, ft
b_s	span of spoiler, ft
b_t	span of tab, ft

$\bar{c}_s$	root-mean-square of upper-surface width of spoiler, ft
d	distance from spoiler hinge axis to midpoint of upper-surface width of spoiler, ft
$\bar{d}$	root-mean-square of distance from spoiler hinge axis to midpoint of upper-surface width of spoiler, ft
t	airfoil section thickness at aileron hinge line, ft
$\bar{t}$	root-mean-square of airfoil section thickness at aileron hinge line over span of aileron, ft
$\bar{t}'$	root-mean-square of airfoil section thickness at aileron hinge line over span of tab, ft
α	angle of attack, deg unless otherwise indicated
$(\Delta\alpha)_p$	effective change in angle of attack caused by rolling velocity, deg
δ_a	deflection of aileron, deg
$\Delta\delta_a$	total deflection of right and left ailerons, deg
$\delta_{a_{cr}}$	critical aileron deflection; that is, deflection at which plain-overhang or Frise balance is no longer effective in reducing slope of hinge-moment curve, deg
δ_t	deflection of tab, deg
δ_f	deflection of lift flap, deg
δ_{bp}	deflection of balance plate of internally balanced ailerons (positive when attached aileron is deflected positively), deg
$\delta_{bp_{limit}}$	limiting deflection of balance plate when horizontal balance-chamber cover plates are used, deg

θ	angular deflection of control (stick deflection with subscript s, wheel deflection with subscript w), deg
β	angle of sideslip, deg
ψ	angle of yaw, deg
ϕ	trailing-edge angle at any aileron section, deg
$\bar{\phi}$	effective aileron trailing-edge angle, deg
y	distance from plane of symmetry to any spanwise station, ft
y_i	distance from plane of symmetry to inboard end of aileron, ft
y_o	distance from plane of symmetry to outboard end of aileron, ft
y_1	distance from plane of symmetry to inboard end of tab, ft
y_2	distance from plane of symmetry to outboard end of tab, ft
l	chordwise location of minimum pressure point for low-drag airfoils, measured in airfoil chords from leading edge
r	moment arm of point of application of control force; that is, control stick length or control wheel radius, ft
s	width of flexible seal of internally balanced aileron, expressed as a fraction of the balance plate chord c_{bp}
g	gap between leading edge of undeflected balance plate and forward wall of balance chamber of internally balanced aileron, expressed as a fraction of the balance-plate chord c_{bp}
A	aspect ratio (b^2/S)

λ wing taper ratio; ratio of wing-tip chord to wing-root chord

M Mach number; also, with subscripts O, A, B, and so forth of figure 24, area moment of exposed-overhang-balance profile about hinge axis

R Reynolds number; also, with subscripts O, A, B, and so forth of figure 24, nose radius of exposed-overhang balance

B_1 factor used in evaluating $(\Delta\alpha)_p$

B_2 factor used in evaluating $\left(\Delta C_{h_\alpha}\right)_{LS}$

F_1, F_2, F_2', F_3, F_4, F_5, F_6 correlation factors

k_1 ratio between angular deflection of control (stick or wheel) and aileron deflection with spring tab fixed

k_2 ratio between angular deflection of control (stick or wheel) and spring-tab deflection with aileron fixed

k_3 ratio of control force to spring-tab deflection when aileron is held fixed and airspeed is zero, lb/deg

k_τ helix-angle reduction factor resulting from wing twist

k_β helix-angle reduction factor resulting from sideslip angle

k_r helix-angle reduction factor resulting from yawing velocity

k_t helix-angle reduction factor resulting from tab deflection

$$c_{l_\alpha} = \left(\frac{\partial c_l}{\partial \alpha}\right)_{\delta_a}$$

$$c_{n_\alpha} = \left(\frac{\partial c_n}{\partial \alpha}\right)_{\delta_a}$$

$$c_{n_\delta} = \left(\frac{\partial c_n}{\partial \delta_a}\right)_{\alpha}$$

$$c_{h_\alpha} = \left(\frac{\partial c_{h_a}}{\partial \alpha}\right)_{\delta_a}$$

$$c_{h_\delta} = \left(\frac{\partial c_{h_\alpha}}{\partial \delta_a}\right)_{\alpha}$$

$$C_{L_\alpha} = \left(\frac{\partial C_L}{\partial \alpha}\right)_{\delta_a}$$

$$c_{l_\delta} = \left(\frac{\partial c_l}{\partial \delta_a}\right)_{\alpha}$$

$$c_{l_\psi} = \left(\frac{\partial c_l}{\partial \psi}\right)_{C_L}$$

$$c_{n_\beta} = \left(\frac{\partial c_n}{\partial \beta}\right)$$

$$c_{h_\alpha} = \left(\frac{\partial c_{h_a}}{\partial \alpha}\right)_{\delta_a}$$

$$C_{h_\delta} = \left(\frac{\partial C_{h_a}}{\partial \delta_a}\right)_\alpha$$

$$P_{R_\alpha} = \left(\frac{\partial P_R}{\partial \alpha}\right)_{\delta_a}$$

$$P_{R_\delta} = \left(\frac{\partial P_R}{\partial \delta_a}\right)_\alpha$$

The subscripts outside the parentheses of the foregoing partial derivatives indicate the factors held constant during measurement of the derivatives.

$\left(C_{h_\alpha}\right)_{LL}$ value of C_{h_α} computed by means of lifting-line theory

$\left(C_{h_\delta}\right)_{LL}$ value of C_{h_δ} computed by means of lifting-line theory

$\left(\Delta C_{h_\alpha}\right)_{LS}$ lifting-surface-theory correction to $\left(C_{h_\alpha}\right)_{LL}$

$\frac{\Delta\alpha}{\Delta\delta}$ aileron effectiveness parameter; effective change in section angle of attack per unit change in aileron deflection

$\left(\frac{\Delta\alpha}{\Delta\delta}\right)_o$ aileron effectiveness parameter for a trailing-edge angle of approximately 10° and for Mach numbers approaching zero (values of fig. 18)

$\left(\frac{\Delta\alpha}{\Delta\delta}\right)_\phi$ aileron effectiveness parameter for a trailing-edge angle ϕ and for Mach numbers approaching zero

$\left(\frac{\Delta\alpha}{\Delta\delta}\right)_{M=0}$ aileron effectiveness parameter for Mach numbers approaching zero

$\left(\frac{\Delta\alpha}{\Delta\delta}\right)_M$ aileron effectiveness parameter for a Mach number M

γ' helix-angle parameter $\left(\frac{C_{l_\delta}/\frac{\Delta\alpha}{\Delta\delta}}{C_{l_p}}\right)$

τ' rolling-moment-loss parameter

m_{θ_y} wing torsional stiffness at station y, ft-lb/deg

k_X radius of gyration about longitudinal axis; fraction of wing span

Subscripts *lt* and st when used in place of the general subscript t, for tabs, refer to linked tabs and to spring tabs, respectively.

REFERENCES

1. Weick, Fred E., and Jones, Robert T.: Résumé and Analysis of N.A.C.A. Lateral Control Research. NACA Rep. No. 605, 1937.

2. Gilruth, R. R., and Turner, W. N.: Lateral Control Required for Satisfactory Flying Qualities Based on Flight Tests of Numerous Airplanes. NACA Rep. No. 715, 1941.

3. Soulé, H. A., and Harmon, S. M.: A Study of the Effect of Increased Size and Speed of Pursuit Airplanes on the Aileron Balancing Problem. NACA RB, Nov. 1942.

4. Lawrence, T. F. C.: Aileron Performance Analysis. Aerodynamics Note No. 50, Council for Sci. and Ind. Res., Commonwealth of Australia, Aug. 1944.

5. Gilruth, R. R.: Requirements for Satisfactory Flying Qualities of Airplanes. NACA ACR, April 1941.

6. Anon.: Stability and Control Characteristics of Airplanes. AAF Specification No. R-1815-A, April 7, 1945.

7. Anon.: Specification for Stability and Control Characteristics of Airplanes. SR-119A, Bur. Aero., April 7, 1945.

8. Gilruth, Robert R.: Analysis of Vertical-Tail Loads in Rolling Pull-Out Maneuvers. NACA CB No. L4H14, 1944.

9. Pearson, Henry A., and Jones, Robert T.: Theoretical Stability and Control Characteristics of Wings with Various Amounts of Taper and Twist. NACA Rep. No. 635, 1938.

10. Swanson, Robert S., and Toll, Thomas A.: Estimation of Stick Forces from Wind-Tunnel Aileron Data. NACA ARR No. 3J29, 1943.

11. Swanson, Robert S., and Priddy, E. LaVerne.: Lifting-Surface-Theory Values of the Damping in Roll and of the Parameter Used in Estimating Aileron Stick Forces. NACA ARR No. L5F23, 1945.

12. Goldstein, S., and Young, A. D.: The Linear Perturbation Theory of Compressible Flow, with Applications to Wind-Tunnel Interference. R. & M. No. 1909, British A.R.C., 1943.

13. Pearson, Henry A., and Aiken, William S., Jr.: Charts for the Determination of Wing Torsional Stiffness Required for Specified Rolling Characteristics or Aileron Reversal Speed. NACA ACR No. L4L13, 1944.

14. Harmon, Sidney M.: Determination of the Effect of Wing Flexibility on Lateral Maneuverability and a Comparison of Calculated Rolling Effectiveness with Flight Results. NACA ARR No. 4A28, 1944.

15. Pugsley, A. G.: The Aerodynamic Characteristics of a Semi-Rigid Wing Relevant to the Problem of Loss of Lateral Control Due to Wing Twisting. R. & M. No. 1490, British A.R.C., 1932.

16. Cox, H. Roxbee, and Pugsley, A. G.: Theory of Loss of Lateral Control Due to Wing Twisting. R. & M. No. 1506, British A.R.C., 1933.

17. Pugsley, A. G., and Brooke, G. R.: The Calculation by Successive Approximation of the Critical Reversal Speed for an Elastic Wing. R. & M. No. 1508, British A.R.C., 1933.

18. Hirst, D. M.: On the Calculation of the Critical Reversal Speeds of Wings. R. & M. No. 1568, British A.R.C., 1934.

19. Shornick, Louis H.: The Computation of the Critical Speeds of Aileron Reversal, Wing Torsional Divergence and Wing-Aileron Divergence. MR No. ENG-M-51/VF18, Addendum 1, Materiel Center, Army Air Forces, Dec. 19, 1942.

20. Horton, W. H.: Critical Reversal Speed. Aircraft Engineering, vol. XV, no. 177, Nov. 1943, pp. 319-324.

21. Rosenberg, Reinhardt: Loss in Aileron Effectiveness Because of Wing Twist and Considerations Regarding the Internal-Pressure Balanced Aileron. Jour. Aero. Sci., vol. 11, no. 1, Jan. 1944, pp. 41-47.

22. Fehlner, Leo F.: A Study of the Effects of Vertical Tail Area and Dihedral on the Lateral Maneuverability of an Airplane. NACA ARR, Oct. 1941.

23. Fehlner, Leo F.: A Study of the Effect of Adverse Yawing Moment on Lateral Maneuverability at a High Lift Coefficient. NACA ARR, Sept. 1942.

24. Fehlner, Leo F.: A Study of the Effects of Radii of Gyration and Altitude on Aileron Effectiveness at High Speed. NACA RB No. 3D26, 1943.

25. Cohen, Doris: A Theoretical Investigation of the Rolling Oscillations of an Airplane with Ailerons Free. NACA ARR No. 4A06, 1944.

26. Theodorsen, Theodore: General Theory of Aerodynamic Instability and the Mechanism of Flutter. NACA Rep. No. 496, 1935.

27. Theodorsen, Theodore, and Garrick, I. E.: Mechanism of Flutter - A Theoretical and Experimental Investigation of the Flutter Problem. NACA Rep. No. 685, 1940.

28. Flax, Alexander H.: Three-Dimensional Wing Flutter Analysis. Jour. Aero. Sci., vol. 10, no. 2, Feb. 1943, pp. 41-47.

29. Küssner, H. G., and Schwarz, L.: The Oscillating Wing with Aerodynamically Balanced Elevator. NACA TM No. 991, 1941.

30. Theodorsen, Theodore, and Garrick, I. E.: Nonstationary Flow about a Wing-Aileron-Tab Combination Including Aerodynamic Balance. NACA Rep. No. 736, 1942.

31. Jones, W. P.: Aerodynamic Forces on an Oscillating Aerofoil-Aileron-Tab Combination. R. & M. No. 1948, British A.R.C., 1941.

32. Krzywoblocki, Zbigniew: Torsional and Aileron Flutter. Jour. Aero. Sci., vol. 10, no. 5, May 1943, pp. 161-168.

33. Becker, John V., and Korycinski, Peter F.: Aerodynamic Tests of a Full-Scale TBF-1 Aileron Installation in the Langley 16-Foot High-Speed Tunnel. NACA ARR No. L4K22, 1944.

34. Cohen, Doris: A Method for Determining the Camber and Twist of a Surface to Support a Given Distribution of Lift. NACA TN No. 855, 1942.

35. Ames, Milton B., Jr., and Sears, Richard I.: Determination of Control-Surface Characteristics from NACA Plain-Flap and Tab Data. NACA Rep. No. 721, 1941.

36. Wood, K. D.: Aspect Ratio Corrections. Jour. Aero. Sci., vol. 10, no. 8, Oct. 1943, pp. 270-272.

37. Swanson, Robert S., and Gillis, Clarence L.: Limitations of Lifting-Line Theory for Estimation of Aileron Hinge-Moment Characteristics. NACA CB No. 3L02, 1943.

38. Anderson, Raymond F.: Determination of the Characteristics of Tapered Wings. NACA Rep. No. 572, 1936.

39. Wolowicz, Chester H.: Prediction of Motions of an Airplane Resulting from Abrupt Movement of Lateral or Directional Controls. NACA ARR No. L5E02, 1945.

40. Jones, Robert T., and Cohen, Doris: Determination of Optimum Plan Forms for Control Surfaces. NACA Rep. No. 731, 1942.

41. Weick, Fred E., Soulé, Hartley A., and Gough, Melvin N.: A Flight Investigation of the Lateral Control Characteristics of Short Wide Ailerons and Various Spoilers with Different Amounts of Wing Dihedral. NACA Rep. No. 494, 1934.

42. Rogallo, F. M.: Collection of Balanced-Aileron Test Data. NACA ACR No. 4A11, 1944.

L-419

43. Sears, Richard I.: Wind-Tunnel Data on the Aerodynamic Characteristics of Airplane Control Surfaces. NACA ACR No. 3L08, 1943. L-663

44. Purser, Paul E., and Gillis, Clarence L.: Preliminary Correlation of the Effects of Beveled Trailing Edges on the Hinge-Moment Characteristics of Control Surfaces. NACA CB No. 3E14, 1943.

45. Rogallo, F. M., and Lowry, John G.: Résumé of Data for Internally Balanced Ailerons. NACA RB, March 1943.

46. Purser, Paul E., and Toll, Thomas A.: Analysis of Available Data on Control Surfaces Having Plain-Overhang and Frise Balances. NACA ACR No. L4E13, 1944.

47. Crandall, Stewart M., and Murray, Harry E.: Analysis of Available Data on the Effects of Tabs on Control-Surface Hinge Moments. NACA TN No. 1049, 1946.

48. Jacobs, Eastman N., Ward, Kenneth E., and Pinkerton, Robert M.: The Characteristics of 78 Related Airfoil Sections from Tests in the Variable-Density Wind Tunnel. NACA Rep. No. 460, 1933.

49. Lockwood, Vernard E.: Wind-Tunnel Investigation of Control-Surface Characteristics. XVII - Beveled-Trailing-Edge Flaps of 0.20, 0.30, and 0.40 Airfoil Chord on an NACA 0009 Airfoil. NACA ACR No. L4D12, 1944.

50. Hoggard, H. Page, Jr., and Bulloch, Marjorie E.: Wind-Tunnel Investigation of Control-Surface Characteristics. XVI - Pressure Distribution over an NACA 0009 Airfoil with 0.30-Airfoil-Chord Beveled-Trailing-Edge Flaps. NACA ARR No. L4D03, 1944.

51. Wenzinger, Carl J., and Delano, James B.: Pressure Distribution over an N.A.C.A. 23012 Airfoil with a Slotted and a Plain Flap. NACA Rep. No. 633, 1938.

52. Bird, J. D.: Effect of Leakage past Aileron Nose on Aerodynamic Characteristics of Plain and Internally Balanced Ailerons on NACA 66(215)-216, a = 1.0 Airfoil. NACA ACR No. L5F13a, 1945.

53. Purser, Paul E., and Riebe, John M.: Wind-Tunnel Investigation of Control-Surface Characteristics. XV - Various Contour Modifications of a 0.30-Airfoil-Chord Plain Flap on an NACA 66(215)-014 Airfoil. NACA ACR No. 3L20, 1943.

54. Swanson, Robert S., and Crandall, Stewart M.: Analysis of Available Data on the Effectiveness of Ailerons without Exposed Overhang Balance. NACA ACR No. L4E01, 1944.

55. Purser, Paul E., and McKinney, Elizabeth G.: Comparison of Pitching Moments Produced by Plain Flaps and by Spoilers and Some Aerodynamic Characteristics of an NACA 23012 Airfoil with Various Types of Aileron. NACA ACR No. L5C24a, 1945.

56. Purser, Paul E., and Johnson, Harold S.: Effects of Trailing-Edge Modifications on Pitching-Moment Characteristics of Airfoils. NACA CB No. L4I30, 1944.

57. Wenzinger, Carl J., and Harris, Thomas A.: Wind-Tunnel Investigation of an N.A.C.A. 23012 Airfoil with Various Arrangements of Slotted Flaps. NACA Rep. No. 664, 1939.

58. Murray, Harry E., and Erwin, Mary A.: Hinge Moments of Sealed-Internal-Balance Arrangements for Control Surfaces. I - Theoretical Investigation. NACA ARR No. L5F30, 1945.

59. Fischel, Jack: Hinge Moments of Sealed-Internal-Balance Arrangements for Control Surfaces. II - Experimental Investigation of Fabric Seals in the Presence of a Thin-Plate Overhang. NACA ARR No. L5F30a, 1945.

60. Harris, Thomas A.: Reduction of Hinge Moments of Airplane Control Surfaces by Tabs. NACA Rep. No. 528, 1935.

61. Lowry, John G., Maloney, James A., and Garner, I. Elizabeth: Wind-Tunnel Investigation of Shielded Horn Balances and Tabs on a 0.7-Scale Model of XF6F Vertical Tail Surface. NACA ACR No. 4C11, 1944.

62. Sears, Richard I., and Hoggard, H. Page, Jr.: Characteristics of Plain and Balanced Elevators on a Typical Pursuit Fuselage at Attitudes Simulating Normal-Flight and Spin Conditions. NACA ARR, March 1942.

63. Garner, I. Elizabeth: Wind-Tunnel Investigation of Control-Surface Characteristics. XX - Plain and Balanced Flaps on an NACA 0009 Rectangular Semi-span Tail Surface. NACA ARR No. L4I11f, 1944.

64. Murray, Harry E., and Warren, S. Anne: Effects of Changes in Aileron Rigging on the Stick Forces of a High-Speed Fighter Airplane. NACA RB No. L4E11, 1944.

65. Wenzinger, Carl J., and Bamber, Millard J.: Wind-Tunnel Tests of Three Lateral-Control Devices in Combination with a Full-Span Slotted Flap on an N.A.C.A. 23012 Airfoil. NACA TN No. 659, 1938.

66. Rogallo, Francis M., and Spano, Bartholomew S.: Wind-Tunnel Investigation of a Plain and a Slot-Lip Aileron on a Wing with a Full-Span Slotted Flap. NACA ACR, April 1941.

67. Rogallo, F. M., and Schuldenfrei, Marvin: Wind-Tunnel Investigation of a Plain and a Slot-Lip Aileron on a Wing with a Full-Span Flap Consisting of an Inboard Fowler and an Outboard Slotted Flap. NACA ARR, June 1941.

68. Davidson, Milton, and Turner, Harold R., Jr.: Tests of an NACA 66,2-216, a = 0.6 Airfoil Section with a Slotted and Plain Flap. NACA ACR No. 3J05, 1943.

69. Wetmore, Joseph W., and Sawyer, Richard H.: Flight Tests of F2A-2 Airplane with Full-Span Slotted Flaps and Trailing-Edge and Slot-Lip Ailerons. NACA ARR No. 3L07, 1943.

70. Soulé, H. A., and McAvoy, W. H.: Flight Investigation of Lateral Control Devices for Use with Full-Span Flaps. NACA Rep. No. 517, 1935.

71. Rogallo, F. M., Lowry, John G., and Fischel, Jack: Wind-Tunnel Investigation of a Full-Span Retractable Flap in Combination with Full-Span Plain and Internally Balanced Ailerons on a Tapered Wing. NACA ARR No. 3H23, 1943.

72. Harris, Thomas A., and Purser, Paul E.: Wind-Tunnel Investigation of Plain Ailerons for a Wing with a Full-Span Flap Consisting of an Inboard Fowler and an Outboard Retractable Split Flap. NACA ACR, March 1941.

73. Rogallo, F. M., and Lowry, John G.: Wind-Tunnel Investigation of a Plain Aileron and a Balanced Aileron on a Tapered Wing with Full-Span Duplex Flaps. NACA ARR, July 1942.

74. Luoma, Arvo A.: Effect of Compressibility on Pressure Distribution over an Airfoil with a Slotted Frise Aileron. NACA ACR No. L4G12, 1944.

75. Mathews, Charles W.: An Analytical Investigation of the Effects of Elevator-Fabric Distortion on the Longitudinal Stability and Control of an Airplane. NACA ACR No. L4E30, 1944.

76. Purser, Paul E., and Turner, Thomas R.: Wind-Tunnel Investigation of Perforated Split Flaps for Use as Dive Brakes on a Rectangular NACA 23012 Airfoil. NACA ACR, July 1941.

77. Laitone, Edmund V.: An Investigation of the High-Speed Lateral-Control Characteristics of a Spoiler. NACA ACR No. 4C23, 1944.

78. Shortal, J. A.: Effect of Retractable-Spoiler Location on Rolling- and Yawing-Moment Coefficients. NACA TN No. 499, 1934.

79. Wenzinger, Carl J., and Rogallo, Francis M.: Wind-Tunnel Investigation of Spoiler, Deflector, and Slot Lateral-Control Devices on Wings with Full-Span Split and Slotted Flaps. NACA Rep. No. 706, 1941.

80. Baker, Paul S.: The Development of a New Lateral-Control Arrangement. NACA ARR, Oct. 1941.

81. Wetmore, J. W.: Flight Tests of Retractable Ailerons on a Highly Tapered Wing. NACA TN No. 714, 1939.

82. Shortal, Joseph A.: Wind-Tunnel and Flight Tests of Slot-Lip Ailerons. NACA Rep. No. 602, 1937.

83. Rogallo, Francis M., and Swanson, Robert S.: Wind-Tunnel Development of a Plug-Type Spoiler-Slot Aileron for a Wing with a Full-Span Slotted Flap and a Discussion of Its Application. NACA ARR, Nov. 1941.

84. Rogallo, F. M., and Spano, Bartholomew S.: Wind-Tunnel Investigation of a Spoiler-Slot Aileron on an NACA 23012 Airfoil with a Full-Span Fowler Flap. NACA ARR, Dec. 1941.

85. Lowry, John G., and Liddell, Robert B.: Wind-Tunnel Investigation of a Tapered Wing with a Plug-Type Spoiler-Slot Aileron and Full-Span Slotted Flaps. NACA ARR, July 1942.

86. Laitone, Edmund V., and Summers, James L.: An Additional Investigation of the High-Speed Lateral-Control Characteristics of Spoilers. NACA ACR No. 5D28, 1945.

87. Rogallo, F. M., and Purser, Paul E.: Wind-Tunnel Investigation of a Plain Aileron with Various Trailing-Edge Modifications on a Tapered Wing. III - Ailerons with Simple and Spring-Linked Balancing Tabs. NACA ARR, Jan. 1943.

88. Phillips, William H.: The Use of Geared Spring Tabs for Elevator Control. NACA RB No. L5A13, 1945. RBL-30

89. Imlay, Frederick H., and Bird, J. D.: Wind-Tunnel Tests of Hinge-Moment Characteristics of Spring-Tab Ailerons. NACA ARR No. 4A26, 1944.

90. Jones, Robert T.: Properties of Low-Aspect-Ratio Pointed Wings at Speeds below and above the Speed of Sound. NACA TN No. 1032, 1946.

91. Letko, William, and Goodman, Alex: Preliminary Wind-Tunnel Investigation at Low Speed of Stability and Control Characteristics of Swept-Back Wings. NACA TN No. 1046, 1946.

TABLE I.- INDEX TO DESIGN FIGURES

	Figure
General:	
Values of damping coefficient C_{l_p}	1
Values of helix-angle parameter γ'	2
Values of angle-of-attack change in roll $(\Delta\alpha)_p$	3
Values of rolling-moment-loss parameter τ'	5
Variation of $V\sigma^{1/2}$ with $q/\sqrt{1 - M^2}$ and with altitude	6
Values of lifting-surface-theory correction $\left(\Delta C_{h_\alpha}\right)_{LS}$	11
Plain ailerons:	
Trailing-edge angles of various airfoils	12
Correlation of section hinge-moment parameters c_{h_α} and c_{h_δ}	13
Effect of trailing-edge angle on C_{h_α} and C_{h_δ}	15
Effect of trailing-edge angle on c_{l_α}	16
Effect of aileron nose gap on c_{l_α}	17
Values of effectiveness parameter $\Delta\alpha/\Delta\delta$	18
Values of section pitching-moment parameter $\left(\partial c_m/\partial\alpha\right)_{c_l}$	20
Effect of trailing-edge angle on $\left(\partial c_m/\partial c_l\right)_{\delta_a}$	21
Ailerons having exposed-overhang balances:	
Expressions for nose-shape factor F_2' for exposed-overhang balances	24
Values of factors F_1 and F_2	25
Effect of exposed-overhang balances on C_{h_α} and C_{h_δ}	26
Variation of $\bar{c}_b/\bar{c}_a$ with F_1F_2' for representative exposed-overhang balances	27
Effect of exposed-overhang balances on critical deflection $\delta_{a_{cr}}$	28
Effect of exposed-overhang balances and gap on $\Delta\alpha/\Delta\delta$	29
Ailerons having sealed-internal balances:	
Values of seal-moment ratio m_s	34
Effect of sealed internal balances on C_{h_α} and C_{h_δ}	35
Effect of vent location on P_{R_α} and P_{R_δ}	36
Effect of cover-plate misalinement on C_{h_α} and C_{h_δ}	37
Effect of leakage on C_{h_δ}	38
Ailerons having linked tabs:	
Values of factors F_3, F_4, and F_5	40
Effect of linked tabs on C_{h_δ}	41
Spoiler devices:	
Values of section pitching-moment parameter $\left(\partial c_m/\partial\alpha\right)_{c_l}$	63

TABLE II.- SUPPLEMENTARY INFORMATION REGARDING MODELS HAVING PLAIN CONTROL SURFACES

Symbol in figures 13, 15, 16	Type of test	Basic airfoil section	Aspect ratio A	Taper ratio λ	$\frac{\bar{c}_a}{\bar{c}}$	Location of control surface $\frac{y_1}{b/2}$	Location of control surface $\frac{y_o}{b/2}$	Air-flow characteristics M	Air-flow characteristics R	Source of data
○	Two-dimensional	NACA 0009	∞	-----	0.15	-----	-----	0.10	1.43 × 10^6	Reference 43, fig. 1
△	Two-dimensional	NACA 0009	∞	-----	.20	-----	-----	.10	1.43	Reference 49
□	Two-dimensional	NACA 0009	∞	-----	.30	-----	-----	.10	1.43	Reference 43, figs. 5, 46, 48, 50, 51, 52
◻	Two-dimensional	NACA 0009	∞	-----	.30	-----	-----	.10	1.43	Reference 49
◻	Two-dimensional	NACA 0009	∞	-----	.30	-----	-----	.10	1.43	Reference 50
◇	Two-dimensional	NACA 0009	∞	-----	.40	-----	-----	.10	1.43	Reference 49
◻	Two-dimensional	NACA 0015	∞	-----	.30	-----	-----	.10	1.43	Reference 43, figs. 59, 69
◻	Two-dimensional	NACA 66-009	∞	-----	.30	-----	-----	.10	1.43	Reference 43, fig. 97
△	Two-dimensional	NACA 23012	∞	-----	.20	-----	-----	.11	2.19	Reference 51
△	Two-dimensional	NACA 66(215)-216, a = 1.0	∞	-----	.20	-----	-----	.20	2.8	Reference 52
○	Two-dimensional	NACA 66(215)-216, a = 0.6	∞	-----	.15	-----	-----	.14 .34	3.8 9.5	Reference 42, model D-1
△	Two-dimensional	NACA 66(215)-216, a = 0.6	∞	-----	.20	-----	-----	.14 .34	3.8 9.5	Reference 42, model D-1
◻	Two-dimensional	NACA 66(215)-014	∞	-----	.30	-----	-----	.10	1.43	Reference 53
▽	Semispan wing	Root, NACA 23015.5 (approx.) Tip, NACA 23008.25 (approx.)	5.6	0.6	.155	0.579	0.984	.08	1.54	Reference 42, model D-IV
◁	Third-span wing	NACA 66-series	7.3	.42	.20	.509	.980	.11	2.35	Reference 42, model D-V
▽	Quarter-span wing	Root, NACA 65(223)-222, a=1.0 Tip, NACA 65(216)-415, a = 0.5	12.0	.32	.225	.641	.945	.11	1.99	Unpublished
◁	Horizontal tail mounted on fuselage	NACA 0009	3.7	.57	.30	0	1.0	.10	.50	Reference 43, figs. 107, 117, 119
▷	Semispan tail surface	NACA 0009	3.0	.5	.30	0	1.0	.10	1.2	Unpublished

TABLE III.- SUPPLEMENTARY INFORMATION REGARDING MODELS HAVING CONTROL SURFACES WITH EXPOSED-OVERHANG BALANCES

Symbol in figures 26 and 28	Type of test	Basic airfoil section	Aspect ratio A	Taper ratio λ	$\frac{\bar{c}_a}{\bar{c}}$	Location of control surface		Air-flow characteristics		Source of data
						$\frac{y_1}{b/2}$	$\frac{y_o}{b/2}$	M	R	
Plain-overhang balances										
○	Two-dimensional	NACA 23012	∞	-----	0.20	-----	-----	0.20	2.8×10^6	Reference 42, model B-I
△	Two-dimensional	NACA 66(215)-216, a = 1.0	∞	-----	.20	-----	-----	.36	5.1	Reference 42, model B-II
□	Two-dimensional	NACA 0009	∞	-----	.30	-----	-----	.10	1.43	Reference 43, figs. 5 to 45
◇	Two-dimensional	NACA 0015	∞	-----	.30	-----	-----	.10	1.43	Reference 43, figs. 59 to 68
◺	Two-dimensional	NACA 0015 (modified)	∞	-----	.30	-----	-----	.10	1.43	Reference 43, figs. 69 to 75
▽	Two-dimensional	NACA 66-009	∞	-----	.30	-----	-----	.10	1.43	Reference 43, figs. 97 to 102
◹	Two-dimensional	NACA 66-009 (modified)	∞	-----	.26	-----	-----	.10	1.43	Reference 43, figs. 103 to 106
◁	Semispan wing	Root, NACA 23015.5 Tip, NACA 23008.25	5.6	0.60	.155	0.579	0.984	.08	1.54	Reference 42, model B-III
▷	Quarter-span wing	Root, NACA 65(223)-222, a = 1.0 Tip, NACA 65(216)-415, a = 0.5	12	.32	.23	.641	.945	.11	1.99	Reference 42, model B-IV
◸	Complete model	Root, NACA 23015 Tip, NACA 4412	7.2	.42	.195 .206	.500	.960	.11	.80	Reference 42, model B-V
Frise balances										
◇	Two-dimensional	NACA 23012	∞	-----	0.20	-----	-----	0.20	2.8	Reference 42, model A-I
∪	Two-dimensional	NACA conventional (approx. 14 percent thick)	∞	-----	.20	-----	-----	.13	1.91	Reference 42, model A-III
◇	Semispan wing	NACA 23012	4.0	1.0	.20	0.63	1.0	.11	2.88	Reference 42, model A-VI
D	Quarter-span wing	Root, NACA 65(223)-222, a = 1.0 Tip, NACA 65(216)-415, a = 0.5	12.0	.32	.23	.641	.945	.11	1.99	Reference 42, model A-IV
⊐	Third-span wing	NACA 66-series	7.3	.42	.20	.509	.980	.11	2.35	Reference 42, model A-V

TABLE IV.- SUPPLEMENTARY INFORMATION REGARDING MODELS HAVING CONTROL SURFACES WITH SEALED INTERNAL BALANCES

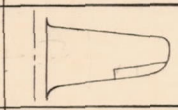
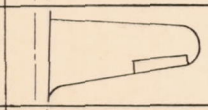
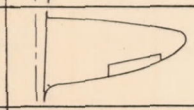
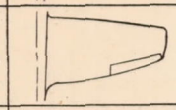
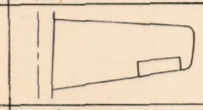
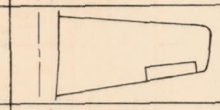
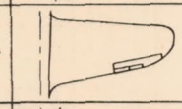
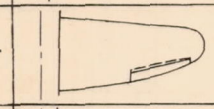
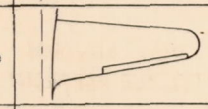
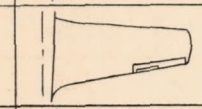
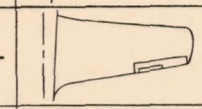
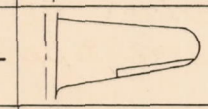
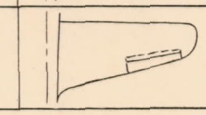
Symbol in figures 35, 37, 38	Type of test	Basic airfoil section	Aspect ratio A	Taper ratio λ	$\frac{c_a}{c}$	Location of control surface $\frac{y_1}{b/2}$	Location of control surface $\frac{y_o}{b/2}$	Air-flow characteristics M	Air-flow characteristics R	Source of data
○	Two-dimensional	NACA 0009	∞	-----	0.30	-----	-----	0.10	1.43×10^6	Reference 43, figs. 5 and 58
△	Two-dimensional	NACA 0015	∞	-----	.30	-----	-----	.10	1.43	Reference 43, figs. 69 and 84
□	Two-dimensional	NACA 66(215)-216, a = 1.0	∞	-----	.20	-----	-----	.20	2.8	Reference 42, model C-VII and unpublished
◇	Two-dimensional	NACA 65,3-018 (modified)	∞	-----	.182	-----	-----	.20	2.8	Unpublished
◹	Two-dimensional	NACA 66(2x15)-216, a = 0.6	∞	-----	.164	-----	-----	.14	4.2	Reference 42, model C-I
◿	Two-dimensional	NACA 66(215)-216, a = 0.6	∞	-----	.20	-----	-----	.33	9.5	Reference 42, model C-IX
◸	Two-dimensional	NACA 66(215)-216, a = 0.6	∞	-----	.172	-----	-----	.20	9.6	Reference 42, model C-V
◺	Two-dimensional	----------	∞	-----	.22	-----	-----	----	----------	Unpublished
◁	Third-span wing	NACA 66-series	7.3	0.42	.20	0.509	0.980	.11	2.35	Reference 42, model C-XV
▷	Semispan wing	Root, NACA 23015.5 (approx.) Tip, NACA 23008.25 (approx.)	5.6	.60	.155	.579	.984	.11	2.05	Reference 42, model C-X
▢	Complete model	Root, NACA 66(215)-1(165), a=1.0 Tip, NACA 67(115)-213, a=0.7	5.4	.60	.25	.54	.953	.11	.99	Reference 42, model C-XVI
▽	Quarter-span wing	Root, NACA 65(223)-222, a=1.0 Tip, NACA 65(216)-415, a=0.5	12.0	.32	.23	.641	.945	.11	1.99	Reference 42, model C-XIV
◇	Semispan wing	Root, NACA 66,2-118, a=1.0 Tip, NACA 66(2x15)-116, a=1.0	6.2	.33	.175 .162 .149	.496	.906 .977	.11	1.9	Reference 42, model C-XI
◇	Quarter-span wing	Root, Clark YH (19 percent thick) Tip, Clark YH (12.2 percent thick)	6.2	.49	.18	.54	.93	.05	1.1	Reference 42, model C-XVII
◇	Semispan wing	Root, NACA 23015.5 Tip, NACA 23008.25	5.6	.60	.08	0	.984	.11	2.05	Reference 42, model C-XVIII
▢	Semispan wing	NACA 23012	4.0	1.0	.15	.63	1.00	.05	1.44	Reference 42, model C-XII
◇	Vertical tail on stub fuselage	NACA 66-series (modified)	2.41	.47	.42	0	1.00	.10	1.51	Reference 43, figs. 131 and 138
▷	Vertical tail on stub fuselage	NACA 65-series (modified)	2.17	-----	.35	-----	-----	.21	3.3	Unpublished
⏢	Semispan horizontal tail	NACA 65_1-012 (modified)	5.00	.50	.32	.09	.942	.21	2.76	Unpublished
▽	Semispan wing	Root, NACA 2416 Tip, NACA 4412	6.24	.43	.20	.430	.966	.21	3.38	Unpublished

TABLE V.- SUPPLEMENTARY INFORMATION REGARDING MODELS

HAVING CONTROL SURFACES WITH BALANCING TABS

Symbol in figure 41	Type of test	Basic airfoil section	Aspect ratio A	Taper ratio λ	Location of control surface $y_1/b/2$	Location of control surface $y_o/b/2$	Location of tab y_1/b_a	Location of tab y_2/b_a	$\bar{c}_a'/\bar{c}'$	$\bar{c}_t/\bar{c}_a'$	$\bar{t}'/2/\bar{c}_a'$	ø (deg)	F_3	Gaps: Control surface	Gaps: Tab	Overhang balance: Type	Overhang balance: $\bar{c}_b'/\bar{c}_a'$	Air-flow characteristics: M	Air-flow characteristics: R	Source of data
○	Complete wing	Clark Y	6.0	1.0	0.700	1.000	0	1.000	0.400	0.100	0.095	13.0	1.000	Unsealed	Sealed	None	0.095	0.11	0.61×10^6	
◇							0	1.000		.200			1.000			None	.095			
▽							.250	.750					.500			Frise	.330			
□							.500	1.000								None	.095			
⬠							0	.500												
☆							.250	.750												
⬡					.600		0	1.000	.250	.100			1.000							Reference 60
△	Third-span wing	Root, NACA 66(215)-2(13.716) Tip, NACA 66(215)-2(13.125)	5.6	.52	.264	.974	0	.156	.200	.190	.160	15.0	.216	Sealed	Sealed	Internal	.505	.11	2.4	
◁												15.0		Unsealed		Frise	.400			
◇						.900		.300		.150		31.0	.388	Sealed		None	.160			Reference 42 model E-VII
▷								.200		.300			.270							
△								.200		.500			.270							
□	Semispan wing	Root, NACA 66,2-118, a=1.0 Tip, NACA 66(2x15)-116, a=1.0	6.2	.33	.499	.894	0	1.000	.149	.260	.195	9.0	.950	Sealed	Sealed	Internal	.688	.11	1.9	Reference 42 model E-VI
▽						.894		.500	.162	.239	.200		.399				.563			
◇						.940		.509	.149	.260	.195		.376				.688			
▽	Semispan wing	Root, NACA 23015.5 Tip, NACA 23008.25	5.6	.60	.579	.984	0	1.000	.155	.200	.110	11.7	1.00	Sealed	Sealed	None	.110	.08	1.5	Reference 42 model E-V
◁							0	.333			.124	13.1	.383				.124			
◇							.667	1.000			.095	10.2	.289				.095			
▷							.333	.667			.110	11.7	.333				.110			
▽							0	1.000			.102	10.9	.625				.102			
◁							0	.667			.117	12.3	.725				.117			
◇	Third-span wing	Root, NACA 2213 Tip, NACA 2205	4.3	Elliptic	.190	.793	0	.858	.22	.158	.122	12.8	.962	Unsealed	Sealed	None	.122	.06	1.3	Reference 42 model F-XI
▽								.858		.329	.122	12.8	.962				.122			
◁								.433		.176	.127	13.4	.621				.127			
▷								.433		.324	.127	13.4	.621				.127			
◻	Partial-span wing	----------	7.2	.60	.143	.925	0	.346	.167	.376	.158	14.5	.345	Unsealed	Sealed	Blunt nose	.41	.3	5.0	Unpublished
○	Semispan wing	NACA 43012	7.6	1.00	.422	.892	.355	.645	.188	.25	.130	14.5	.291	Unsealed	Sealed	Frise	.330	.16	2.5	Unpublished
▽	Semispan wing	Root, NACA 0015 Tip, NACA 0009	10.8	.26	.564	.965	.011	.254	.121	.236	.145	10.4	.245	Sealed	Sealed	Internal	.365	.175	8.9	Unpublished
R			10.8	.26	.564	.965	.011	.496	.130	.236	.145	10.4	.435	Sealed	Sealed	Internal	.365	.175	8.9	
△	Tail surface model	NACA 0006	3.0	.64	0	1.000	0	.686	.385	.10	.063	7.0	.794	Unsealed	Sealed	None	.063	.08	1.2	Reference 60
◁			↓	↓	↓	↓	↓	↓	.385	.20	.063	↓	↓	↓	↓	↓	.063	↓	↓	
◇			1.5						.564	↓	.054						.054			
▷									.564		.054						.054			
▽	Semispan horizontal tail	----------	3.9	.58	.04	.953	.150	.342	.491	.20	.095	8.2	.282	Unsealed	Sealed	Blunt nose	.260	.11	2.0	Reference 43, figs. 127 to 130
R			3.9	.58	.04	.953	.094	.892	.340	.35	.095	7.3	.962	Sealed	Sealed	Blunt nose	.500	.11	2.0	
○	Semispan tail	NACA 16-series (modified)	2.9	.39	0	1.000	.343	.554	.318	.30	.152	14.1	.225	Sealed	Sealed	None	.152	.08	2.3	Reference 61
▷	Horizontal tail mounted on fuselage	NACA 0009	3.7	.57	0	1.000	.195	.834	.306	.20	.093	11.6	.834	Sealed	Sealed	Blunt nose	.093	.11	.5	Reference 62
R			↓	↓	↓	↓	↓	↓	↓	↓	↓	↓	↓	↓	↓	↓	.35	↓	↓	
△	Semispan horizontal tail	----------	3.1	1.00	0	.669	0	.586	.310	.410	.125	16.1	.585	Sealed	Sealed	Blunt nose	.50	.11	1.0	Unpublished
◻	Tail-surface model	NACA 0020	2.0	1.00	0	.300	0	1.00	.40	.200	.447	25.6	1.00	Sealed	Sealed	None	.280	.11	1.0	Unpublished
○	Semispan horizontal tail	NACA 0009	3.0	1.00	0	1.00	.193	.679	.300	.200	.093	11.6	.486	Sealed	Sealed	None	0	.05	1.0	Unpublished
◁	Partial-span wing	Root, NACA 2416 Tip, NACA 4412	4.6	.50	.167	.950	0	.242	.20	.25	.17	19.0	.295	Sealed	Unsealed	Internal	.093	.10	1.43	Reference 63
R			4.6	.50	.167	.950	.242	.348	.20	.25	.17	19.0	.118	Sealed	Unsealed	Internal	.410	.21	3.38	Unpublished
▽	Vertical tail with stub fuselage	NACA 65-series (modified)	2.17	.557	.238	.932	0	.533	.350	.209	.120	14.0	.570	Sealed	Unsealed	Internal	.410	.21	3.38	Unpublished
▷	Semispan horizontal tail	NACA 65_1-012 (modified)	5.00	.50	.094	.943	0	.413	.32	.20	.131	16.0	.545	Sealed	Unsealed	Internal	.325	.21	3.30	Unpublished
○	Vertical tail with stub fuselage	NACA 0009	2.40	.50	0	1.000	.141	.340	.25	.25	.10	19.0	.253	Unsealed	Unsealed	Blunt nose	.410	.21	2.76	Unpublished
																	.360	.40	1.9	Unpublished

Table VI.- SUPPLEMENTARY INFORMATION REGARDING THE FIGHTER-TYPE AIRPLANES FOR WHICH ROLLING-PERFORMANCE CHARACTERISTICS ARE PRESENTED IN FIGURES 46 AND 47

Airplane	Wing-aileron arrangement	Type of aileron	Wing span (ft)	$\frac{y_1}{b/2}$	$\frac{b_a}{b/2}$	$\frac{\bar{c}_a}{\bar{c}}$
Focke-Wulf 190		Frise	34.5	0.57	0.43	0.20
Typhoon		Frise	41.58	.595	.35	-----
Spitfire (normal wings)		Frise	36.92	.495	.375	.165
Spitfire (clipped wings)		Frise	32.5	.563	.425	.165
F4F-3		Frise	38	.6875	.275	.225
F6F-3		Frise with spring tab	42.83	.64	.30	.20
P-39D-1-BE		Frise with balance tabs	34	.55	.376	.175
P-47C-1-RE		Frise	40.78	.54	.408	.18
Japanese Zero		Frise	39.33	.37	.545	-----
Mustang XP-51		Plain with balance tabs	37.03	.61	.355	.187
P-51B-1-NA		Internal balance and seal	37.03	.61	.355	.187
P-63A-1-BE		Internal balance and seal	38.33	.442	.525	.15
P-40F		Beveled Frise and seal	37.5	.544	.368	.20

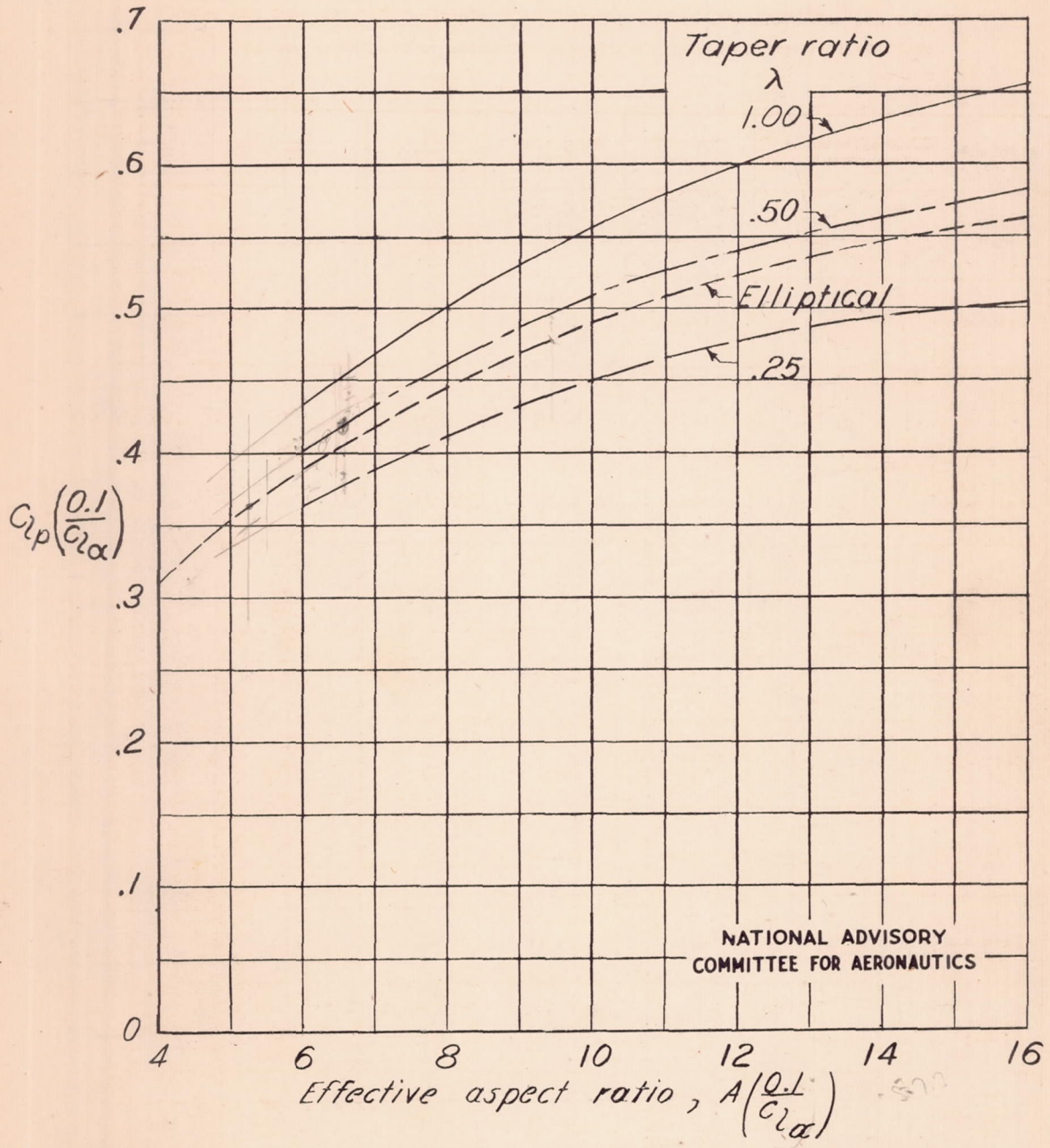


Figure 1.- Chart for determining values of damping coefficient C_{l_p} of round-tipped wings. Reference 11.

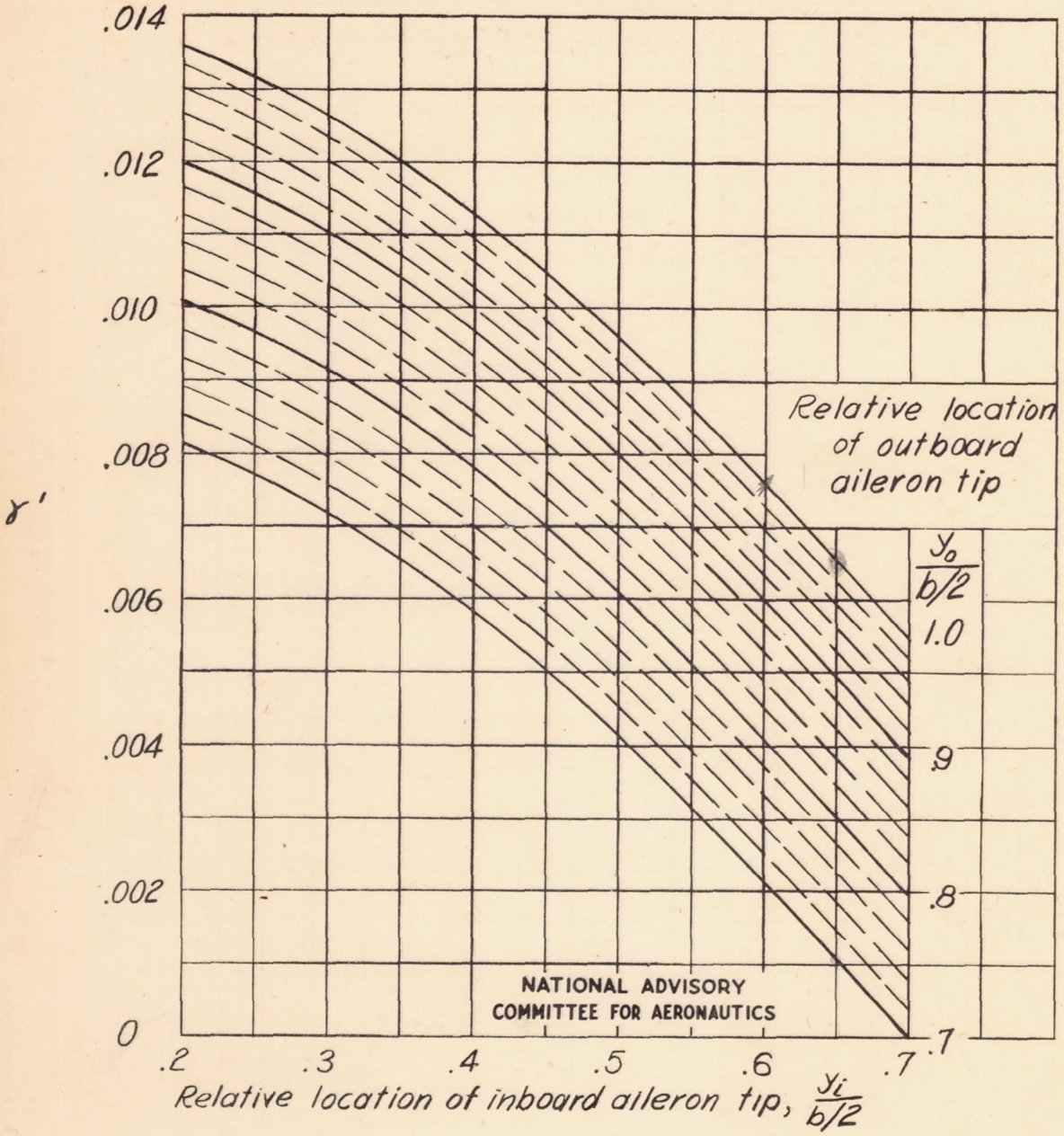
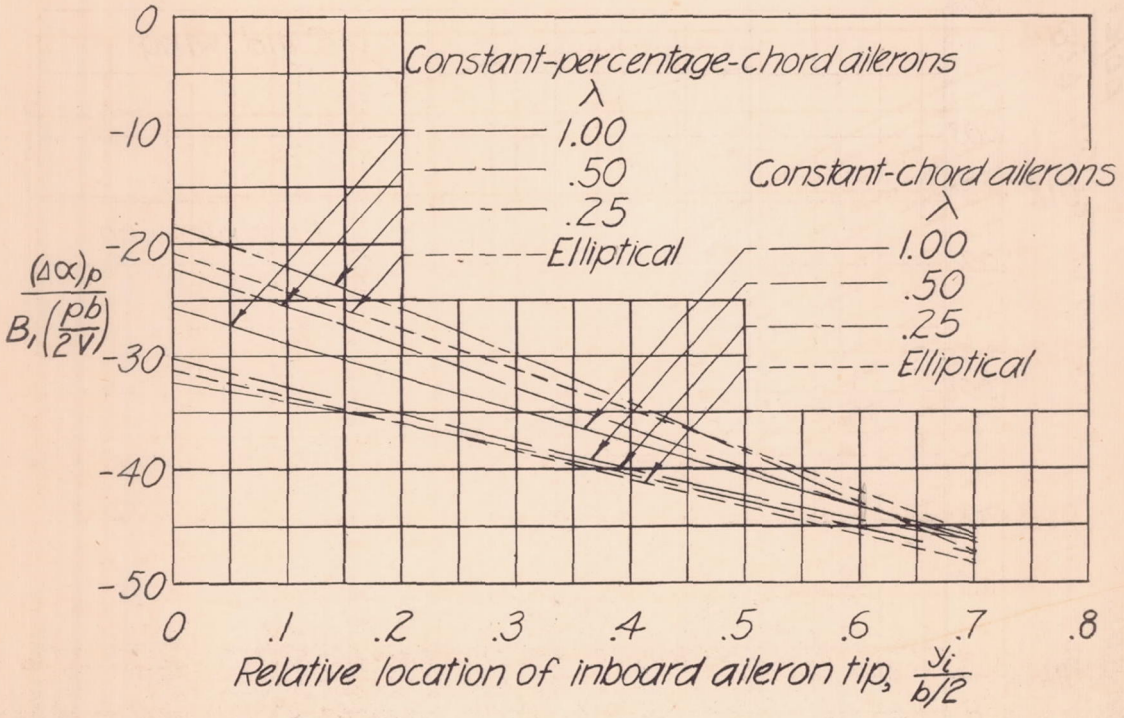


Figure 2.- Values of the helix-angle parameter γ' for wings having taper ratios between 0.25 and 1.0 and aspect ratios between 5 and 16. Constant-percentage-chord ailerons. Derived from reference 13.



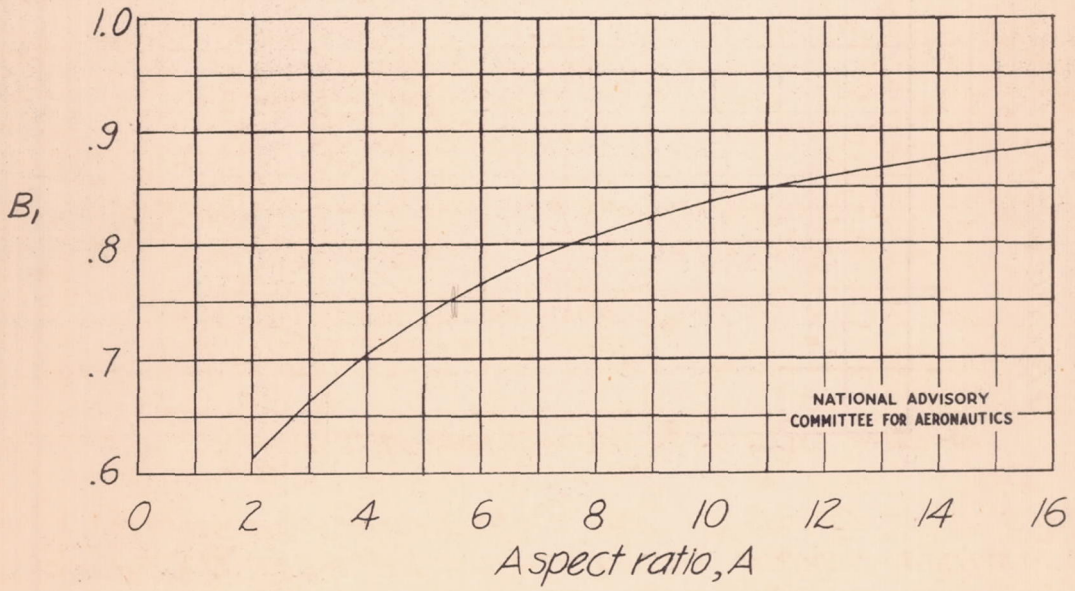


Figure 3.- Chart for determining the effective change in angle of attack, caused by steady roll, at the aileron. Outboard aileron-tip locations between $0.9\frac{b}{2}$ and $1.0\frac{b}{2}$. Derived from reference 11.

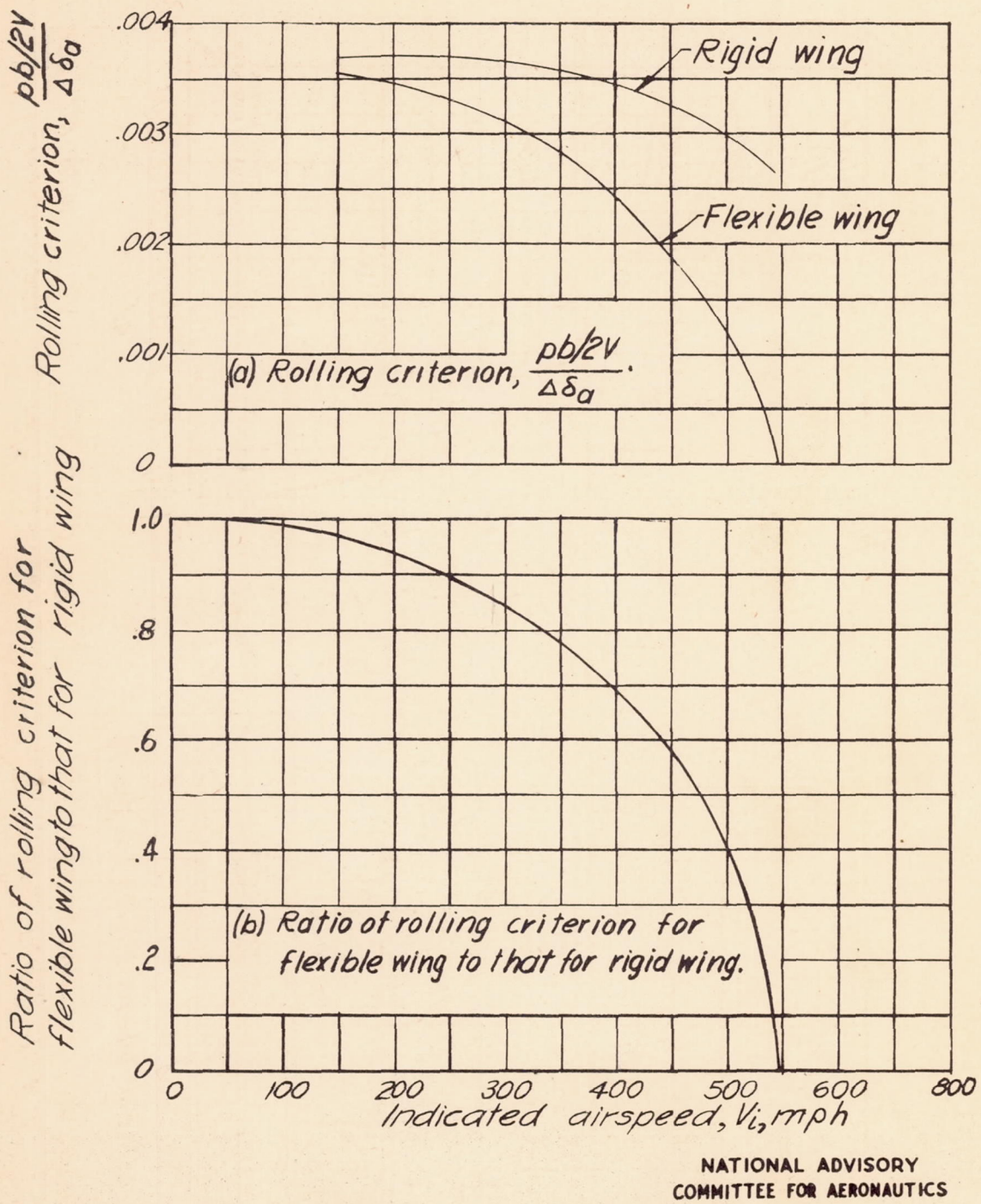


Figure 4.- Variation with indicated airspeed of calculated effect of wing flexibility on rolling. P-47C-1-RE airplane; $\Delta\delta_a = 8°$; altitude ≈ 4000 feet. Reference 14.

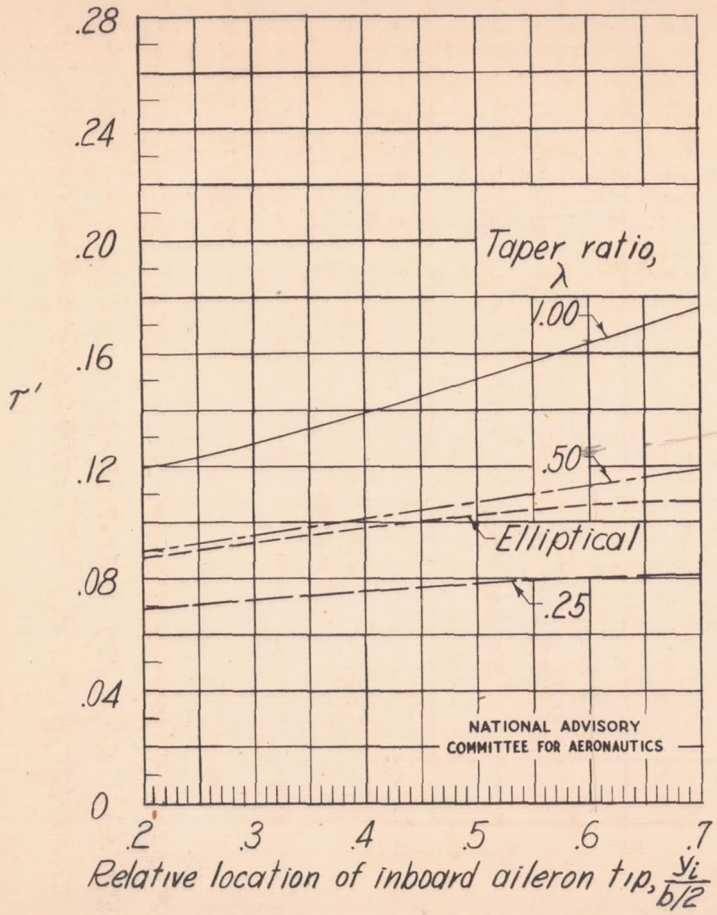


Figure 5.—Values of the rolling-moment-loss parameter T' for wings having aspect ratios between 5 and 16 and outboard aileron-tip locations between 0.8 $\frac{b}{2}$ and 1.0 $\frac{b}{2}$. Derived from reference 13.

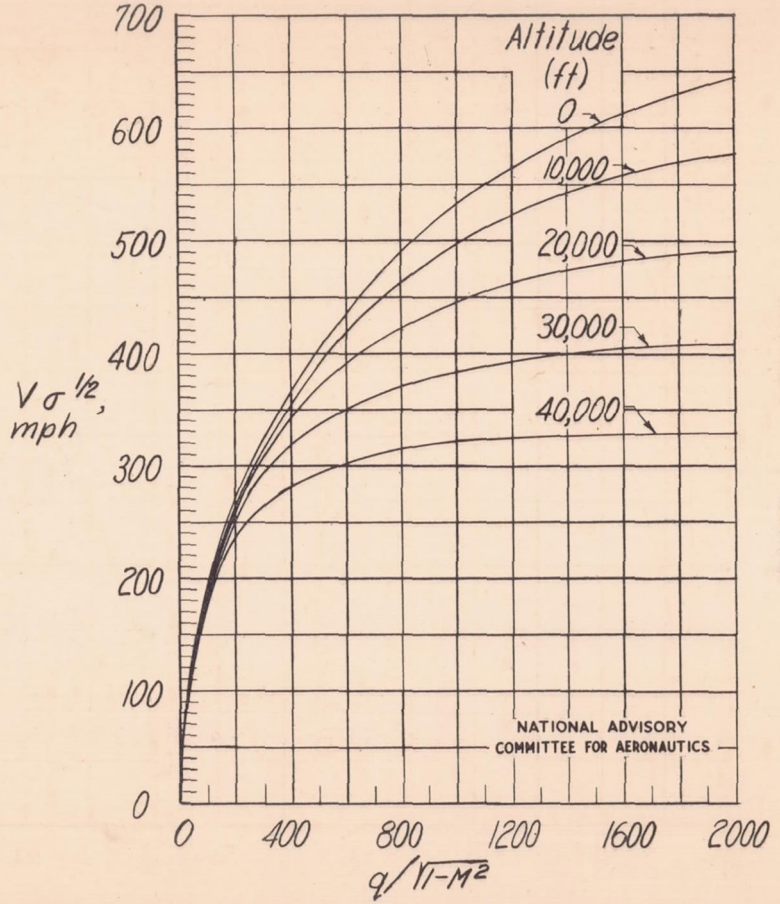


Figure 6.- Variation of $V\sigma^{1/2}$ with altitude and with $q/\sqrt{1-M^2}$. Reference 13.

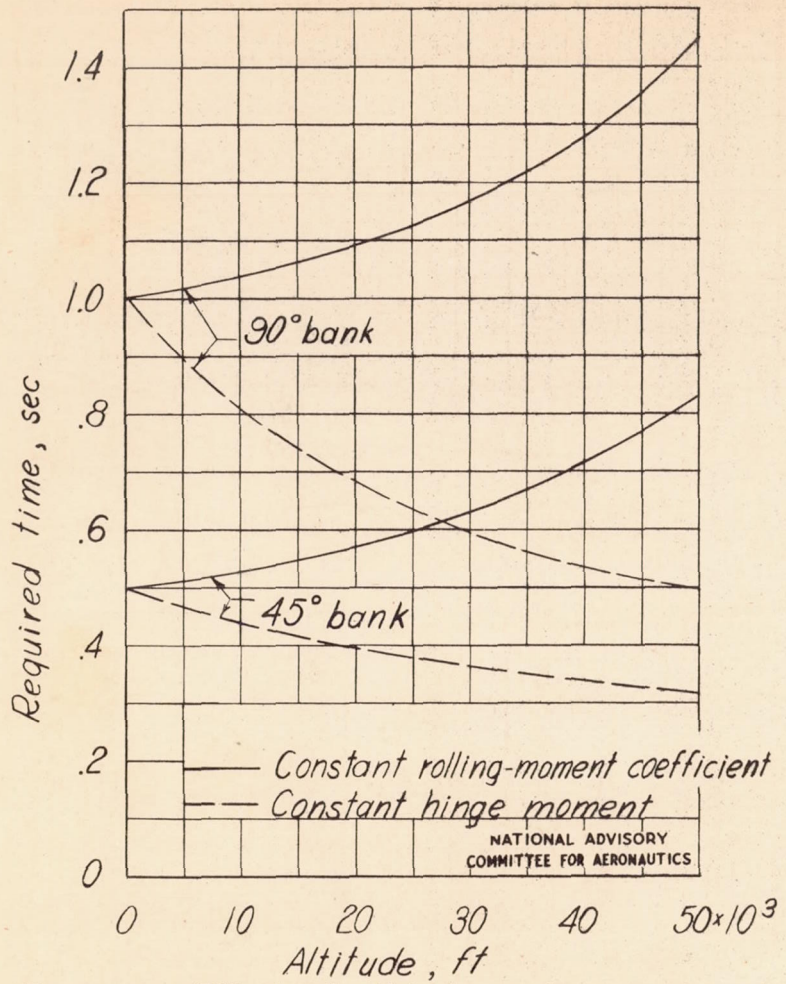


Figure 7.- Effect of altitude on time required to bank to 45° and to 90° with constant rolling-moment coefficient and with constant hinge moment. V, 530 miles per hour. Reference 24.

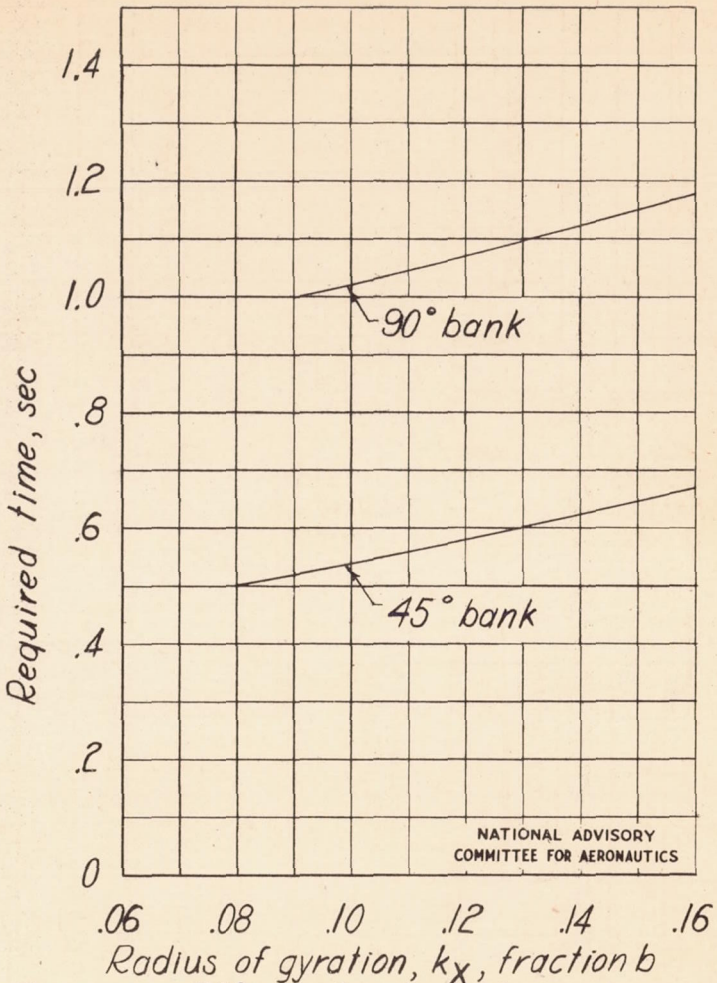


Figure 8.- Effect of radius of gyration in roll on time required to bank to 45° and to 90°. Constant rolling-moment coefficient. Reference 24.

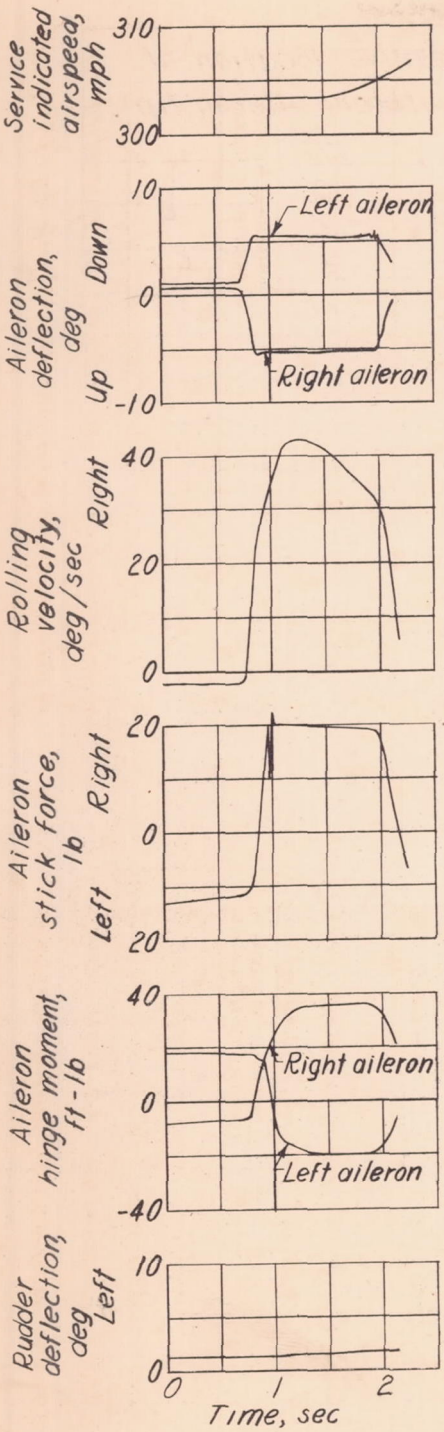


Figure 9.- Time history of a typical rudder-fixed aileron roll made with ailerons partly deflected to determine rolling performance.

NATIONAL ADVISORY COMMITTEE FOR AERONAUTICS

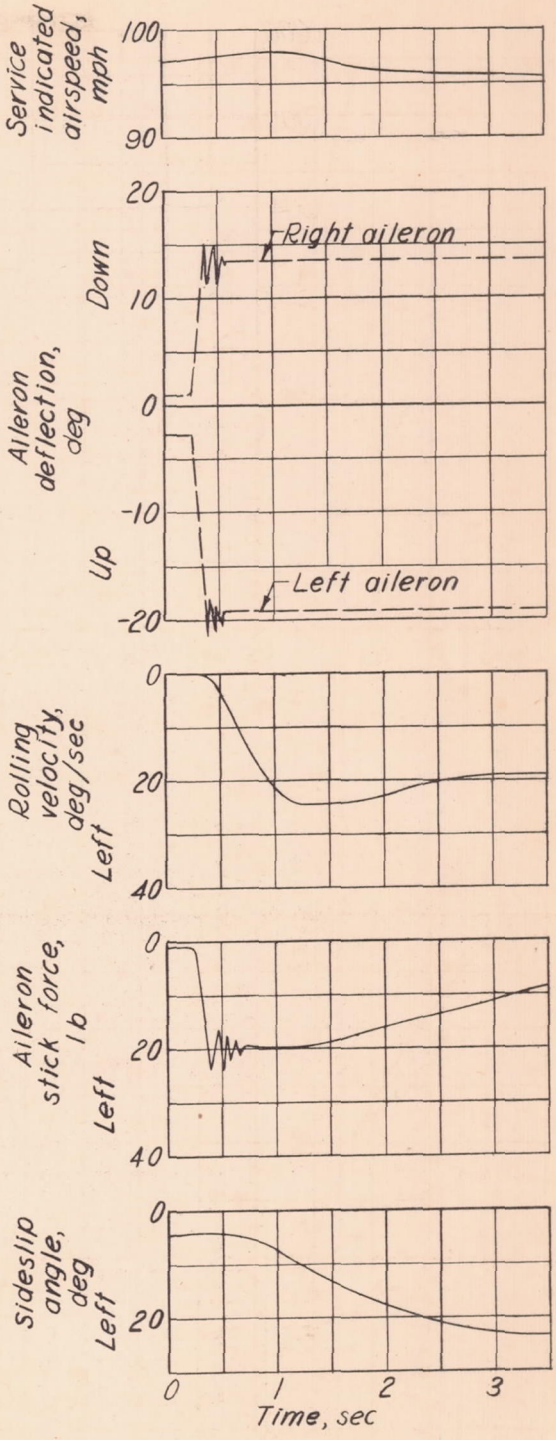


Figure 10.- Time history of a typical rudder-fixed aileron roll made with ailerons fully deflected to determine adverse yaw.

NATIONAL ADVISORY COMMITTEE FOR AERONAUTICS

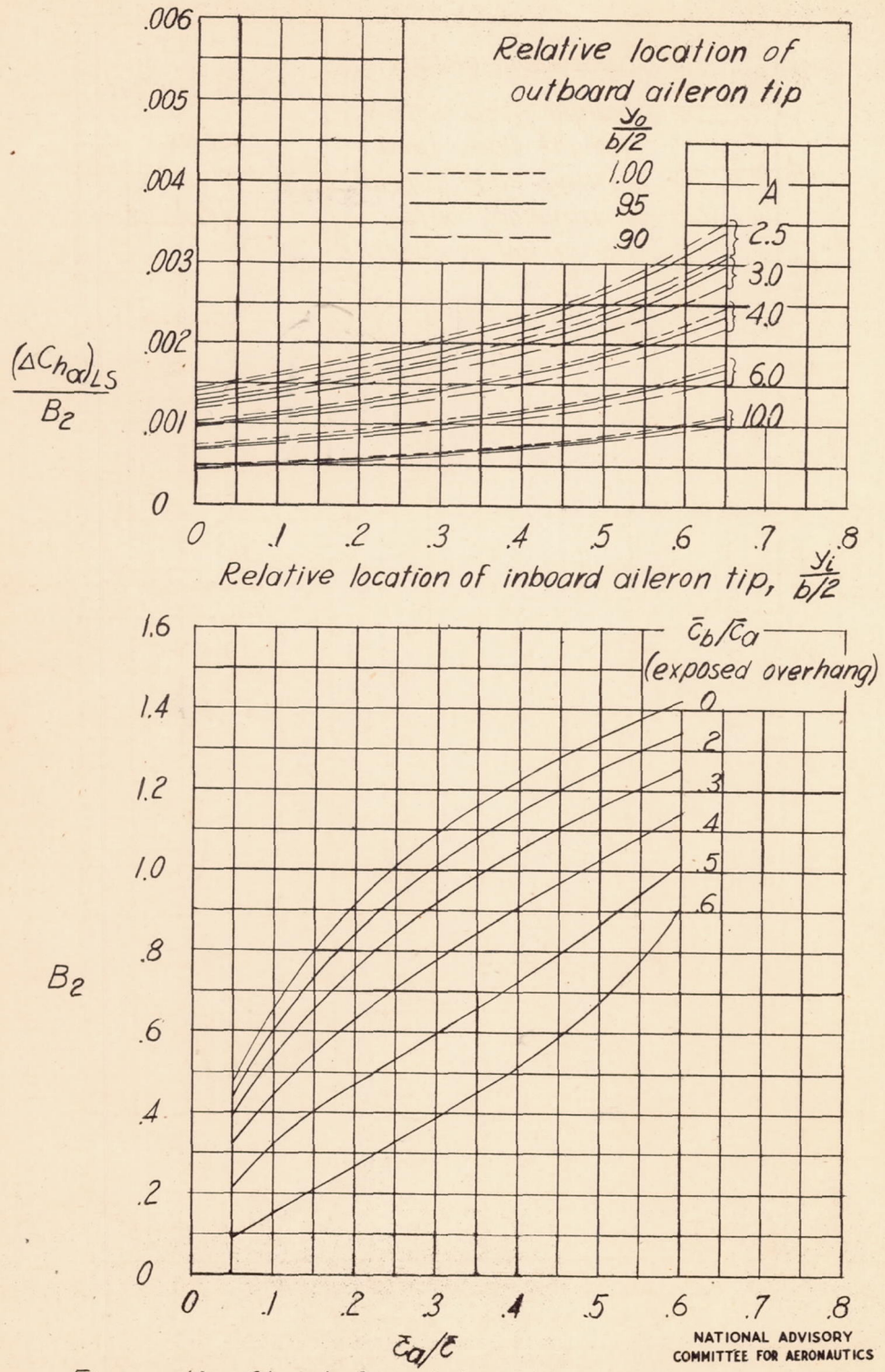


Figure 11.- Chart for determining lifting-surface-theory correction to the slope of the curve of hinge-moment coefficient against angle of attack. Reference 11.

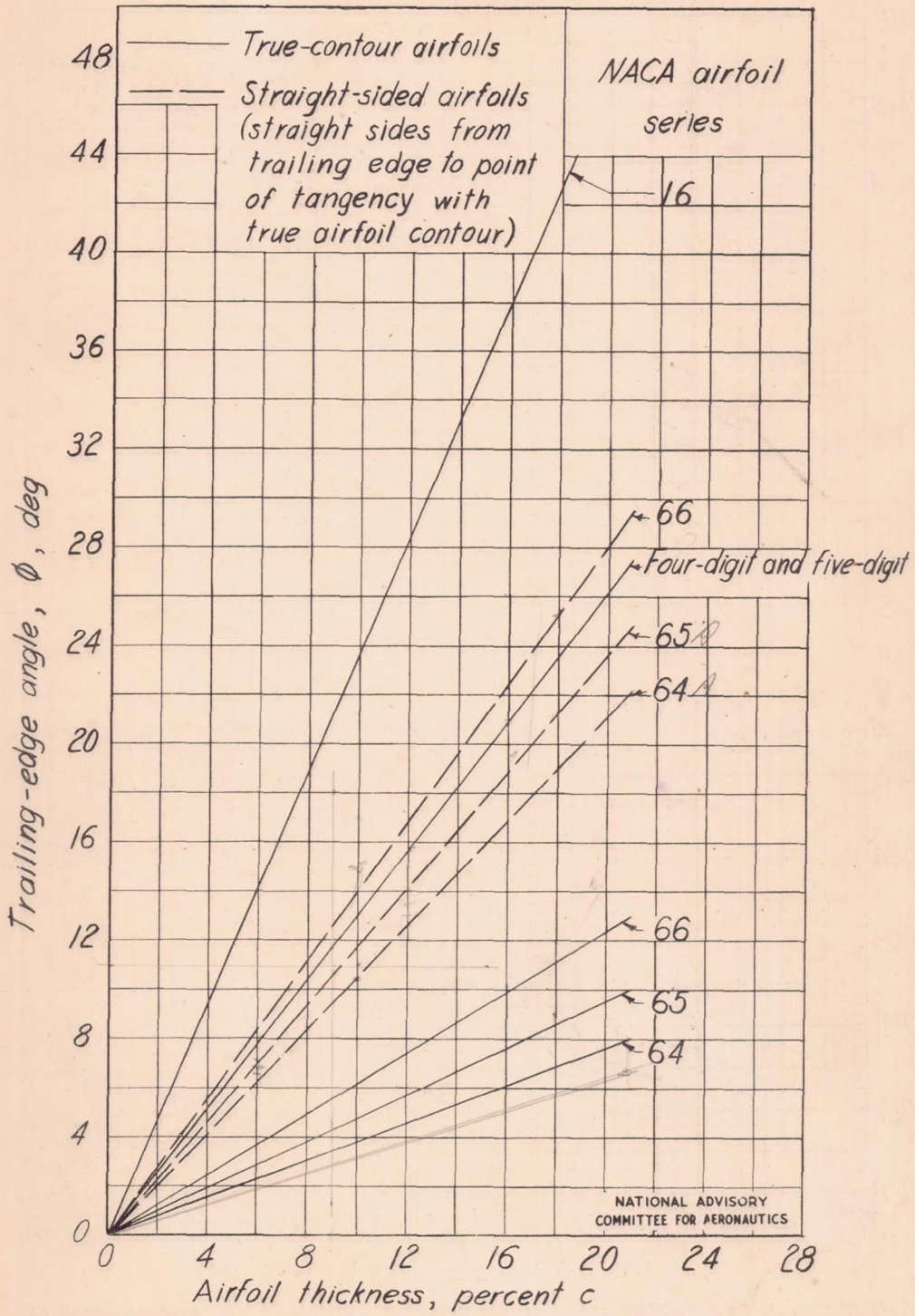


Figure 12.- Variation of trailing-edge angle with airfoil thickness for several series of NACA airfoils. Trailing-edge angle measured between lines drawn from airfoil surfaces at trailing edge to airfoil surfaces at 0.98c.

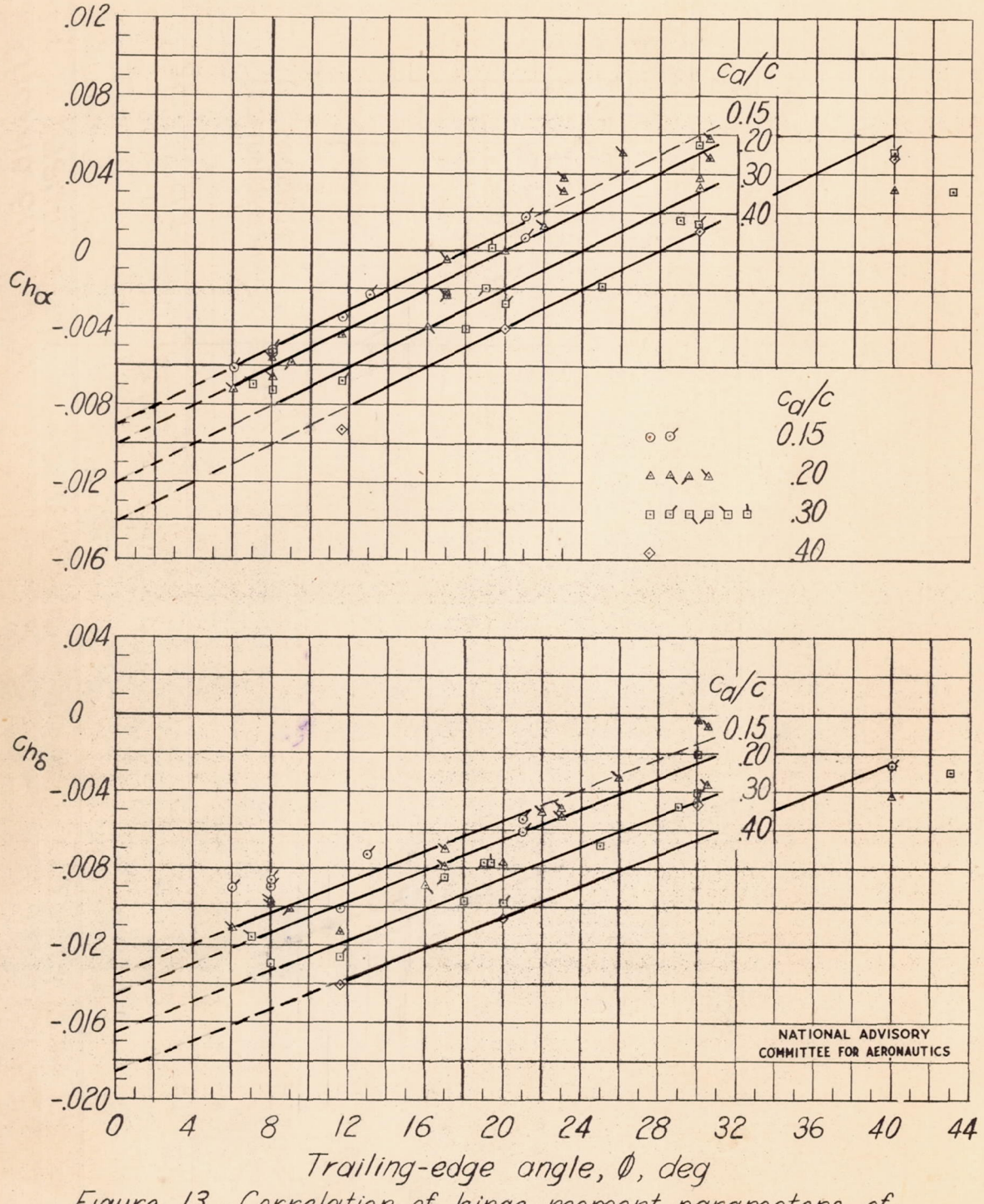


Figure 13.- Correlation of hinge-moment parameters of plain two-dimensional ailerons having various chords and various trailing-edge angles. Gaps sealed; M, 0.34 or less. Symbols identified in table II.

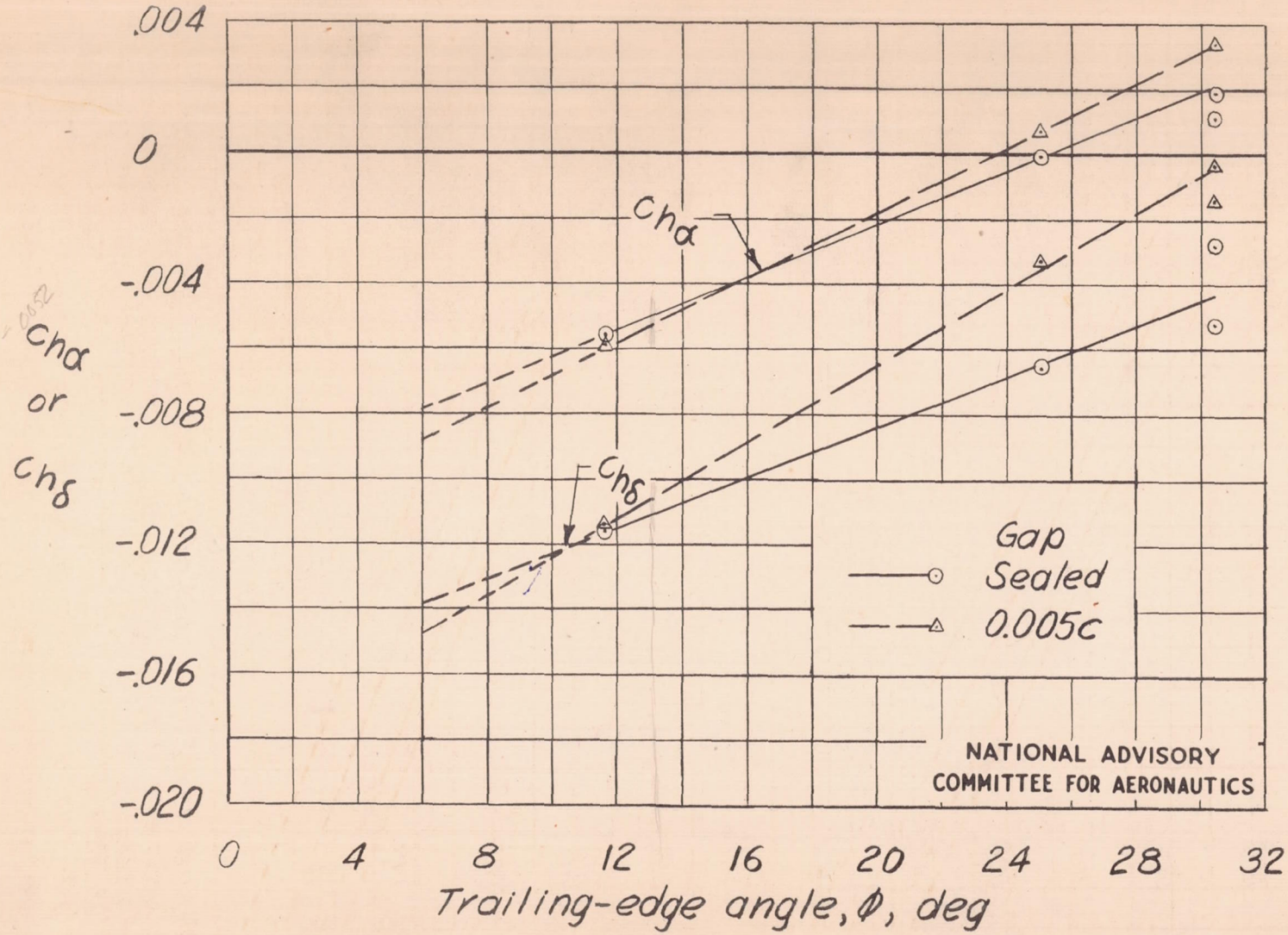


Figure 14.- Effect of gap on variation of hinge-moment parameters with trailing-edge angle. NACA 0009 airfoil; two-dimensional model; c_a/c, 0.30. Reference 50.

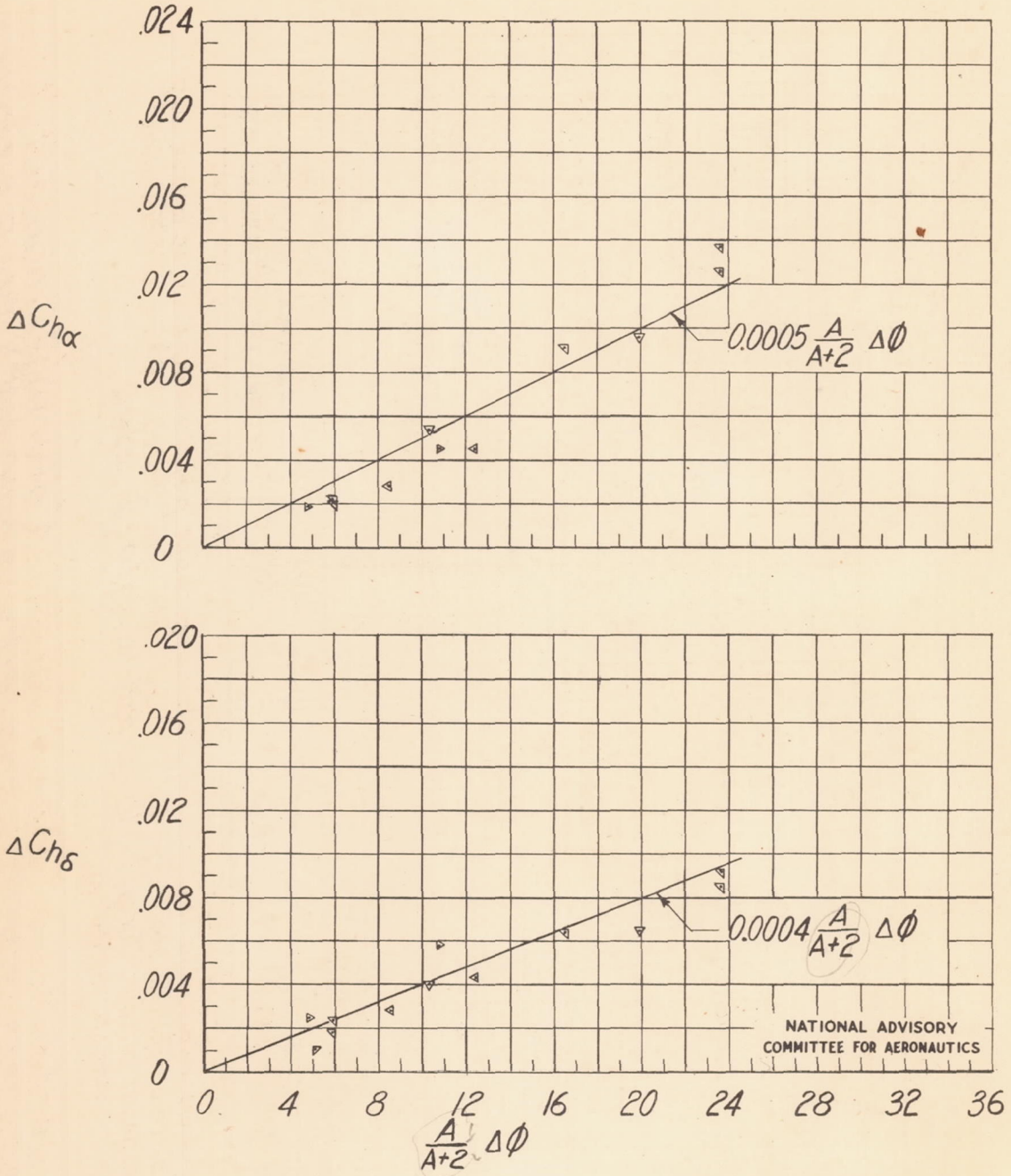


Figure 15.- Effect of trailing-edge angle on the hinge-moment characteristics of plain control surfaces on finite-span models. Gaps sealed; M, 0.11 or less. Symbols identified in table II.

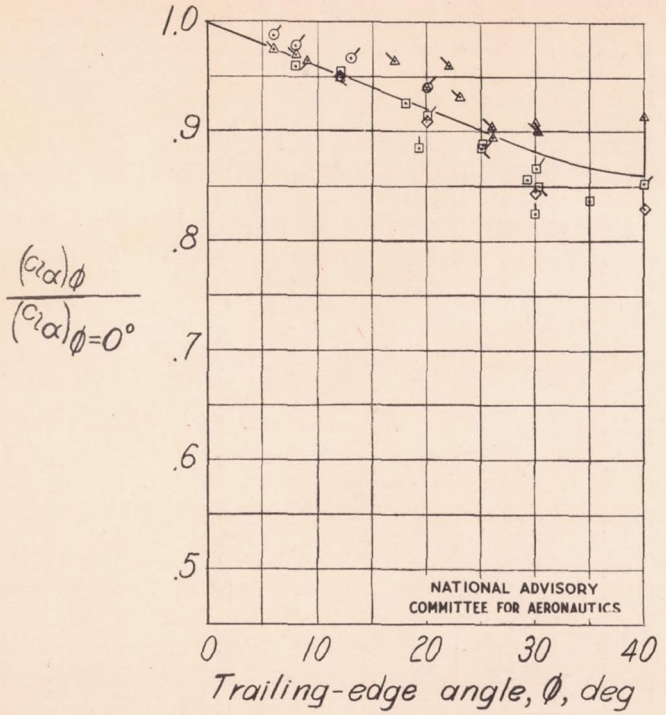


Figure 16.- Effect of trailing-edge angle on the lift-curve slope, relative to the lift-curve slope at zero trailing-edge angle, of two-dimensional airfoils. Gaps, sealed; M, 0.34 or less. Symbols identified in table II.

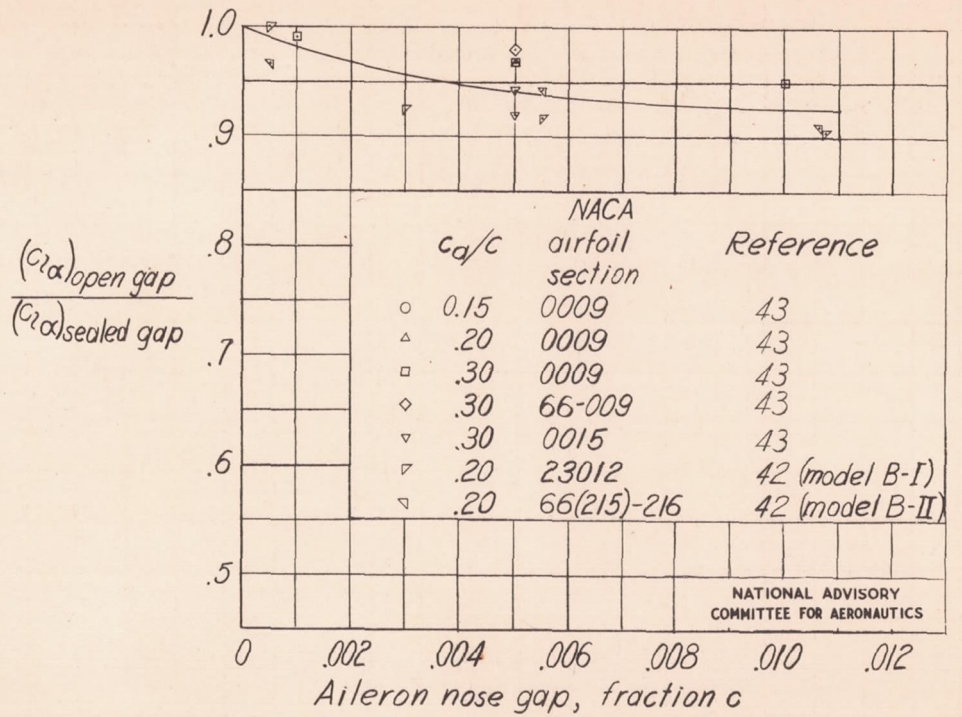


Figure 17.- Effect of aileron nose gap on the lift-curve slope, relative to the lift-curve slope with gap sealed, of two-dimensional models. M, 0.2 or less.

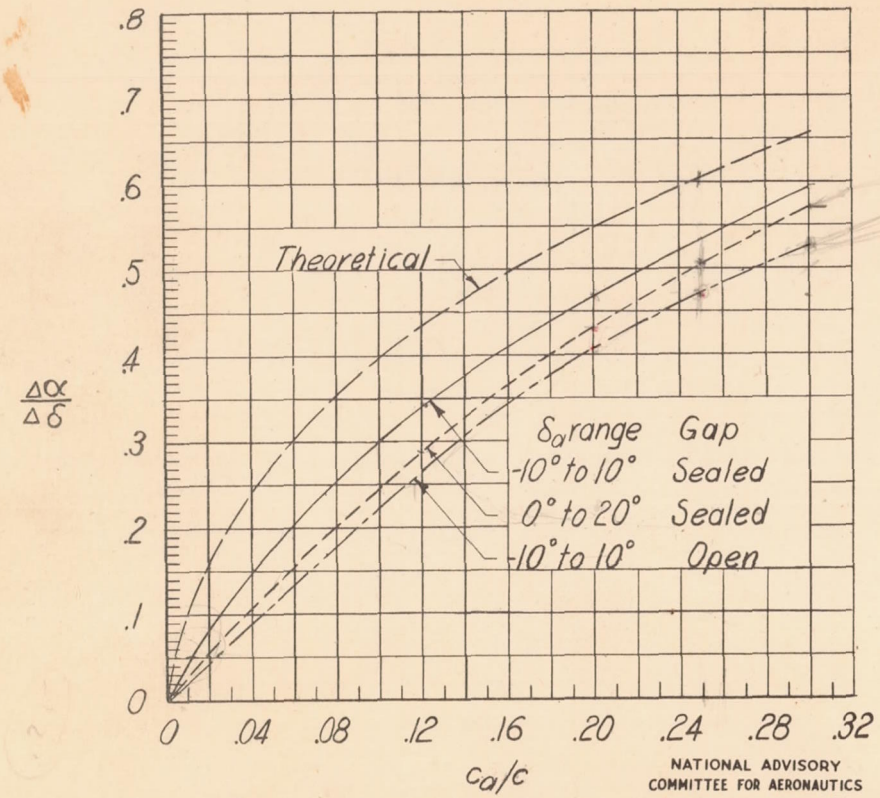


Figure 18.- Variation of lift-effectiveness parameter with flap chord ratio. Average trailing-edge angle, about 10°; M, 0.20 or less. Faired curves from reference 54.

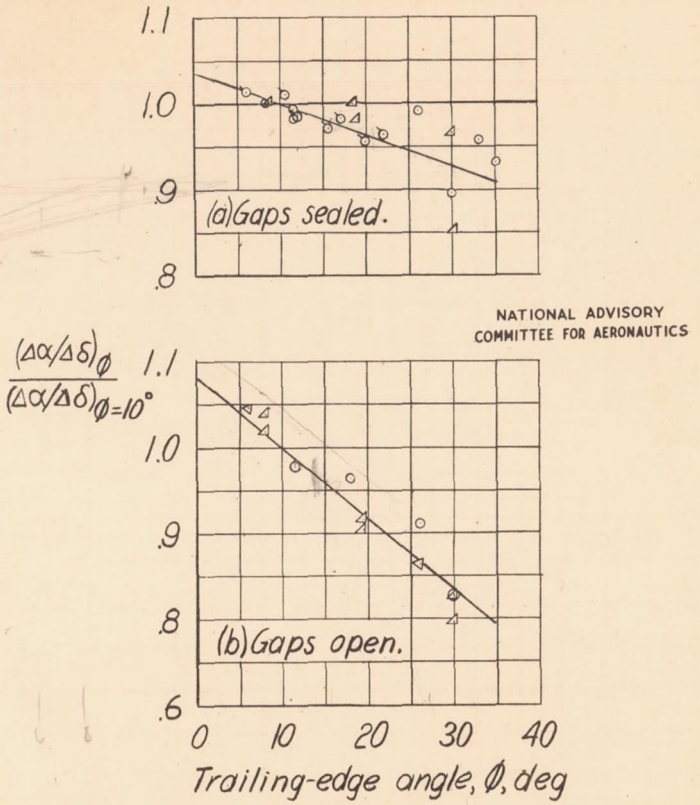


Figure 19.- Effect of trailing-edge angle on the lift-effectiveness parameter, relative to lift-effectiveness parameter at ϕ=10°. M, 0.20 or less. Data from reference 54.

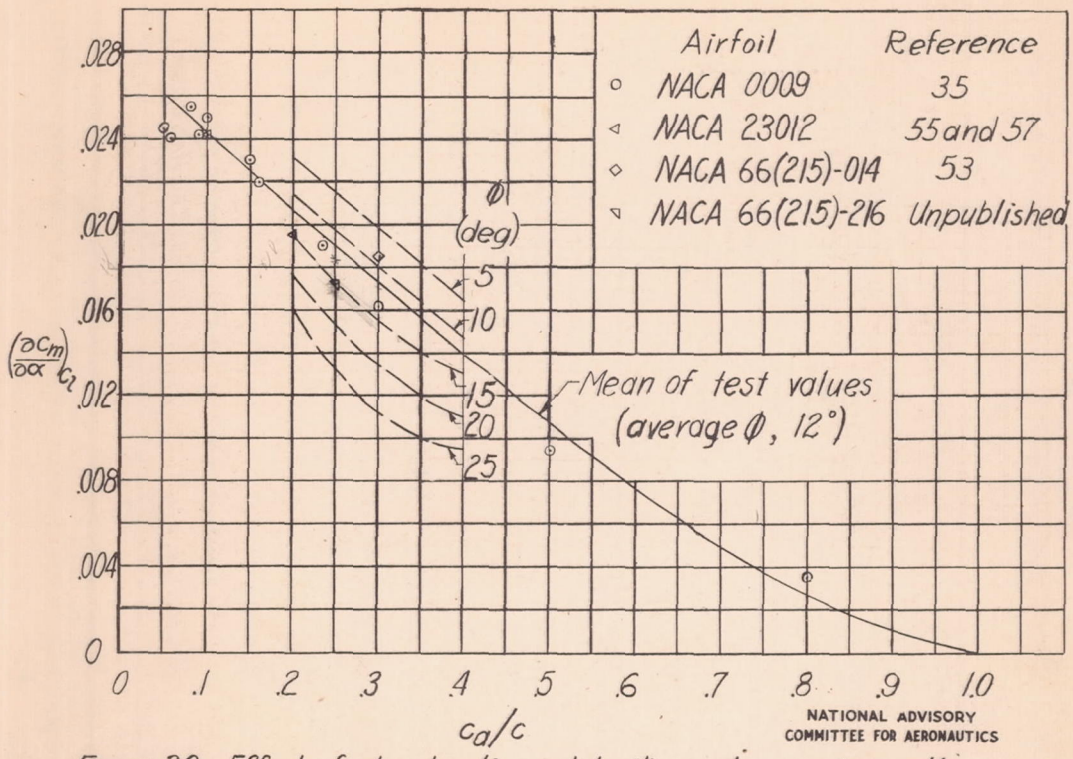


Figure 20.-Effect of chord ratio and trailing-edge angle on the parameter $\left(\frac{\partial c_m}{\partial \alpha}\right)_{c_l}$ of plain sealed ailerons. Derived from references 55 and 56.

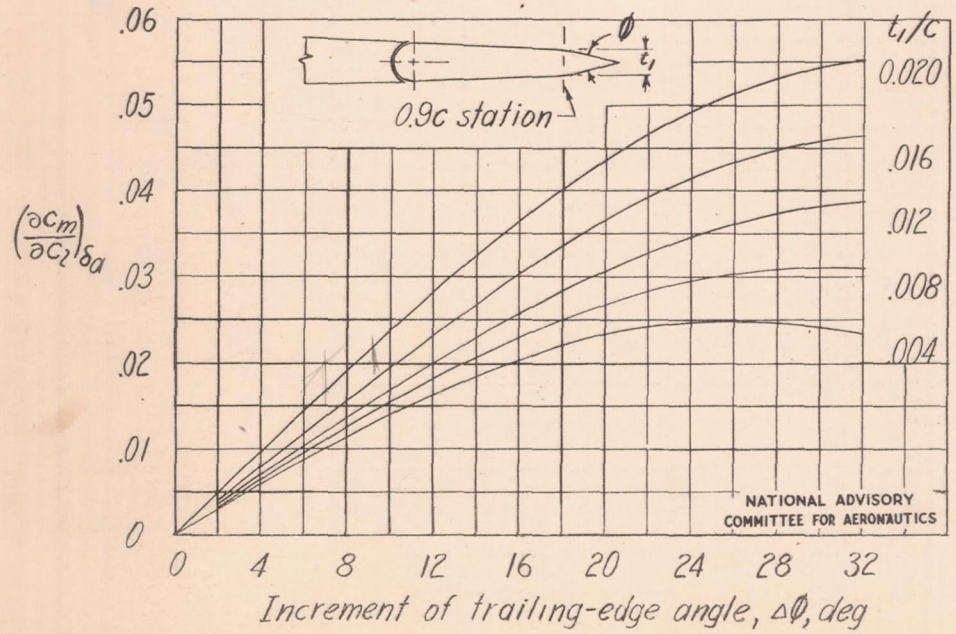


Figure 21.-Effect of trailing-edge modifications on the parameter $\left(\frac{\partial c_m}{\partial c_l}\right)_{\delta_a}$. Reference 56.

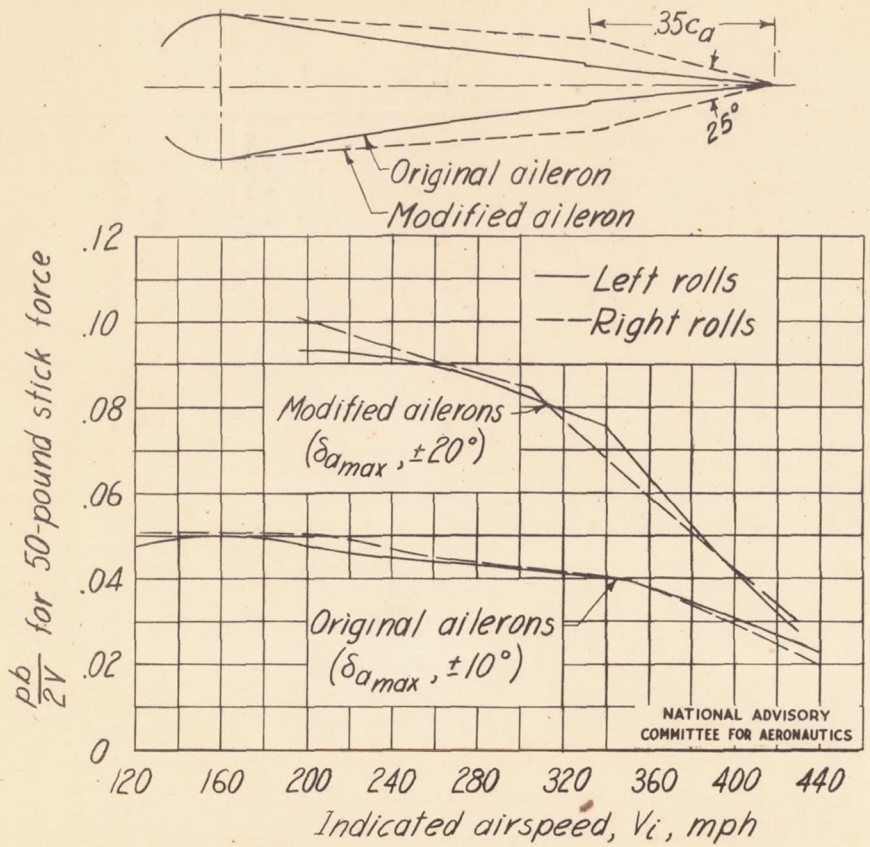


Figure 22.- Comparison of characteristics of original ailerons and modified ailerons on XP-51 airplane. Both sets of ailerons equipped with balancing tabs, aileron nose gaps unsealed.

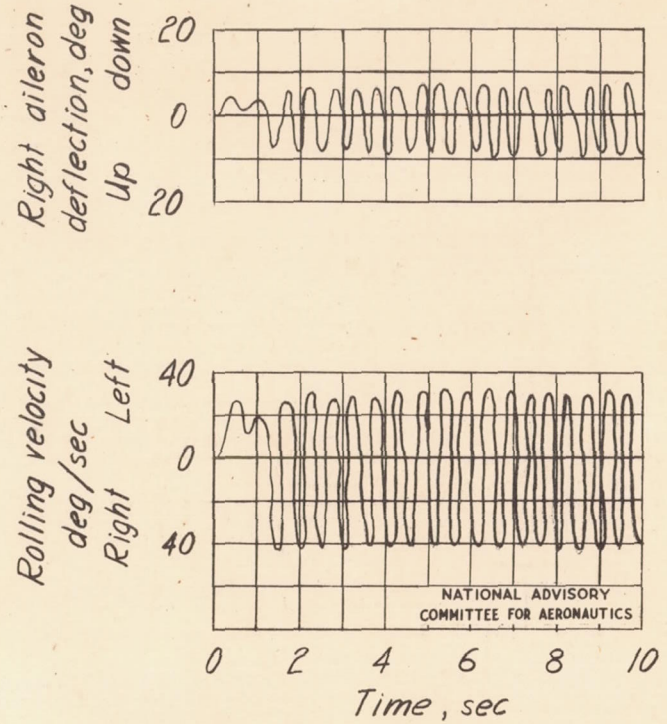


Figure 23.- Time history showing stick-free characteristics of XP-51 airplane equipped with sealed ailerons having trailing-edge angles of 32°. V_i, 320 miles per hour.

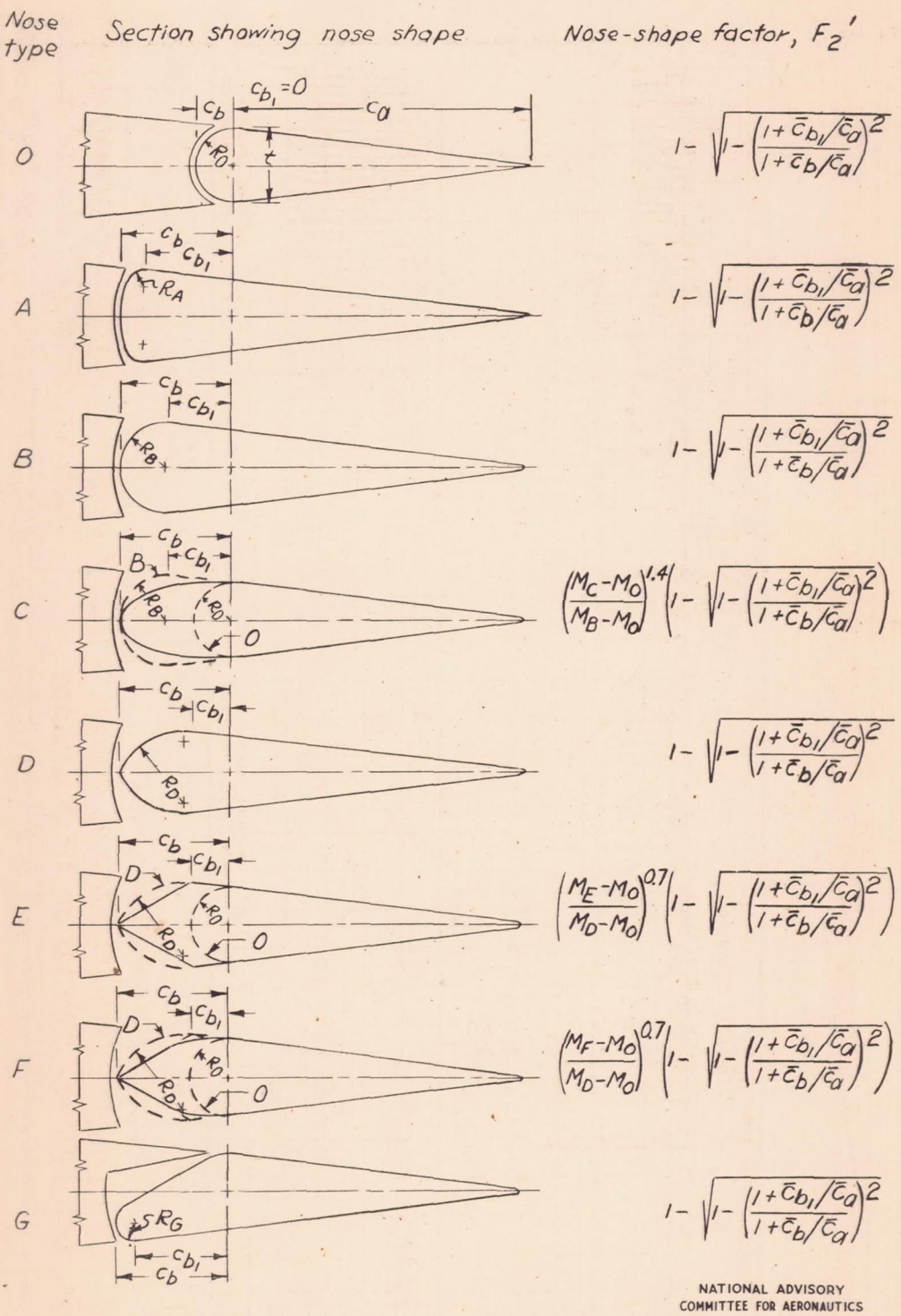


Figure 24.-Various nose shapes considered in correlation of plain-overhang and Frise balances and corresponding expressions for nose-shape factor.

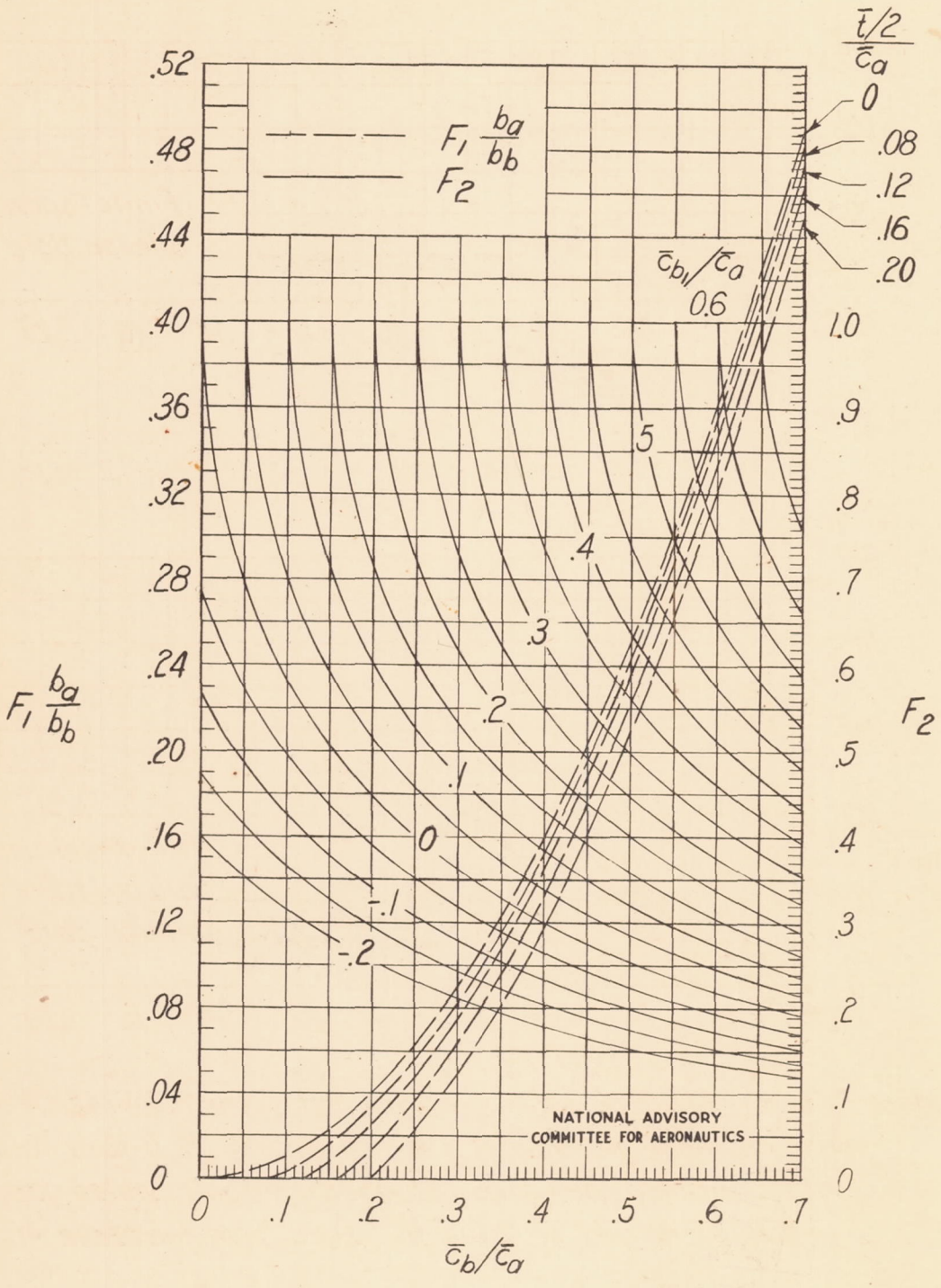
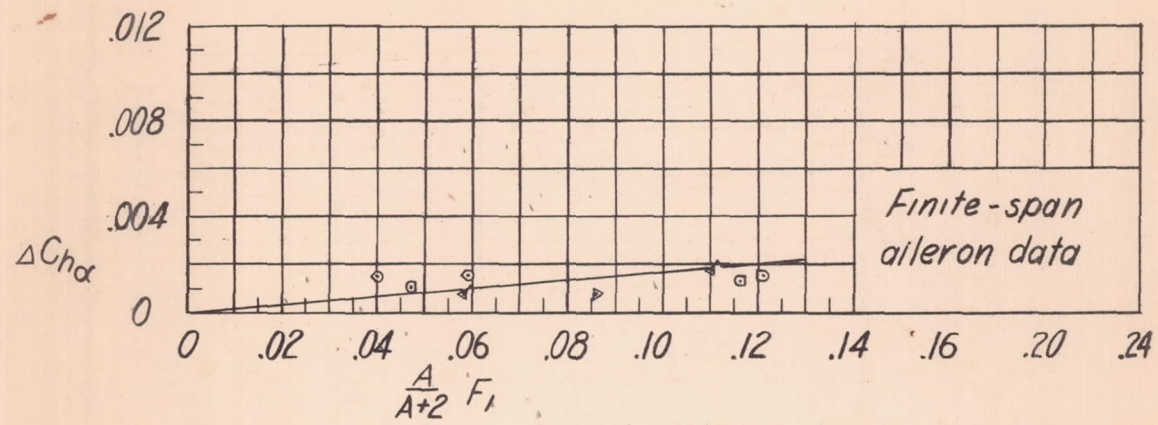


Figure 25.- Charts for determining numerical values of overhang factor F_1 and of nose-shape factor F_2 from geometric constants of balanced ailerons.



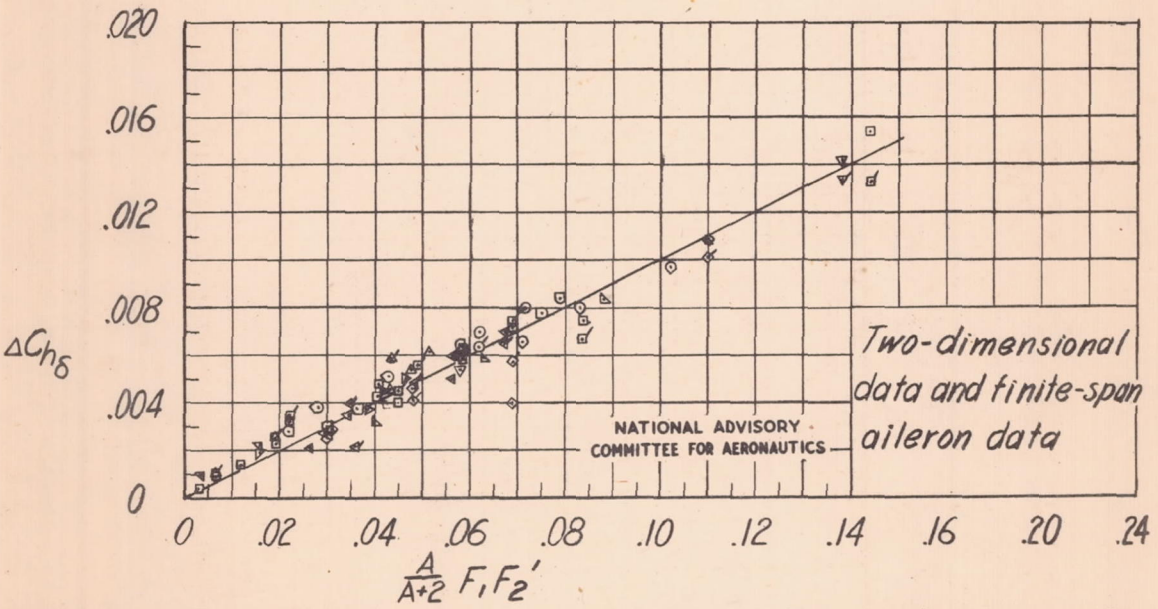


Figure 26.- Effect of plain-overhang and Frise balances on the hinge-moment parameters of ailerons. M, 0.36 or less. Plain symbols, open gaps; flagged symbols, sealed gaps. Symbols identified in table III. Data from reference 46.

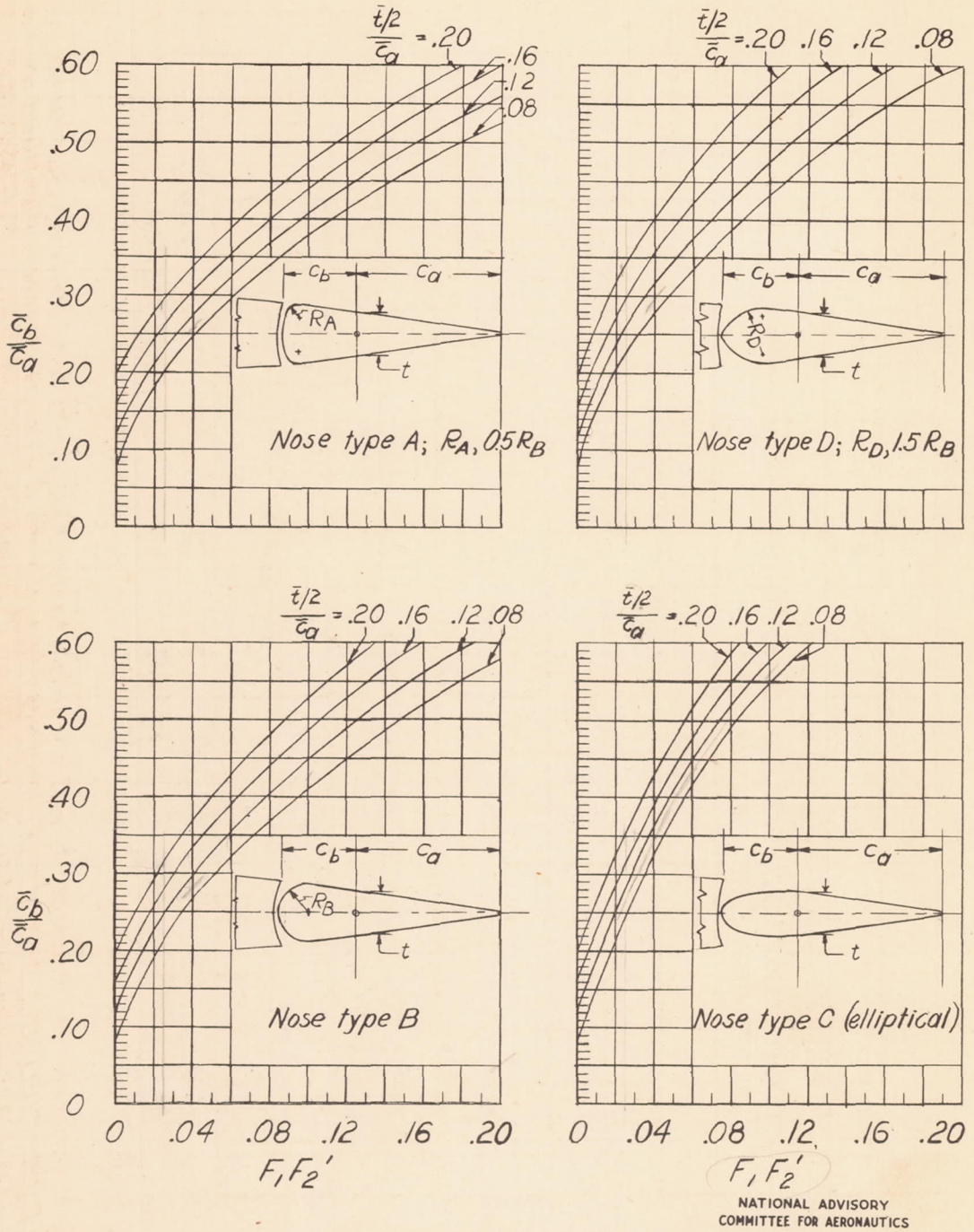


Figure 27.— Charts for estimating the required lengths of overhangs having various nose shapes. Letters A, B, C, and D refer to the corresponding nose shapes of figure 24.

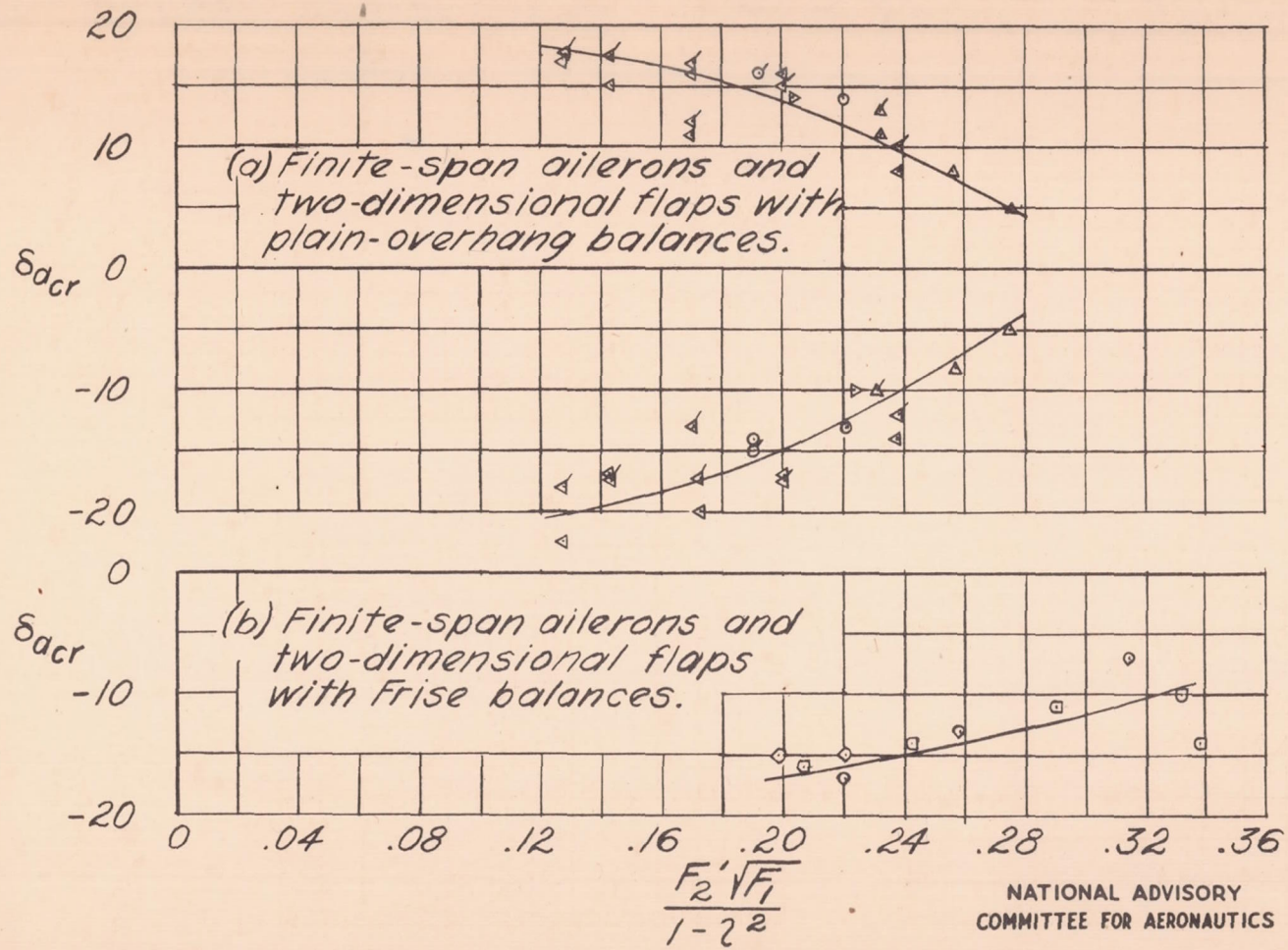


Figure 28.— Variation of critical deflection with factor $F_2'\sqrt{F_1}/(1-\tau^2)$ for control surfaces with plain-overhang and Frise balances. M, 0.1 to 0.2; α, 0°. Symbols identified in table III; plain symbols, open gaps; flagged symbols, sealed gaps. Reference 46.

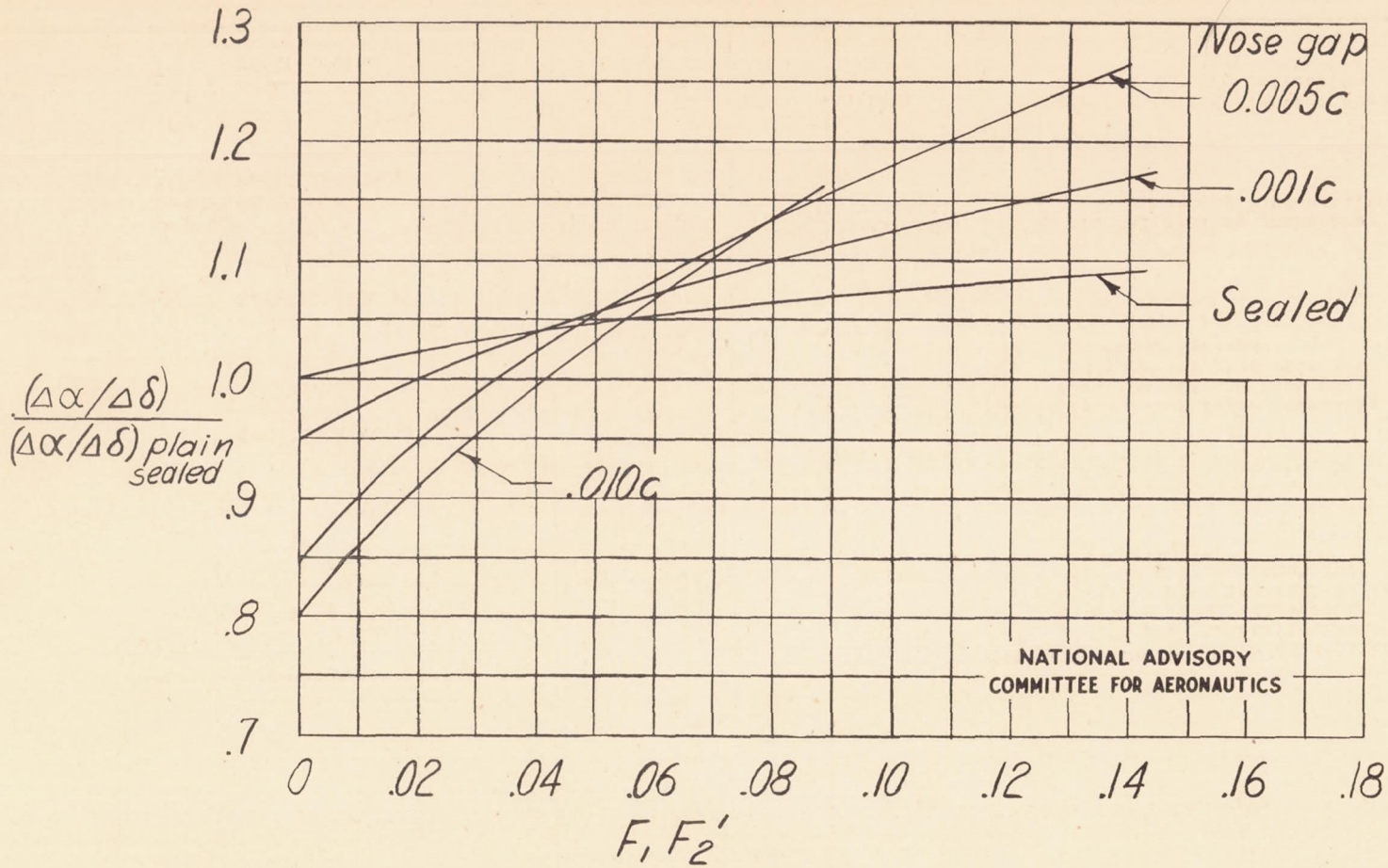
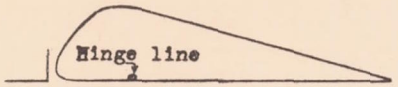
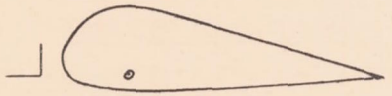
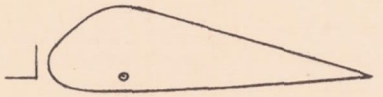
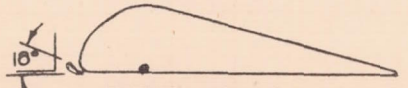
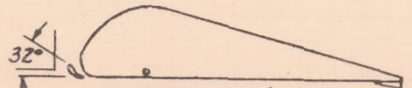


Figure 29.- Variation of lift-effectivenes parameter, relative to lift-effectiveness parameter for plain-sealed ailerons, with the product F_1F_2' and with nose gap. M, 0.2 or less. Faired curves from figure 6 of reference 46.

Aileron arrangement	Characteristics in level flight				
	Maximum $\frac{pb}{2V}$	Control force at 230 mph (lb)		Shake	Remarks
		3/4 full deflection	Full deflection		
 Original	0.055	16	45	Violent	Shake set in at 3/4 deflection at 100 mph, intensity increasing with speed; apparently control force for full deflection much larger than for 3/4 deflection
 Modification 1	.052	38	53	Very slight	Large aileron force caused by downfloating tendency of ailerons combined with differential linkage
 Modification 2	.050	28	43	Slight	
 Modification 3	.058	21	37	Sometimes violent	Occasional violent shake probably caused by slat stalling
 Modification 4	.065	26	29	Slight	Force for full deflection about same as for 3/4 deflection

NATIONAL ADVISORY COMMITTEE FOR AERONAUTICS

Figure 30.- Summary of results of flight tests of the original ailerons and various modified ailerons of the XF4U-1 airplane.

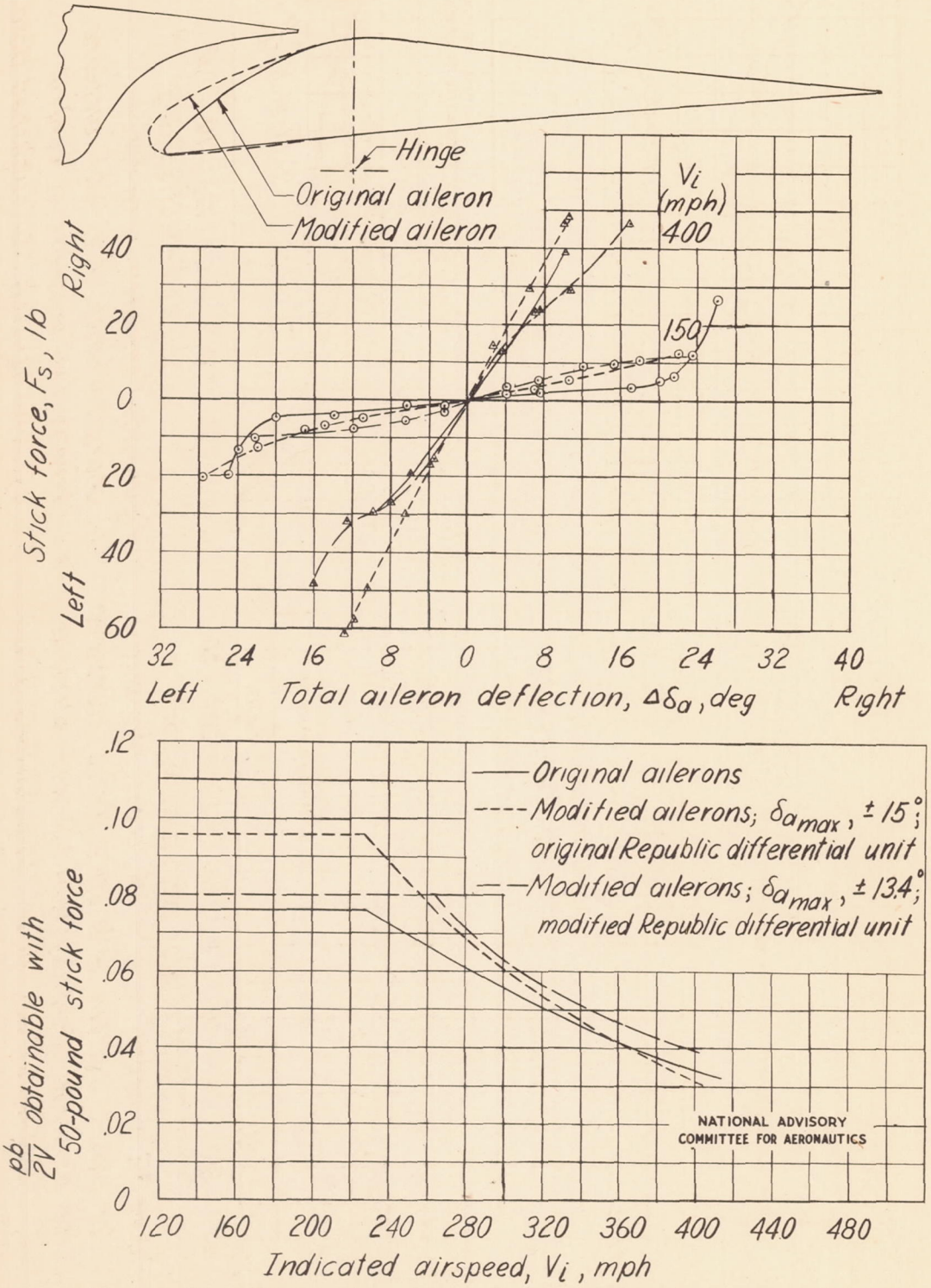


Figure 31.- Characteristics of original ailerons and modified ailerons on P-47C-1-RE airplane. Unpublished data.

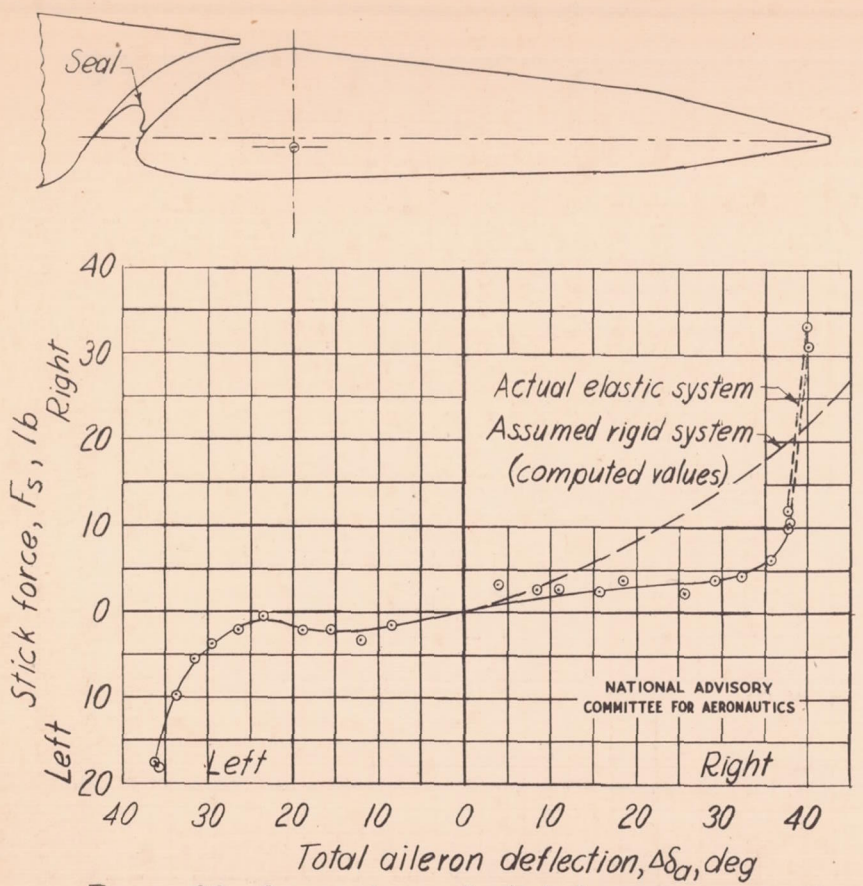


Figure 32.- Comparison of stick forces measured for elastic system with stick forces computed for assumed rigid system. P-40F airplane; V_i, 202 miles per hour. Unpublished data.

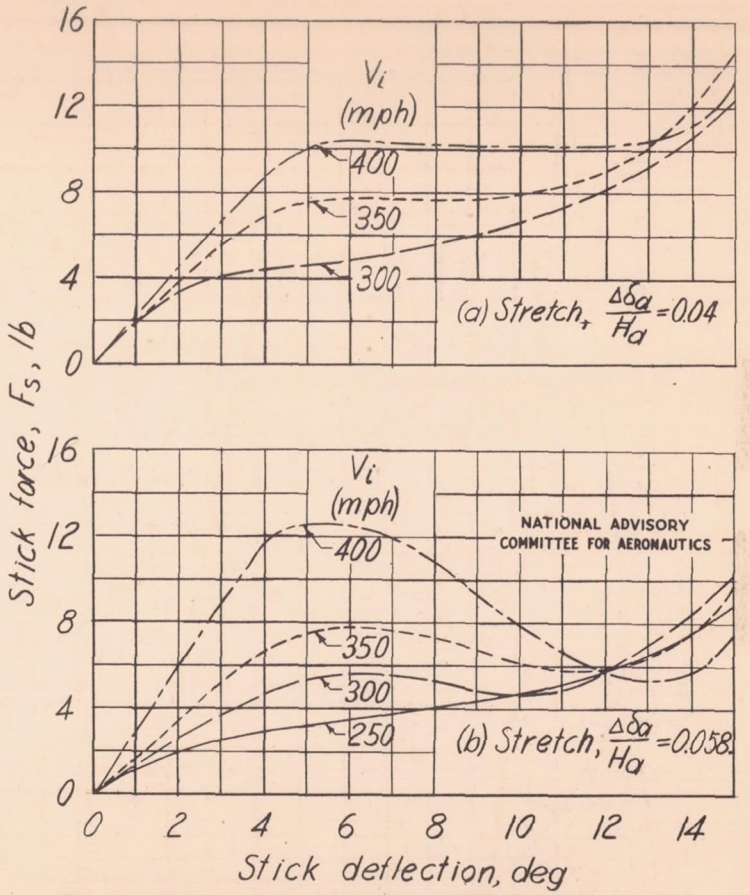


Figure 33.- Computed stick-force characteristics of P-40F airplane having two amounts of control-system stretch. Unpublished data.

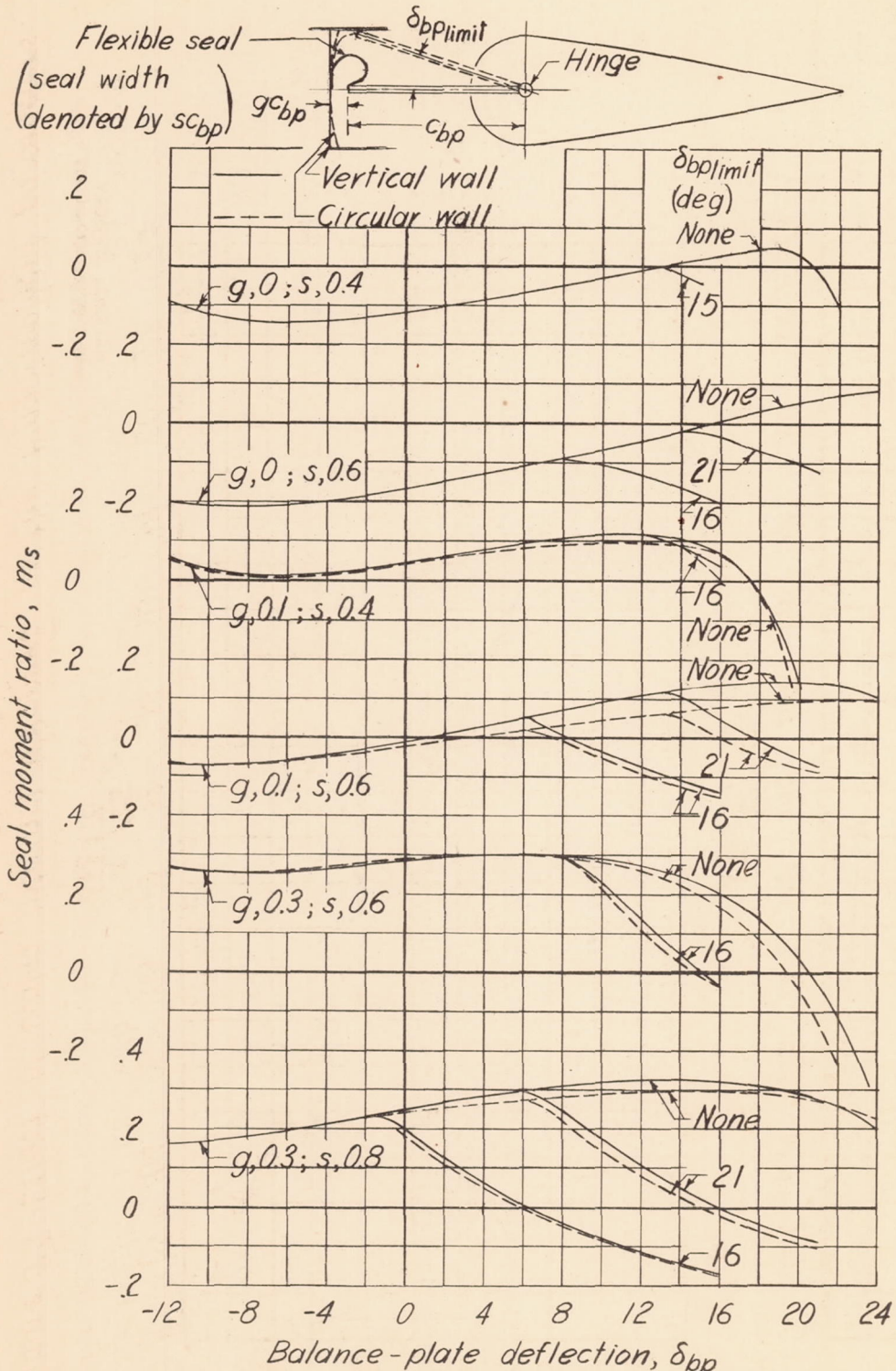


Figure 34. – Values of the seal-moment ratio m_s for various arrangements of sealed internal balances. Reference 59.

NATIONAL ADVISORY COMMITTEE FOR AERONAUTICS

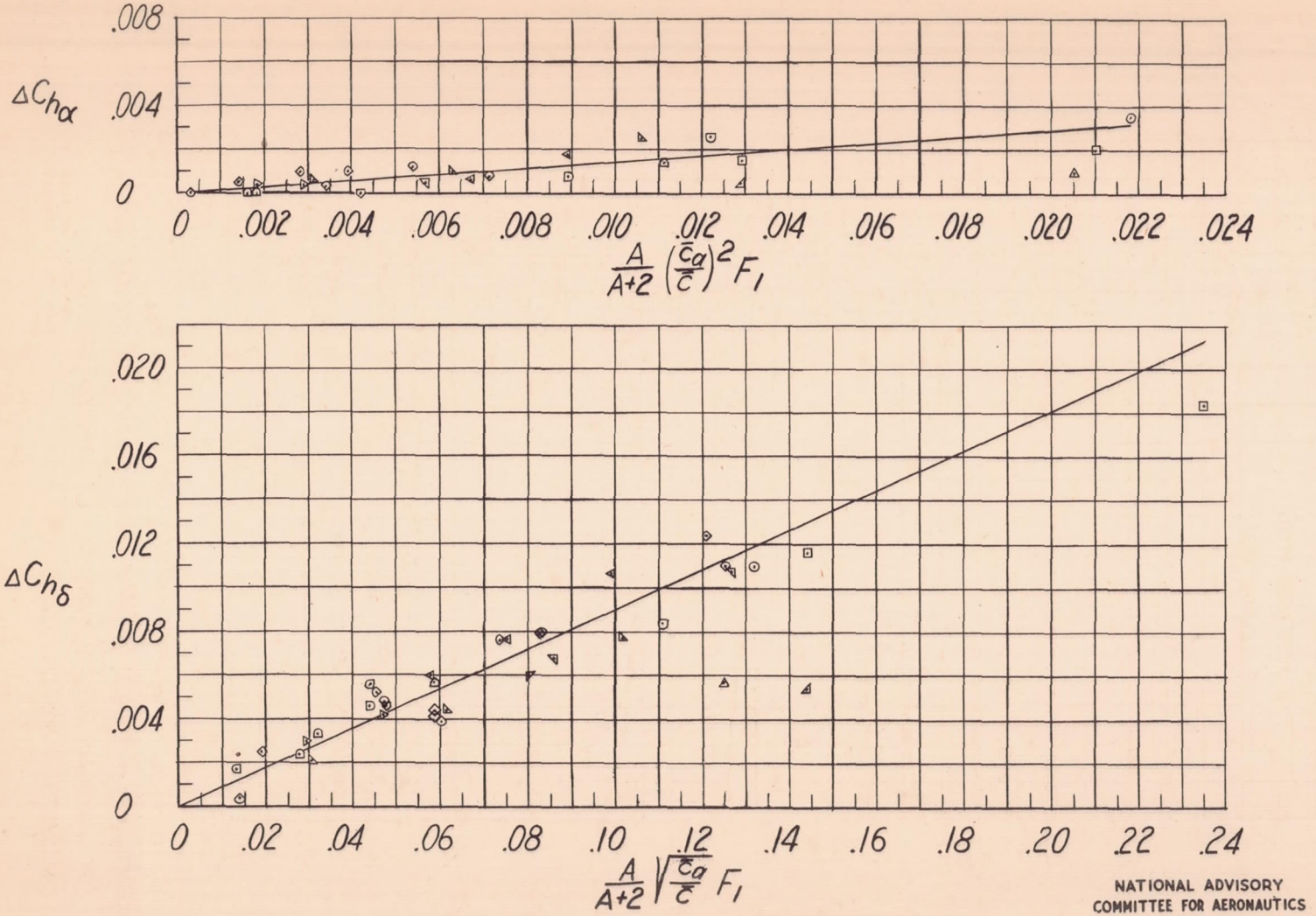


Figure 35.- Effect of sealed internal balances on the hinge-moment parameters of control surfaces. M, 0.2 or less. Symbols identified in table IV.

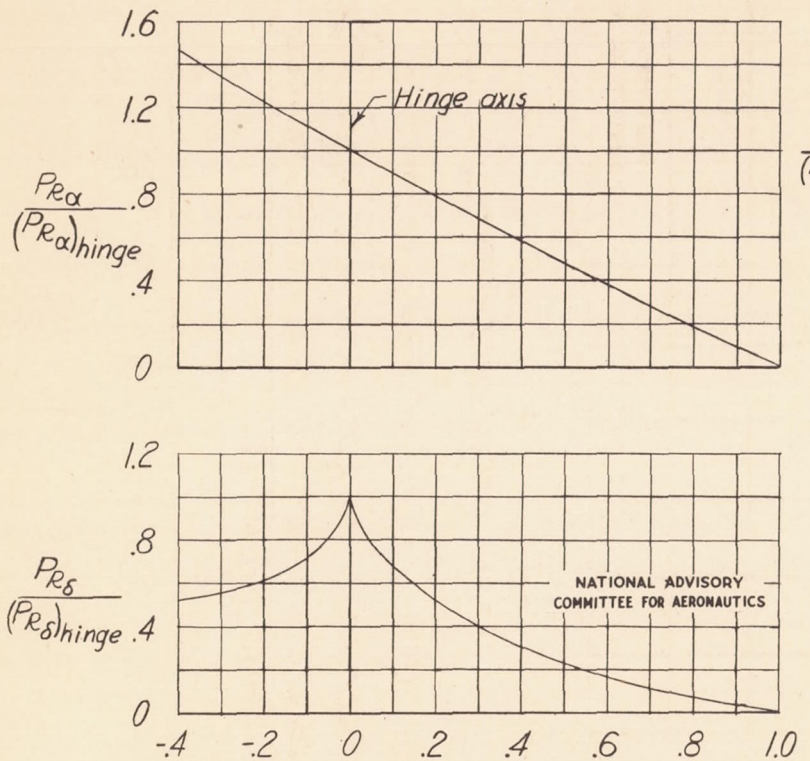


Figure 36.-Effect of location of balance-chamber vents on variation of resultant-pressure coefficient with angle of attack and with aileron deflection. c_a/c, 0.18. References 43 and 45.

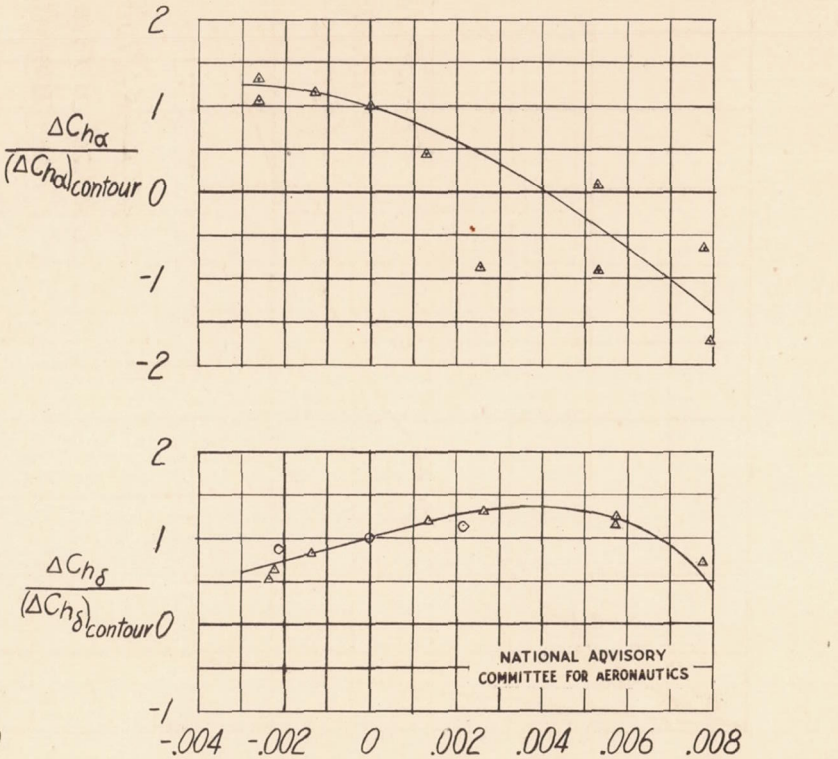


Figure 37.-Effect of cover-plate misalinement on the incremental hinge-moment parameters caused by sealed internal balances. Symbols identified in table IV. Reference 45.

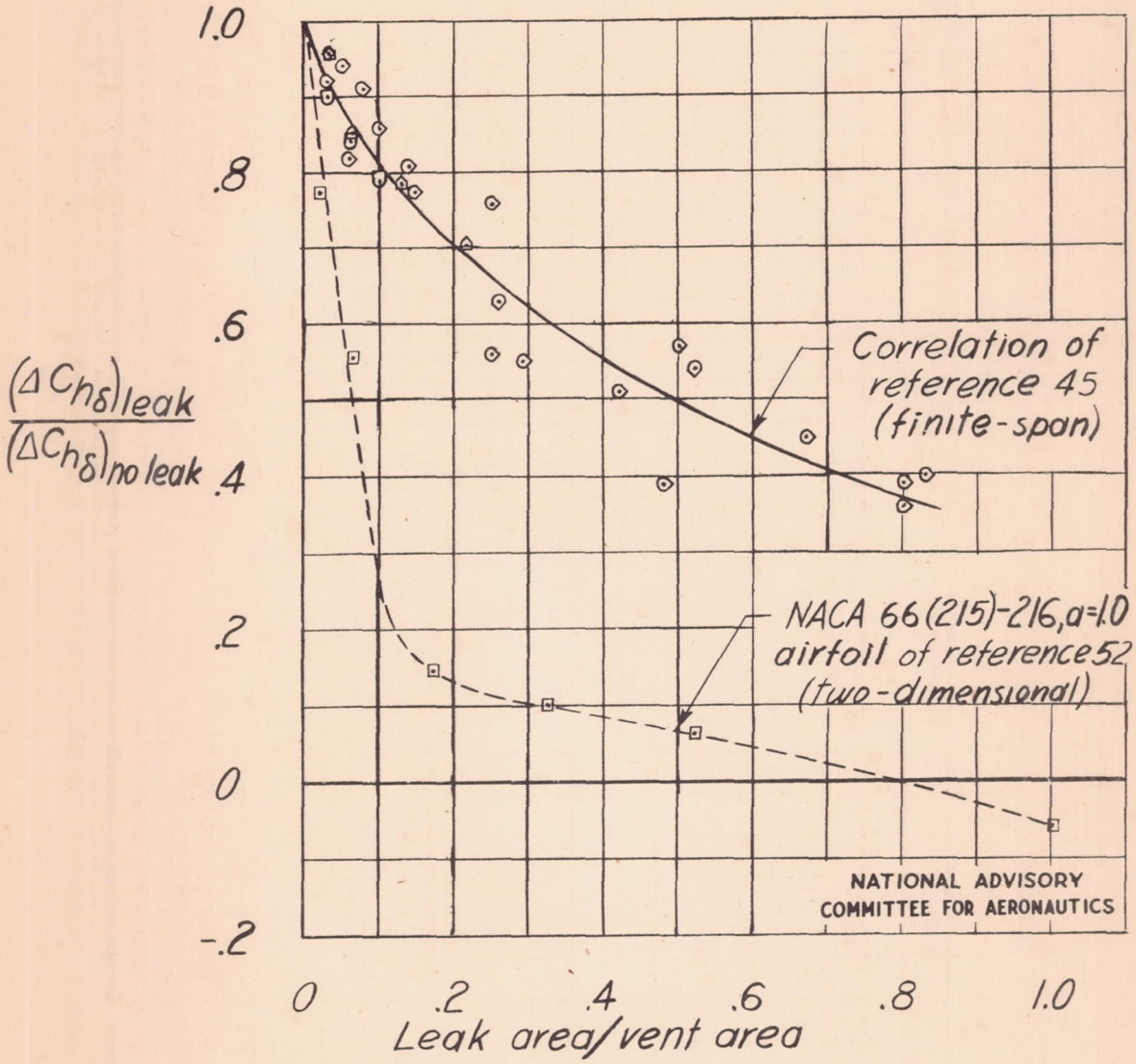


Figure 38.- Effect of leakage on the incremental hinge-moment slope ΔC_{h_δ} caused by internal balances. Symbols identified in table IV.

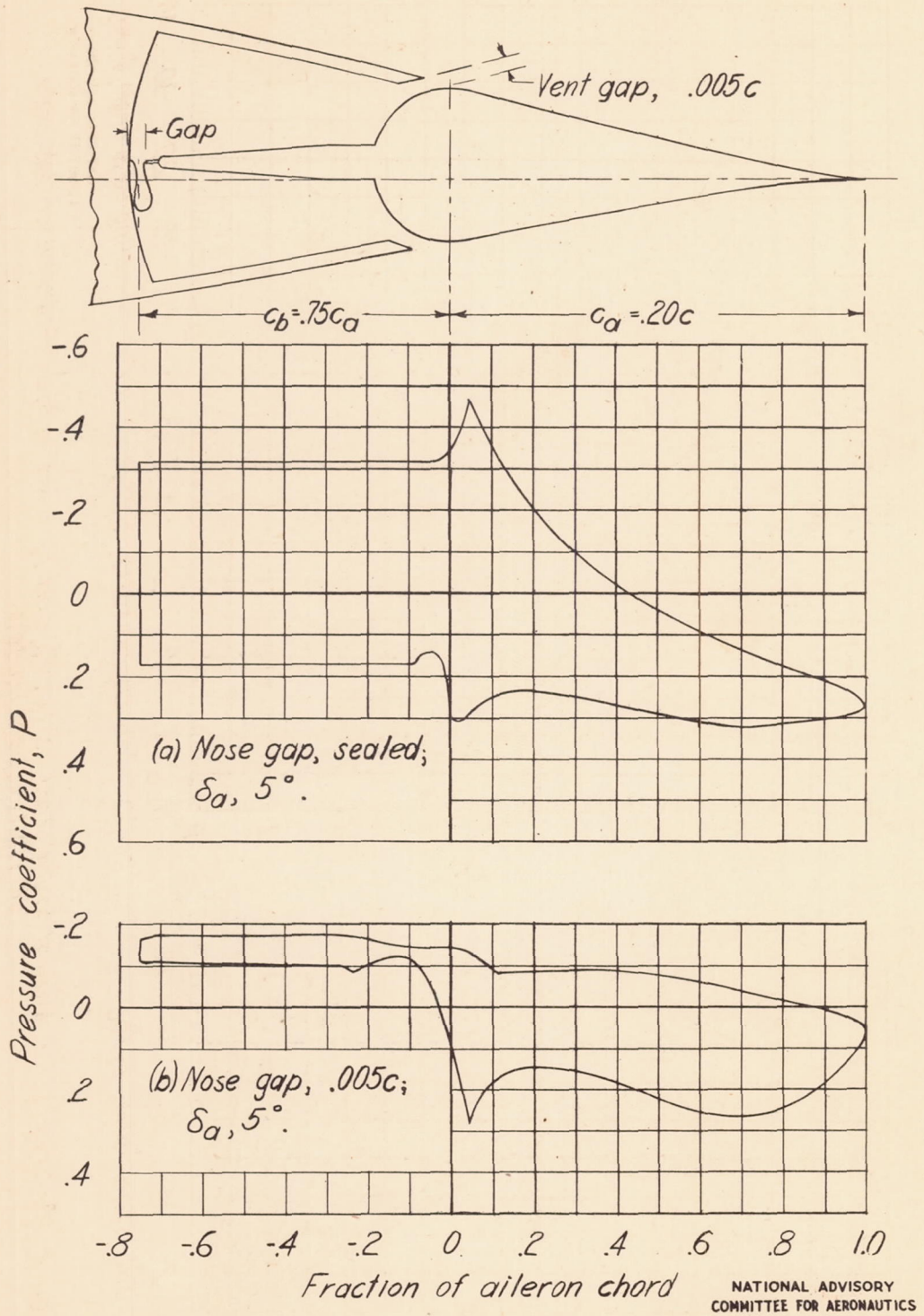


Figure 39.- Effect of nose gap on the pressure distribution of an internally balanced 0.20c flap on an NACA 66(215)-216 airfoil. c_b/c_a, 0.75; two-dimensional data; α, 0°. Reference 52.

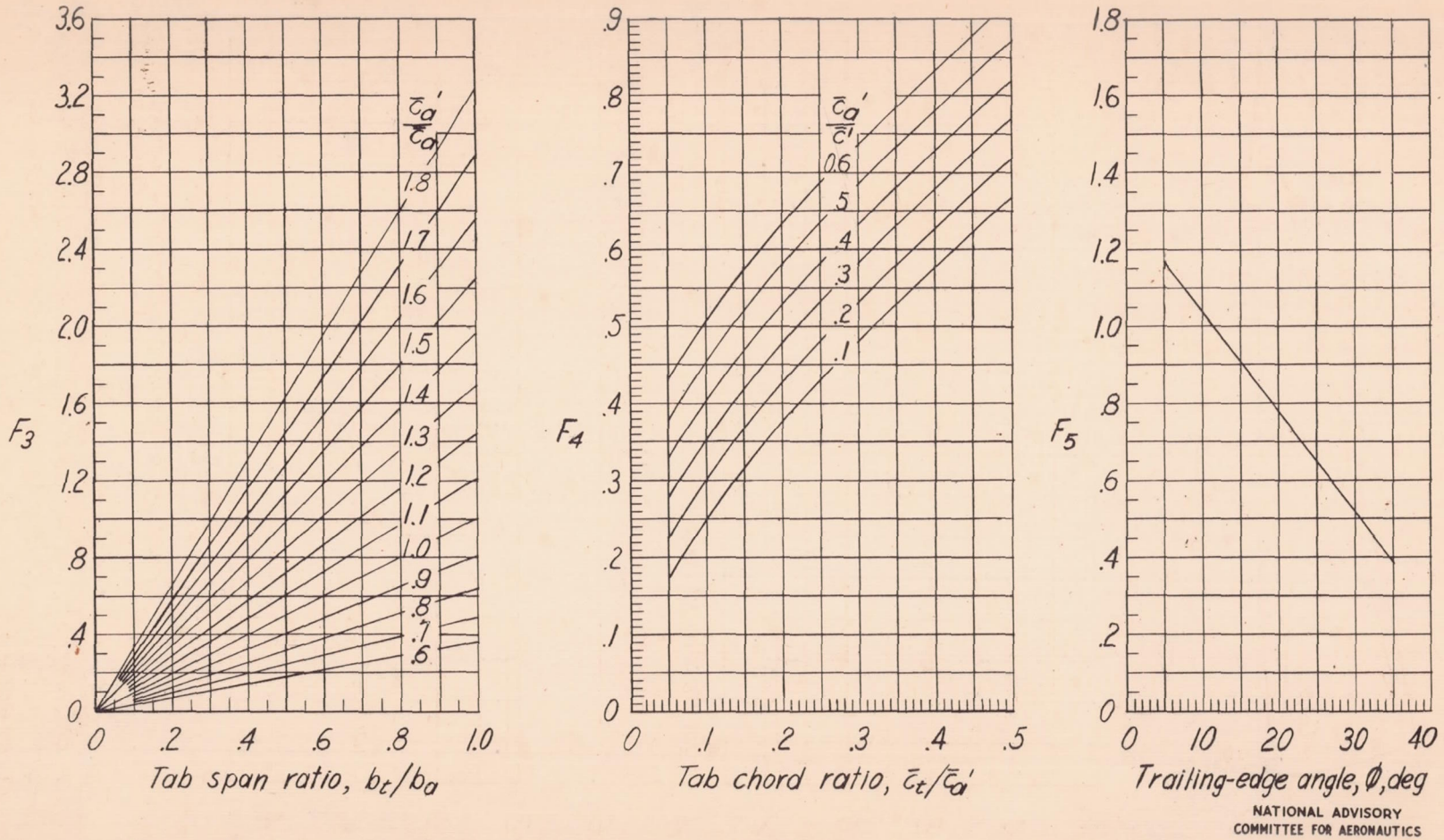


Figure 40.-Charts for evaluating the factors F_3, F_4, and F_5 used in the correlation of tab data on finite-span models.

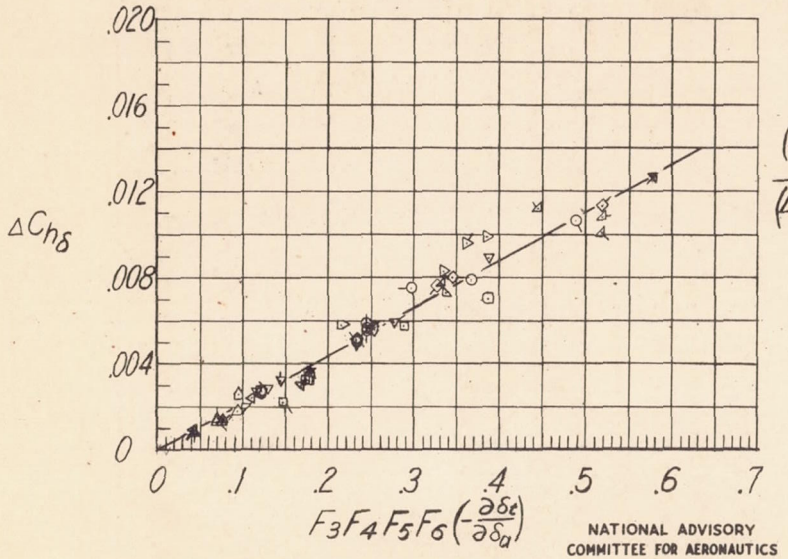


Figure 41.-Effect of linked tabs on the hinge-moment parameter C_{h_δ}. Finite-span data from reference 47. Symbols identified in table V.

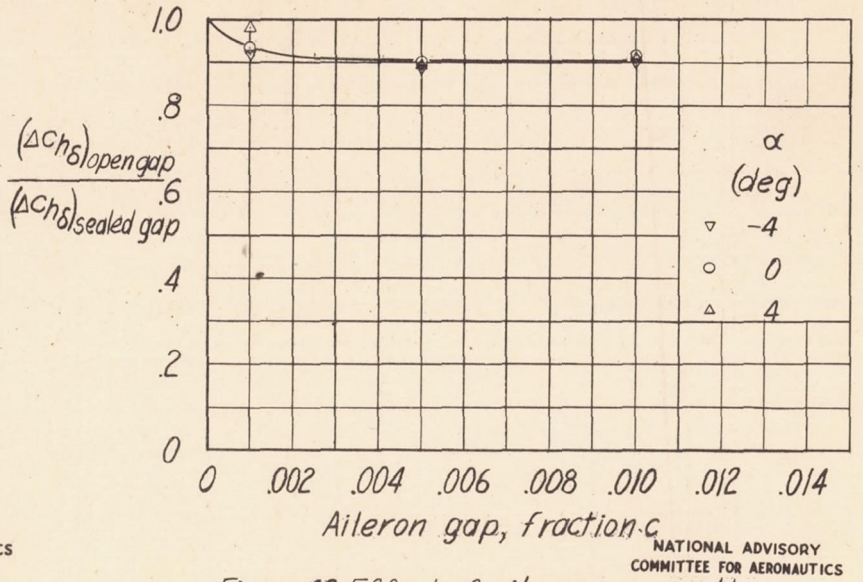
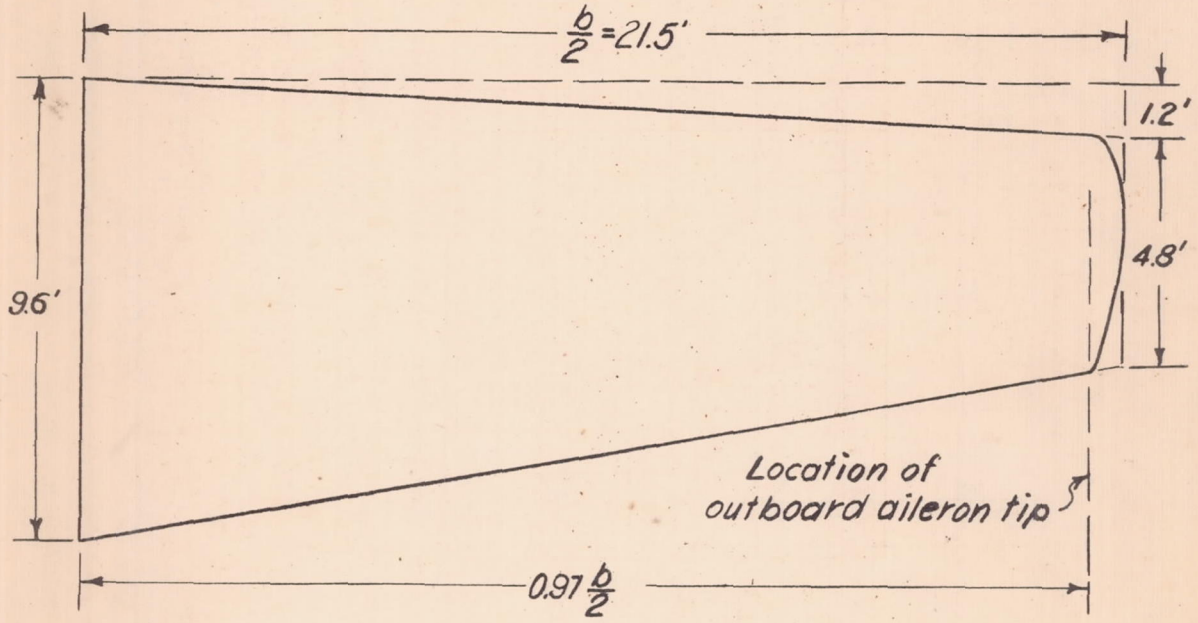


Figure 42.-Effect of aileron gap on the incremental hinge-moment slope ΔC_{h_δ} due to a linked tab. NACA 0009 airfoil.



Airplane constants

Wing span, b, ft	43
Wing area, S, sq ft	308
Aspect ratio, A	6.0
Taper ratio, λ	.5
Root airfoil section	NACA 23015
Tip airfoil section	NACA 23009
Airplane weight, lb	12,000
Stick length, ft	2.33

NATIONAL ADVISORY
COMMITTEE FOR AERONAUTICS

Figure 43.- Wing plan form and airplane constants for assumed fighter airplane.

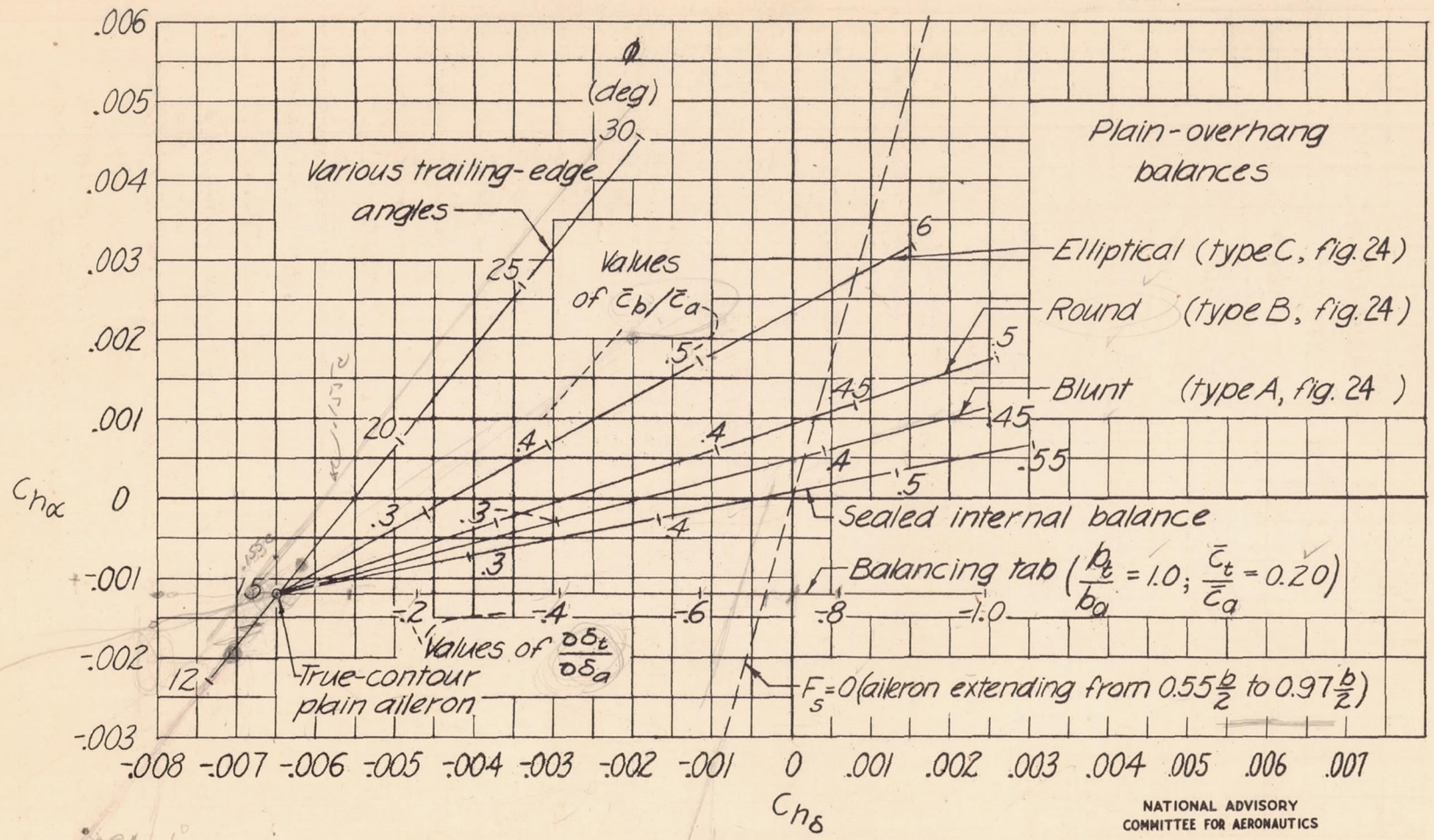


Figure 44.- Comparison of the effects of the various aerodynamic balances on the aileron hinge-moment parameters of the airplane wing of figure 43. c_a/c, 0.25; incremental hinge-moment parameters estimated from correlations.

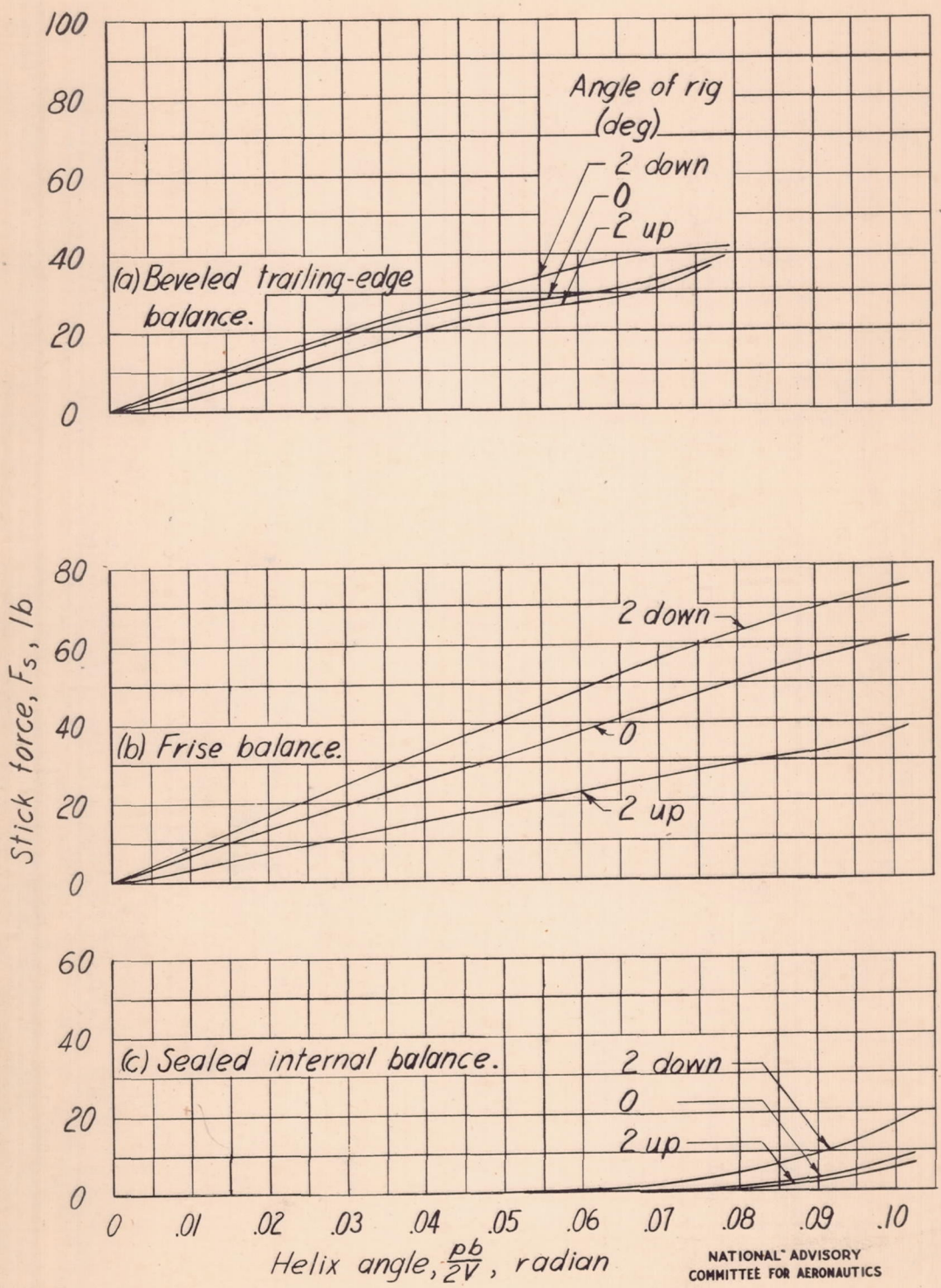


Figure 45. - Effects of changes in aileron rigging on the estimated stick forces of a high-speed fighter airplane. V_i, 300 miles per hour; no differential in linkage system. Reference 64.

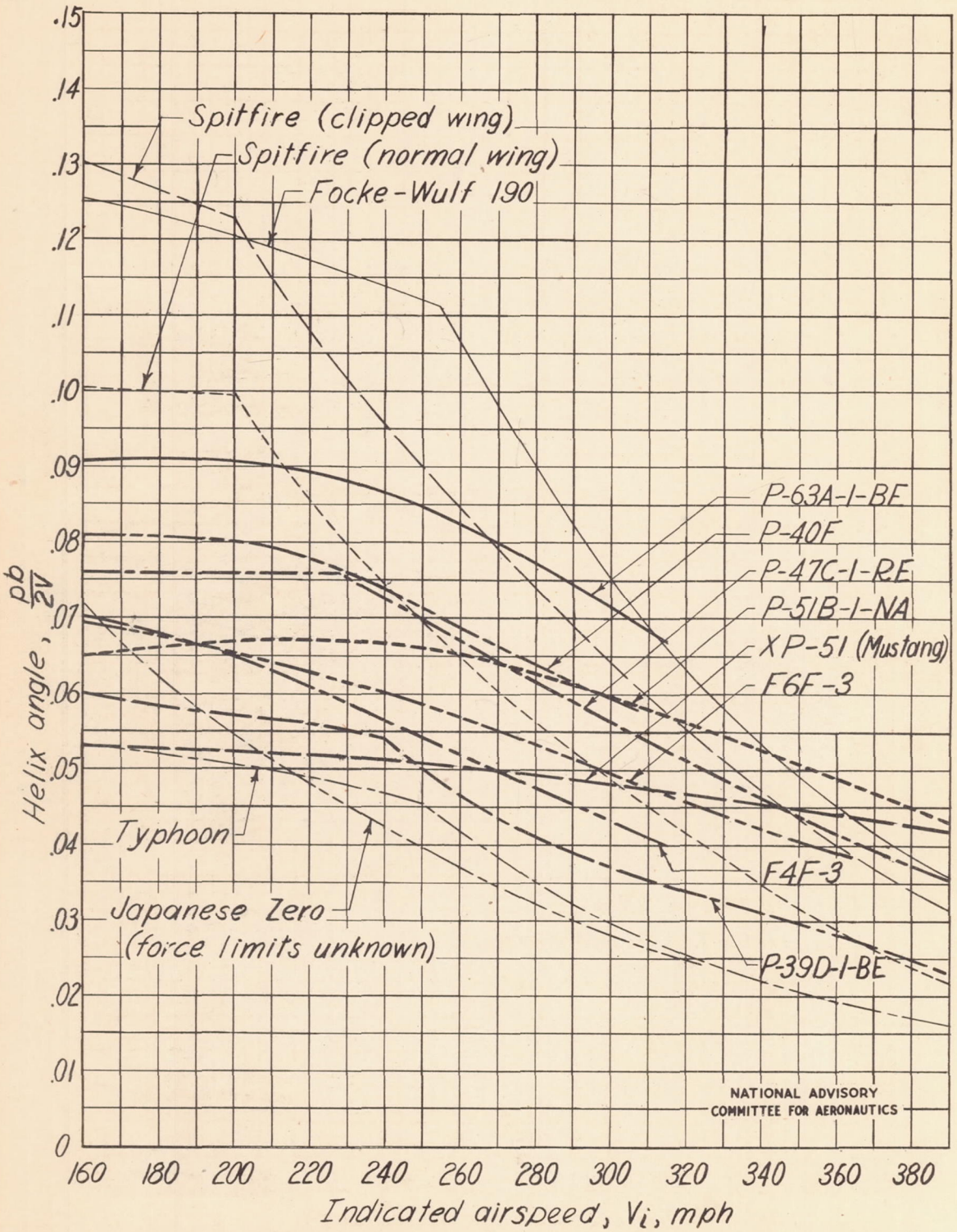


Figure 46.- Variation with indicated airspeed of helix angle pb/2V obtainable with 50-pound stick force. Altitude, 10,000 feet.

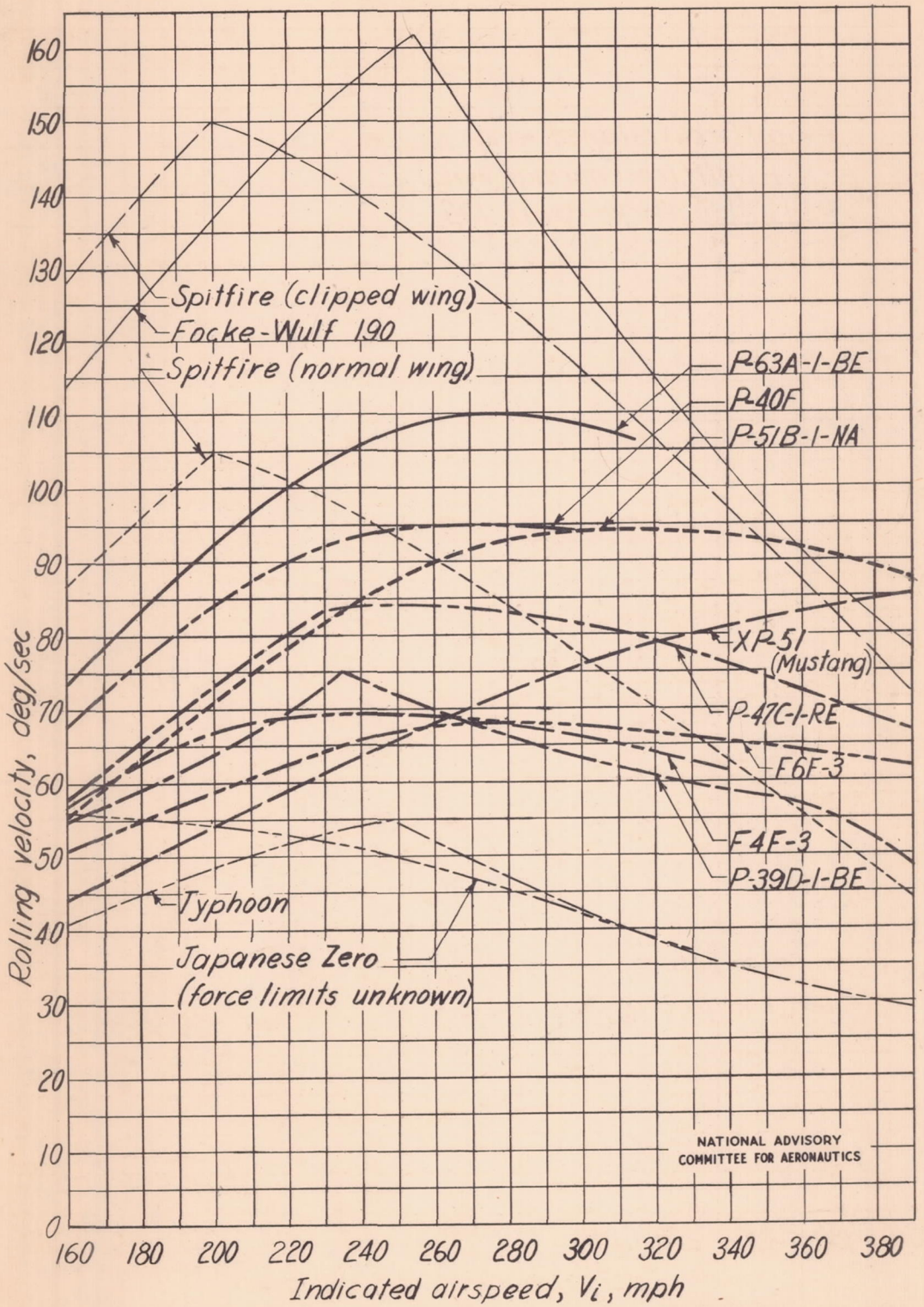
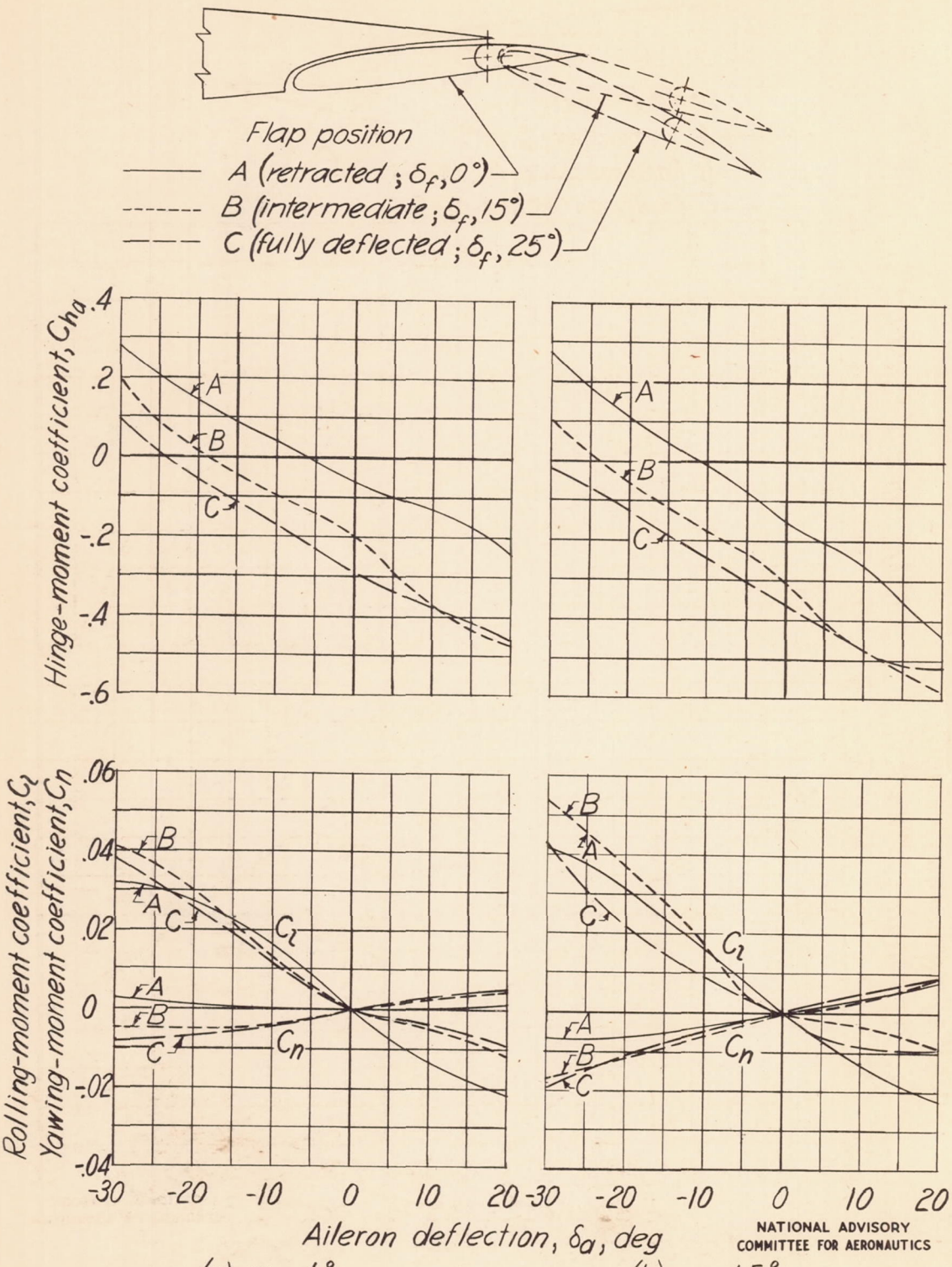
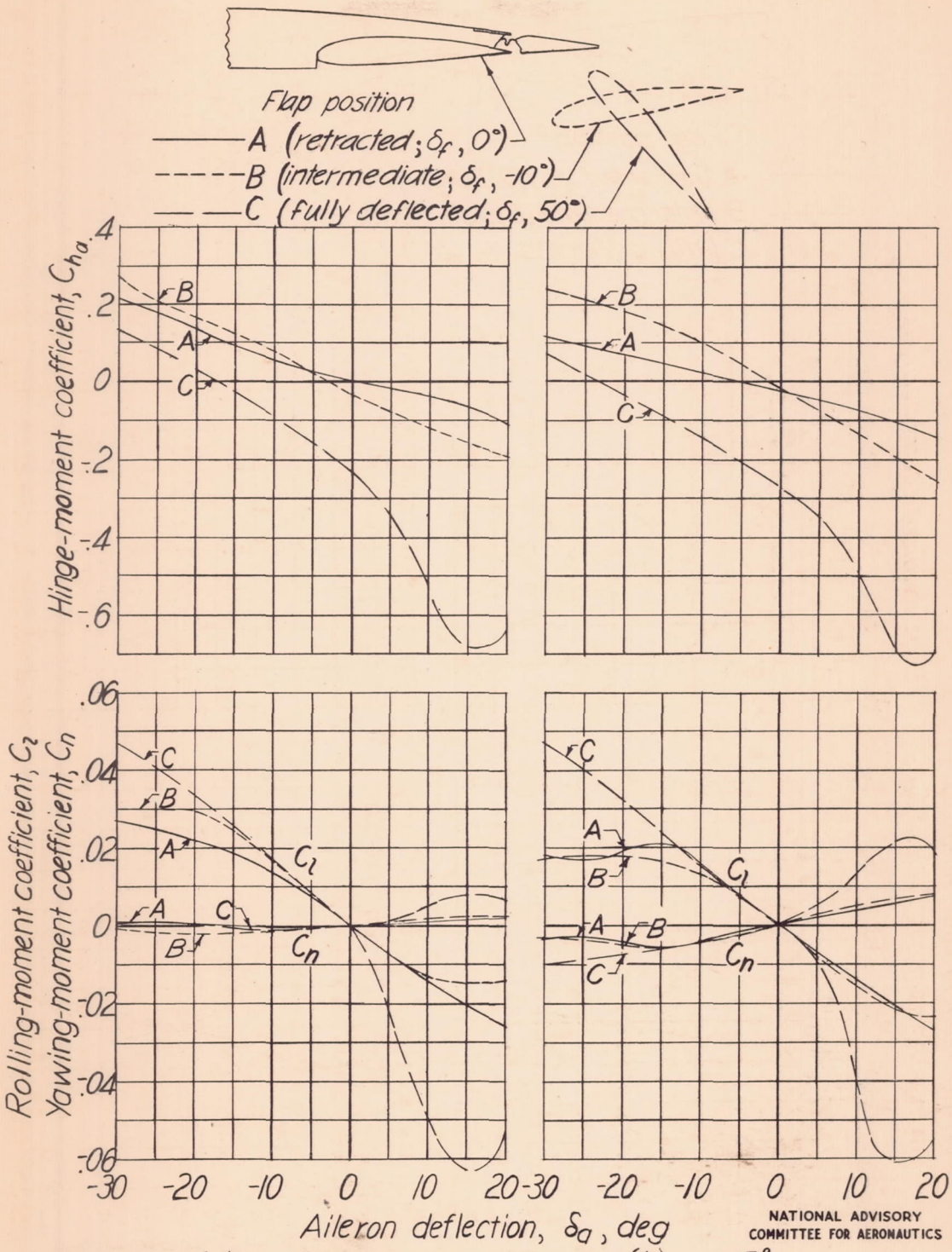


Figure 47.- Variation with indicated airspeed of rolling velocity obtainable with 50-pound stick force. Altitude, 10,000 feet.



(a) α, 1°. (b) α, 15°.

Figure 48.- Effect of flap position on the characteristics of a flap-trailing-edge aileron. Reference 67.



(a) α, 1°. (b) α, 15°.

Figure 49.- Effect of retractable-flap position on the characteristics of a narrow-chord conventional aileron. Reference 71.

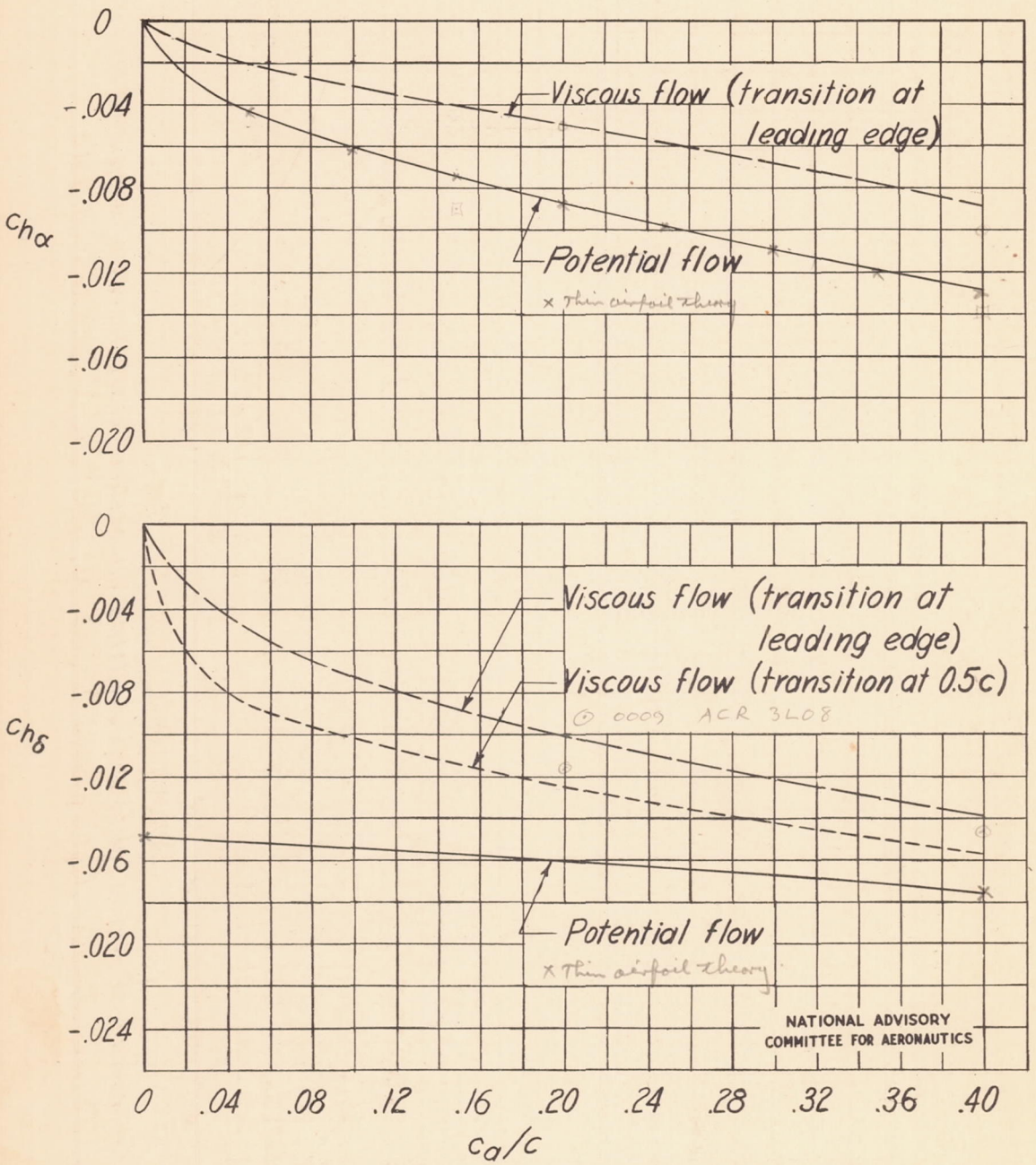


Figure 50.-Comparisons of theoretical hinge-moment parameters for viscous and potential flow. Unpublished data.

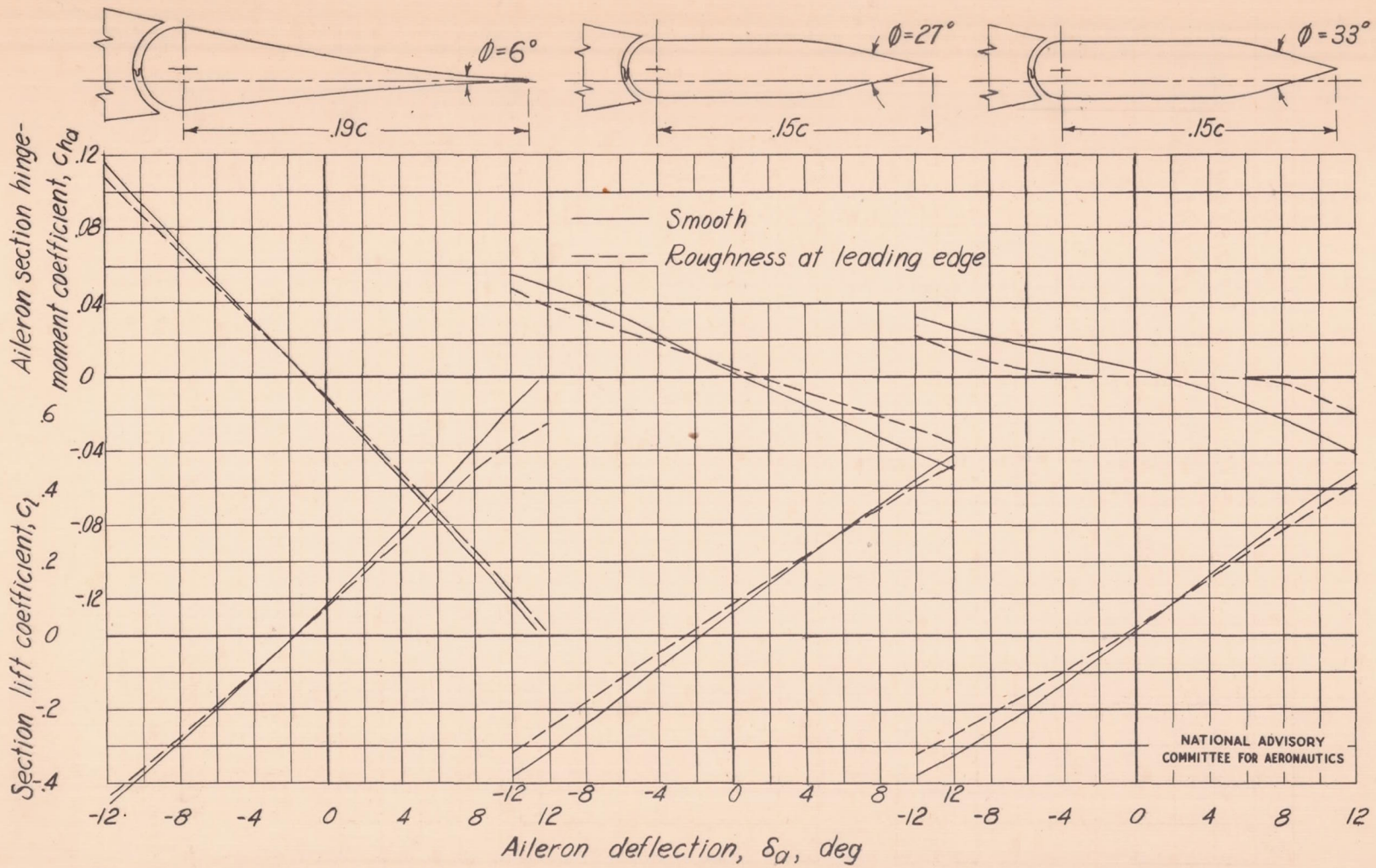


Figure 51.-Comparison of effects of roughness strips on section characteristics of an aileron having various trailing-edge angles. R, 4×10^6; α, 0°. Unpublished data.

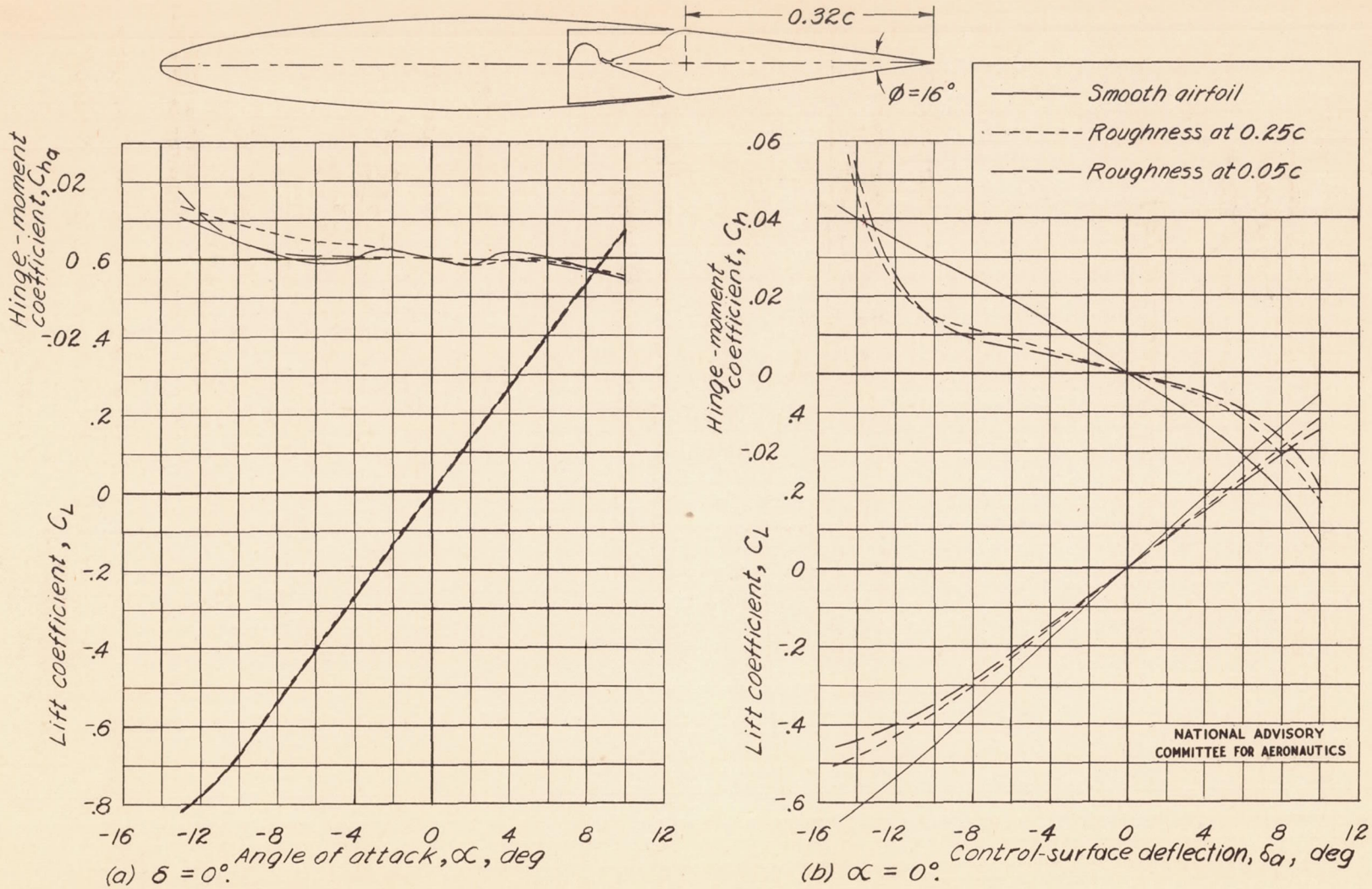
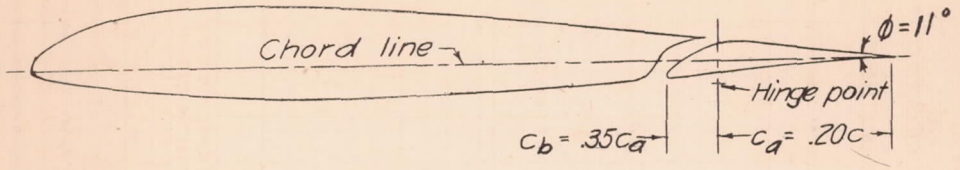
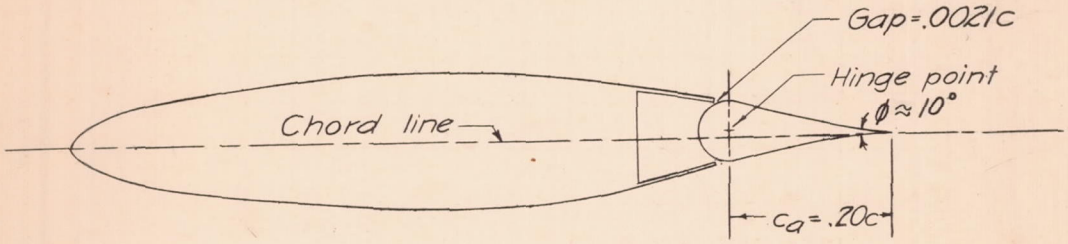


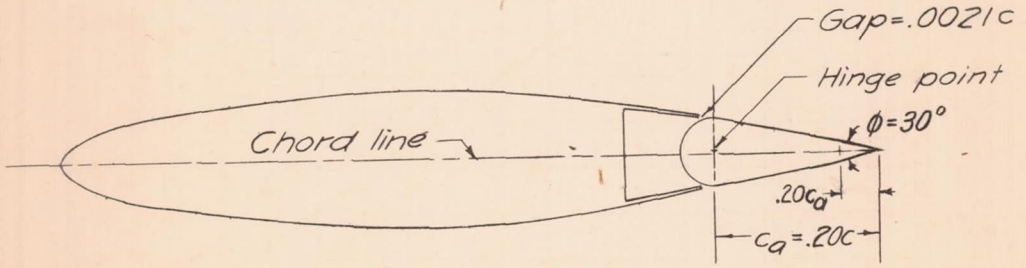
Figure 52.-Effect of roughness strips on the characteristics of a semispan horizontal-tail model having a modified NACA 65_1-012 airfoil section. A, 5.0; λ, 0.5; R, 2.8×10^6; M, 0.2. Unpublished data.



(a) Frise aileron (reference 74).



(b) True contour plain aileron on NACA 66,1-115 airfoil (unpublished).



(c) Beveled aileron on NACA 66,1-115 airfoil (unpublished).

NATIONAL ADVISORY COMMITTEE FOR AERONAUTICS

Figure 53. - Cross sections of two-dimensional models with 0.20c ailerons tested in the Langley 8-foot high-speed tunnel.

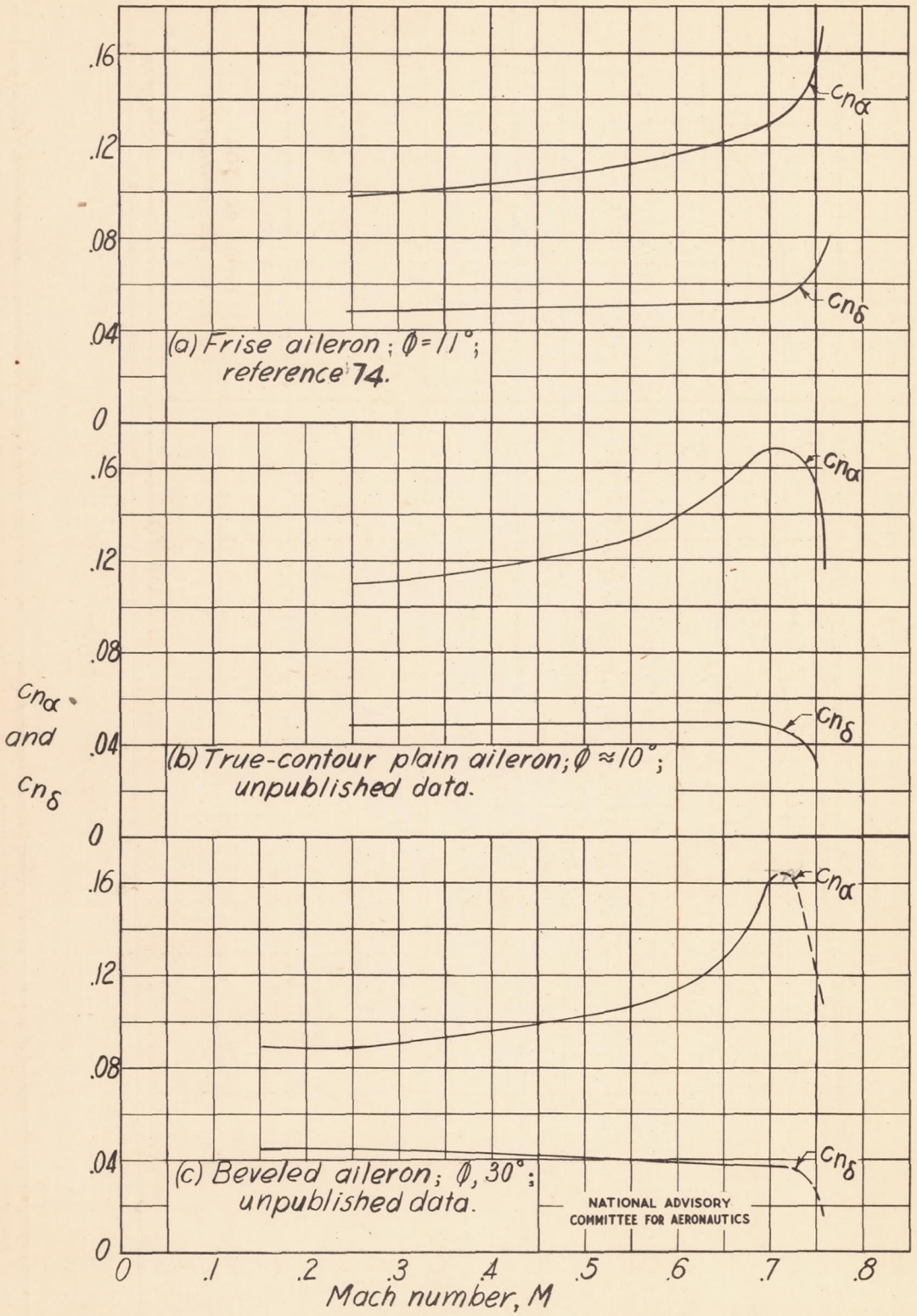


Figure 54.-Effect of Mach number on the section normal-force parameters c_{n_α} and c_{n_δ} of the ailerons shown in figure 53.

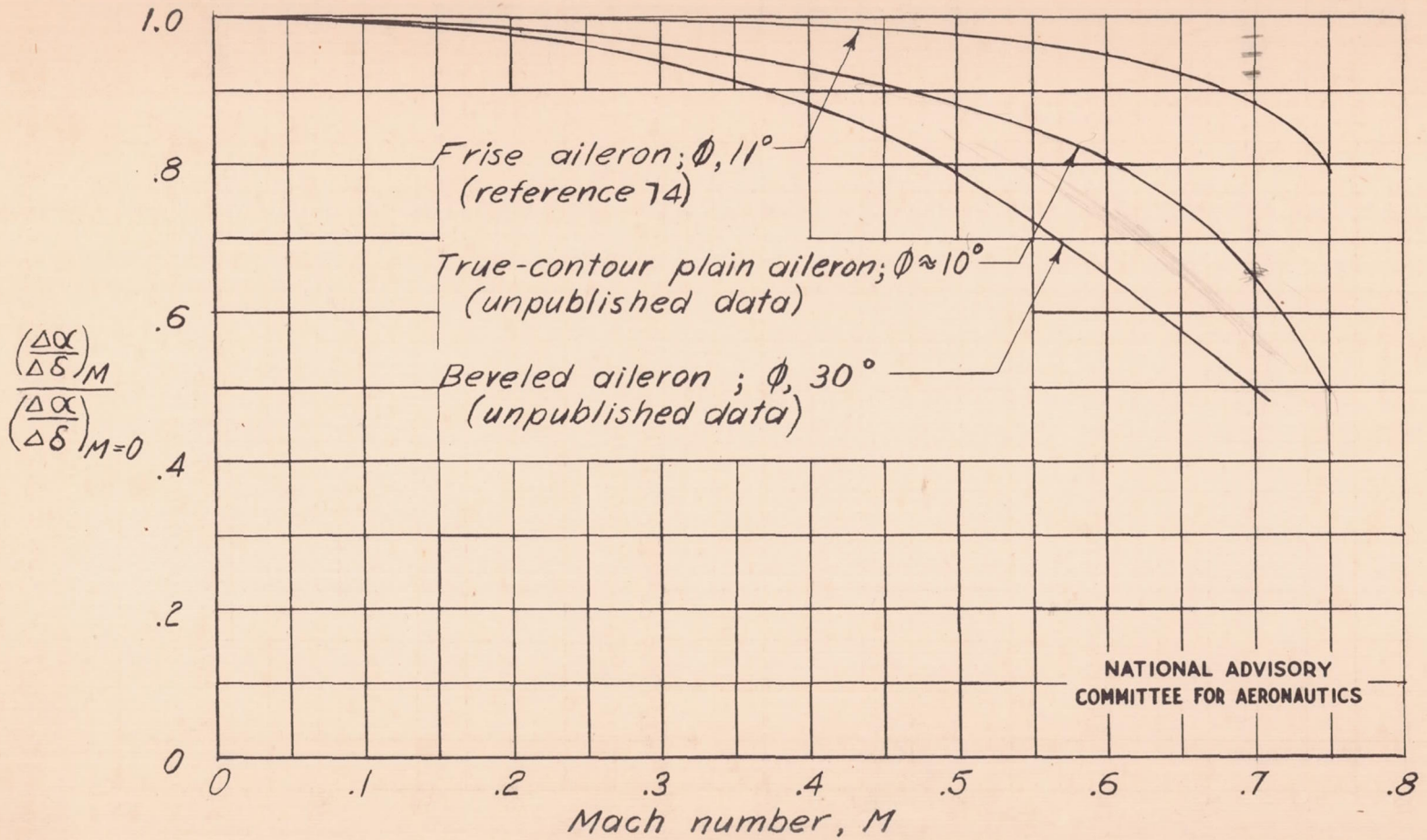


Figure 55.- Effect of Mach number on the effectiveness parameters, relative to the effectiveness parameters at zero Mach number, for the ailerons shown in figure 53.

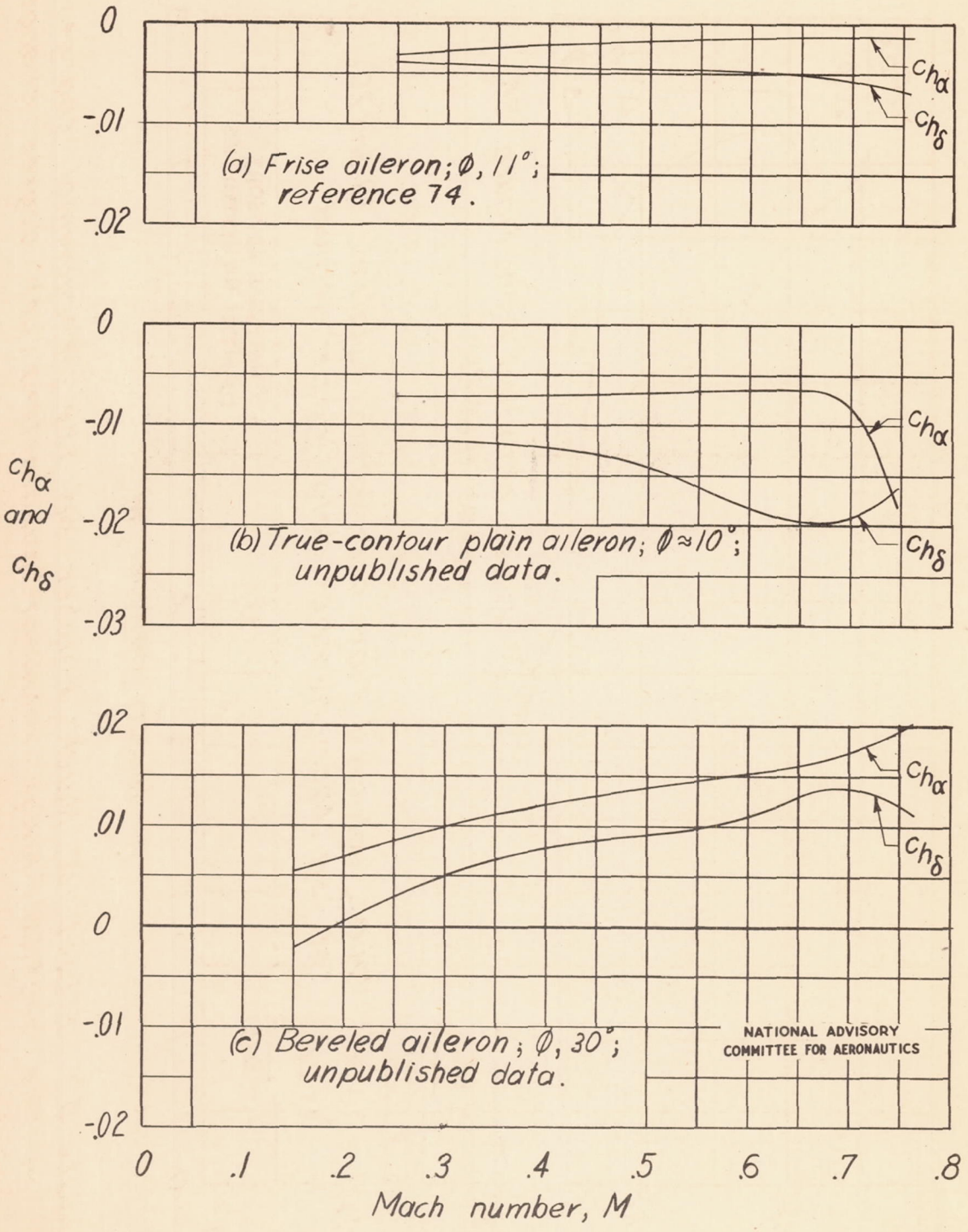


Figure 56.- Effect of Mach number on the section hinge-moment parameters c_{h_α} and c_{h_δ} of the three ailerons shown in figure 53.

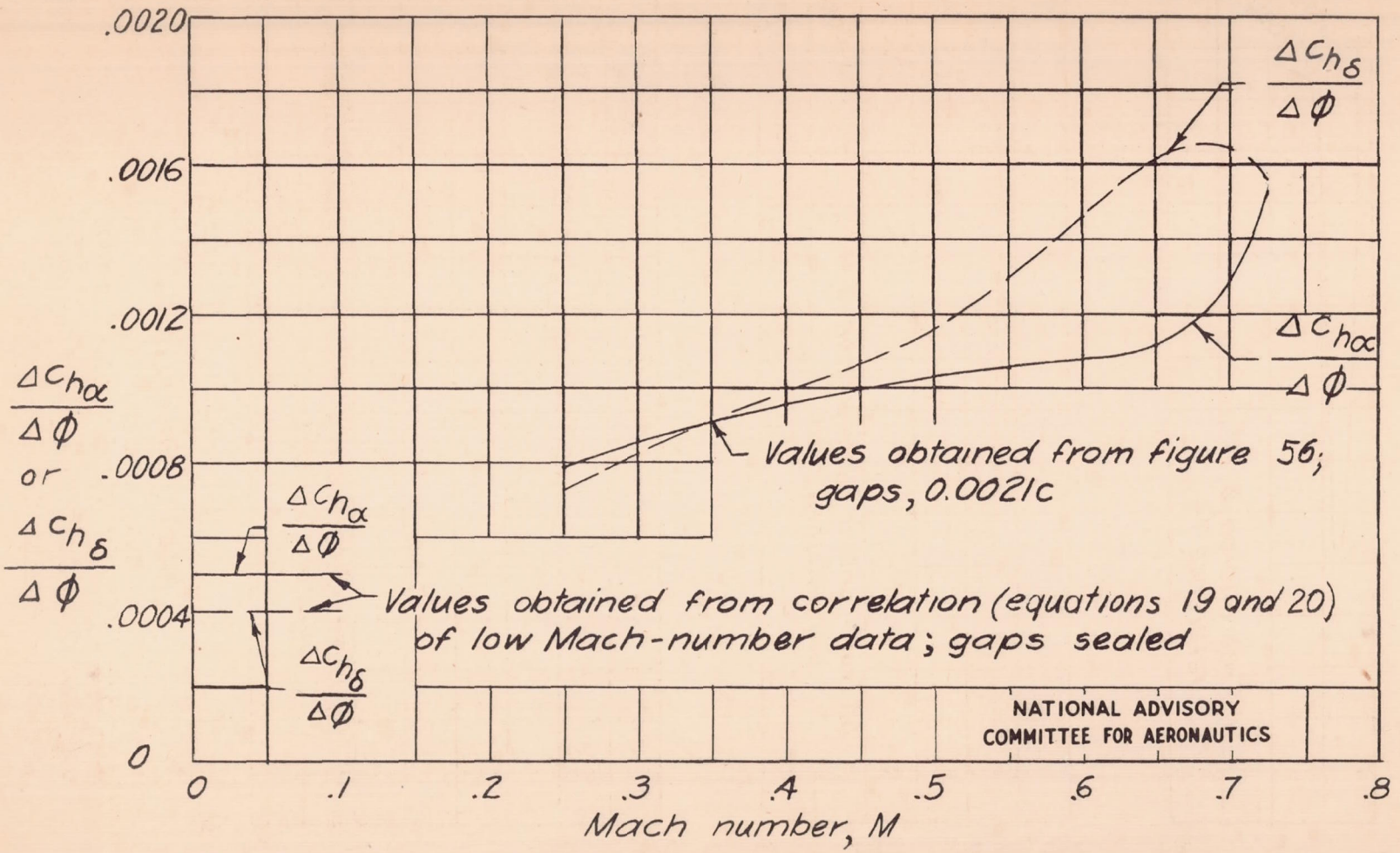


Figure 57.- Effect of Mach number on the incremental changes in the section hinge-moment parameters per degree change in trailing-edge angle.

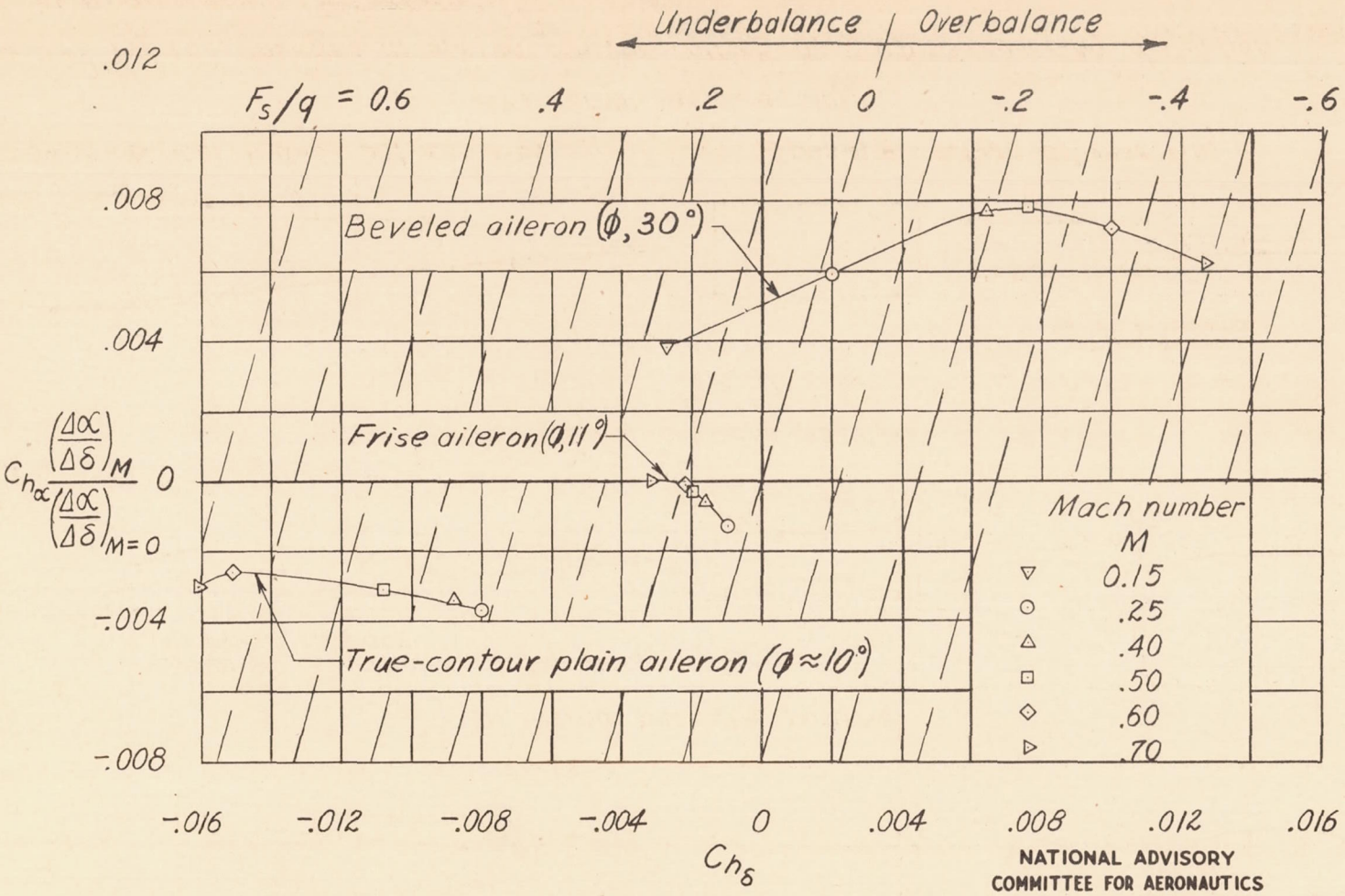
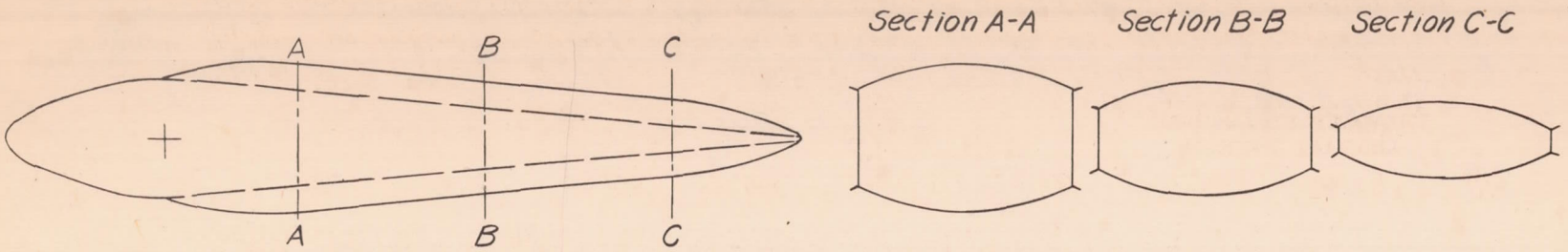
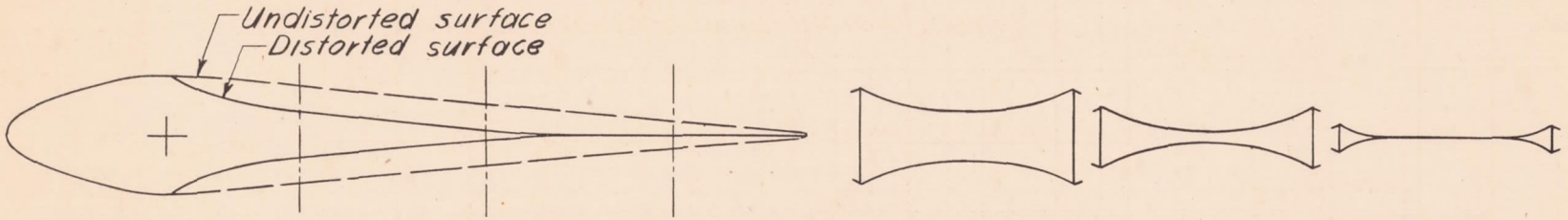


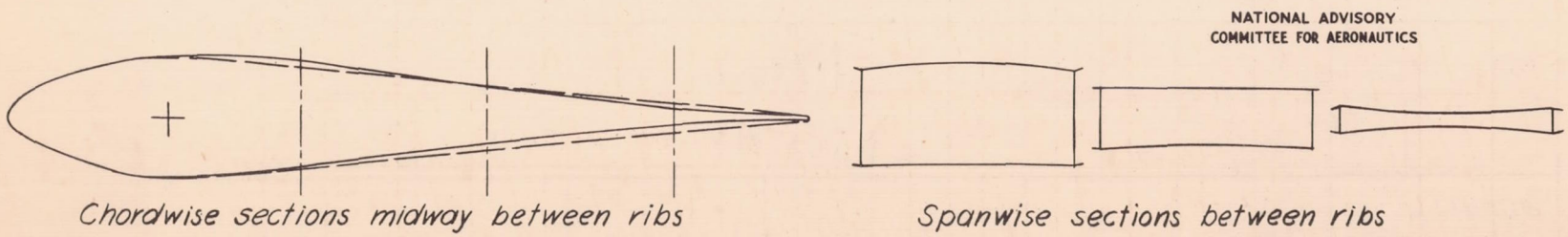
Figure 58.- Effect of Mach number on the estimated finite-span hinge-moment characteristics and the estimated stick-force characteristics (for $\delta_a = \pm 5°$) of a fighter airplane (fig. 43) equipped with each of the ailerons of figure 53. $\frac{b_a}{b/2}$, 0.42; c_a/c, 0.20; $\partial\delta_a/\partial\theta_s$, 0.833.



(a) Internal pressure, positive.



(b) Internal pressure, negative.



(c) Internal pressure, static.

Figure 59.- Typical changes in aileron contour caused by surface-covering distortion at high airspeeds. Reference 15.

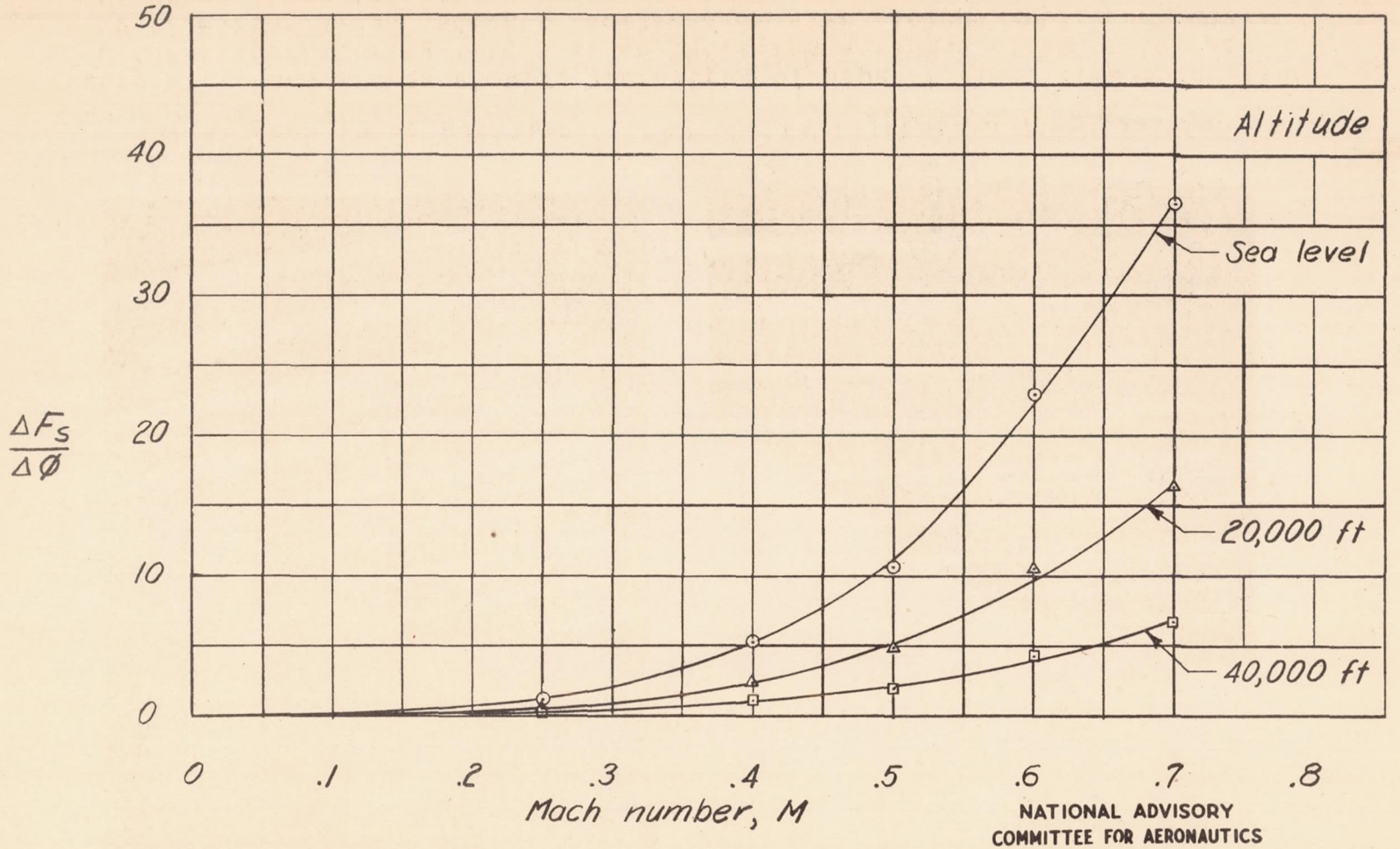
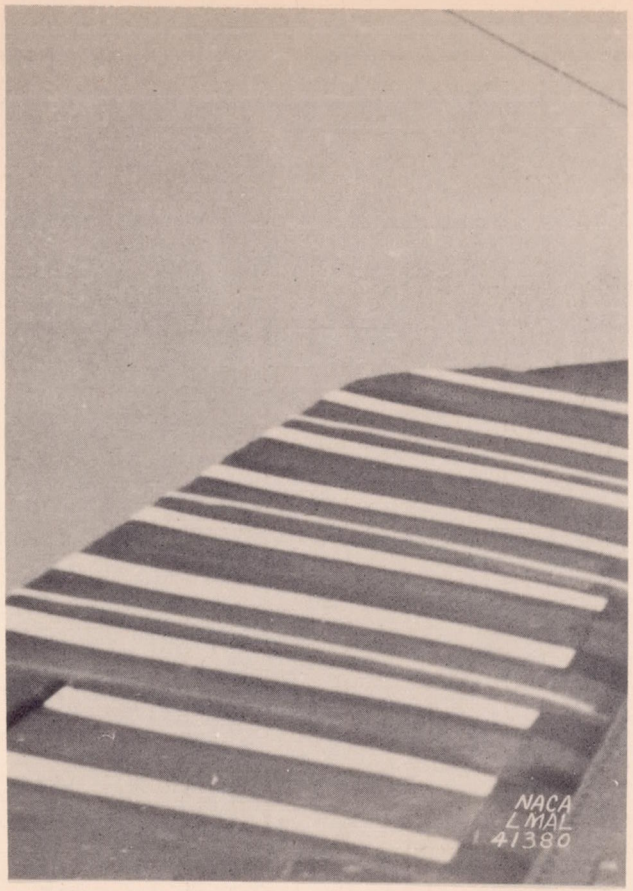
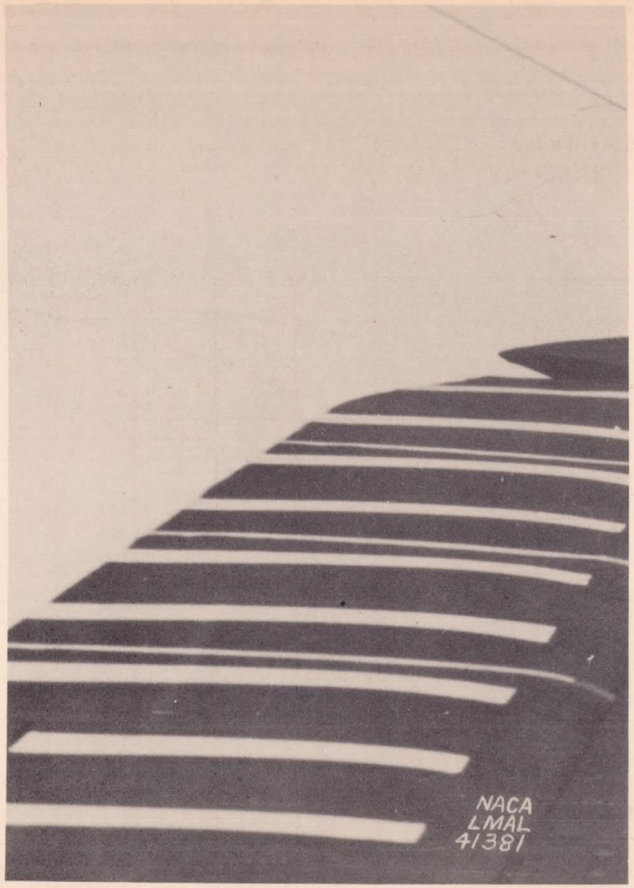


Figure 60.- Effect of Mach number and altitude on the change in stick force per degree change in trailing-edge angle for ±5° aileron deflection. Assumed airplane of figure 43. $\frac{b_a}{b/2}$, 0.42; c_a/c, 0.20; $\partial\delta_a/\partial\theta_s$, 0.833.



(a) Aileron in up position.



(b) Aileron in down position.

Figure 61.- Photographs showing distortion of upper surface of a production P-40F aileron during flight at an indicated airspeed of 350 miles per hour. Narrow lines indicate locations of every second rib; lower edges of broad lines indicate centers of panels.

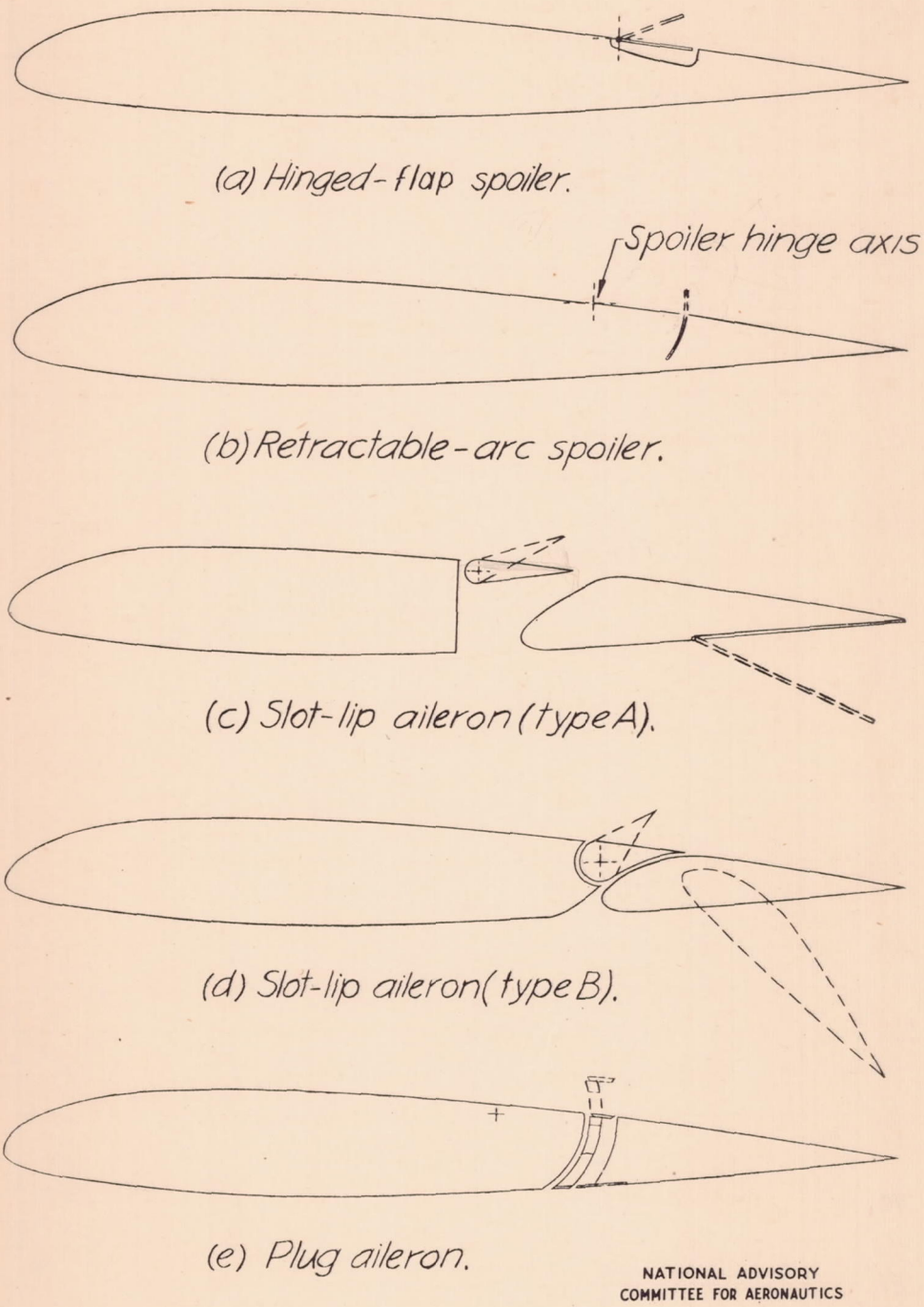


Figure 62.-Sketches of typical spoiler-type lateral-control devices.

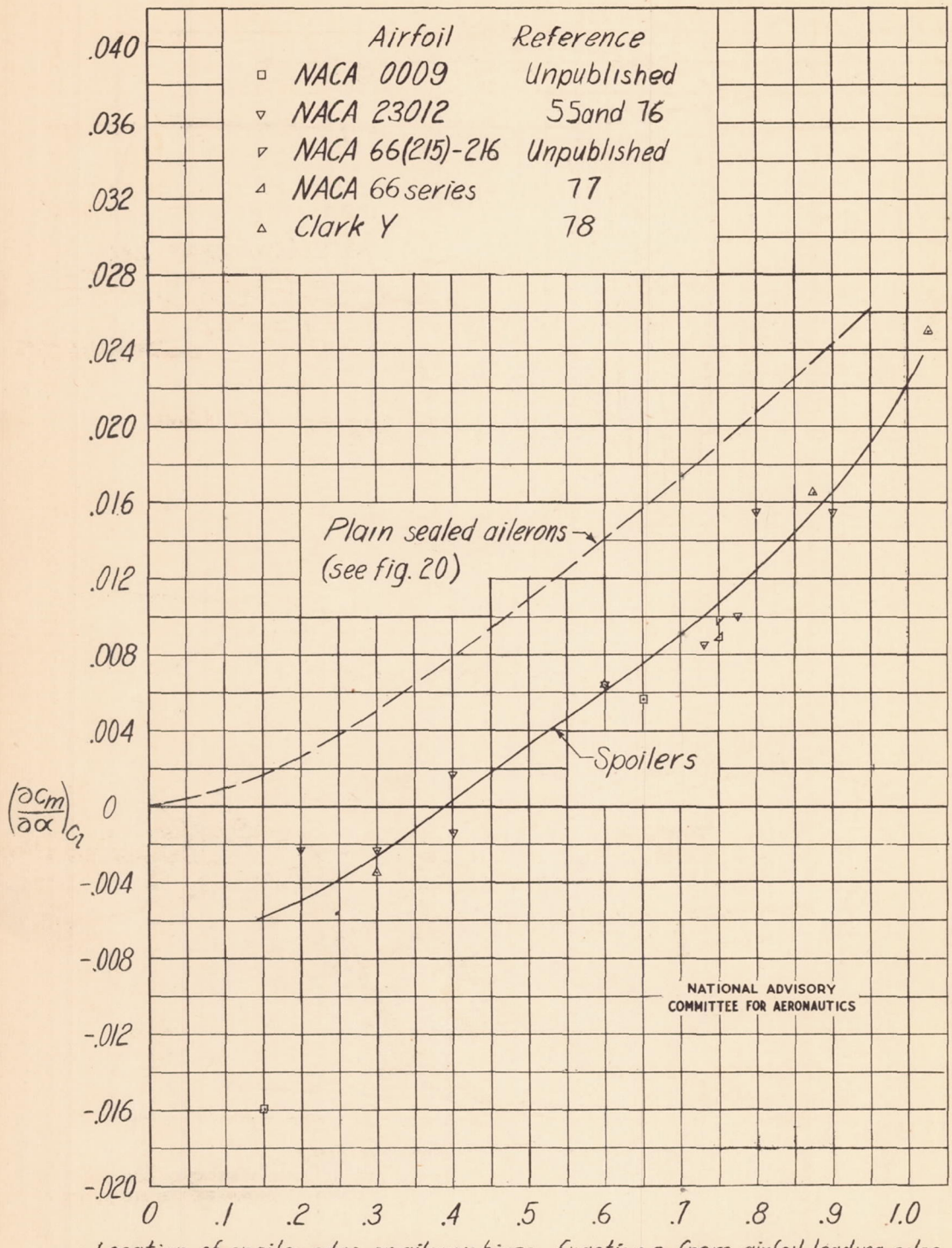
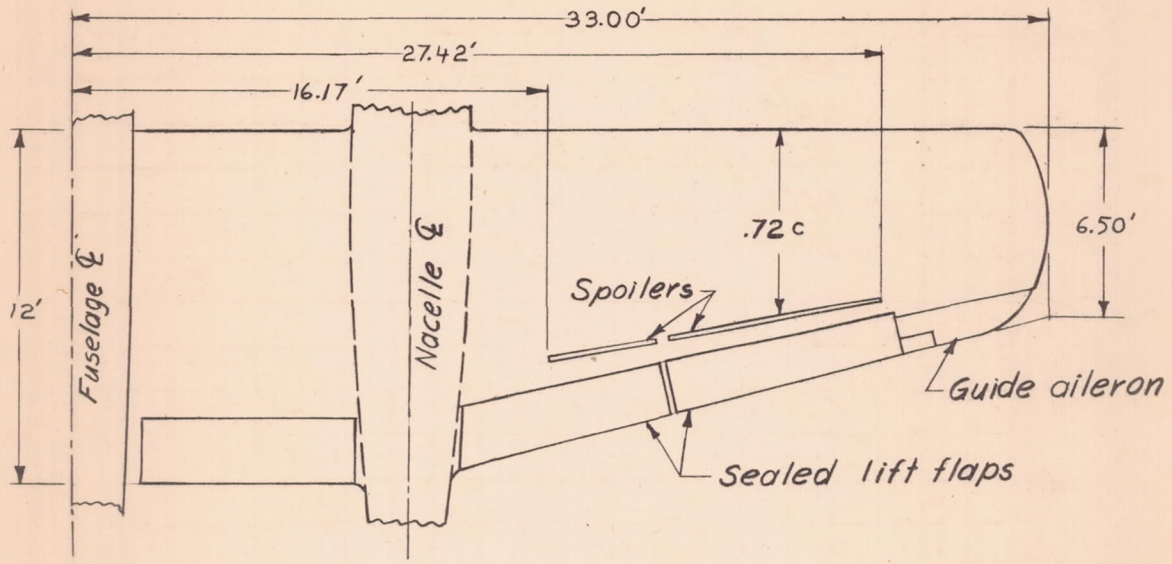


Figure 63.- Comparison of effects of chordwise location of spoiler edge or of aileron hinge on the parameter $(\partial c_m/\partial \alpha)_{c_l}$ of spoilers and of plain sealed ailerons. Reference 55.



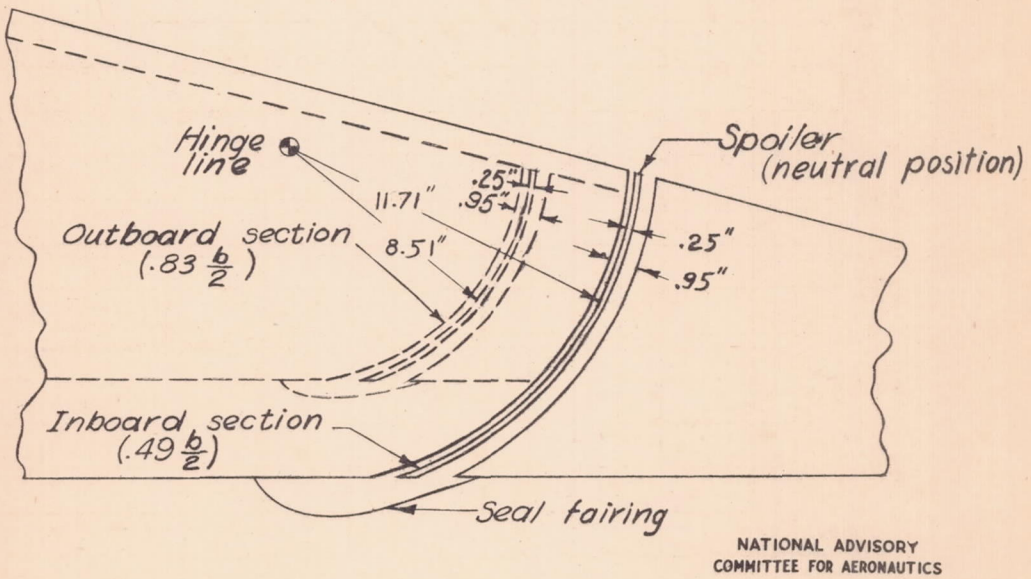


Figure 64.- Wing plan form and wing section showing spoiler arrangement on P-61 airplane.

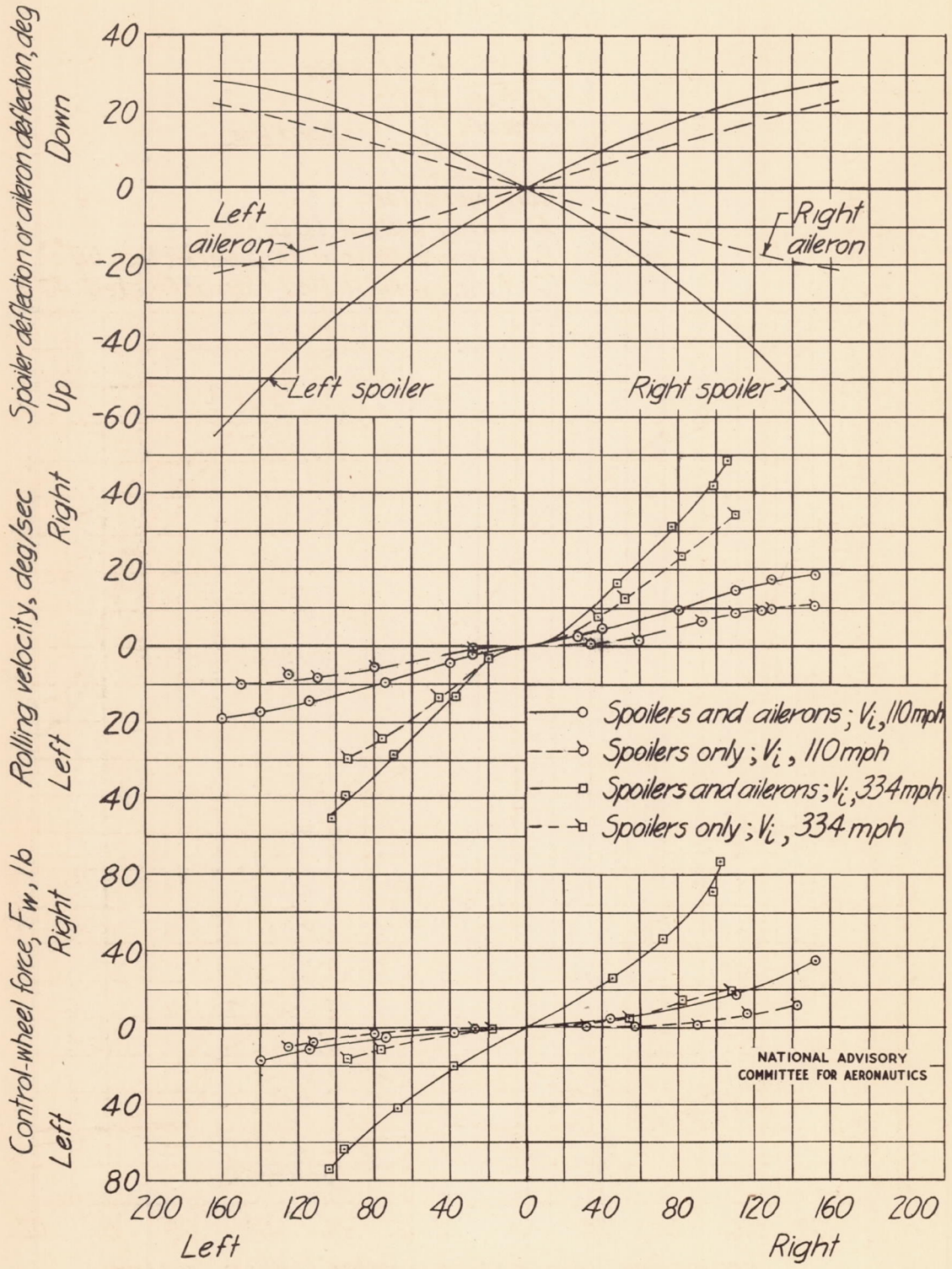


Figure 65.- Lateral-control characteristics of P-61 airplane. Unpublished data.

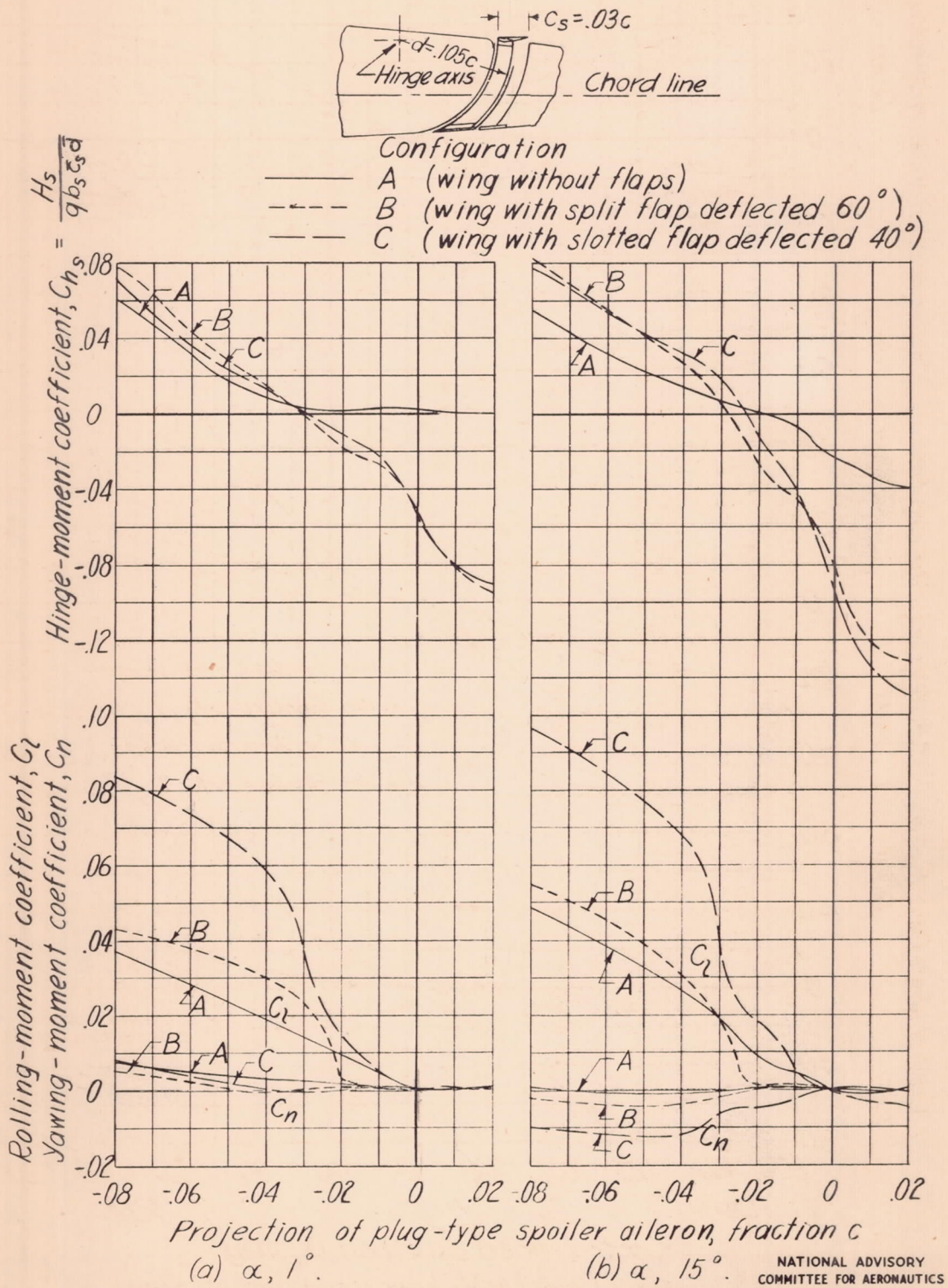
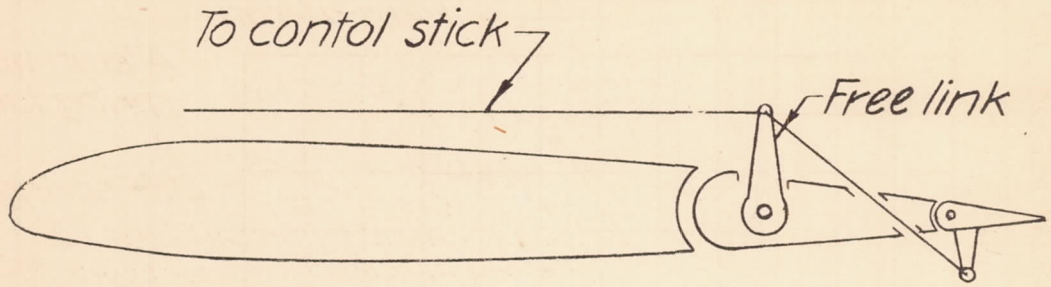
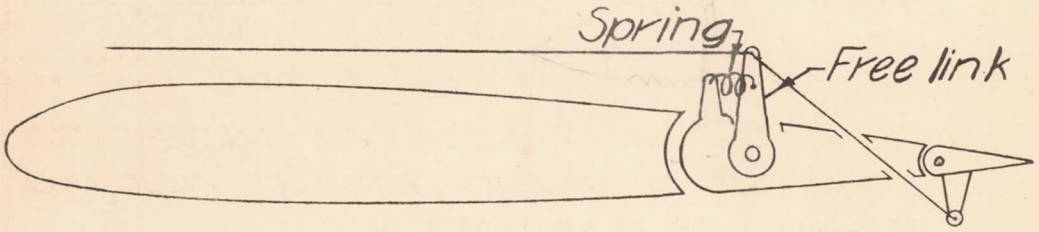


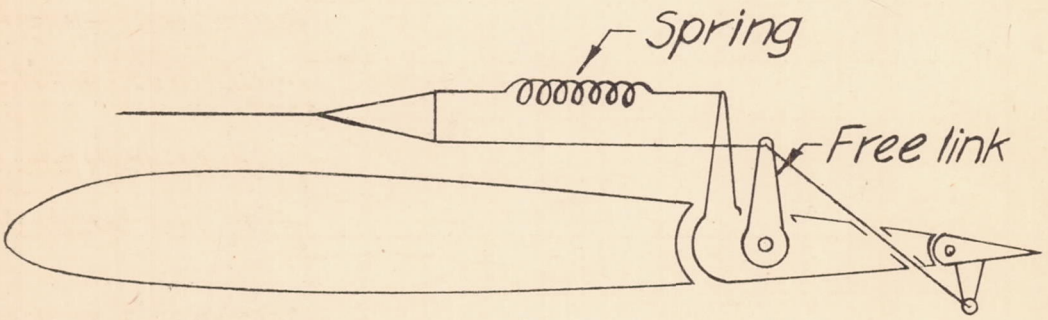
Figure 66.- Effects of lift flaps on the characteristics of a plug-type spoiler aileron. Reference 79.



(a) Servotab.



(b) Spring tab.



(c) Geared spring tab.

NATIONAL ADVISORY
COMMITTEE FOR AERONAUTICS

Figure 67. - Arrangements of tab-type aileron booster mechanisms.

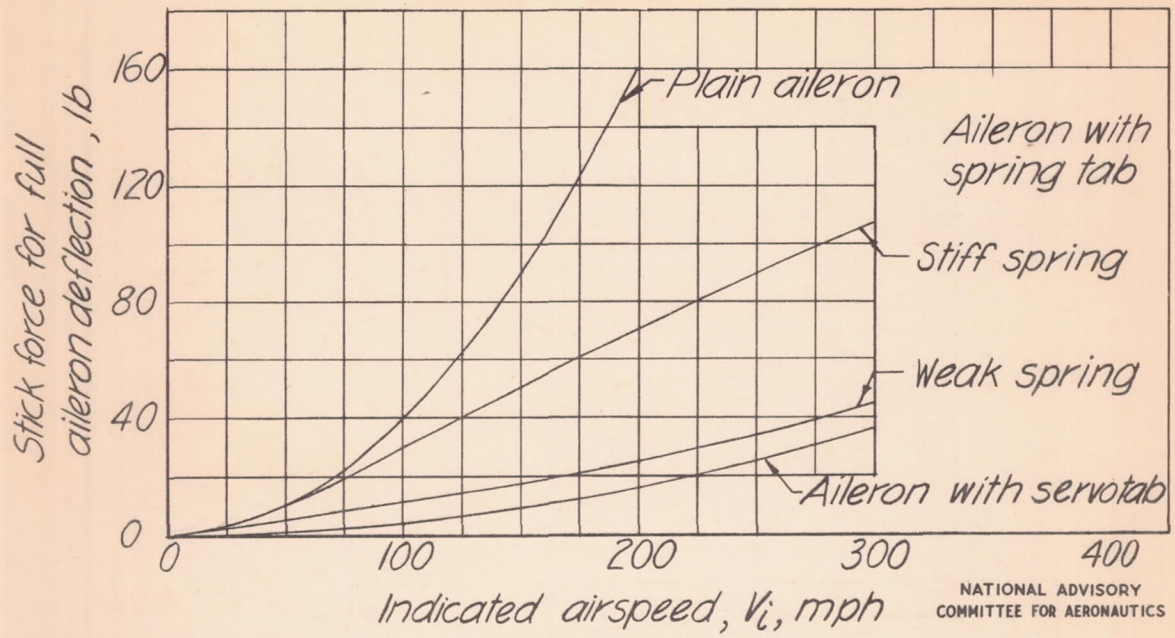


Figure 68.- Comparison of stick-force characteristics of a plain aileron, an aileron with a spring tab, and an aileron with a servo tab.

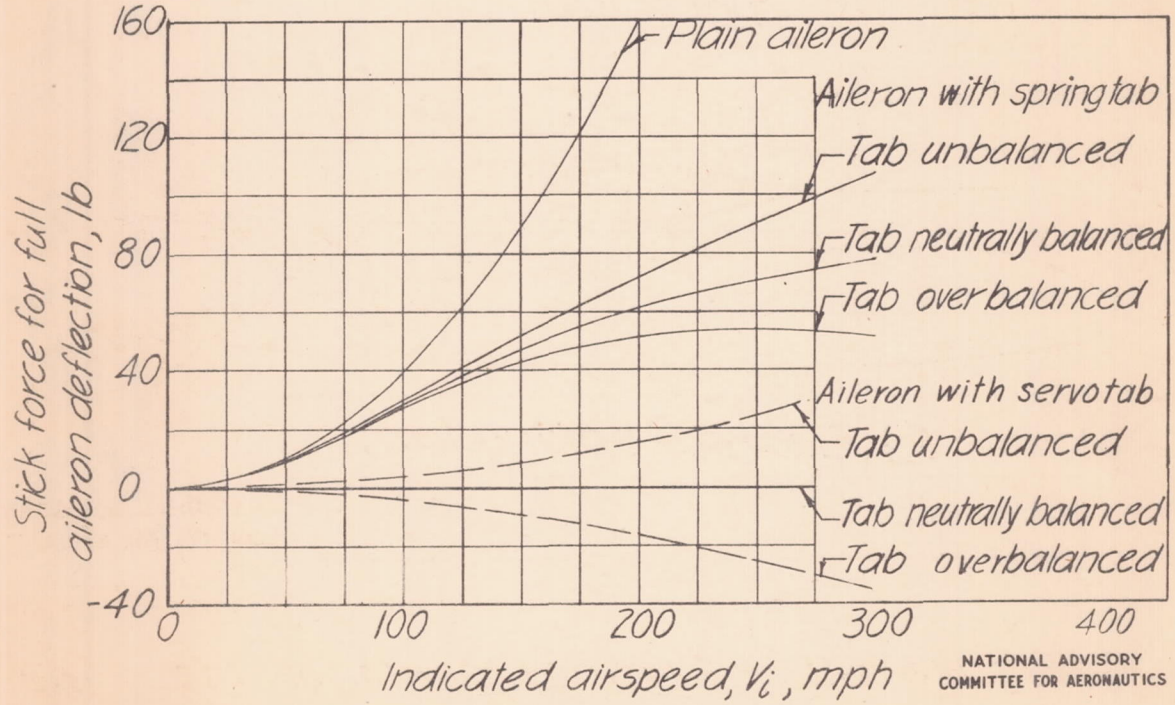


Figure 69.- Effect of aerodynamic balance of tab on stick-force characteristics of aileron with spring tab and of aileron with servotab.

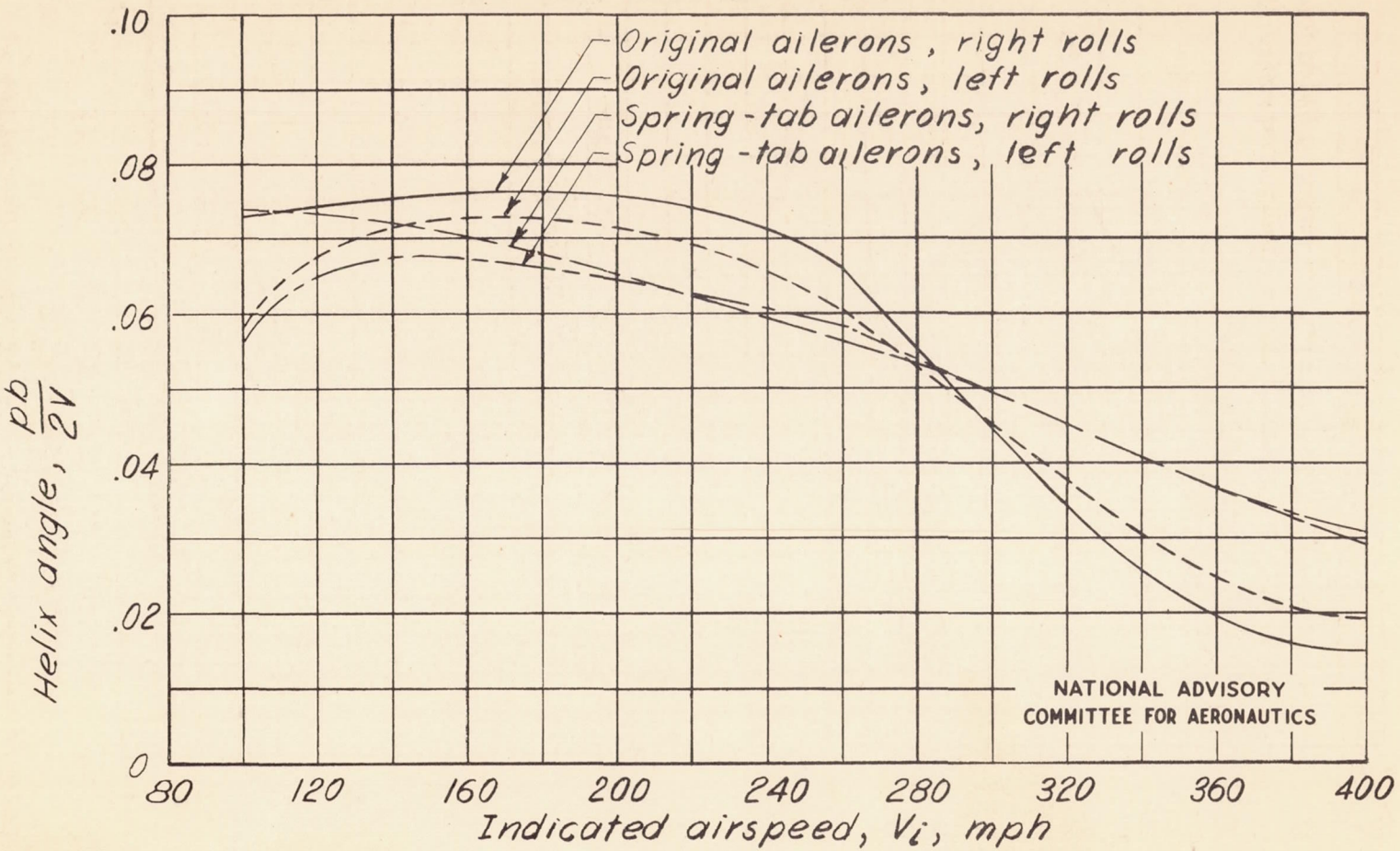


Figure 70. - Comparisons of rolling performance of F6F-3 airplane with original ailerons and with spring-tab ailerons. Stick-force limit, 30 pounds. Unpublished data

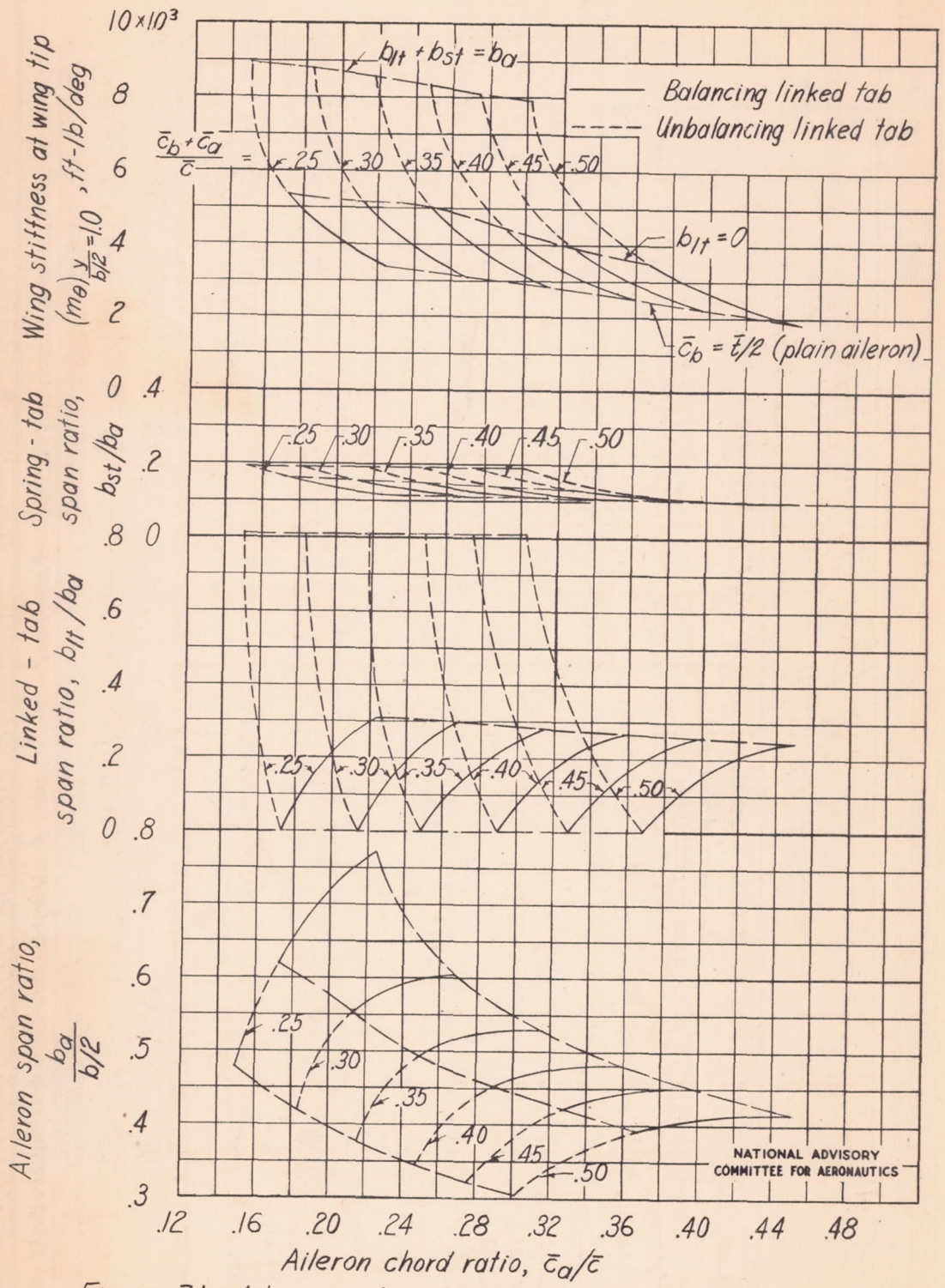


Figure 71.- Aileron configurations estimated to be capable of producing a $pb/2V$ of 0.09 with 30 pounds stick force at 320 miles per hour for airplane of figure 43. δ_a, $\pm 12°$; δ_{lt}, $\pm 15°$; δ_{st}, $\pm 15°$; $\bar{c}_{lt}/\bar{c}_a'$, 0.25; $\bar{c}_{st}/\bar{c}_a'$, 0.25; $\theta_{s_{max}}$, 14.8°.

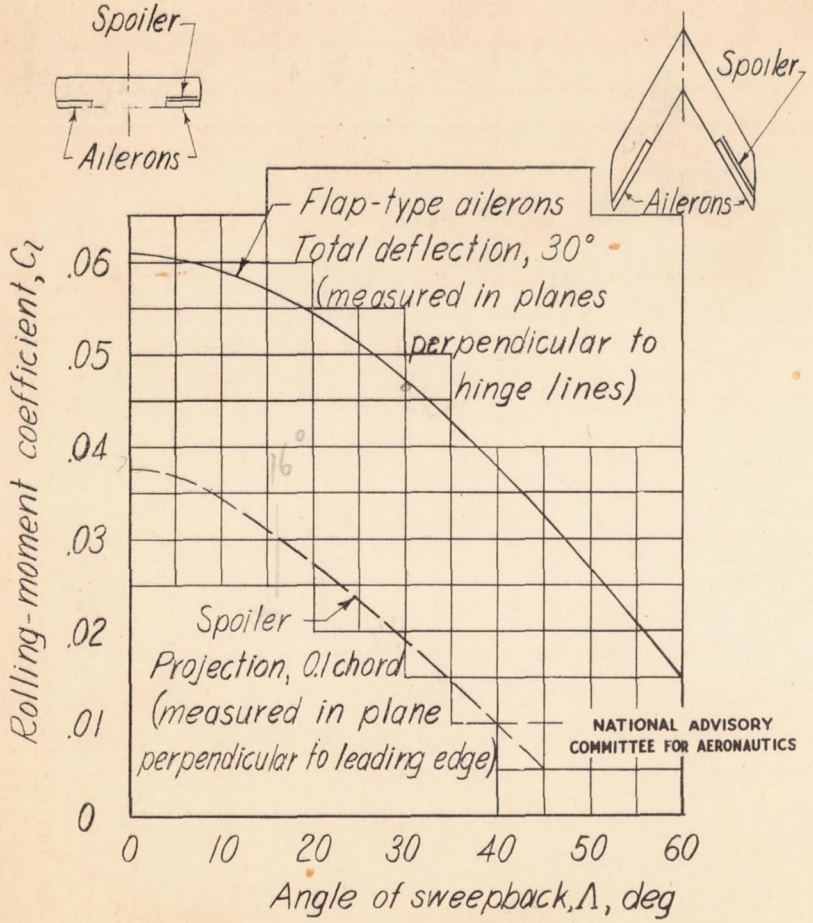


Figure 72.-Effect of angle of sweepback on rolling-moment coefficients produced by flap-type ailerons and by spoilers. c_a/c, 0.20; $\frac{b_a}{b/2} \approx 0.5$; $\frac{b_s}{b/2} \approx 0.5$; spoiler at 0.7c. Reference 91.

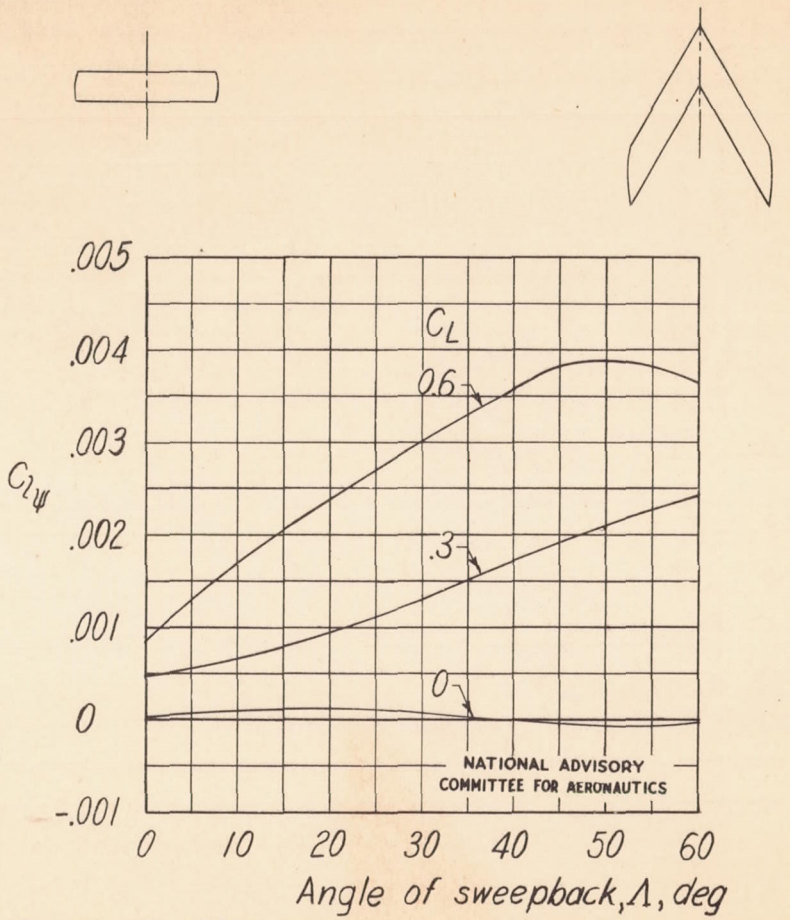


Figure 73.-Effect of angle of sweepback on variation of rolling-moment coefficient with angle of yaw. Reference 91.